EFFICIENT BIOSYNTHESIS OF ORGANIC ACIDS FROM RENEWABLE MATERIALS

EDITED BY: Hui Wu, Yu Deng and Rongming Liu

PUBLISHED IN: Frontiers in Bioengineering and Biotechnology

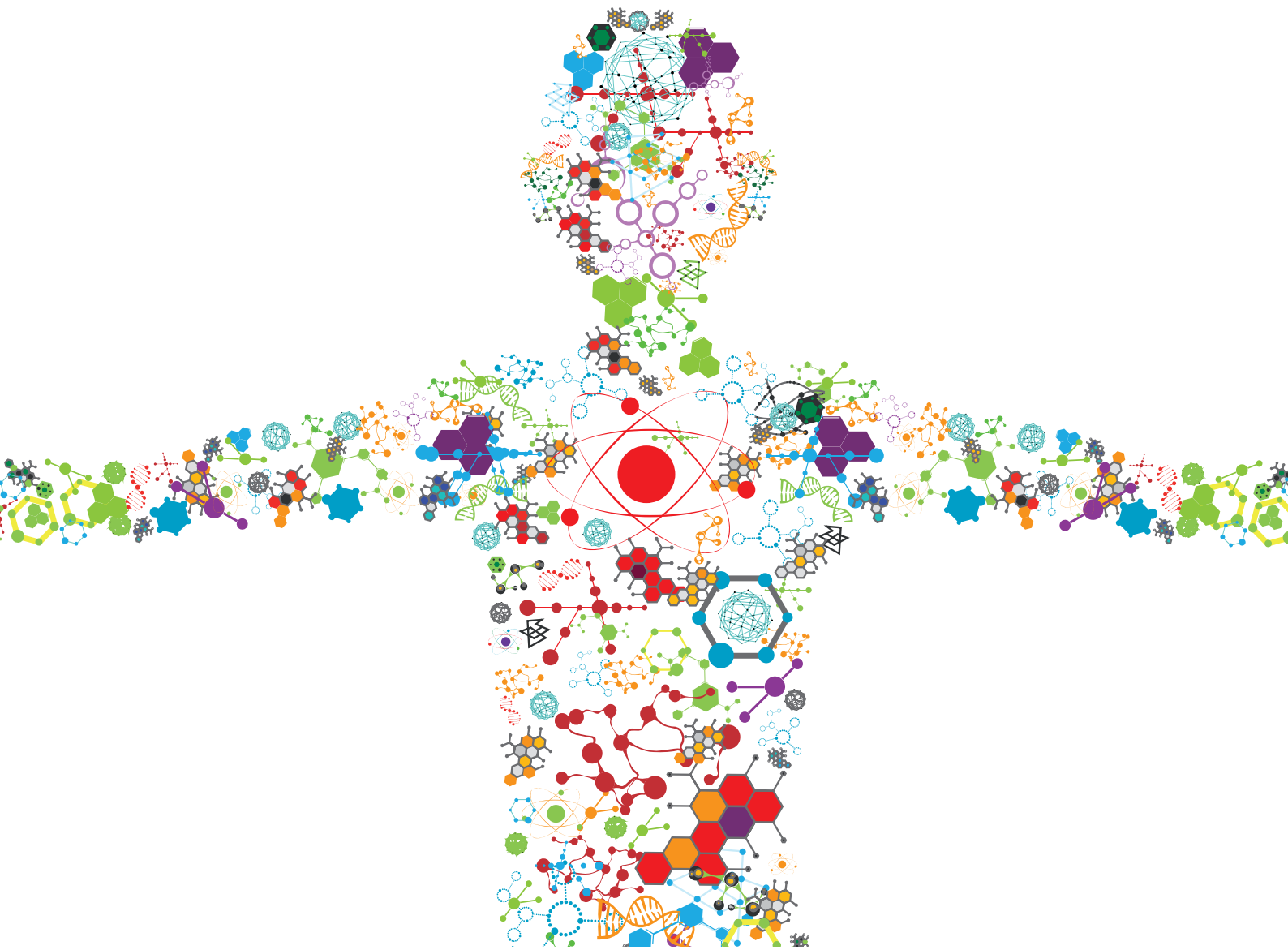

frontiers Research Topics

frontiers

ISSN 1664-8714
ISBN 978-2-88971-138-3
DOI 10.3389/978-2-88971-138-3

About Frontiers

Frontiers is more than just an open-access publisher of scholarly articles: it is a pioneering approach to the world of academia, radically improving the way scholarly research is managed. The grand vision of Frontiers is a world where all people have an equal opportunity to seek, share and generate knowledge. Frontiers provides immediate and permanent online open access to all its publications, but this alone is not enough to realize our grand goals.

Frontiers Journal Series

The Frontiers Journal Series is a multi-tier and interdisciplinary set of open-access, online journals, promising a paradigm shift from the current review, selection and dissemination processes in academic publishing. All Frontiers journals are driven by researchers for researchers; therefore, they constitute a service to the scholarly community. At the same time, the Frontiers Journal Series operates on a revolutionary invention, the tiered publishing system, initially addressing specific communities of scholars, and gradually climbing up to broader public understanding, thus serving the interests of the lay society, too.

Dedication to Quality

Each Frontiers article is a landmark of the highest quality, thanks to genuinely collaborative interactions between authors and review editors, who include some of the world's best academicians. Research must be certified by peers before entering a stream of knowledge that may eventually reach the public - and shape society; therefore, Frontiers only applies the most rigorous and unbiased reviews.
Frontiers revolutionizes research publishing by freely delivering the most outstanding research, evaluated with no bias from both the academic and social point of view. By applying the most advanced information technologies, Frontiers is catapulting scholarly publishing into a new generation.

What are Frontiers Research Topics?

Frontiers Research Topics are very popular trademarks of the Frontiers Journals Series: they are collections of at least ten articles, all centered on a particular subject. With their unique mix of varied contributions from Original Research to Review Articles, Frontiers Research Topics unify the most influential researchers, the latest key findings and historical advances in a hot research area! Find out more on how to host your own Frontiers Research Topic or contribute to one as an author by contacting the Frontiers Editorial Office: frontiersin.org/about/contact

EFFICIENT BIOSYNTHESIS OF ORGANIC ACIDS FROM RENEWABLE MATERIALS

Topic Editors:
Hui Wu, East China University of Science and Technology, China
Yu Deng, Jiangnan University, China
Rongming Liu, University of Colorado Boulder, United States

Citation: Wu, H., Deng, Y., Liu, R., eds. (2021). Efficient Biosynthesis of Organic Acids from Renewable Materials. Lausanne: Frontiers Media SA. doi: 10.3389/978-2-88971-138-3

Table of Contents

frontiers in Bioengineering and Biotechnology

REVIEW
published: 08 August 2019
doi: 10.3389/fbioe.2019.00191

Biomethane Production From Lignocellulose: Biomass Recalcitrance and Its Impacts on Anaerobic Digestion

*Ning Xu[1,2], Shixun Liu[1], Fengxue Xin[1], Jie Zhou[1], Honghua Jia[1], Jiming Xu[2], Min Jiang[1,3] and Weiliang Dong[1,3]**

[1] State Key Laboratory of Materials-Oriented Chemical Engineering, College of Biotechnology and Pharmaceutical Engineering, Nanjing Tech University, Nanjing, China, [2] Jiangsu Key Laboratory for Biomass-Based Energy and Enzyme Technology, Huaiyin Normal University, Huai'an, China, [3] Jiangsu National Synergetic Innovation Center for Advanced Materials (SICAM), Nanjing Tech University, Nanjing, China

OPEN ACCESS

Edited by:
Rongming Liu,
University of Colorado Boulder,
United States

Reviewed by:
Elisabeth Jacobsen,
Norwegian University of Science and Technology, Norway
Jiufu Qin,
Technical University of Denmark,
Denmark

***Correspondence:**
Weiliang Dong
dwl@njtech.edu.cn

Specialty section:
This article was submitted to Industrial Biotechnology, a section of the journal Frontiers in Bioengineering and Biotechnology

Received: 15 May 2019
Accepted: 24 July 2019
Published: 08 August 2019

Citation:
Xu N, Liu S, Xin F, Zhou J, Jia H, Xu J, Jiang M and Dong W (2019) Biomethane Production From Lignocellulose: Biomass Recalcitrance and Its Impacts on Anaerobic Digestion. Front. Bioeng. Biotechnol. 7:191. doi: 10.3389/fbioe.2019.00191

Anaerobic digestion using lignocellulosic material as the substrate is a cost-effective strategy for biomethane production, which provides great potential to convert biomass into renewable energy. However, the recalcitrance of native lignocellulosic biomass makes it resistant to microbial hydrolysis, which reduces the bioconversion efficiency of organic matter into biogas. Therefore, it is necessary to critically investigate the correlation between lignocellulose characteristics and bioconversion efficiency. Accordingly, this review comprehensively summarizes the anaerobic digestion process and rate-limiting step, structural and compositional properties of lignocellulosic biomass, recalcitrance and inhibitors of lignocellulose and their major effects on anaerobic digestion for biomethane production. Moreover, various type of pretreatment strategies applied to lignocellulosic biomass was discussed in detail, which would contribution to cell wall degradation and improvement of biomethane yields. In the view of current knowledge, high energy input and cost requirements are the main limitations of these pretreatment methods. In addition to optimization of fermentation process, further studies should focus much more on key structural influence factors of biomass recalcitrance and anaerobic digestion efficiency, which will contribute to improvement of biomethane production from lignocellulose.

Keywords: biomethane, anaerobic digestion, lignocellulose, cell wall composition, biomass recalcitrance

INTRODUCTION

Lignocellulose is one of the most abundant renewable organic resources with an increasing annual yield of 200 billion tons, which can be produced from agriculture, forestryand urban wastes (Patinvoh et al., 2017). The prominent abundance and low cost of lignocellulose make it a potential substrate for second generation bioenergy production, such as bioethanol and biomethane (Florian et al., 2013). During these, biomethane production is one of the most cost-effective methods for energy generation from lignocellulosic cellulose, which has been implemented worldwide (Grosser, 2017).

Biomethane production through anaerobic digestion is a naturally occurring biological process, which can be divided into four steps (**Figure 1**). In the beginning of the process, complex organic polymers are decomposed to their component units, e.g., amino acids, fatty acids, and sugars, respectively. Then, these monomers are converted into a mixture of short chain volatile fatty acids by fermentative bacteria (Acidogens). Acetogenic bacteria or acetogens further convert the volatile fatty acids to acetate, carbon dioxide, and hydrogen, which are natural substrates for Methanogenesis to generate biomethane. Theoretically, AD process can decompose the organic fraction of any feedstocks to produce biomethane, such as crop and livestock residues, food waste and lignocellulosic feedstocks (Hagos et al., 2016). However, methane production varies greatly with different types of substrates. For example, high methane yields up to 450 mL CH_4/g volatile solids can be achieved with sugar and starch crops (Frigon and Guiot, 2010), while no more than 330 mL CH_4/g volatile solids can be produced from lignocellulosic biomass (**Table 1**). The complexity of biomass structure is the major challenge, which makes lignocellulosic biomass highly recalcitrant to anaerobic degradation and ultimately results in low biomethane yield (Sawatdeenarunat et al., 2016). The stubborn anti-degradation characteristics of native lignocellulose was known as biomass recalcitrance, which extremely restricts the hydrolysis during the first step of anaerobic digestion process and finally limits the commercial biomethane production from lignocellulose (Himmel et al., 2007).

In order to overcome this recalcitrance, lignocellulose must be pretreated and many pretreatment methods have been developed in recent years. The positive effects of various pretreatments (e.g., increase of surface area, lignin removal, decrease of cellulose crystallinity) have been reviewed elsewhere (Paudel et al., 2017). However, an overall review and assessment about the impacts of lignocellulose recalcitrance on anaerobic digestion and biomethane production is still needed and imperative for further biomethane development. Hence, the aim of this paper is to provide a comprehensive review of lignocellulose recalcitrance and its relative effects on anaerobic fermentation and biomethane production. In addition, the technology for acceleration of anaerobic digestion of lignocellulose and future prospective was also discussed.

BASIC STRUCTURAL PROPERTIES OF PLANT CELL WALL AND LIGNOCELLULOSE RECALCITRANCE

Lignocellulosic biomass is mainly composed of cellulose, hemicellulose and lignin, which vary a lot based on types of plants, growth conditions and maturation both in quantity and quality (**Table 2**). The detailed structure has been comprehensively reviewed elsewhere (Jeoh et al., 2017). Biomass recalcitrance refers to the anti-degradation characteristics of native lignocellulose, which protect plant cell wall from pathogen attack or degradation by microorganisms and enzymes. It was caused by the complicated compositions and structure of plant cell wall (**Figure 1**). Cellulose is a relative homogeneous substance in terms of the composition and structure, which provides the basic backbone to lignin-carbohydrate complexes. Hemicelluloses are embedded through the cell wall and form covalent bonds to the surface of cellulose fibrils (Somerville et al., 2004), which help strengthen the cell wall. As a filler compound, lignin wrappers itself in the interspace of cellulose and hemicellulose chains and formed a hydrophobic lignification structure, which plays an important role in maintaining the structural integrity of the cell wall (Yuan et al., 2013). Besides the three main compositions, cell wall proteins, lipids, pectin, mineral and other matters are also involved in the formation of biomass recalcitrance. Moreover, in addition to chemical composition and physical structure, the arrangement and density of the vascular bundles, epidermal protection and some process-induced causes also play considerable role in building the cell wall matrix.

As discussed above, biomass recalcitrance refers to lignocellulosic building blocks which are naturally evolved to block their microbial and enzymatic deconstruction. This is the result of a sophisticated combination of the crystalline cellulose in microfibrils, heteropolysaccharides, lignin, and other components (**Table 3**). In the first step of anaerobic digestion process (**Figure 1**), biomass recalcitrance protects itself from degradation by microorganisms and enzymes, which result in lower monosaccharide production and finally limits the biomethane efficiency. It is known that the degree of recalcitrance varies depending on the composition of the lignocellulosic biomass, which closely correlated to genotype, environmental conditions, crop management practices and plant parts (Surendra et al., 2018). However, there are some basic components and major influencing factors which generally exist in different plants. The detailed of these properties and its impacts on anaerobic digestion for biomethane production are discussed in the following.

Accessible Surface Area of Cellulose

Accessible surface area of substrate refers to the surface area, by which cellulases can contact with cellulose. In anaerobic digestion process, it could directly affect the biodegradability of lignocellulosic materials, which limits the contact between lignocellulose and enzyme, microbial or chemical reagents and result in insufficient fermentable sugars for the subsequent process (Kratky and Jirout, 2015). Accessible surface area can be affected by many indirect factors, e.g., epidermal feature, particle size of raw material powder, chemical and physical characteristics of plant cell wall (Florian et al., 2013). Accessible surface area can be divided into two forms: interior surface area which is determined by substrate porosity and exterior surface area which is correlated with particle size (Zhao et al., 2012). Generally, natural lignocellulosic substrates have very small interior surfaces, especially for dried material (Park et al., 2006). Arantes and Saddler (2011) have reported that cellulose accessibility to enzymes or chemical regents is mainly through the inside pores of substrate (about 90%) rather than the external surface, suggesting that the external surface only plays less important role in hydrolysis progress.

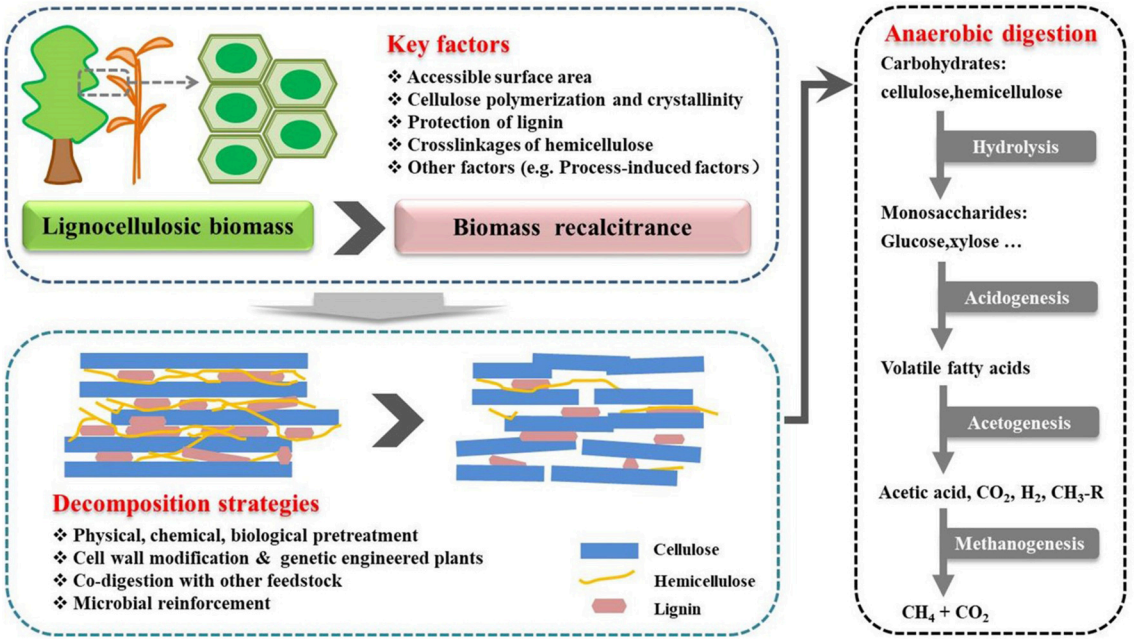

FIGURE 1 | Process stages of the conversion of lignocellulosic biomass to biomethane. Biomethane production is a naturally occurring biological process, which can be divided into four stages. Recalcitrance of lignocellulose restricts the hydrolysis during the first stage. Pretreatment is necessary step for biomethane production. The positive effects of pretreatment strategies can help to facilitate the hydrolysis of lignocellulosic in the first stage (Florian et al., 2013; Hagos et al., 2016).

Lignocellulosic biomass is hydrolyzed by hydrolytic bacteria to release saccharides for biomethane production. These microorganisms will bind to the lignocellulose surface through physical contact, and then secrete extracellular multi-enzyme complexes to initiate the hydrolysis. Accessible surface area is considered as an important factor for the biodegradability of lignocellulosic materials and the substrate should have enough pores for efficient hydrolysis (Karimi and Taherzadeh, 2016). Generally, the diameter of the pore ranged from 0.2 to 20 μm, which is similar to the size of the bacteria. During the anaerobic digestion progress, the accessible surface area will increase along with the removal of partial cell wall component, resulting in higher surface availability. However, enzymatic hydrolysis is usually faster at the beginning and slower in the latter stages (Vivekanand et al., 2014), indicating that the surface area is not the only controlling factor for the hydrolysis. At the initial stage, lager surface area allows sufficient contact between enzymes and digestible amorphous cellulose, resulting in faster hydrolysis. But in the later period of anaerobic digestion, even though the accessible surface area is increasing, the remaining higher crystalline cellulose and the compact structure become the main factors which finally limit the hydrolysis efficiency (Khodaverdi et al., 2012).

Cellulose Polymerization and Crystallinity

Degree of cellulose polymerization referring to the molecular weight of cellulose chains is an important factor affecting the enzymatic hydrolysis of cellulose. In the last few decades, many methods have been developed to give more accurate polymerization degree of cellulose (Hubbell and Ragauskas, 2010). It is known that the enzymatic hydrolysis of cellulose is the depolymerization process of cellulose by cellulase, which is directly related with cellulose polymerization degree. With the prominent reduction of cellulose polymerization degree from 247 to 151, steam explosion pretreatment yields 5–6 folds enhancements of enzymatic saccharification (Huang et al., 2015). Generally, more intramolecular hydrogen bond in long cellulose chains will hinder the cellulose conversion compared to shorter ones (Karimi and Taherzadeh, 2016). According to Waliszewska et al. (2018), the partial cellulose with lower polymerization was hydrolyzed preferentially in anaerobic digestion; resulting in the increase of cellulose polymerization degree after the methane fermentation process.

Cellulose crystallinity refers to the proportion of crystalline region of cellulose, which generally ranges from 30 to 80%. Hydrogen bonds and van der Waals forces are main acting forces to form crystalline structure (Zhang et al., 2013). Cellulose chains have different orientations, leading to three different levels of crystallinity including crystalline, sub-crystalline and amorphous forms. There are several crystalline and non-crystalline regions in microfibrils, however, no obvious boundary exists between different regions (Park et al., 2010). The crystallization zone is characterized by the good chain orientation, compact arrangement, high density and strong intermolecular bonding. The non-crystalline region is characterized by the poor chains orientation of cellulose, unordered molecular arrangement, large distance between molecules, low density and less hydrogen bonding between molecules (Park et al., 2010).Because of the

TABLE 1 | Biomethane production of selected lignocellulosic biomass.

Biomass	Inoculum	Operation conditions	Methane production	References
Hydrolysis lignin (lignin content of 80%) of Birch wood chips	CSTR[c] running with food waste and cow manure	37°C, 90 rpm, 39 days	125 mL CH_4/g VS	Mulat et al., 2018
Paper paste	Anaerobic sludge	Pretreated with cellulolytic microbial consortium, then pH 7.3, 55°C, 90 days	101 mL CH_4/g cellulose	Kinet et al., 2015
Rice straw	Anaerobic sludge	Fungal pretreatment, then SS-AD reactors, 37 ± 1°C for 45 days	152∼263 mL CH_4/g VS	Mustafa et al., 2016
Reed canary grass (Cultivated and wild)	Sewage sludge	35 ± 1°C, pH 7.0, 20∼40 days	Cultivated: 406 ± 21; Wild: 120 ± 16 mL CH_4/g VS	Oleszek et al., 2014
Miscanthus. *giganteus*	Mesophilic digestate	35°C, 90 days	285∼333 mL CH_4/g VS	Wahid et al., 2015
Miscanthus. *sinensis*	Mesophilic digestate	35°C, 90 days	291∼320 mL CH_4/g VS	Wahid et al., 2015
Switchgrass (WHS[a])	–	Different pretreatment (G[d], GA[e], GAA[f]), 35°C anaerobic fermentation for 38 days	G: 112.4 ± 8.4; GA: 132.5 ± 9.7; MA A:139.8 mL CH_4/g VS	Frigon et al., 2011
Switchgrass (SHS[b])	–	Different pretreatment (C[g], M[h], MA[i]), 35°C anaerobic fermentation for 36 days	C: 94.7 ± 4.4; M: 152.3 ± 1.2; MA: 256.6 ± 8.2 mL CH_4/g VS	Frigon et al., 2011
Barley	AD reactor digesting cattle slurry and grass silage	37°C, 35 days	314.8 mL CH_4/g VS	Himanshu et al., 2018
Wheat straw	Anaerobic sludge	Laccase, versatile peroxidase pretreatment, then 37°C anaerobic fermentation for 30 days	250.5 mL CH_4/g VS	Schroyen et al., 2015
Sunflower	Digestate	35°C, pH 8.1 ± 0.3, 30 days	210∼286.1 mL CH_4/g ODM[j]	Herrmann et al., 2016
Sorghum	Digestate	35°C, pH 8.1 ± 0.3, 30 days	298.9∼311.3 mL CH_4/ g ODM[j]	Herrmann et al., 2016
Corn straw	Biogas slurry	55°C and 5 ml/g O_2 pretreatment, then 37°C anaerobic fermentation	325.7 mL CH_4/g VS	Fu et al., 2015

[a] *WHS, winter harvested Switchgrass.*
[b] *SHS, summer harvested Switchgrass.*
[c] *CSTR, continuously stirred tank reactor.*
[d] *G, ground.*
[e] *GA, ground and alkalinization.*
[f] *GAA, ground, alkalinization and autoclaving.*
[g] *C, chopped.*
[h] *M, mulched.*
[i] *MA, mulched and alkalinization.*
[j] *ODM, organic dry matter.*

high endo-glucanase activity of cellulase with the amorphous (non-crystalline) region, cellulose crystallinity plays noticeable role in affecting initial hydrolysis of cellulose. The yield of monosaccharides decreased with the increased crystallinity of the substrate, indicating that amorphous domains are hydrolyzed first before the hydrolysis of crystalline parts (Zhe et al., 2017). Mirahmadi et al. (2010) found that alkaline pretreatment with NaOH resulted in the significant reduction of crystallinity, which improved enzymatic hydrolysis and led to 83 and 74% improvement in methane production from birch and spruce.

In order to understand the mechanism of impacts of cellulose crystallinity on cellulose hydrolysis, several functional quantitative models have been designed. Jeoh et al. (2017) pointed out that cellulose crystallinity greatly impacted the adsorption of cellobiohydrolase Cel7A (CBHI), which resulted in lower cellulase hydrolysis efficiency. Moreover, with constant concentration of adsorbed enzyme, the initial enzymatic hydrolysis rate decreased with increasing cellulose crystallinity, which means that cellulose crystallinity can also affect the effectiveness of adsorbed cellulase components (Hall et al., 2010). In addition, different cellulase components showed different capacities and activities of adsorption with various cellulose forms (Zhang and Lynd, 2004). For example, endoglucanase I showed greater capacity of adsorption than CBHI and its higher crystallinity resulted in increasing adsorption of a non-hydrolytic protein named fibril-forming protein from *Trichoderma reesei* (Ding and Xu, 2004).

Cellulose is the most important component of plant cell wall, and the negative effect of cellulose polymerization degree and cellulose crystallinity on enzymatic hydrolysis has been recognized as mentioned above. However, more investigation is needed regarding the various cellulose properties and parameters, e.g., changes of cellulose structure during fermentation process (Waliszewska et al., 2018), the cellulase

TABLE 2 | Biochemical composition of selected lignocellulosic biomass (w/w, %).

Biomass	Cellulose	Hemicellulose	Lignin	References
Sunflower stalk	31.0	15.6	29.2	Monlau et al., 2012
Barley straw	34.3	23.0	13.3	Saha and Cotta, 2010
Wheat straw	35.0	22.3	15.6	Boladorodríguez et al., 2016
Miscanthus	38.2	24.3	25.1	Vrije et al., 2002
Rice straw	38.6	19.7	13.6	Zhu et al., 2005
Pine	43.3	21.5	28.3	Florian et al., 2013
Polar	44.5	22.5	19.5	Florian et al., 2013
Corn straw	45.4	22.7	10.8	Fu et al., 2015
Spruce	45.5	22.9	27.9	Florian et al., 2013
Eucalyptus	54.1	18.4	21.5	Florian et al., 2013

adsorption and desorption (Yang et al., 2011), combined effect of cellulose and other cell wall properties (Jeoh et al., 2017).

Crosslinkages of Hemicellulose and Lignin

In contrast to cellulose, hemicellulose is a branched polysaccharide consisting of various sugar units. Xylan, the backbone chains of 1, 4-linked β-d-xylopyranose is the most abundant component of hemicellulose. The matrix properties of hemicellulose are complicated and significantly influenced by crosslinking agents (e.g., ferulic acid), monosaccharides characteristics and abundance of side chains (Somerville et al., 2004; Vogel, 2008).

It is generally believed that hemicellulose can increase the structural strength of plant cell wall and the space resistance, resulting in decreased hydrolysis efficiency. Pretreatment can effectively remove or dissolve lignin and hemicellulose, thereby increase the accessibility of the cellulose to microorganisms or enzymes (Hendriks and Zeeman, 2009). By carefully controlling the solids retention time, methane production can be enhanced from hemicellulose exclusively, while cellulose and lignin are left over in the residues. For anaerobic bioconversion of lignocellulose, hemicellulose was commonly removed earlier which decreased the structural obstacle degree for downstream enzymatic hydrolysis. Therefore, some result indicated that hemicelluloses were might be a positive factor to promote biomass digestibility by negatively affecting lignocellulosic recalcitrance. Our previous study suggested that the hemicellulose branch connected to the cellulose crystalline region and construct the non-crystalline region, thus positively reduce the crystallinity of cellulose, resulting in much more easy hydrolysis site and higher hydrolysis efficiency of cellulose consequently (Xu et al., 2012). Moreover, branched arabinose (Ara) might be an important influence factor, which could build interlinking (β-1, 4-glucans) to cellulose fibers to decrease cellulose crystallinity, and would improve the saccharification efficiency (Li et al., 2015). In a word, because of the complexity of hemicellulose structure and cross-linking between cell wall components, more research is still needed to carefully interpret the hemicellulose properties and its effect on methane production.

Lignin is a complex polymer of phenylpropane units that form a three-dimensional network inside the cell wall. It is generally considered to be the most important factor which limiting the biodegradability of lignocellulose. Studies have shown that 1% increase of lignin content would result in an average reduction of 7.49 L CH_4/kg total solid (Thomsen et al., 2014). Moreover, Triolo et al. (2012) found that the excess of lignin (>100 g/kg volatile solid) would result in notable lower methane yield. Lignin restricts the degradation of structural polysaccharides by hydrolytic enzymes, thereby limiting the bioconversion of lignocellulose (Ahring et al., 2015). Generally, two main mechanisms have been proposed to illustrate this phenomenon. First, lignin consolidates the cell wall structure by covalent linkages with other cell wall components, which increases space resistance and prevents the carbohydrate from enzymatic hydrolysis (Yuan et al., 2013). A comparison between woody materials and grass revealed that the higher abundant of covalent linking and the phenyl groups in lignin result in harder digestion in wood than grass (Ververis et al., 2004). Moreover, the lignin structural units also have influence in biomass degradation efficiency. A previous study reported that different contents of three lignin monolignols (Syringyl, Guaiacyl, and *p*-Hydroxyphenyl), syringyl/guaiacyl ratio and interlinked-phenolics could affect enzymatic digestion after NaOH and H_2SO_4 pretreatments (Li et al., 2014).

Another influence of lignin is its adsorption capacity to enzymes (Lu et al., 2016). Lignin can affect enzymatic hydrolysis by non-specific or non-productive adsorption of cellulase (Palonen et al., 2004). The adsorption of cellulase to lignin has been mediated by three mechanism: hydrogen bonding (Berlin et al., 2006), hydrophobic (Eriksson et al., 2002) and electrostatic interactions (Nakagame et al., 2011). In lignocellulose digestion progress, three types of interactions may be involved in the non-productive adsorption of cellulases to lignin. Most studies suggested that hydrophobic interaction is the major cause for non-productive adsorption of enzyme to lignin, while less attention has been paid on hydrogen bonding and electrostatic interactions. However, until now, it is difficult to point out which one is the dominant in the specific reaction because of complex structure of different substrate (Saini et al., 2016). Electrostatic action was a main factor influencing the adsorption of endo-beta-1, 4-glucanases and xylanase onto lignin, while hydrophobicity mainly affected the adsorption of cellobiohydrolases and β-Glucosidase onto lignin (Lu et al., 2016). Thermodynamic analysis of enzyme adsorption onto lignin indicated that the adsorption was a spontaneous process and higher temperature would accelerate the process (Tu et al., 2009). This provides enlightenment that the enzymatic hydrolysis should be conducted at as low temperature as possible to avoid cellulase adsorption with lignin.

Non-structural and Other Factors Restricting Lignocellulose Degradation

Besides physical and chemical characteristics of cell wall as mentioned above, there are also some other factors which may reduce lignocellulose biodegradation. For example,

TABLE 3 | Different factors constructing biomass recalcitrance.

Factors	Relative effects	References
Epidermal protection	The epidermal tissue of the plant body, particularly the bark, cuticle and epicuticular waxes	Greenshields et al., 2004; Zhao et al., 2012
Cellulose characteristic	High degree of CrI and DP of cellulose, challenges for enzymes acting on insoluble substrate	Himmel et al., 2007; Zhang et al., 2013
Chemical compositions	Heterogeneity and complexity of constituents, degree of lignification, and complexity of chemical cross-linkages	Karimi and Taherzadeh, 2016
Cell wall physical structure	Arrangement and density of the vascular bundles; the relative amount of sclerenchymatous tissue	Vogel, 2008; Zhang et al., 2013
Process-induced causes	Inhibitors are generated during conversion processes (e.g., cellulose realignment)	Himmel et al., 2007

bioconversion processes may generate some additional inhibitors or negative variation of cell wall structure. Reduction of article size to 0.36–0.55 mm and 0.71–1.0 mm could achieve lower methane yield when compared with size of 1.4–2.0 mm (Rubia et al., 2011). This result might be attributed to inhibitors (e.g., overproduction of volatile fatty acid) and chemical transformation generated from excessive particle size reduction. Moreover, delignification beyond 50% might cause collapse of cellulose matrix, resulting in compact and chaotic structure and subsequent decrease in cellulose accessibility (Zhu et al., 2008). In addition, the crystal structure of cellulose can be transformed. For example, alkali extraction can transform cellulose I to cellulose II, and cellulose II are antiparallel configuration which generally do not exist in the natural cell wall (Zhang et al., 2013). Such structural changes or hazardous substances caused by the pretreatment processes are additional inhibitors to anaerobic digestion, and should be taken into consideration as part of the biomass recalcitrance. But compared with the native structures and characteristics of the plant cell wall, these additional inhibitors are by-products of the process of cracking cell wall recalcitrance and are just minor contributors to restrict the fermentation efficiency. In the process of biomethane production from lignocellulose, the ideal process strategy is efficiently breaking down the lignocellulosic recalcitrance while minimizing the production of by-products.

STRATEGIES TO OVERCOME RECALCITRANCE FOR HIGHER BIOMETHANE PRODUCTION

Pretreatment prior to biomethane fermentation is an effective method to reduce the biomass recalcitrance and increase the accessibility in AD (Weiland, 2010). Recent years, many studies have provided various physical, chemical or biological pretreatments in the production of biomethane, and their major effects are summarized in **Table 4**.

Physical Pretreatment of Lignocellulose

Physical (mechanical) pretreatment refers to the pretreatment processes without chemicals or microorganisms, which includes comminution (e.g., milling and grinding), irradiation (e.g., ultrasound, gamma ray, and microwave), steam explosion, liquid hot water pretreatment and others.

Comminution is mainly used to reduce the particle size, which increases the accessible surface area, alters the ultrastructure, and reduces the cellulose crystallinity and polymerization degree of cellulose for improved digestibility (Kratky and Jirout, 2015). Generally, comminution is the most common pretreatment method and always the first step ahead of the whole biomethane production process. Biogas production would be increased with the reduction of particle size. However, to the different lignocellulose compositions of the various particle size ranges, excessive particle size reduction may produce inhibitors and decrease biogas production (Rubia et al., 2011). Therefore, particle size should be carefully considered when different lignocellulose substrate was employed. Irradiation could preferentially dissociate the glucoside bonds of the cellulose and degrade cellulose chains into brittle fibers, oligosaccharides, or even cellobiose. Siddique et al. (2017) found that microwave and ultrasonic pre-treatments on the waste sludge resulted in supplementary 53 and 25% enhancement of biomethane, respectively. However, some research reported that excessive microwave pretreatment at high temperature may have adverse effect on methane yield due to the side effect of heat-induced inhibitors, such as phenolic compounds and furfural (Li et al., 2012). Steam explosion has been used to treat various kinds of lignocellulosic biomass for enhancement of methane production. After steam explosion, hemicellulose was hydrolyzed and lignin was reduced to a certain degree, thus resulting in degradation of lignin-carbohydrate complexes (Zhou et al., 2016). Moreover, steam explosion is often facilitated by additional acids, such as 6% SO_2 (Vivekanand et al., 2014), diluted H_2SO_4 (Huang et al., 2015), and other chemicals. Liquid hot water pretreatment can enlarge the accessible surface area of substrate for higher cellulose degradability to cellulase. Under high temperature and pressure, water can penetrate into the interior of cell wall structure, solubilize hemicellulose, slightly remove lignin and hydrate cellulose. This method causes less corrosion to reactors and produces little amounts of byproducts and inhibitors, thereby has considerable potential of pentose recovery (Monlau et al., 2012; Yu et al., 2013).

Chemical Pretreatment of Lignocellulose

Chemical pretreatment refers to the use of chemicals (e.g., acids, bases, oxidizing agents, organic solvents) to change physical and chemical characteristics of native lignocellulose.

TABLE 4 | Conventional pretreatments and notable effects.

Pretreatment	Notable effects	References
Grining/milling	Size reduction, larger surface area and pore size, lower crystallinity	Kratky and Jirout, 2015
Irradiation	Cleavage of chemical bonds, lager surface area	Siddique et al., 2017
Steam explosion	Increase of surface area and pore size, solubilization of hemicellulose	Zhou et al., 2016
Liquid hot water	Lager surface area, solubilization of hemicellulose	Yu et al., 2013
Alkali	Cleavage of lignin, dissolution of hemicellulose, increase of internal surface area, reduction of polymerization	Boladorodríguez et al., 2016
Acid	Hydrolysis of hemicellulose, alteration of cellulose structure, larger surface area	Zhou et al., 2014
Oxidizing agents	Removal of hemicellulose and lignin, increase of cellulose accessibility	Florian et al., 2013
Organic solvent	Solubilization of hemicellulose or lignin, larger surface area	Zheng et al., 2014
Ammonia fiber explosion	Solubilization of lignin, disruption of LCC structure, increase of cellulose accessibility	Huang et al., 2015; Zhou et al., 2016
Ionic liquids	Solubilization of cellulose, reduction of crystallinity	Xu et al., 2016; Cao et al., 2017
Fungal	Delignification and partial hydrolysis of hemicellulose, alteration of LCC structure	Kudanga and Roes-Hill, 2014

It has attracted the most research interest because of its higher efficiency on decreasing the resistant characteristics for better bioconversion performance. The positive effects of conventional chemical pretreatments are summarized in **Table 4** and discussed below.

Acid pretreatment can prominently hydrolyze hemicellulose to mono saccharides, which will increase the pore size or volume of cell wall and make cellulose more susceptible to enzymatic degradation (Zhou et al., 2014). It can also disrupt lignin to a high degree, but only can dissolve little lignin in most cases. Considering the cost, toxicity by-products and equipment requirements, dilute acid is usually used for pretreatment in practical applications (Mussoline et al., 2013). Alkali is another popular pretreatment method. The function of alkali is believed to be two important effects: saphonication and solvation of lignin-carbohydrate linkages, which result in the enlargement and decrystallization of substrates (Van der Pol et al., 2014). The solvation can significantly remove lignin, acetyl groups and uronic acid of hemicellulose, which disrupts the lignin structure and breaks down the intramolecular bonds between lignin and other components. Therefore, the effectiveness of alkali pretreatment is associated closely with lignin content of lignocellulosic feedstock. Compared with traditional chemicals, ionic liquids possess some advantages of low toxicity, thermal stability, low hydrophobicity, enhanced electrochemical stability and so on. It has been proven to be positive on the improvement of biofuel production (Cao et al., 2017). During the pretreatment, ionic liquid can dissolve large amount of cellulose at mild conditions, and it is feasible to recover almost 100% of used liquid with high purity and leave little residues for the downstream anaerobic fermentation. The dissolution mechanism of cellulose in ionic liquids is the chemical interaction between its molecules and the oxygen and hydrogen atoms of cellulose hydroxyl groups (Xu et al., 2016). In the interaction, separation of oxygen and hydrogen atoms results in the opening of the hydrogen bonds between cellulose chains, which leads to the dissolution of cellulose (Feng and Chen, 2008). Then, dissolved cellulose can be regenerated by adding some specific chemical solvents which can precipitate cellulose from ionic liquid, such as ethanol, methanol, acetone, or water. The p mrecipitates have a higher enzymatic digestibility than native cellulose due to the changes in macro- and micro-structures. Crystallinity analysis of dissolved lignocellulose showed that the cellulose precipitates are different with either amorphous cellulose or cellulose II (Wahlstrom and Suurnakki, 2015).

Biological Pretreatment of Lignocellulose

Biological pretreatment can be classified into three categories including fungal, microbial consortium and enzymatic pretreatment (Wei, 2016). Fungus has two specific systems including oxidative lignolytic system which exclusively attacks the phenyl bonds in lignin, and the hydrolytic enzyme system which degrades cellulose and hemicellulose. This pretreatment specifically degrades lignin, resulting in enhanced digestibility of cellulose (Kudanga and Roes-Hill, 2014). Cellulose is more recalcitrant to fungal attack than other components. Degradation of lignin and hemicellulose result in increased digestibility of cellulose, which is preferred for the following anaerobic fermentation. Microbial consortium pretreatment is conducted by microbes screened from natural environments in which rotten lignocellulosic biomass is the substrate. It is a complex microbial agent containing yeast and cellulolytic bacteria, heat-treated sludge, clostridium thermocellum, and mixture of fungi and composting microbes (Zhang et al., 2011). In contrast to fungal pretreatment, microbial consortium usually has high cellulose- and hemicellulose-degradation ability which mainly degrade cellulose and hemicellulose. Compared with physical and chemical pretreatment, the above two biological methods usually conducted in mild conditions which required far lower energy and chemicals input, and generated scarcely any inhibitors. However, the long pretreatment time limited the use of these processes in commercial applications. In addition, another important issue should be considered is that certain levels of carbohydrates are required by microbes during biological pretreatment, which resulted the competition between pretreatment and downstream biomethane production.

Therefore, one major objective of biological pretreatment is to minimize the loss of carbohydrates and maximize the lignin removal. Enzymatic pretreatment prior to or in anaerobic digestion usually employs pure enzymes to accelerate the degradation of lignocellulose. The most commonly used enzymes mainly included cellulase, hemicellulose, and lignin-degrading enzyme, such as laccases and manganese peroxidase (Wei, 2016). These enzymes will help to release fermentable sugars from cellulose and hemicellulose to promote biomethane production from lignocellulosic biomass. However, the effect of enzymes in enhancing biogas production was minimal in most cases, and the cost of enzymes was high (Romano et al., 2011). Therefore, the application of enzymatic pretreatment has been limited.

Pretreatments have been proven to decrease the recalcitrance of native lignocellulose to obtain higher biomethane production. Generally, every pretreatment method has its major effect on different chemical or physical characteristics of the recalcitrance. Such as increasing accessible surface area, reducing crystallinity and polymerization, removing lignin content and so on (**Table 4**). However, all of these have the positive effect on the accessible area of lignocellulose. Therefore, grinding or milling is the most common first step for all pretreatment in biomethane production. Due to the complexity of lignocellulose chemical structures and different fermentation processes, the selection of pretreatment technologies must consider several factors, e.g., the type of lignocellulosic biomass, void the formation of by-products that are inhibitory to microorganisms, the downstream biological conversion processes, and the cost of pretreatment.

Cell Wall Modification and Genetically Engineered Plants

Besides previous studies on pretreatment methods and management of anaerobic fermentation, some researches focusing on plant cell wall modification and even energy crops. Recently, performance of energy crops under various management practices has been extensively discussed elsewhere (Knoll et al., 2015; Cole et al., 2017). There are some strategies can be applied to modify plant cell wall *in vivo*, such as modification or interference of key enzymes in the biosynthesis pathways, expression of heterologous proteins or enzymes. These plant cell wall artificial modification would change the native biomass characteristics and got desired substrate (Vermerris and Abril, 2015). Li et al. (2018) over-expressed *Trichoderma reesei* β-1,4-D-glucosidasein the cell walls, and this significantly increased biomass porosity and reduced cellulose features (crystallinity or polymerization degree), resulting in enhanced biomass enzymatic hydrolysis. Fan et al. (2017) demonstrated that AtCesA8 -driven OsSUS3 expression in transgenic rice could reduce cellulose crystallinity and increase cell wall thickness, resulting in improved biomass saccharification. Another report found that lasalocid sodium pretreatment on *Arabidopsis* could upregulate type III peroxidase genes and change the cellular arrangement of hypocotyls, resulting in enhanced enzymatic saccharification (Okubo-kurihara et al., 2016). Moreover, research about synthesis and assembly mechanism of cellulose and hemicellulose provide great possibility to control and alter these processes in ways that would render the cell walls more easily. It can help to get better hydrolysis efficiency and considerable reduction of costly enzymes.

Compared to pretreatment, cell wall artificial modification or genetic engineered plants has more advantages because it does not require additional energy or chemicals input, produces fewer toxic by-products and causes less pollution to environment. At present, these researches have made some progress in improvement of bioethanol production. It is capable to create the desired breakthrough to overcome biomass recalcitrance. However, there are very limited studies on the changes in quality or composition of plant cell wall of tropical energy crops. An in-depth understanding of the precise plant cell wall structure and identification of the key affecting factors are still needed for optimizing the conversion of lignocellulosic biomass to biomethane in the future.

Process Controlling and Optimization of Anaerobic Fermentation Process

Compared to mono-digestion, co-digestion of lignocellulose with animal feces shows significant potential for commercial biomethane production (Giuliano et al., 2013; Wei et al., 2014). Wang et al. (2017) reported 256.57 mL/g volatile solids methane was produced through the co-digestion of corn stalk and pig manure, which was increased by 17.4% than that using corn stalk mono-digestion. The higher efficiency of co-digestion mainly associated with process stability, e.g., optimal C/N ratio, ammonia reduction, and essential trace elements, which help maintain a steady condition for better performance of microorganisms to break down lignocellulose recalcitrance (Siddique and Wahid, 2018). Moreover, microbial reinforcement is another promising option to enhance enzymatic hydrolysis of lignocellulose and improve the biogas yield. Zhang et al. (2015) utilized 10% inoculation of *Acetobacteroides hydrogenigenes* as reinforcement, and got 19–23% increase of methane yield finally. Due to abundant enzymes (e.g., cellulase and xylanase) and sufficient nutrient content, digested manures have better adaptability in digesting lignocellulose for higher biomethane production (Gu et al., 2014). There are some basic requirements for anaerobic microorganism those degrade the particular lignocellulose in terms of environmental conditions and feed compositions inside the reactor (Mao et al., 2015). Different from pretreatment and cell wall modification, process optimization is an indirect strategy, which aims to provide a more reasonable environment for anaerobic bacteria to grow better and secrete more relevant enzymes to degrade lignocellulose more efficiently. For example, thermophilic microaerobic pretreatment (oxygen loads of 5 ml/g volatile solids substrate) on corn straw could promote the growth of aerobic microorganisms which secreted more hydrolytic enzymes in the early stage of the fermentation process. These enzymes would decrease cellulose crystallinity and cause substantial

structural disruption of plant cell wall, which finally resulted in 16.24% higher methane production than that of untreated (Fu et al., 2015).

CONCLUSIONS AND FUTURE PERSPECTIVES

Lignocellulose substrate shows great potential for biomethane production. Due to the inherent complicated recalcitrance of the plant cell wall, lignocellulosic biomass cannot be efficiently utilized during anaerobic digestion process. Generally, the direct factor affecting hydrolysis of biomass is the accessible surface area which is constructed by its chemical compositions that build a spatial network as a protection barrier. It plays more important role in reducing the initial enzymatic hydrolysis by limiting the substrate accessibility to enzymes or chemical regents. During the anaerobic digestion progress, accessible surface area will increase along with the removal of partial cell wall components, resulting in higher surface availability. Then the indirect factors such as chemical compositions (lignin, hemicelluloses, and acetyl group), and cellulose structure-relevant factors (cellulose crystallinity and polymerization degree), will play more important role in restricting the decomposition of substrate. As cross-linked polysaccharide networks, different influencing factors are not isolated, but closely related to each other and have synergetic impact on bioconversion. Although much is known about the structure of the plant cell wall and recalcitrance, there are still some fundamental questions that need further investigation, especially for the decomposition process in anaerobic digestion.

In the view of current knowledge, current strategies have positive contribution to improve biomethane production from lignocellulose. Pretreatment is still the most effective way to overcome the biomass recalcitrance, and selection of proper pretreatment method is very crucial for commercial biomethane production. However, high energy input and cost requirements of decomposing biomass recalcitrance are the main limitations. Cost-effective production of biomethane from lignocellulosic feedstocks depends much on significant improvement in both biomass quality and conversion efficiency. So, further studies should focus much more on investigating the relationship between the precise structure of cell wall recalcitrance and the key factor affecting the anaerobic digestion progress, which will be used to explore new methods to improve the biomethane production. Recently, some researches indicated that plant cell wall modification and artificial energy croup are fascinating strategies, which can improve quality, quantity and digestibility of traditional biomass material. With the development of biotechnology, transgenic plant may will be frequently applied in the anaerobic digestion system for biomethane production.

AUTHOR CONTRIBUTIONS

NX, SL, and JZ wrote the paper. FX and HJ provided the literature and data. JX, MJ, and WD contributed to the writing of the paper and the overall paper design.

FUNDING

This work was financially supported by National Key Research and Development Program of China (2018YFA0902200), the National Natural Science Foundation of China (No. 31700092), the Natural Science Foundation of Jiangsu Province (BK20170997), the project of State Key Laboratory of Materials-Oriented Chemical Engineering (ZK201601, KL17-09), the China Postdoctoral Innovative Talents Support Program (BX20180140), the China Postdoctoral Science Foundation (2018M642238), the Jiangsu Synergetic Innovation Center for Advance Bio-Manufacture, the open foundation of Jiangsu Key Laboratory for Biomass-Based Energy and Enzyme Technology (BEETKB1801).

REFERENCES

Ahring, B. K., Biswas, R., Ahamed, A., Teller, P. J, and Uellendahl, H. (2015). Making lignin accessible for anaerobic digestion by wet-explosion pretreatment. *Bioresour. Technol.* 175, 182–188. doi: 10.1016/j.biortech.2014.10.082

Arantes, V., and Saddler, J. N. (2011). Cellulose accessibility limits the effectiveness of minimum cellulase loading on the efficient hydrolysis of pretreated lignocellulosic substrates. *Biotechnol. Biofuels* 4, 1–17. doi: 10.1186/1754-6834-4-3

Berlin, A., Balakshin, M., Gilkes, N., Kadla, J., Maximenko, V., Kubo, S., et al. (2006). Inhibition of cellulase, xylanase and beta-glucosidase activities by softwood lignin preparations. *J. Biotechnol.* 125, 198–209. doi: 10.1016/j.jbiotec.2006.02.021

Boladorodríguez, S., Toquero, C., Martínjuárez, J., Travaini, R., and Garcíaencina, P. A. (2016). Effect of thermal, acid, alkaline and alkaline-peroxide pretreatments on the biochemical methane potential and kinetics of the anaerobic digestion of wheat straw and sugarcane bagasse. *Bioresour. Technol.* 201, 182–190. doi: 10.1016/j.biortech.2015.11.047

Cao, Y., Zhang, R., Cheng, T., Guo, J., Xian, M., and Liu, H. (2017). Imidazolium-based ionic liquids for cellulose pretreatment: recent progresses and future perspectives. *Appl. Microbiol. Biotechnol.* 101, 1–12. doi: 10.1007/s00253-016-8057-8

Cole, M. R., Eggleston, G., Petrie, E., Uchimiya, S. M., and Dalley, C. (2017). Cultivar and maturity effects on the quality attributes and ethanol potential of sweet sorghum. *Biomass Bioenerg.* 96, 183–192. doi: 10.1016/j.biombioe.2016.12.001

Ding, H., and Xu, F. (2004). Productive cellulase adsorption on cellulose. *ACS Symp. Ser.* 889, 154–169. doi: 10.1021/bk-2004-0889.ch009

Eriksson, T., Börjesson, J., and Tjerneld, F. (2002). Mechanism on surfactant effect in enzymatic hydrolysis of lignocellulose. *Enzym. Microb. Tech.* 31, 353–364. doi: 10.1016/s0141-0229(02)00134-5

Fan, C. F., Feng, S. Q., Huang, J. F., Wang, Y. T., Wu, L. M., Li, X. K., et al. (2017). *Atcesa*8-driven *OsSUS3* expression leads to largely enhanced biomass saccharification and lodging resistance by distinctively altering lignocellulose features in rice. *Biotechnol. Biofuels* 10:221. doi: 10.1186/s13068-017-0911-0

Feng, L., and Chen, Z. L. (2008). Research progress on dissolution and functional modification of cellulose in ionic liquids. *J. Mol. Liq.* 142, 1–5. doi: 10.1016/j.molliq.2008.06.007

Florian, M., Abdellatif, B., Eric, T., Claire, D., JeanPhilippe, S., and Hélène, C. (2013). Lignocellulosic materials into biohydrogen and biomethane: impact of structural features and pretreatment. *Crit. Rev. Env. Sci. Technol.* 43, 260–322. doi: 10.1080/10643389.2011.604258

Frigon, J. C., and Guiot, S. R. (2010). Biomethane production from starch and lignocellulosic crops: acomparative review. *Biofuels Bioprod. Bioresour.* 4, 447–458. doi: 10.1002/bbb.229

Frigon, J. C., Mehta, P., and Guiot, S. R. (2011). Impact of mechanical, chemical and enzymatic pre-treatments on the methane yield from the anaerobic digestion of switchgrass. *Biomass Bioenerg.* 36, 1–11. doi: 10.1016/j.biombioe.2011.02.013

Fu, S. F., Wang, F., Yuan, X. Z., Yang, Z. M., Luo, S. J., Wang, C. S., et al. (2015). The thermophilic (55°C) microaerobic pretreatment of corn straw for anaerobic digestion. *Bioresour. Technol.* 175, 203–208. doi: 10.1016/j.biortech.2014.10.072

Giuliano, A., Bolzonella, D., Pavan, P., Cavinato, C., and Cecchi, F. (2013). Co-digestion of livestock effluents, energy crops and agro-waste: feeding and process optimization in mesophilic and thermophilic conditions. *Bioresour. Technol.* 128, 612–618. doi: 10.1016/j.biortech.2012.11.002

Greenshields, D. L., Liu, G. S., Selvaraj, G., and Wei, Y. D. (2004). New insights in to ancient resistance: the molecular side of cell wall appositions. *Phytoprotection* 85, 49–52. doi: 10.7202/008907ar

Grosser, A. (2017). The influence of decreased hydraulic retention time on the perfor-mance and stability of co-digestion of sewage sludge with grease trap sludge andorganic fraction of municipal waste. *J. Environ. Manag.* 203, 1143–1157. doi: 10.1016/j.jenvman.2017.04.085

Gu, Y., Chen, X., Liu, Z., Zhou, X., and Zhang, Y. (2014), Effect of inoculum sources on the anaerobic digestion of rice straw. *Bioresour. Technol.* 158, 149–155. doi: 10.1016/j.biortech.2014.02.011

Hagos, K., Zong, J., Li, D., Liu, C., and Lu, X. H. (2016). Anaerobic co-digestion process for biogas production: progress, challenges and perspectives. *Renew. Sust. Energ. Rev.* 76, 1485–1496. doi: 10.1016/j.rser.2016.11.184

Hall, M., Bansal, P., Lee, J. H., Realff, M. J., and Bommarius, A. S. (2010). Cellulose crystallinity-a key predictor of the enzymatic hydrolysis rate. *FEBS. J.* 277, 1571–1582. doi: 10.1111/j.1742-4658.2010.07585.x

Hendriks, A. T., and Zeeman, G. (2009). Pretreatments to enhance the digestibility of lignocellulosic biomass. *Bioresour. Technol.* 100, 10–18. doi: 10.1016/j.biortech.2008.05.027

Herrmann, C., Idle, C., and Heiermann, M. (2016). Biogas crops grown in energy crop rotations: linking chemical composition and methane production characteristics. *Bioresour. Technol.* 206, 23–35. doi: 10.1016/j.biortech.2016.01.058

Himanshu, H., Murphy, J. D., Grant, J., O'Kiely, P. (2018). Synergies from co-digesting grass or clover silages with cattle slurry in in vitro batch anaerobic digestion. *Renew. Energ.* 127, 474–480. doi: 10.1016/j.renene.2018.04.086

Himmel, M. E., Ding, S. Y., Johnson, D. K., Adney, W. S., Nimlos, M. R., Brady, J. W., et al. (2007). Biomass recalcitrance: engineering plants and enzymes for biofuels production. *Science* 315, 804–807. doi: 10.1126/science.1137016

Huang, Y., Wei, X. Y., Zhou, S. G., Liu, M. Y., Tu, Y. Y., Li, A., et al. (2015). Steam explosion distinctively enhances biomass enzymatic saccharification of cotton stalks by largely reducing cellulose polymerization degree in *G. barbadense* and *G. hirsutum*. *Bioresour. Technol.* 181, 224–230. doi: 10.1016/j.biortech.2015.01.020

Hubbell, C. A., and Ragauskas, A. J. (2010). Effect of acid-chlorite delignification on cellulose degree of polymerization. *Bioresour. Technol.* 101, 7410–7415. doi: 10.1016/j.biortech.2010.04.029

Jeoh, T., Cardona, M. J., Karuna, N., Mudinoor, A. R., and Nill, J. (2017). Mechanistic kinetic models of enzymatic cellulose hydrolysis-a review. *Biotechnol. Bioeng.* 114, 1369–1385. doi: 10.1002/bit.26277

Karimi, K., and Taherzadeh, M. J. (2016). A critical review on analysis in pretreatment of lignocelluloses: degree of polymerization, adsorption/desorption and accessibility. *Bioresour. Technol.* 203, 348–356. doi: 10.1016/j.biortech.2015.12.035

Khodaverdi, M., Jeihanipour, A., Karimi, K., and Taherzadeh, M. J. (2012). Kinetic modeling of rapid enzymatic hydrolysis of crystalline cellulose after pretreatment by NMMO. *J. Ind. Microbiol. Biotechnol.* 39, 429–438. doi: 10.1007/s10295-011-1048-y

Kinet, R., Destain, J., Hiligsmann, S., Thonart, P., Delhalle, L., Taminiau, B., et al. (2015). Thermophilic and cellulolytic consortium isolated from composting plants improves anaerobic digestion of cellulosic biomass: toward a microbial resource management approach. *Bioresour. Technol.* 189, 138–144. doi: 10.1016/j.biortech.2015.04.010

Knoll, J. E., Johnson, J. M., Huang, P., Lee, R. D., and Anderson, W. F. (2015). Effects of delayed winter harvest on biomass yield and quality of Napiergrass and Energycane. *Biomass Bioenerg.* 80, 330–337. doi: 10.1016/j.biombioe.2015.06.018

Kratky, L., and Jirout, T. (2015). Biomass size reduction machines for enhancing biogas production. *Chem. Eng. Technol.* 34, 391–399. doi: 10.1002/ceat.201000357

Kudanga, T., and Roes-Hill, M. L. (2014), Laccase applications in biofuels production: current status and future prospects. *Appl. Microbiol. Biotechnol.* 98, 6525–6542. doi: 10.1007/s00253-014-5810-8

Li, F. C., Zhang, M. L., Guo, K., Hu, Z., Zhang, R., Feng, Y. Q., et al. (2015). High-level hemicellulosic arabinose predominately affects lignocellulose crystallinity for genetically enhancing both plant lodging resistance and biomass enzymatic digestibility in rice mutants. *Plant Biotechnol. J.* 13, 514–525. doi: 10.1111/pbi.12276

Li, L. H., Kong, X. Y., Yang, F. Y., Dong, L., Yuan, Z. H., and Sun, Y. M. (2012). Biogas production potential and kinetics of microwave and conventional thermal pretreatment of grass. *App. Biochem. Biotechnol.* 166, 1183–1191. doi: 10.1007/s12010-011-9503-9

Li, Y., Liu, P., Huang, J. F., Zhang, R., Hu, H. Z., Feng, S. Q., et al. (2018). Mild chemical pretreatments are sufficient for bioethanol production in the transgenic glucosidase-overproduced rice straw. *Green Chem.* 20, 2047–2056. doi: 10.1039/C8GC00694F

Li, Z. R., Zhao, C. Q., Zha, Y., Wan, C., Si, S. L., Liu, F., et al. (2014). The minor wall-networks between monolignols and interlinked-phenolics predominantly affect biomass enzymatic digestibility in miscanthus. *PLoS ONE* 9, 105–115. doi: 10.1371/journal.pone.0105115

Lu, X., Zheng, X., Li, X., and Jian, Z. (2016). Adsorption and mechanism of cellulase enzymes onto lignin isolated from corn stover pretreated with liquid hot water. *Biotechnol. Biofuels* 9:118. doi: 10.1186/s13068-016-0531-0

Mao, C. L., Feng, Y. Z., Wang, X. J., and Ren, G. X. (2015). Review on research achievements of biogas from anaerobic digestion. *Renew. Sust. Energy Rev.* 45, 540–555. doi: 10.1016/j.rser.2015.02.032

Mirahmadi, K., Kabir, M. M., Jeihanipour, A., Karimi, K., and Taherzadeh, M. J. (2010). Alkaline pretreatment of spruce and birch to improve bioethanol and biogas production. *Bioresources* 5, 928–938. doi: 10.1007/s00226-009-0268-z

Monlau, F., Barakat, A., Steyer, J. P., and Carrere, H. (2012). Comparison of seven types of thermo-chemical pretreatments on the structural features and anaerobic digestion of sunflower stalks. *Bioresour. Technol.* 120, 241–247. doi: 10.1016/j.biortech.2012.06.040

Mulat, D. G., Dibdiakova, J., and Horn, S. J. (2018). Microbial biogas production from hydrolysis lignin: insight into lignin structural changes. *Biotechnol. Biofuels* 11:61. doi: 10.1186/s13068-018-1054-7

Mussoline, W., Esposito, G., Giordano, A., and Lens, P. (2013). The anaerobic digestion of rice straw: a review. *Crit. Rev. Environ. Sci. Technol.* 43, 895–915. doi: 10.1080/10643389.2011.627018

Mustafa, A. M., Poulsen, T. G., and Sheng, K. (2016). Fungal pretreatment of rice straw with pleurotus ostreatus, and trichoderma reesei, to enhance methane production under solid-state anaerobic digestion. *Appl. Energy* 180, 661–671. doi: 10.1016/j.apenergy.2016.07.135

Nakagame, S., Chandra, R. P., Kadla, J. F., and Saddler, J. N. (2011). The isolation, characterization and effect of lignin isolated from steam pretreated douglas-fir on the enzymatic hydrolysis of cellulose. *Bioresour. Technol.* 102, 4507–4517. doi: 10.1016/j.biortech.2010.12.082

Okubo-kurihara, E., Ohtani, M., Kurihara, Y., Kakegawa, K., Kobayashi, M., Nagata, N., et al. (2016). Modification of plant cell wall structure accompanied by enhancement of saccharification efficiency using a chemical, lasalocid sodium. *Sci. Rep.* 6:34602. doi: 10.1038/srep34602

Oleszek, M., Król, A., Tys, J., Matyka, M., and Kulik, M. (2014). Comparison of biogas production from wild and cultivated varieties of reed canary grass. *Bioresour. Technol.* 156, 303–306. doi: 10.1016/j.biortech.2014.01.055

Palonen, H., Tjerneld, F., Zacchi, G., and Tenkanen, M. (2004). Adsorption of *Trichoderma reesei* CBH I and EG II and their catalytic domains on steam pretreated softwood and isolated lignin. *J. Biotechnol.* 107, 65–72. doi: 10.1016/j.jbiotec.2003.09.011

Park, S., Baker, J. O., Himmel, M. E., Parilla, P. A., and Johnson, D. K. (2010). Cellulose crystallinity index: measurement techniques and their

impact on interpreting cellulase performance. *Biotechnol. Biofuels* 3:10. doi: 10.1186/1754-6834-3-10

Park, S., Venditti, R. A., Jameel, H., and Pawlak, J. J. (2006). Changes in pore size distribution during the drying of cellulose fibers as measured by differential scanning calorimetry. *Carbohydr. Polym.* 66, 97–103. doi: 10.1016/j.carbpol.2006.02.026

Patinvoh, R. J., Osadolor, O. A., Chandolias, K., Sárvári, H. I., and Taherzadeh, M. J. (2017). Innovative pretreatment strategies for biogas production. *Bioresour. Technol.* 224, 13–24. doi: 10.1016/j.biortech.2016.11.083

Paudel, S. R., Banjara, S. P., Choi, O. K., Park, K. Y., Kim, Y. M., and Lee, J. W. (2017). Pretreatment of agricultural biomass for anaerobic digestion: current state and challenges. *Bioresour. Technol.* 245, 1194–1205. doi: 10.1016/j.biortech.2017.08.182

Romano, R. T., Zhang, R. H., Teter, S., and McGarvey, J. A. (2011). The effect of enzyme addition on anaerobic digestion of jose tall wheat grass. *Bioresour. Technol.* 100, 4564–4571. doi: 10.1016/j.biortech.2008.12.065

Rubia, M. A. D. L., Fernández-Cegrí, V., Raposo,. F., and Borja,. R. (2011). Influence of particle size and chemical composition on the performance and kinetics of anaerobic digestion process of sunflower oil cake in batch mode. *Biochem. Eng. J.* 58–59, 162–167. doi: 10.1016/j.bej.2011.09.010

Saha, B. C., and Cotta, M. A. (2010). Comparison of pretreatment strategies for enzymatic saccharification and fermentation of barley straw to ethanol. *New Biotechnol.* 27, 10–16. doi: 10.1016/j.nbt.2009.10.005

Saini, J. K., Patel, A. K., Adsul, M., and Singhania, R. R. (2016). Cellulase adsorption on lignin: a roadblock for economic hydrolysis of biomass. *Renew. Energy* 98, 29–42. doi: 10.1016/j.renene.2016.03.089

Sawatdeenarunat, C., Nguyen, D., Surendra, K. C., Shrestha, S., Rajendran, K., Oechsner, H., et al. (2016). Anaerobic biorefinery: current status, challenges, and opportunities. *Bioresour. Technol.* 215, 304–313. doi: 10.1016/j.biortech.2016.03.074

Schroyen, M., Vervaeren, H., Vandepitte, H., Van Hulle, S. W., and Raes, K. (2015). Effect of enzymatic pretreatment of various lignocellulosic substrates on production of phenolic compounds and biomethane potential. *Bioresour. Technol.* 192, 696–702. doi: 10.1016/j.biortech.2015.06.051

Siddique, M. N. I., Munaim, M. S. A., and Wahid, Z. B. A. (2017). The combined effect of ultrasonic and microwave pre-treatment on bio-methane generation from co-digestion of petrochemical wastewater. *J. Clean. Prod.* 145, 303–309. doi: 10.1016/j.jclepro.2017.01.061

Siddique, M. N. I., and Wahid, Z. A. (2018). Achievements and perspectives of anaerobic co-digestion: a review. *J. Clean. Prod.* 194, 359–371. doi: 10.1016/j.jclepro.2018.05.155

Somerville, C., Bauer, S., Brininstool, G., Facette, M., Hamann, T., Milne, J., et al. (2004). Toward a systems approach to understanding plant cell walls. *Science* 306, 2206–2211. doi: 10.1126/science.1102765

Surendra, K. C., Ogoshi, R., Zaleski, H. M., Hashimoto, A. G., and Khanal, S. K. (2018). High yielding tropical energy crops for bioenergy production: effects of plant components, harvest years and locations on biomass composition. *Bioresour. Technol.* 251, 218–229. doi: 10.1016/j.biortech.2017.12.044

Thomsen, S.T., Spliid, H., and Østergård, H. (2014). Statistical prediction of biomethane potentials based on the composition of lignocellulosic biomass. *Bioresour. Technol.* 154, 80–86. doi: 10.1016/j.biortech.2013.12.029

Triolo, J. M., Pedersen, L., Qu, H., and Sommer, S. G. (2012). Biochemical methane potential and anaerobic biodegradability of non-herbaceous and herbaceous phytomass in biogas production. *Bioresour. Technol.* 125, 226–232. doi: 10.1016/j.biortech.2012.08.079

Tu, M., Pan, X., and Saddler, J. N. (2009). Adsorption of cellulase on cellulolytic enzyme lignin from lodgepole pine. *J. Agr. Food. Chem.* 57, 7771–7778. doi: 10.1021/jf901031m

Van der Pol, E. C., Bakker, R. R., Baets, P., and Eggink, G. (2014). By-products resulting from lignocellulose pretreatment and their inhibitory effect on fermentations for (bio)chemicals and fuels. *Appl. Microbiol. Biotechnol.* 98, 9579–9593. doi: 10.1007/s00253-014-6158-9

Vermerris, W., and Abril, A. (2015). Enhancing cellulose utilization for fuels and chemicals by genetic modification of plant cell wall architecture. *Curr. Opin. Biotechnol.* 32, 104–112. doi: 10.1016/j.copbio.2014.11.024

Ververis, C., Georghiou, K., Christodoulakis, N., Santas, P., and Santas, R. (2004). Fiber dimensions, lignin and cellulose content of various plant materials and their suitability for paper production. *Ind. Crop. Prod.* 19, 245–254. doi: 10.1016/j.indcrop.2003.10.006

Vivekanand, V., Olsen, E. F., Eijsink, V. G., and Horn, S. J. (2014). Methane potential and enzymatic saccharification of steam-exploded bagasse. *Bioresources* 9, 1311–1324. doi: 10.15376/biores.9.1.1311-1324

Vogel, J. (2008). Unique aspects of the grass cell wall. *Curr. Opin. Plant. Biol.* 11, 301–307. doi: 10.1016/j.pbi.2008.03.002

Vrije, T. D., Haas, G. G. D, Tan, G. B., Keijsers, E. R. P., and Claassen, P. A. M. (2002). Pretreatment of *Miscanthus* for hydrogen production by *Thermotoga elfii*. *Int J. Hydrogen Energ.* 27, 1381–1390. doi: 10.1016/s0360-3199(02)00124-6

Wahid, R., Nielsen, S. F., Hernandez, V. M., Ward, A. J., Gislum, R., Jørgensen, U., et al. (2015). Methane production potential from *Miscanthus* sp.: effect of harvesting time, genotypes and plant fractions. *Biosyst. Eng.* 133, 71–80. doi: 10.1016/j.biosystemseng.2015.03.005

Wahlstrom, R. M., and Suurnakki, A. (2015). Enzymatic hydrolysis of lignocellulosic polysaccharides in the presence of ionic liquids. *Green Chem.* 17, 694–714. doi: 10.1039/C4GC01649A

Waliszewska, H., Zborowska, M., Waliszewska, B., Borysiak, S., Antczak, A., and Czekała, W. (2018). Transformation of miscanthus, and sorghum, cellulose during methane fermentation. *Cellulose* 25, 1207–1216. doi: 10.1007/s10570-017-1622-1

Wang, M., Zhou, J., Yuan, Y. X., Dai, Y. M., Li, D., Li, Z. D., et al. (2017). Methane production characteristics and microbial community dynamics of mono-digestion and co-digestion using corn stalk and pig manure. *Int. J. Hydrogen Energy* 42, 4893–4901. doi: 10.1016/j.ijhydene.2016.10.144

Wei, S. (2016). The application of biotechnology on the enhancing of biogas production from lignocellulosic waste. *Appl. Microbiol. Biotechnol.* 100, 9821–9836. doi: 10.1007/s00253-016-7926-5

Wei, S., Zhang, H., Cai, X., Xu, J., Fang, J., and Liu, H. (2014). Psychrophilic anaerobic co-digestion of highland barley straw with two animal manures at high altitude for enhancing biogas production. *Energ. Convers Manag.* 88, 40–48. doi: 10.1016/j.enconman.2014.08.018

Weiland, P. (2010). Biogas production: current state and perspectives. *Appl. Microbiol. Biotechnol.* 85, 849–860. doi: 10.1007/s00253-009-2246-7

Xu, J., Xiong, P., and He, B. (2016). Advances in improving the performance of cellulase in ionic liquids for lignocellulose biorefinery. *Bioresour. Technol.* 200, 961–970. doi: 10.1016/j.biortech.2015.10.031

Xu, N., Zhang, W., Ren, S. F., Liu, F., Zhao, C. Q., Liao, H. F., et al. (2012). Hemicelluloses negatively affect lignocellulose crystallinity for high biomass digestibility under NaOH and H_2SO_4 pretreatments in *Miscanthus*. *Biotechnol. Biofuels* 5:58. doi: 10.1186/1754-6834-5-58

Yang, B., Dai, Z. Y., Ding, S. Y., and Wyman, C. E. (2011). Enzymatic hydrolysis of cellulosic biomass. *Biofuels* 2, 421–449. doi: 10.4155/bfs.11.116

Yu, Q., Zhuang, X., Lv, S., He, M., Zhang, Y., and Yuan, Z. (2013). Liquid hot water pretreatment of sugarcane bagasse and its comparison with chemical pretreatment methods for the sugar recovery and structural changes. *Bioresour. Technol.* 129, 592–598. doi: 10.1016/j.biortech.2012.11.099

Yuan, T. Q., You, T. T., Wang, W., Xu, F., and Sun, R. C. (2013). Synergistic benefits of ionic liquid and alkaline pretreatments of poplar wood. Part 2: characterization of lignin and hemicelluloses. *Bioresour. Technol.* 136, 345–350. doi: 10.1016/j.biortech.2013.03.042

Zhang, J., Guo, R. B., Qiu, Y. L., Qiao, J. T., Yuan, X. Z., Shi, X. S., et al. (2015). Bioaugmentation with an acetate-type fermentation bacterium Acetobacteroides hydrogenigenes improves methane production from corn straw. *Bioresour. Technol.* 179, 306–313. doi: 10.1016/j.biortech.2014.12.022

Zhang, Q., He, J., Tian, M., Mao, Z., Tang, L., Zhang, J., et al. (2011). Enhancement of methane production from cassava residues by biological pretreatment using a constructed microbial consortium. *Bioresour. Technol.* 102, 8899–8906. doi: 10.1016/j.biortech.2011.06.061

Zhang, W., Yi, Z. Z., Huang, J. F., Li, F. C., Hao, B., Li, M., et al. (2013). Three lignocellulose features that distinctively affect biomass enzymatic digestibility under NaOH and H_2SO_4 pretreatments in miscanthus. *Bioresour. Technol.* 130, 30–37. doi: 10.1016/j.biortech.2012.12.029

Zhang, Y. H., and Lynd, L. R. (2004). Toward an aggregated understanding of enzymatic hydrolysis of cellulose: noncomplexed cellulase systems. *Biotechnol. Bioeng.* 88, 797–824. doi: 10.1002/bit.20282

Zhao, X. B., Zhang, L. H., and Liu, D. H. (2012). Biomass recalcitrance. Part I: the chemical compositions and physical structures affecting the enzymatic hydrolysis of lignocellulose. *Biofuels Bioprod. Bioresour.* 6, 465–482. doi: 10.1002/bbb.1331

Zhe, L., Sheng, C., Xun, Z., and Feng,. X. (2017). Exploring crystalline-structural variations of cellulose during alkaline pretreatment for enhanced enzymatic hydrolysis. *Bioresour. Technol.* 224, 611–617. doi: 10.1016/j.biortech.2016.10.064

Zheng, Y., Zhao, J., Xu, F.Q., Li, Y. (2014). Pretreatment of lignocellulosic biomass for enhanced biogas production. *Prog. Energy. Combust. Sci.* 42, 35–53. doi: 10.1016/j.pecs.2014.01.001

Zhou, J., Yan, B. H., Wang, Y., Yong, X. Y., Yang, Z. H., Jia, H. H., et al. (2016). Effect of steam explosion pretreatment on the anaerobic digestion of rice straw. *RSC Adv*. 6, 88417–88425. doi: 10.1039/C6RA15330E

Zhou, X., Ma, J., Ji, Z., Zhang, X., Ramaswamy,. S., Xu, F., et al. (2014). Dilute acid pretreatment differentially affects the compositional and architectural features of *Pinus bungeana* Zucc. compression and opposite wood tracheid walls. *Ind. Crop. Prod.* 62, 196–203. doi: 10.1016/j.indcrop.2014.08.035

Zhu, L., O'Dwyer, J. P., Chang, V. S., Granda, C. B., and Holtzapple, M. T. (2008). Structural features affecting biomass enzymatic digestibility. *Bioresour. Technol.* 99, 3817–3828. doi: 10.1016/j.biortech.2007.07.033

Zhu, S., Wu, Y., Yu, Z., Liao, J., and Zhang, Y. (2005). Pretreatment by microwave/alkali of rice straw and its enzymic hydrolysis. *Process Biochem.* 40, 3082–3086. doi: 10.101 6/j.procbio.2005.03.016

Conflict of Interest Statement: The authors declare that the research was conducted in the absence of any commercial or financial relationships that could be construed as a potential conflict of interest.

frontiers in Bioengineering and Biotechnology

ORIGINAL RESEARCH
published: 18 September 2019
doi: 10.3389/fbioe.2019.00216

Metabolic Regulation of Organic Acid Biosynthesis in *Actinobacillus succinogenes*

Wenming Zhang[1,2], *Qiao Yang*[1], *Min Wu*[1], *Haojie Liu*[1], *Jie Zhou*[1], *Weiliang Dong*[1,2], *Jiangfeng Ma*[1,2], *Min Jiang*[1,2*] *and Fengxue Xin*[1,2*]

[1] State Key Laboratory of Materials-Oriented Chemical Engineering, College of Biotechnology and Pharmaceutical Engineering, Nanjing Tech University, Nanjing, China, [2] Jiangsu National Synergetic Innovation Center for Advanced Materials, Nanjing Tech University, Nanjing, China

Actinobacillus succinogenes is one of the most promising strains for succinic acid production; however, the lack of efficient genetic tools for strain modification development hinders its further application. In this study, a markerless knockout method for *A. succinogenes* using in-frame deletion was first developed. The resulting Δ*pflA* (encode pyruvate formate lyase 1-activating protein) strain displayed distinctive organic acid synthesis capacity under different cultivation modes. Additional acetate accumulation was observed in the Δ*pflA* strain relative to that of the wild type under aerobic conditions, indicating that acetate biosynthetic pathway was activated. Importantly, pyruvate was completely converted to lactate under anaerobic fermentation. The transcription analysis and enzyme assay revealed that the expression level and specific activity of lactate dehydrogenase (LDH) were significantly increased. In addition, the mRNA expression level of *ldh* was nearly increased 85-fold compared to that of the wild-type strain during aerobic–anaerobic dual-phase fermentation, resulting in 43.05 g/L lactate. These results demonstrate that *pflA* plays an important role in the regulation of C3 flux distribution. The deletion of *pflA* leads to the improvement of acetic acid production under aerobic conditions and activates lactic acid biosynthesis under anaerobic conditions. This study will help elaborate the mechanism governing organic acid biosynthesis in *A. succinogenes*.

Keywords: *Actinobacillus succinogenes*, organic acid, pyruvate formate lyase 1-activating enzyme, metabolic engineering, fermentation

OPEN ACCESS

Edited by:
Rongming Liu,
University of Colorado Boulder, United States

Reviewed by:
Jianmin Xing,
Institute of Process Engineering (CAS), China
Chuang Xue,
Dalian University of Technology (DUT), China

***Correspondence:**
Min Jiang
bioengine@njtech.edu.cn
Fengxue Xin
xinfengxue@njtech.edu.cn

Specialty section:
This article was submitted to Industrial Biotechnology, a section of the journal Frontiers in Bioengineering and Biotechnology

Received: *19 July 2019*
Accepted: *27 August 2019*
Published: *18 September 2019*

Citation:
Zhang W, Yang Q, Wu M, Liu H, Zhou J, Dong W, Ma J, Jiang M and Xin F (2019) Metabolic Regulation of Organic Acid Biosynthesis in Actinobacillus succinogenes. Front. Bioeng. Biotechnol. 7:216. doi: 10.3389/fbioe.2019.00216

INTRODUCTION

Microbial production of organic acid from renewable resources is a promising and sustainable approach due to its ecological and economical advantages (Kamzolova et al., 2014). For example, succinic acid has been identified as one of the top 12 chemical building blocks according to the US Department of Energy, which can be synthesized through microbial fermentation (Mckinlay et al., 2007b; Zhang et al., 2018b). *Actinobacillus succinogenes*, a facultative anaerobe and natural succinate producer, is one of the most promising strains for succinic acid production due to its wide carbon utilization spectrum and robustness to environment (Mckinlay et al., 2005; Pateraki et al., 2016). Various low-cost feedstocks have been used for succinate production by using *A. succinogenes*, including corncob (Zhong et al., 2015), corn stover

(Borges and Pereira, 2011), sugarcane bagasse hemicellulose hydrolysate (Li et al., 2011), etc. It should be noticed that other organic acids, such as pyruvic and lactic acids, were also accumulated under different cultivation modes, taking advantage of its unique incomplete TCA cycle. For instance, *A. succinogenes* NJ113 has been reported to be a potential industrial application for the bioproduction of pyruvic acid under microaerobic fermentation condition, and dissolved oxygen environment was found to have a vital role in promoting pyruvic acid production (Wang et al., 2016). Initial oxygen aeration was also necessary to enhance lactic acid biosynthetic capacity for *A. succinogenes* 130Z^T in subsequent anaerobic cultivation (Li et al., 2010). Conversely, physiological changes during aerobic growth of engineered *E. coli* strain could significantly affect succinate production in the subsequent anaerobic phase (Vemuri et al., 2002).

Currently, metabolic engineering strategy has attracted increasing attention to develop industrially competitive microorganisms, such as *Mannheimia succiniciproducens*, *Escherichia coli*, *Corynebacterium glutamicum*, *Clostridium acetobutylicum*, *Saccharomyces cerevisiae*, and *Yarrowia lipolytica* (Li et al., 2016; Ahn et al., 2017; Chung et al., 2017; Cui et al., 2017; Franco-Duarte et al., 2017; Xue et al., 2017). To improve succinic acid production, some cases regarding genetic modification of *A. succinogenes* have been reported, including enhancement of pathways involved in succinic acid synthesis and deletion of pathways involved in byproduct accumulation (Joshi et al., 2014; Guarnieri et al., 2017). For example, overexpression of the key enzymes (such as malate dehydrogenase) in the reductive branch of the TCA cycle enhanced flux to succinic acid, resulting in titer, rate, and yield enhancements (Guarnieri et al., 2017). A single-knockout mutant of the pyruvate formate lyase (PFL, encoded by *pflB*) was obtained using natural transformation method employing a positive selection marker (isocitrate dehydrogenase), which will effectively eliminate formate biosynthesis (Joshi et al., 2014). Thereafter, a series of single-knockout mutants and double-knockout mutants were constructed using electroporation employing antibiotic resistance marker to drive carbon flux into succinic acid (Guarnieri et al., 2017). However, it should be noticed that delayed bacterial growth, sugar utilization, and succinic acid biosynthesis were observed in knockout mutants compared with the wild strain, though formation of by-products including acetate and formate were effectively reduced. Thus, the strategy to improve the production of succinic acid through the removal of competitive pathways in *A. succinogenes* was still in vain.

Compared to metabolic gene knockouts, change of corresponding protein activity might be better to improve strain's growth performance. For instance, there is an activation system composed of activating factor and coenzyme under anaerobic conditions, which can convert the inactive PFL pro-enzyme into active PFL by amino acid free radical activation (Rodel et al., 1988). Pyruvate formate lyase 1-activating protein (encoded by *pflA*) is usually an activator to *pflB*. It was reported that deletion of *pflA* can increase succinic acid production from glycerol in *E. coli* under anaerobic conditions (Mienda et al., 2018). Protein homology analysis method showed that *pflA* can activate *pflB* under anaerobic conditions in *A. succinogenes* (Zhang et al., 2018a). These data provide a novel gene knockout target for increasing succinate production in *A. succinogenes*.

In this study, genetic tools for markerless gene knockout by in-frame deletion was first developed. The metabolic regulation of organic acid biosynthetic in *A. succinogenes* Δ*pflA* strain under different fermentation strategies was also investigated. To elucidate the mechanism underlying the increased different organic acids production, the transcriptional level of key genes involved in metabolic pathway was evaluated. In this work, the effect of the deletion of *pflA* on organic acids production in *A. succinogenes* was studied. Additionally, the engineered strain represents a promising role for acetate or lactate production.

MATERIALS AND METHODS

Strains and Media

Actinobacillus succinogenes 130Z (ATCC 55618) was obtained from the American Type Culture Collection. Wild-type and engineered strains were cultivated in sterile seed medium YC (containing the following: 5 g/L yeast extract, 9.6 g/L $NaH_2PO_4{\cdot}2H_2O$, 15.5 g/L $K_2HPO_4{\cdot}3H_2O$, 10 g/L $NaHCO_3$, 10 g/L glucose, 1 g/L NaCl, and 2.5 g/L corn steep liquor) at 37°C and 200 rpm. *E. coli* SM10 λ*pir*, provided by Professor Lianrong Wang (Wuhan University), was used as the donor strain to allow efficient replication of the suicide plasmid and grown in Luria-Bertani (LB) medium. The fermentation medium consisted of 10 g/L yeast extract, 1.36 g/L NaAc, 0.3 g/L $Na_2HPO_4{\cdot}12H_2O$, 1.6 g/L $Na_2HPO_4{\cdot}2H_2O$, 3 g/L K_2HPO_4, 1 g/L NaCl, 0.2 g/L $MgCl_2{\cdot}6H_2O$, 7.5 g/L corn steep liquor, and 0.2 g/L $CaCl_2$. Glucose was added after sterilization at a concentration of 30–50 g/L for fermentation.

DNA Manipulation and Conjugation

To construct a knockout cassette, the 1.5-kb up- and downstream regions of *pflA* gene were individually amplified by PCRs from genomic DNA of *A. succinogenes* using primers listed in **Supplementary Table 1**. Two purified fragments were ligated to a shuttle suicide plasmid pJC4 using One Step Cloning Kit (Vazyme, China), thereafter naturally transformed into *E. coli* SM10 λ*pir*.

Recipient strain *A. succinogenes* and donor bacteria were grown in media until exponential phase. Cells were mixed at an equal ratio. Then, mixture cultures were harvested by centrifugation (4,500 × *g*, 3 min) and washed three times with LB medium at room temperature. Pellets were resuspended in 50 μl of LB medium and spotted onto an LB plate. During anaerobic cultivation at 37°C, the shuttle suicide plasmid might enter the recipient strain from the donor bacteria. After 16 h of conjugation, cells were washed with LB medium and plated on the YC medium. For the selection of the first crossing-over and elimination of the donor strain, 34 μg/ml of chloramphenicol was supplemented. Clones were checked by PCR analysis (with primers F_0 and down-rev, up-fwd and R_0). Subsequently, positive colony was plated on YC agar plates with 15% sucrose, which is a counter selectable marker to promote the second crossing-over. The plasmid could be excited from the chromosome, generating

wild-type strain or deletion mutant. Clones were checked with primers *pflA*-F_0 and *pflA*-R_0 by colony PCR.

Fermentation in Seal Bottles and Bioreactors

A 6% seed inoculum from overnight YC culture was added to 100-ml sealed bottles containing 30 ml of fermentation medium supplement with 30 g/L glucose and 16 g/L magnesium carbonate hydroxide to maintain the pH at 6.8 and the fermentation was carried out at 200 rpm and 37°C. The anaerobic condition was achieved by sparging CO_2 for 2 min (Dessie et al., 2018).

Bioreactor fermentations were performed in a 5-L fermentor (Bioflo 110, USA) containing 2 L of fermentation medium. The temperature was controlled at 37°C and the agitation at 300 rpm. The pH was maintained at 6.8 by supplementing 20% Na_2CO_3. During aerobic fermentation conditions, air was sparged at 1 vvm. While anaerobic conditions were created by sparging with CO_2 at a flow rate of 0.2 L/min. When the glucose concentration was lower than 10 g/L, 600 g/L glucose was fed into the fermentation medium until the final concentration was 50 g/L.

Enzymatic Assays

Cultures were harvested by centrifugation (4°C, 10,000 × *g*, 10 min) and washed twice with 50 mM Tris-HCl buffer (pH at 7.0). Pellets were resuspended in 100 mM Tris–HCl buffer (pH at 7.0) containing 2 mM DTT and 0.1 mM EDTA. Cell disruption by sonication was followed *via* centrifugation for 10 min at 10,000 × *g* at 4°C. The supernatant was used for all enzyme assays. The protein concentration was determined by the method of Bradford (1976).

The enzyme activity of pyruvate formate lyase was measured as described previously (Melchiorsen et al., 2002). The lactate dehydrogenase (LDH) assay was performed based on Vanderwerf et al. (1997). One unit (U) was defined as the amount of enzyme catalyzing the conversion of 1 μmol of substrate per minute into specific products. Specific activity was defined as units per milligram of protein (Li et al., 2010).

Quantitative RT-PCR

Cultures grown under different cultivation conditions were subject to RNA extraction during 8 h in aerobic/anaerobic or 20 h in dual-phase fermentation. Takara RNAiso Plus (Takara) was used to extract total RNA. After eliminating genomic DNA by RNase-free DNase I (Takara), RNA was converted into cDNA using a cDNA synthesis kit (Takara).

SYBRs Premix Ex TaqTM kit purchased from Takara was used for RT-PCR. All experiments were performed in biological triplicates in 96-well plates using the ABI 7500 Real-Time PCR system (Applied Biosystems). The 16S rRNA gene was used to standardize the mRNA levels. Primer sequences for qRT-PCR are indicated in **Supplementary Table 1**. The mRNA level of the target genes was calculated *via* the $2^{-\Delta\Delta CT}$ method (Livak and Schmittgen, 2001).

Analytical Methods

Cell growth was determined by OD_{600} in an AOE INSTRUMENTS-UV1800 spectrophotometer. Organic acids were measured by high-performance liquid chromatography (UitiMate 3000 HPLC system, Dionex, USA) equipped with an ion exchange column (Bio Rad Aminex HPX-87H column, USA) at 55°C, using a mobile phase of 5 mM H_2SO_4 at a flow rate of 0.6 ml/min and a UVD 170U ultraviolet detector at 215 nm for detection, as described previously (Zhang et al., 2018c). Glucose concentration in the fermentation broth was detected by a chronoamperometry method. In this detection process, a calibration line of current response vs. glucose concentration was first fitted by the continuous additions of a standard glucose concentration into a buffer solution. Then, the target sample was added to calculate its glucose concentration by using the calibration line (Jiang et al., 2016; Yang et al., 2017).

RESULTS AND DISCUSSION

A Markerless Knockout Method for *A. succinogenes* by In-Frame Deletion

Different from previous transformation methods, which adopted the positive selection marker with natural transformation or antibiotic resistance marker with electroporation (Joshi et al., 2014; Guarnieri et al., 2017), a markerless knockout method for *A. succinogenes* using conjugation was first developed. To create the gene deletion method in *A. succinogenes*, a shuttle suicide vector (pJC4) was employed, which carried *R6K ori* (the replication functional in *E. coli*), *cat* gene conferring chloramphenicol resistance, and *sacB* gene from *Bacillus subtilis* (the sucrose-sensitivity system). The replacement cassette contains two 1.5-kb regions flanking the target gene on the chromosome of *A. succinogenes*. After single crossing-over screened by chloramphenicol resistance and second crossing-over by sucrose counter selection, a markerless knockout mutant was obtained (**Figure 1**). Although markerless knockout method has been reported, the residual "scar" still exists in the chromosome at the site of the deletion, such as Flp sites, which will lead to large sections of the genome rather than two FRT sequences flanking the marker incorrect deletion when multiple genes have been consecutively deleted from one strain (Joshi et al., 2014). The mutants generated through in-frame deletion method in this study solved this problem efficiently and achieved real markerless knockout, providing a research basis for the metabolic engineering of *A. succinogenes*. Based on this method, pyruvate formate lyase 1-activating protein encoded by *pflA* in *A. succinogenes* 130Z was successfully knocked out and mutant was generated markerless.

Redistribution of Metabolic Products by Mutant With *pflA* Deletion

Generally, metabolic flux in *A. succinogenes* will be split into the following two branches under anaerobic conditions: (i) C3 pathways for formate, acetate, ethanol, and lactate production, and (ii) C4 pathway for succinate production. As known, the insufficient supply of reducing power is one main obstacle to achieve high succinic acid yield under anaerobic conditions, as succinic acid yield from glucose or other carbon sources strongly depends on ATP and NADH levels, which were mainly

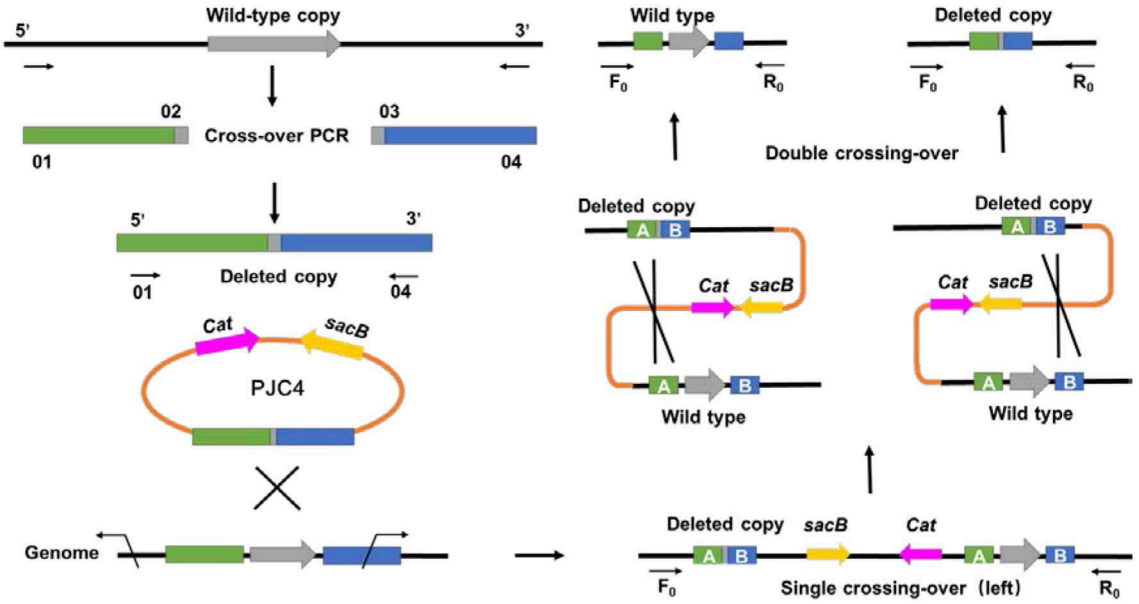

FIGURE 1 | General diagram representing an alternative method for markerless gene deletion by allelic exchange in *Actinobacillus succinogenes*.

produced by C3 pathways (Singh et al., 2011; Zhang et al., 2018c). However, the accumulation of by-products synthesized through C3 pathways will not only reduce the substrate utilization but also cause difficulties in the separation and purification steps. It was found that formate could be significantly reduced when PFLB catalyzing pyruvate into acetyl coenzyme A and formate was knocked out. However, the cell growth rate was also significantly decreased in Δ*pflB* strain. Succinate yield was still similar to that of wild-type strain. To relieve the negative effect by *pflB* knockout, pyruvate formate lyase 1-activating protein (*pflA*) was further knocked out.

Wild-type and Δ*pflA* strain were cultivated in sealed bottles containing 30 g/L glucose. The titers of succinate, formate, and acetate in the Δ*pflA* strain were 15.78, 4.53, and 8.23 g/L, respectively, which were approximately equal to those of the wild-type strain (**Figure 2**). Results demonstrated that the absence of activating protein (PFLA) did not affect the expression of pyruvate formate lyase, and succinic acid production was not increased significantly. Interestingly, pyruvate, and lactate production were significantly changed. Pyruvate accumulation was observed in both wild-type and Δ*pflB* strains (Guarnieri et al., 2017), while traces of pyruvate accumulation (< 1 g/L) were observed in the Δ*pflA* strain, indicating that pyruvic acid was completely assimilated. Surprisingly, the Δ*pflA* strain displayed a significantly increased lactate accumulation capacity (6.92 g/L) with 5.77-fold improvement, which coincided with pyruvate assimilation (**Figure 2**). Conversely, no lactic acid accumulation was observed in the wild-type or Δ*pflB* strains.

To further investigate the effect of *pflA* deletion on cell growth and metabolite profiles, batch fermentation of wild-type and Δ*pflA* strains was carried out under anaerobic conditions in a 5-L fermentor with 50 g/L of glucose. As illustrated

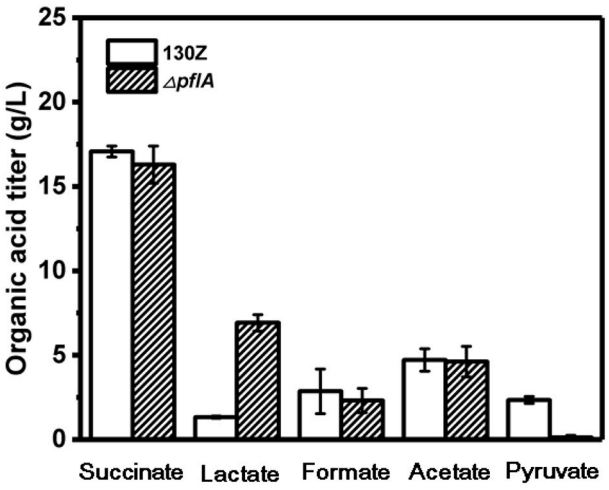

FIGURE 2 | Comparison of different organic acids production between wild-type *A. succinogenes* 130Z and Δ*pflA* strains.

in **Figure 3A**, 40 g/L of glucose was consumed after 18 h of fermentation by the wild-type strain, and the maximal OD_{600} reached 7.07. However, cell growth and glucose consumption rates were slightly decreased by the Δ*pflA* strain with a maximal OD_{600} of 6.07 at 21 h. Complete glucose consumption was ultimately achieved after 50 h of cultivation (**Figure 3B**). Delayed glucose consumption and cell growth coincided well with delayed succinic acid production relative to that of the 130Z strain. 30.25 g/L succinic acid with a yield of 0.62 g/g was achieved, which was decreased by 10% when compared to that of control strain. The

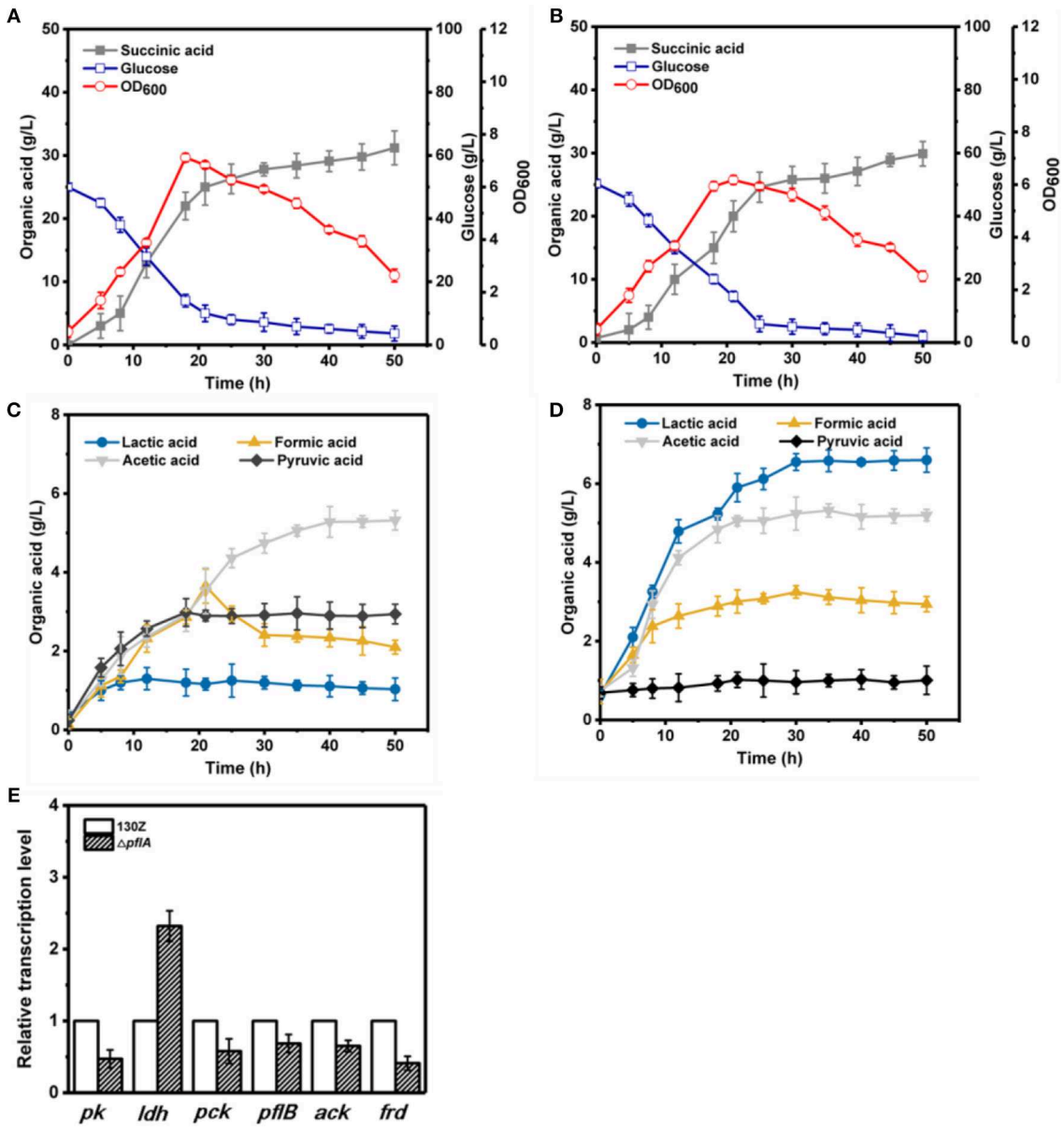

FIGURE 3 | Evaluation of different fermentation and metabolic parameters in wild-type *A. succinogenes* 130Z **(A,C)** compared to those of the Δ*pflA* strain **(B,D)** under anaerobic conditions. The bar graph **(E)** represents the expression levels of genes related to organic acid biosynthesis pathway.

strain Δ*pflA* showed similar acetic and formic acid accumulation profiles to that of wild type; acetic and formic production reached 5.32 and 2.26 g/L, respectively (**Figure 3C**). Notably, negligible amount of lactate accumulation was observed in strain 130Z, which is in agreement with the previously reported wild-type strain. Conversely, more lactate accumulation (6.43 g/L) and nearly complete elimination of pyruvate was observed by using the Δ*pflA* strain (**Figure 3D**), indicating that lactate flux was activated after removal of *pflA*. Although lactate accumulation was also observed in the Δ*pflB* Δ*ackA* strain, pyruvate was still accumulated at early exponential phase and yet completely assimilated following 24 h of cultivation (Guarnieri et al., 2017), which is different from this study. Therefore, in addition to knockout of both *ackA* and *pflB*, deletion of *pflA* can also lead to lactic acid generation, indicating that *pflA* plays a critical role in lactic acid biosynthesis in *A. succinogenes*.

Effect of *pflA* Knockout on the Expression of Key Genes Involved in Metabolic Pathway

To examine the effect of *pflA* knockout on the gene expression in *A. succinogenes*, the expression levels of several key genes involved in succinic acid (*pck* encoding phosphoenolpyruvate carboxykinase, *frd* encoding fumarate reductase), pyruvic acid (*pk* encoding pyruvate kinase), acetic acid (*pfl* encoding

pyruvate formate lyase, *ack* encoding acetate kinase), and lactic acid formation (*ldh* encoding 6-lactate dehydrogenase) were investigated. Relative mRNA transcription levels of these genes at exponential phase for strain 130Z and Δ*pflA* were measured with RT-PCR. 16S rRNA copy number was used as internal reference.

As shown in **Figure 3E**, knockout of *pflA* could slightly down-regulate mRNA levels of all metabolite synthesis genes except *ldh*, which coincides with the prolonged bacterial growth and product synthesis in the Δ*pflA* strain. For example, the expression level of *pk* and *frd* was nearly 0.4-fold lower than that of strain 130Z.

TABLE 1 | Comparison of enzyme activities involved in organic acid formation in *Actinobacillus succinogenes* 130Z and Δ*pflA* grown anaerobically.

Strain	Total protein (mg/ml)	PFL activity (U/ml)	Specific activity (U/mg)	LDH activity (U/ml)	Specific activity (U/mg)
130Z	0.25 ± 0.02	4.56 ± 0.12	18.25 ± 0.26	3.25 ± 0.08	11.61 ± 0.32
Δ*pflA*	0.29 ± 0.01	4.06 ± 0.15	17.65 ± 0.42	10.62 ± 0.27	30.34 ± 1.21

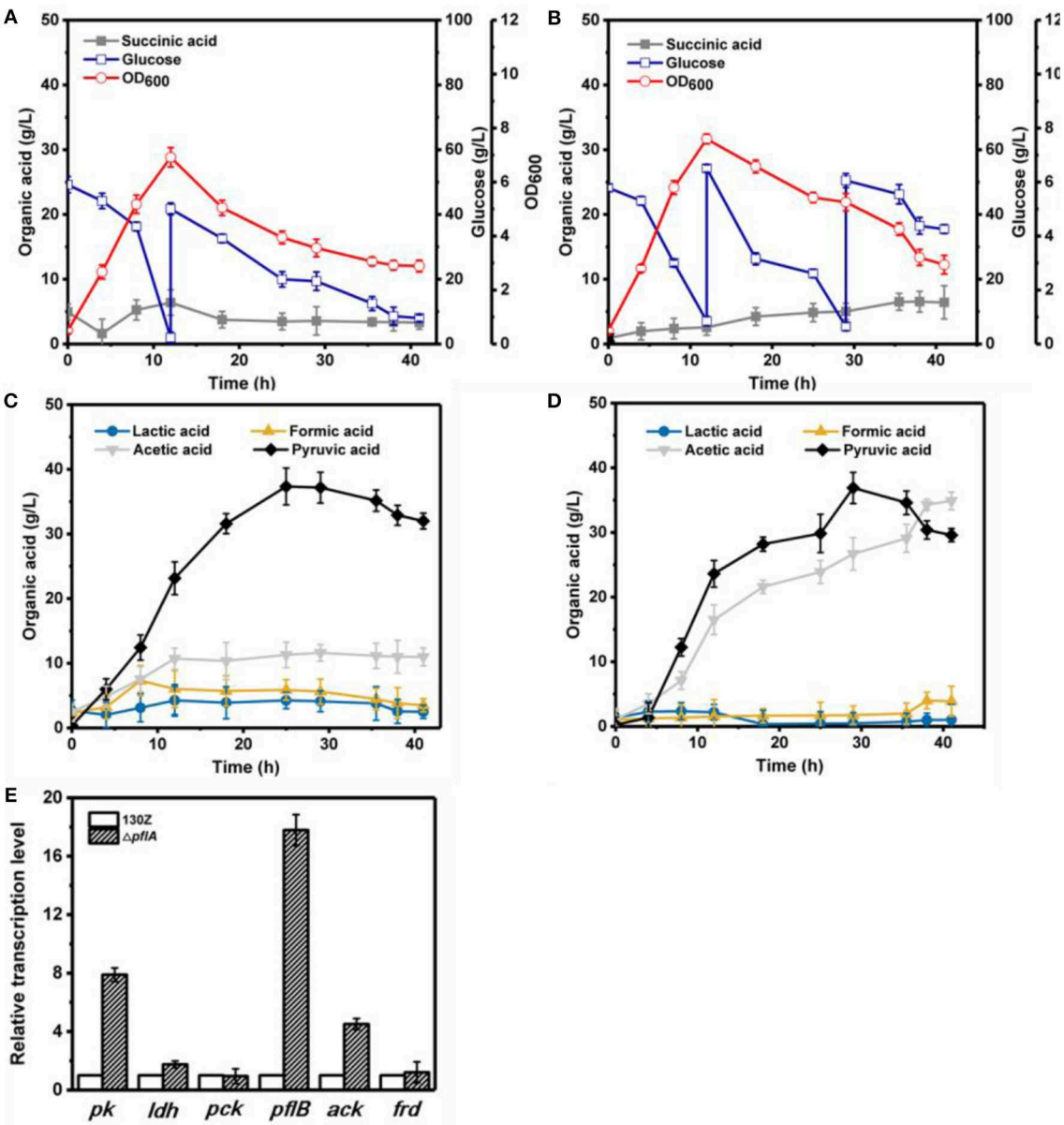

FIGURE 4 | Evaluation of different fermentation and metabolic parameters in the 130Z strain **(A,C)** compared to those of the Δ*pflA* strain **(B,D)** under aerobic conditions. The bar graph **(E)** represents the expression levels of genes related to organic acid biosynthesis pathway.

Surprisingly, the mRNA level of *ldh* in the Δ*pflA* strain was 2.3-fold higher than that of the wild-type strain, indicating that the lactic acid biosynthesis pathway might be activated by deletion of *pflA*.

In order to further investigate the metabolic regulation mechanism, the activities of two key enzymes PFL (pyruvate formate lyase) and LDH involved in C3 branch pathways were investigated. As shown in **Table 1**, PFL enzyme activities were similar between the wild-type (18.25 U/mg) and Δ*pflA* strains (17.65 U/mg), which is in agreement with the fermentation results. However, LDH specific activity was significantly increased in the Δ*pflA* strain, which was 2.62-fold higher than that of the wild-type strain. The maximum activity was 30.34 U/mg, which coincides well with the mRNA level and lactate production. Taken together, these results indicated that the expression of pyruvate formate lyase in *A. succinogenes* does not depend on the activation of pyruvate formate lyase 1-activating protein, though its function notation in NCBI is to activate pyruvate formate lyase 1 under anaerobic conditions. Moreover, the absence of this protein might be beneficial for the carbon flux to lactic acid. Therefore, we speculated that the function of pyruvate formate lyase 1-activating protein might be a repressor for *ldh* gene transcription, which is different from *E. coli*.

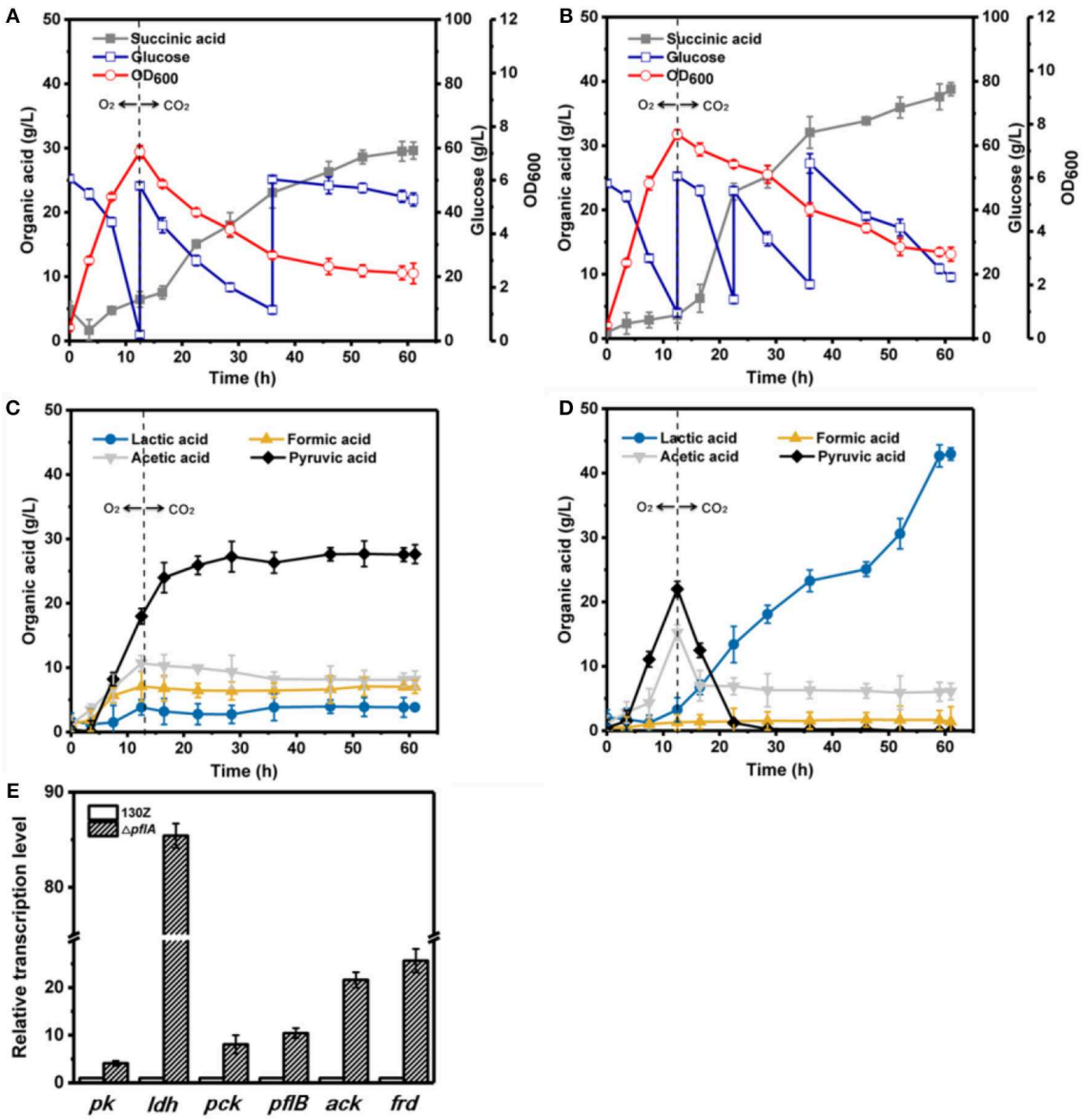

FIGURE 5 | Evaluation of different fermentation and metabolic parameters in the 130Z strain **(A,C)** compared to those of the Δ*pflA* strain **(B,D)** under aerobic–anaerobic dual-phase conditions. The bar graph **(E)** represents the expression levels of genes related to organic acid biosynthesis pathway.

Organic Acid Production Under Different Fermentation Strategies

Actinobacillus succinogenes will change cell physiology and metabolite profile under different cultivation conditions, such as aerobic and anaerobic conditions. As mentioned above, the lactic acid biosynthesis pathway was activated after deletion of *pflA* under anaerobic conditions. To further investigate the effect of *pflA* deletion on cell growth and metabolic performance under aerobic and aerobic–anaerobic dual-phase cultivation modes, the fed-batch fermentation using wild-type 130Z and Δ*pflA* strain was conducted in a 5-L fermentor.

Under aerobic conditions, 82 g/L of glucose was completely consumed after 41 h by strain 130Z with a maximal OD_{600} of 6.92 at 12 h (**Figure 4A**). Interestingly, strain Δ*pflA* displayed higher growth rate, which is obviously different from that under anaerobic conditions (**Figure 4B**). As a result, more glucose (105 g/L) was consumed with a maximal OD_{600} of 7.64. As a main product, pyruvic acid accumulation profiles were similar between strain Δ*pflA* and 130Z, and the highest titer reached 36.90 and 37.36 g/L, respectively. The latter is in agreement with a previous study reported under microaerobic fermentation (Wang et al., 2016). Surprisingly, massive acetic acid accumulation was also observed in the Δ*pflA* strain. The highest titer of acetic acid can reach 34.92 g/L, 13.7-fold titer enhancement (**Figure 4D**), indicating that acetic acid biosynthesis was enhanced and carbon flux was shifted to acetic acid after the deletion of *pflA* under aerobic conditions. As known, ATP generation is accompanying by acetic acid production (Guarnieri et al., 2017), leading to cell growth and glucose consumption improvement. Additionally, the Δ*pflA* strain displayed increased succinic acid accumulation capacity (6.43 g/L) with 48.06% enhancement. Conversely, a greater reduction in lactic and formic acid titer was observed in the Δ*pflA* strain relative to that of the wild type.

Under aerobic-anaerobic conditions, succinic, and pyruvic acids were main metabolic products with 29.62 and 27.64 g/L, respectively, from 96 g/L of glucose by using strain 130Z (**Figure 5A**). Pyruvic acid was significantly accumulated in the aerobic phase and still produced and even shifted to anaerobic condition (**Figure 5C**). Surprisingly, 142 g/L glucose (32.39% higher) was consumed in the Δ*pflA* strain, indicating the superior performance of bacteria growth. Final succinic acid titer (38.82 g/L) was also significantly enhanced with 23.72% improvement (**Figure 5B**). However, the pyruvic acid concentration was dramatically decreased in the Δ*pflA* strain when shifted to anaerobic condition. In addition, no pyruvic acid accumulation was observed at the end of fermentation with almost complete pyruvate reassimilation. As shown in **Figure 5C**, acetic acid production was slowly decreased under anaerobic phase with a final titer of 8.15 g/L. Moreover, lactic and formic acids production remained stable in the wild-type strain. These results showed that carbon flux distribution was shifted from C3 (pyruvic acid synthesis) toward C4 flux (succinic acid synthesis) when cultivation condition was shifted from an aerobic to an

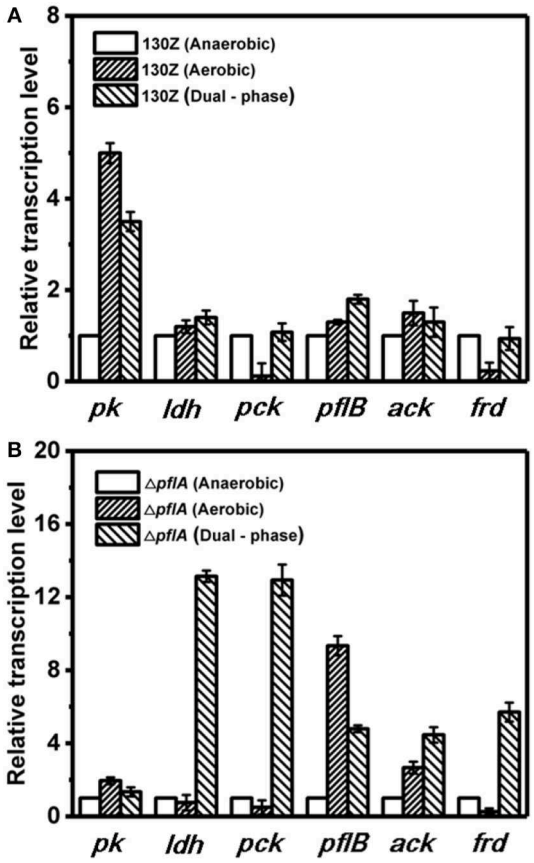

FIGURE 6 | Expression levels of genes related to organic acid biosynthesis pathway in the 130Z strain **(A)** and Δ*pflA* strain **(B)** under different cultivation modes.

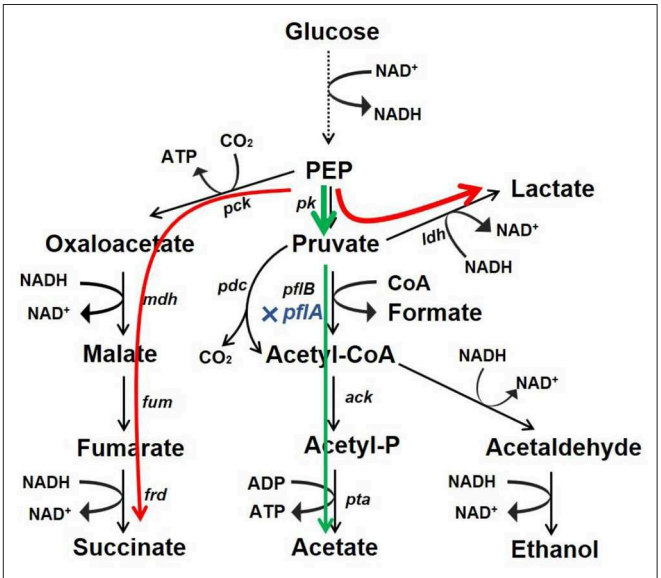

FIGURE 7 | Redistribution of metabolic products by mutant with *pflA* deletion. Glucose carbon flux in strain Δ*pflA* under aerobic condition (green) and anaerobic or dual-phase condition (red).

anaerobic one. By contrast, sharp accumulation of lactic acid was observed by using Δ*pflA* strain under anaerobic conditions. The maximum of lactic acid production was 43.05 g/L at 60 h of cultivation, which was a nearly 11-fold increase compared to that of the wild-type strain (**Figure 5D**). Conversely, the acetic acid accumulation profiles were similar between wild-type and engineered strains, and a negligible amount of formic acid was detected in the whole fermentation. These results indicated that the removal of *pflA* could significantly enhance carbon flux to lactic acid under dual-phase cultivation conditions.

Qrt-PCR Analysis Under Different Cultivation Modes

To further elaborate the underlying mechanism responsible for organic acid synthesis, the expression levels of related genes were investigated. Previous work showed that the expression level of *ldh* in strain Δ*pflA* was much higher than that of the wild-type strain, while the expression level of other metabolite synthesis genes was slightly lower under anaerobic conditions (**Figure 3**). The expression levels of *pk*, *pfl*, and *ack* genes from the Δ*pflA* strain are significantly increased relative to that of the 130Z strain during aerobic fermentation, which coincides with acetic acid accumulation in the Δ*pflA* strain (**Figures 4D,E**). However, the mRNA level of all genes was significantly increased (> 4-fold) in the Δ*pflA* strain under dual-phase fermentation conditions, indicating that the strain has the superior performance of cell growth and metabolism (**Figure 5E**). Notably, the transcription level of *ldh* was increased nearly 85-fold, displaying a dramatically increased lactic acid accumulation capacity relative to that of the wild type. It is known that LDH is indeed encoded in its genome, while no lactate was produced in *A. succinogenes* (Mckinlay et al., 2007a). The finding in the current paper suggests that a finely tuned system might be used to lactic acid biosynthesis.

Next, mRNA levels of key genes in the same strain under different conditions were also compared. As shown in **Figure 6A**, wild-type *A. succinogenes* showed the same transcription levels of *ldh* and *ack* among three kinds of cultivation modes. The expression levels of *pck* and *frd* genes were significantly down-regulated under aerobic conditions, in accordance with low carbon flux of SA-producing reductive C4 pathway. A similar phenomenon was observed in the Δ*pflA* strain. Specifically, the expression levels of *ldh*, *pck*, and *frd* genes under dual-phase conditions were much higher than those under other fermentation modes in the Δ*pflA* strain, leading to massive lactic acid and succinic acid accumulation (**Figure 6B**). However, although the expression level of *ack* was up-regulated in the Δ*pflA* strain under both aerobic and dual-phase cultivation, higher acetic acid accumulation was observed in the aerobic condition. Instead, no difference in acetic acid production was found between anaerobic and dual-phase cultivation conditions (**Figures 3D**, **5D**). Thus, it was speculated that an alternative route to acetic acid biosynthesis exists in *A. succinogenes*.

CONCLUSIONS

Microbial production of organic acid is a promising approach owing to advantages of being low cost, efficient, and environment friendly. In this work, we developed a markerless knockout method for *A. succinogenes*. It was found that C3 metabolic pathways were regulated by *pflA*, which was vital for organic acid synthesis. Moreover, the resulting Δ*pflA* strain was able to accumulate acetic acid under aerobic conditions and lactic acid under dual-phase fermentation (**Figure 7**). These results reveal a potential finely tuned mechanism in organic acid biosynthesis. Moreover, the study indicates that *A. succinogenes* is not only a promising succinate producer, but also potentially an excellent strain for the bioproduction of acetic acid and lactic acid.

DATA AVAILABILITY

All datasets generated for this study are included in the manuscript/**Supplementary Files**.

AUTHOR CONTRIBUTIONS

WZ designed and performed the experiments, analyzed the results, and wrote the manuscript. QY, MW, and HL assisted in experimental work and analytical work. JZ, WD, and JM assisted in the design of the study. MJ and FX revised the manuscript. All authors read and approved the final manuscript.

FUNDING

This work was supported by the National Natural Science Foundation of China (Grant No. 21706124) and the Jiangsu Synergetic Innovation Center for Advanced Bio-Manufacture of China.

SUPPLEMENTARY MATERIAL

The Supplementary Material for this article can be found online at: https://www.frontiersin.org/articles/10.3389/fbioe.2019.00216/full#supplementary-material

REFERENCES

Ahn, J. H., Bang, J., Kim, W. J., and Lee, S. Y. (2017). Formic acid as a secondary substrate for succinic acid production by metabolically engineered *Mannheimia succiniciproducens*. *Biotechnol. Bioeng.* 114, 2837–2847. doi: 10.1002/bit.26435

Borges, E. R., and Pereira, N. Jr. (2011). Succinic acid production from sugarcane bagasse hemicellulose hydrolysate by *Actinobacillus succinogenes*. *J. Ind. Microbiol. Biotechnol.* 38, 1001–1011. doi: 10.1007/s10295-010-0874-7

Bradford, M. M. (1976). A rapid and sensitive method for the quantitation of microgram quantities of protein utilizing the principle of protein-dye binding. *Anal. Biochem.* 72, 248–254. doi: 10.1016/0003-2697(76)90527-3

Chung, S. C., Park, J. S., Yun, J., and Park, J. H. (2017). Improvement of succinate production by release of end-product inhibition in *Corynebacterium glutamicum*. *Metab. Eng.* 40, 157–164. doi: 10.1016/j.ymben.2017.02.004

Cui, Z. Y., Gao, C. J., Li, J. J., Hou, J., Lin, C. S. K., and Qi, Q. S. (2017). Engineering of unconventional yeast *Yarrowia lipolytica* for efficient

succinic acid production from glycerol at low pH. *Metab. Eng.* 42, 126–133. doi: 10.1016/j.ymben.2017.06.007

Dessie, W., Zhu, J., Xin, F., Zhang, W., Jiang, Y., Wu, H., et al. (2018). Bio-succinic acid production from coffee husk treated with thermochemical and fungal hydrolysis. *Bioproc. Biosyst. Eng.* 41, 1461–1470. doi: 10.1007/s00449-018-1974-4

Franco-Duarte, R., Bessa, D., Goncalves, F., Martins, R., Silva-Ferreira, A. C., Schuller, D., et al. (2017). Genomic and transcriptomic analysis of *Saccharomyces cerevisiae* isolates with focus in succinic acid production. *FEMS Yeast Res.* 17:fox057. doi: 10.1093/femsyr/fox057

Guarnieri, M. T., Chou, Y. C., Salvachua, D., Mohagheghi, A., John, P. C. S., Peterson, D. J., et al. (2017). Metabolic engineering of *Actinobacillus succinogenes* provides insights into succinic acid biosynthesis. *Appl. Environ. Microbiol.* 83:e00996–17. doi: 10.1128/AEM.00996-17

Jiang, D. F., Chu, Z. Y., Peng, J. M., and Jin, W. Q. (2016). Screen-printed biosensor chips with Prussian blue nanocubes for the detection of physiological analytes. *Sens. Actuators Chem.* 228, 679–687. doi: 10.1016/j.snb.2016.01.076

Joshi, R. V., Schindler, B. D., Mcpherson, N. R., Tiwari, K., and Vieille, C. (2014). Development of a markerless knockout method for *Actinobacillus succinogenes*. *Appl. Environ. Microbiol.* 80, 3053–3061. doi: 10.1128/AEM.00492-14

Kamzolova, S. V., Vinokurova, N. G., Shemshura, O. N., Bekmakhanova, N. E., Lunina, J. N., Samoilenko, V. A., et al. (2014). The production of succinic acid by yeast *Yarrowia lipolytica* through a two-step process. *Appl. Microbiol. Biotechnol.* 98, 7959–7969. doi: 10.1007/s00253-014-5887-0

Li, J., Zheng, X. Y., Fang, X. J., Liu, S. W., Chen, K. Q., Jiang, M., et al. (2011). A complete industrial system for economical succinic acid production by *Actinobacillus succinogenes*. *Bioresour. Technol.* 102, 6147–6152. doi: 10.1016/j.biortech.2011.02.093

Li, Q., Wu, H., Li, Z. M., and Ye, Q. (2016). Enhanced succinate production from glycerol by engineered *Escherichia coli* strains. *Bioresour. Technol.* 218, 217–223. doi: 10.1016/j.biortech.2016.06.090

Li, Q. A., Wang, D., Song, Z. Y., Zhou, W., Wu, Y., Xing, J. M., et al. (2010). Dual-phase fermentation enables *Actinobacillus succinogenes* 130Z(T) to be a potential role for high-level lactate production from the bioresource. *Bioresour. Technol.* 101, 7665–7667. doi: 10.1016/j.biortech.2010.04.058

Livak, K. J., and Schmittgen, T. D. (2001). Analysis of relative gene expression data using real-time quantitative PCR and the 2(T)(–Delta Delta C) method. *Methods* 25, 402–408. doi: 10.1006/meth.2001.1262

Mckinlay, J. B., Shachar-Hill, Y., Zeikus, J. G., and Vieille, C. (2007a). Determining *Actinobacillus succinogenes* metabolic pathways and fluxes by NMR and GC-MS analyses of 13C-labeled metabolic product isotopomers. *Metab. Eng.* 9, 177–192. doi: 10.1016/j.ymben.2006.10.006

Mckinlay, J. B., Vieille, C., and Zeikus, J. G. (2007b). Prospects for a bio-based succinate industry. *Appl. Microbiol. Biotechnol.* 76, 727–740. doi: 10.1007/s00253-007-1057-y

Mckinlay, J. B., Zeikus, J. G., and Vieille, C. (2005). Insights into *Actinobacillus succinogenes* fermentative metabolism in a chemically defined growth medium. *Appl. Environ. Microbiol.* 71, 6651–6656. doi: 10.1128/AEM.71.11.6651-6656.2005

Melchiorsen, C. R., Jokumsen, K. V., Villadsen, J., Israelsen, H., and Arnau, J. (2002). The level of pyruvate-formate lyase controls the shift from homolactic to mixed-acid product formation in *Lactococcus lactis*. *Appl. Microbiol. Biotechnol.* 58, 338–344. doi: 10.1007/s00253-001-0892-5

Mienda, B. S., Adamu, A., and Shamsir, M. S. (2018). Model-guided metabolic gene knockout of pflA in *Escherichia coli* increases succinic acid production from glycerol carbon source. *Curr. Metabolomics* 6, 201–206. doi: 10.2174/2213235X066661810121 43004

Pateraki, C., Patsalou, M., Vlysidis, A., Kopsahelis, N., Webb, C., Koutinas, A. A., et al. (2016). *Actinobacillus succinogenes*: advances on succinic acid production and prospects for development of integrated biorefineries. *Biochem. Eng. J.* 112, 285–303. doi: 10.1016/j.bej.2016.04.005

Rodel, W., Plaga, W., Frank, R., and Knappe, J. (1988). Primary structures of *Escherichia coli* pyruvate formate-lyase and pyruvate-formate-lyase-activating enzyme deduced from the DNA nucleotide sequences. *Eur. J. Biochem.* 177, 153–158. doi: 10.1111/j.1432-1033.1988.tb14356.x

Singh, A., Soh, K. C., Hatzimanikatis, V., and Gill, R. T. (2011). Manipulating redox and ATP balancing for improved production of succinate in *E. coli*. *Metab. Eng.* 13, 76–81. doi: 10.1016/j.ymben.2010.10.006

Vanderwerf, M. J., Guettler, M. V., Jain, M. K., and Zeikus, J. G. (1997). Environmental and physiological factors affecting the succinate product ratio during carbohydrate fermentation by *Actinobacillus* sp. 130Z. *Arch. Microbiol.* 167, 332–342. doi: 10.1007/s002030050452

Vemuri, G. N., Eiteman, M. A., and Altman, E. (2002). Succinate production in dual-phase *Escherichia coli* fermentations depends on the time of transition from aerobic to anaerobic conditions. *J. Ind. Microbiol. Biotechnol.* 28, 325–332. doi: 10.1038/sj.jim.7000250

Wang, Z., Xiao, W., Zhang, A. L., Ying, H. X., Chen, K. Q., and Ouyang, P. K. (2016). Potential industrial application of *Actinobacillus succinogenes* NJ113 for pyruvic acid production by microaerobic fermentation. *Korean J. Chem. Eng.* 33, 2908–2914. doi: 10.1007/s11814-016-0168-5

Xue, C., Zhao, J., Chen, L., Yang, S. T., and Bai, F. (2017). Recent advances and state-of-the-art strategies in strain and process engineering for biobutanol production by *Clostridium acetobutylicum*. *Biotechnol. Adv.* 35, 310–322. doi: 10.1016/j.biotechadv.2017.01.007

Yang, P. Q., Peng, J. M., Chu, Z. Y., Jiang, D. F., and Jin, W. Q. (2017). Facile synthesis of Prussian blue nanocubes/silver nanowires network as a water-based ink for the direct screen-printed flexible biosensor chips. *Biosens. Bioelectron.* 92, 709–717. doi: 10.1016/j.bios.2016.10.013

Zhang, H., Naikun, S., Qin, Y., Zhu, J., Li, Y., Jiafa, W., et al. (2018a). Complete genome sequence of *Actinobacillus succinogenes* GXAS137, a highly efficient producer of succinic acid. *Genome Announc.* 6:e01562–17. doi: 10.1128/genomeA.01562-17

Zhang, W., Zhu, J., Zhu, X., Song, M., Zhang, T., Xin, F., et al. (2018b). Expression of global regulator IrrE for improved succinate production under high salt stress by *Escherichia coli*. *Bioresour. Technol.* 254, 151–156. doi: 10.1016/j.biortech.2018.01.091

Zhang, W. M., Zhang, T., Song, M., Dai, Z. X., Zhang, S. J., Xin, F. X., et al. (2018c). Metabolic engineering of *Escherichia coli* for high yield production of succinic add driven by methanol. *ACS Synth. Biol.* 7, 2803–2811. doi: 10.1021/acssynbio.8b00109

Zhong, Y., Ruan, Z., Zhong, Y., Archer, S., Liu, Y., and Liao, W. (2015). A self-sustaining advanced lignocellulosic biofuel production by integration of anaerobic digestion and aerobic fungal fermentation. *Bioresour. Technol.* 179, 173–179. doi: 10.1016/j.biortech.2014.12.013

Conflict of Interest Statement: The authors declare that the research was conducted in the absence of any commercial or financial relationships that could be construed as a potential conflict of interest.

frontiers in Bioengineering and Biotechnology

ORIGINAL RESEARCH
published: 17 October 2019
doi: 10.3389/fbioe.2019.00273

Biosynthesis of Medium-Chain ω-Hydroxy Fatty Acids by AlkBGT of *Pseudomonas putida* GPo1 With Native FadL in Engineered *Escherichia coli*

Qiaofei He[1], *George N. Bennett*[5], *Ka-Yiu San*[4,5] *and Hui Wu*[1,2,3]*

[1] State Key Laboratory of Bioreactor Engineering, East China University of Science and Technology, Shanghai, China, [2] Shanghai Collaborative Innovation Center for Biomanufacturing Technology, Shanghai, China, [3] Key Laboratory of Bio-based Material Engineering of China National Light Industry Council, Shanghai, China, [4] Department of Bioengineering, Rice University, Houston, TX, United States, [5] Department of Chemical and Biomolecular Engineering, Rice University, Houston, TX, United States

OPEN ACCESS

Edited by:
Zhi-Qiang Liu, Zhejiang University of Technology, China

Reviewed by:
Lidan Ye, Zhejiang University, China
*Simon, Congqiang Zhang, Agency for Science, Technology and Research (A*STAR), Singapore*
Laura R. Jarboe, Iowa State University, United States

***Correspondence:**
Hui Wu
hwu@ecust.edu.cn

Specialty section:
This article was submitted to Industrial Biotechnology, a section of the journal Frontiers in Bioengineering and Biotechnology

Received: *10 July 2019*
Accepted: *01 October 2019*
Published: *17 October 2019*

Citation:
He Q, Bennett GN, San K-Y and Wu H (2019) Biosynthesis of Medium-Chain ω-Hydroxy Fatty Acids by AlkBGT of Pseudomonas putida GPo1 With Native FadL in Engineered Escherichia coli. Front. Bioeng. Biotechnol. 7:273. doi: 10.3389/fbioe.2019.00273

Hydroxy fatty acids (HFAs) are valuable compounds that are widely used in medical, cosmetic and food fields. Production of ω-HFAs *via* bioconversion by engineered *Escherichia coli* has received a lot of attention because this process is environmentally friendly. In this study, a whole-cell bio-catalysis strategy was established to synthesize medium-chain ω-HFAs based on the AlkBGT hydroxylation system from *Pseudomonas putida* GPo1. The effects of blocking the β-oxidation of fatty acids (FAs) and enhancing the transportation of FAs on ω-HFAs bio-production were also investigated. When *fadE* and *fadD* were deleted, the consumption of decanoic acid decreased, and the yield of ω-hydroxydecanoic acid was enhanced remarkably. Additionally, the co-expression of the FA transporter protein, FadL, played an important role in increasing the conversion rate of ω-hydroxydecanoic acid. As a result, the concentration and yield of ω-hydroxydecanoic acid in NH03(pBGT-*fadL*) increased to 309 mg/L and 0.86 mol/mol, respectively. This whole-cell bio-catalysis system was further applied to the biosynthesis of ω-hydroxyoctanoic acid and ω-hydroxydodecanoic acid using octanoic acid and dodecanoic acid as substrates, respectively. The concentrations of ω-hydroxyoctanoic acid and ω-hydroxydodecanoic acid reached 275.48 and 249.03 mg/L, with yields of 0.63 and 0.56 mol/mol, respectively. This study demonstrated that the overexpression of AlkBGT coupled with native FadL is an efficient strategy to synthesize medium-chain ω-HFAs from medium-chain FAs in *fadE* and *fadD* mutant *E. coli* strains.

Keywords: *Escherichia coli*, AlkBGT, medium-chain fatty acids, ω-hydroxy fatty acids, FadL

INTRODUCTION

Production of bio-based chemicals has received a lot of attention due to concerns around limited non-renewable fossil fuels and the global environment. Fatty acids (FAs) from plant oils are among the most abundant resources in nature (USDA, 2018). FAs are renewable industrial chemical feedstocks, and some artificial microbial pathways have been established to synthesize

high-value chemicals based on FA utilization. These reactions in the microbial pathways are mainly related to double-bond generation, double-bond oxidation, double-bond cleavage, epoxidation and functionalization of C-H bonds in alkyl chains (Biermann et al., 2011). Hydroxy fatty acids (HFAs), one kind of FA derivative, are the direct products of FA hydroxylation via C-H bond oxygenation.

HFAs are valuable chemicals due to their hydroxyl functional group and carboxyl group. HFAs have also gained great interest from various industries because of their special properties: higher reactivity, solvent miscibility, stability, and viscosity. Therefore, HFAs have wide applications and can be used as pharmaceutical intermediates and synthetic precursors (Cross et al., 1995), cosmetic ingredients, surfactants, foam improvers, emulsified agents in deodorant sticks, etc. (Koay et al., 2011), and as food bio-preservatives because of their strong antifungal activity (Cheng et al., 2010). Additionally, ω-HFAs are the ideal building blocks of green synthetic fibers for polymer materials due to the location of hydroxyl groups on the terminus of long carbon chains, which provide superior material properties (Weng and Wu, 2008; Cao and Zhang, 2013). ω-Hydroxydecanoic acid can be further derivatized to sebacic acid, which is an important precursor in the production of nylon and polyamides (PAs), primarily 4,10-PA and 5,10-PA (Bowen et al., 2016). ω-Hydroxydodecanoic acid has the potential to enable commercially relevant production of C12 α, ω-DCA, a valuable precursor of nylon-6,12 (Sugiharto et al., 2018).

Currently, considerable effort has been expended to produce HFAs by chemical synthesis; however, there are still various problems, e.g., lack of environmentally friendly solutions, complicated extraction methods, poor selectivity and harsh reaction conditions (Liu et al., 2011). Bio-catalysis is therefore regarded as a promising alternative approach because it has several advantages such as high selectivity, broad substrate spectrum, high catalytic efficiency, mufti-step reaction in a single strain, and is environmentally friendly (Manfred et al., 2011; Lin and Tao, 2017). Among all ω-HFAs produced by C-H bond oxygenases, most ω-HFAs are usually produced *via* cytochrome P450 monooxygenase (CYP)-based platforms. For example, these include CYP52A13 and CYP52A17 (Craft et al., 2003; Eschenfeldt et al., 2003), CYP4 (Fer et al., 2008), CYP704B2 (Li et al., 2010), CYP102A1 (Xiao et al., 2018), CYP153 (Bordeaux et al., 2012), and the $CYP153A_{M.aq.}$-CPR_{BM3} fusion protein (Scheps et al., 2013; Ahsan et al., 2018; Joo et al., 2019). Some of these enzymes can ω-oxidize terminal methyl groups and have been applied to ω-HFA production, but there is a limitation, in that most of these enzymes are specific for chain lengths of $\geq$12 (Picataggio et al., 1992).

The alkane hydroxylase of *Pseudomonas putida* GPo1, which consists of three components (AlkB, AlkG, and AlkT), could be another notable ω-oxidation enzyme system of FAs. This system has high specificity for medium-chain fatty acid (C_5-C_{12}) oxidation at terminal positions (Grant et al., 2011; Manfred et al., 2011; Tsai et al., 2017). The mono-oxygenase encoded by *alkB* belongs to a large class of membrane-bound proteins and is an essential component of the alkane hydroxylase system (Grund et al., 1975; Menno et al., 1989; Beilen et al., 1992). Rubredoxin encoded by *alkG* and rubredoxin reductase encoded by *alkT* are two electron transfer proteins. The hydroxylase system *in vivo* operates as follows: AlkG transfers an electron from AlkT, which reduces its flavin adenine dinucleotide at the expense of NADH, then further delivers the electron to AlkB to achieve hydroxylation (Jan et al., 2002). As reported, the AlkBGT hydroxylation system has been investigated in the bioconversion of the fatty acids methyl ester and alkane (Grant et al., 2011; Manfred et al., 2011; Julsing et al., 2012; Call et al., 2016; van Nuland et al., 2016; Kadisch et al., 2017), but there are no reports on ω-HFA production.

E. coli is the ideal host to employ to exploit the hydroxylation activity of these enzymes because of its clarified metabolic background. FA metabolism in *E. coli* has been expounded in previous work. FA β-oxidation in *E. coli* is induced by the presence of FAs in the growth medium. The FA β-oxidation cycle is activated by acyl-CoA synthetase (FadD), which plays an important role in FA degradation. The catabolic oxidation cycle consists of dehydrogenation by FadE, hydration and dehydrogenation by FadB or FadJ, and thiolation with CoA by FadA or FadI (Lennen and Pfleger, 2012; Wu and San, 2014). Regulation of FA oxidation is performed by the control protein FadR, which represses the *fad* regulon. FadD and FadE are the critical enzymes associated with β-oxidation (Wang et al., 2015; Bule et al., 2016). An important approach is deletion of *fadD* and *fadE*, which block the breakdown of fatty acids into acyl-CoA (Steen et al., 2010; Handke et al., 2011). Cao et al. (2016) constructed a *fadD* knockout strain, and the engineered strain showed an enhanced ability to produce HFAs. The titer of HFAs reached 58.7 mg/L, which is 1.6-fold higher than that of the original strain. Kirtz et al. (2016) and Sung et al. (2015) observed improved production of ω-hydroxy fatty acids with a *fadD* knockout strain. In addition, FA transport through the cell membrane to reach intracellular enzymes is one of the hurdles in ω-HFA production. There are two approaches to overcome this hurdle: one is the addition of chemical reagents such as surfactants to enhance membrane permeabilization, and another is using a transporter protein. Many studies have been done with transporter proteins. For example, AlkL from *Pseudomonas putida* GPo1 was reported to transport alkanes and fatty acid methyl esters into *E. coli* but was not active for fatty acids (Jeon et al., 2018). In fact, the outer membrane FA transport mechanism was also clarified in *E. coli*. It was clearly demonstrated that FA transport is mediated by a membrane protein pump (Bonen et al., 2007). FadL is a typical transporter for FAs; it can use spontaneous conformational changes to transport hydrophobic substrates by diffusion (van den Berg, 2005). There have been many notable cases of the use of FadL to achieve increased production (Bae et al., 2014; Tan et al., 2017; Jeon et al., 2018; Wu et al., 2019).

In this study, the medium-chain alkane hydroxylation system, AlkBGT, from *P. oleovorans* GPo1 was introduced in *E. coli* strains for ω-hydroxydecanoic acid biosynthesis from decanoic acid (C10FA). Metabolic engineering strategies to reduce the fatty acid metabolism of the host strains were also investigated here. Blocking the β-oxidation of fatty acids by deletion of

TABLE 1 | Strains and plasmids.

Strains and plasmids	Relevant characteristics	Source
Strains		
E. coli DH5α	Wild-type	Laboratory collection
E. coli W3110	Wild-type	Laboratory collection
NH01	W3110 Δ*fadE*	This study
NH02	W3110 Δ*fadD*	This study
NH03	W3110 Δ*fadE* Δ*fadD*	This study
Plasmids		
pBGT	pTrc99a carries *alkB, alkG, alkT* from *Pseudomonas putida* P1	This study
pBGT-*fadL*	pBGT carries *fadL* from *E. coli*	This study
pGRB	Amp^R, bla, gRNA expression vector	Li et al., 2015
pREDCas9	Spe^R, Cas9, λ Red recombinase expression vector	Li et al., 2015

TABLE 2 | Primers of plasmid and strain construction.

ptrc99aF	CCATGGAATTCGAGCTCGGTAC
H-ptrc99aR	CTCCTTACCCTTTTTGCGAATTGTTATCCGC TCACAATTCCACAC
AlkB-HF	CGCAAAAAGGGTAAGGAGGTATTATATGAATGG CAAAAGCAGCGTTC
AlkB-R	CTATGATGCTACCGCGGTTG
AlkG-HF	GCGGTAGCATCATAGCTACTATATAGAAAAGAGG AGGTAATTCATGGCTAGGTATCAGTGTCCAG
Alk-R	TTAGCCTAACTTTTCCTGATAGAGTACATAG
AlkT-HF	GAAAAGTTAGGCTAAACCTAATATAATTATTTTAAGGA GGAAAAACATGGCAATTGTTATTGTTGGCGCTG
AlkT-R	GAGCTCGAATTCCATCTAATCAGGTAATT TTATACTCCCGCCAAG
pBGT-F	TCTAGAGTCGACCTGCAGGC
pBGT-R	GGATCCCCGGGTACCGAGC
FadL-F	AGCTCGGTACCCGGGGATCCTTGACAATTA ATCATCCGGCTCGTAT
FadL-R	GCCTGCAGGTCGACTCTAGATCAGAACGCGTAG TTAAAGTTAGTACC
FadE-SF	GCCTGCAGGTCGACTCTAGACCGCCGACCCAATT CATCAG
FadE-SR	AGCTCGGTACCCGGGGATCCCTGATGAATTGGG TCGGCGG
FadE-D1F	AGGTGGAGATCCCCAGCAGTAC
FadE-D1R	CTTTCGGCTCCGTTATTCATAACGAAAAGCC CCTTACTTGTAGGAG
FadE-D2F	CAAGTAAGGGGCTTTTCGTTATGAATAACG GAGCCGAAAGG
FadE-D2R	CGTGTTATCGCCAGGCTTTAGG
FadD-SF	GCCTGCAGGTCGACTCTAGATCCAGTCT GCATCTTTCCGC
FadD-SR	AGCTCGGTACCCGGGGATCCGCGGAAAG ATGCAGACTGGA
FadD-D1F	AAGGGAAAACTCGCCTGGAA
FadD-D1R	TCTGACGACTGACTTAACGCTTCTTCAC CTCTAAAATGCGTGTTC
FadD-D2F	ATTTTAGAGGTGAAGAAGCGTTAAGT CAGTCGTCAGA
FadD-D2R	TAACAGATACCAGACATCCGC

fadE and *fadD* highly increased the yield of ω-hydroxydecanoic acid. In addition, co-expression of the native FA transporter protein, FadL, enhanced the consumption rate of decanoic acid as well as the yield of ω-hydroxydecanoic acid. Octanoic acid and dodecanoic acid were also used as substrates in this hydroxylation system. The results showed that this established system has good efficiency for the synthesis of ω-hydroxyoctanoic acid and ω-hydroxydodecanoic acid. To our knowledge, the current study constitutes the first report of AlkBGT to be applied to FA hydroxylation, and it provides a generalizable framework for the production of medium-chain ω-HFAs via AlkBGT in engineered whole-cell systems. Meanwhile, this study provides a new platform for medium-chain ω-HFA production.

MATERIALS AND METHODS

Strains and Plasmids

The strains and plasmids used in this study are listed in **Table 1**. *E. coli* DH5α was used for plasmid construction, and *E. coli* W3110 was used as the host and initial strain for further genetic manipulation. Ribosome binding sites (RBS) between *alkB-alkG* and *alkG-alkT* were calculated by online software (https://salislab.net/software/forward). The *alkB*, *alkG*, and *alkT* genes with optimized ribosome binding sites were cloned into pTrc99a, and the formed plasmid was named pBGT. The strains with *fadD* and *fadE* deletion were constructed using a CRISPR–Cas9 and λ Red recombination system-based genome editing system, which is composed of five elements: Cas9-expressing cassette, gRNA expression plasmid, λ Red recombination, donor template DNA, and inducible plasmid curing system for eliminating gRNA plasmid from the cells (Li et al., 2015). In brief, to construct the gRNA expression plasmid, the pGRB backbone was amplified by PCR with a pair of primers that included 20-bp spacer sequences specific for the target gene. The PCR product was then ligated via homologous recombination to obtain the desired gRNA expression plasmid. To construct donor dsDNA, a pair of 300–500-bp homologous sequences, which are upstream and downstream sequences of the target gene, were amplified by PCR separately and then fused together by overlapping PCR. The mutant strain was verified with genomic PCR after construction to ensure that the target gene had been deleted. For construction of the AlkBGT and FadL expression plasmids, the one-step cloning method was applied. The primers used in this study are listed in **Table 2**. Gene segments of *alkB*, *alkG*, *alkT* from *P. putida* GPo1 were amplified by PCR. Ribosome binding sites inside the *trc-alkB*, *alkB-alkG*, and *alkG-alkT* genes were calculated by online software version 2.0 (https://salislab.net/software/forward). The *alkB*, *alkG*, and *alkT* genes with optimized ribosome binding sites were cloned into pTrc99a, and the formed plasmid was named pBGT. The native *fadL* was further added behind *alkT* in pBGT with optimized

ribosome binding sites, and the newly formed plasmid was named pBGT-*fadL*.

Media and Culture Conditions

The medium for strain construction and primary preculture was Luria-Bertani Broth (LB), containing tryptone 10 g/L, yeast extract 5 g/L, and sodium chloride 10 g/L. The modified M9 medium used for whole-cell bioconversion contained $Na_2HPO_4{\cdot}12H_2O$ 15.12 g/L, KH_2PO_4 3.0 g/L, NaCl 0.5 g/L, $MgSO_4{\cdot}7H_2O$ 0.5 g/L, $CaCl_2$ 0.011 g/L, 1% (w/v) vitamin B1 0.2 ml/L, glucose 5 g/L, and trace elements solution 0.2 ml/L. The total amount of decanoic acid was ∼500 mg/L. The trace elements solution contained (per liter): $FeCl_3{\cdot}6H_2O$ 5 g; $MnCl_2{\cdot}4H_2O$ 2 g; $ZnCl_2$ 0.684 g; $CoCl_2{\cdot}6H_2O$ 0.476 g, $CuCl_2{\cdot}2H_2O$ 0.17 g; H_3BO_3 0.062 g; $Na_2MoO_4{\cdot}2H_2O$ 0.005 g.

To prepare the cell culture, the primary precultures were prepared by transferring one single colony to 3 ml of LB medium with a specific concentration of antibiotics (ampicillin 100 mg/L) at 37°C overnight. In the secondary precultures, 1 ml of the primary preculture was inoculated into 50 ml of LB medium at 37°C for 8 h. Then, a fresh 1 ml of the secondary preculture was transferred into 500-ml flasks containing 100 ml of LB medium with 2 g/L glucose at 30°C, 220 rpm. The expression of target genes was induced with IPTG when the OD_{600} reached 0.5–0.6, and the cells were grown for 12 h at 30°C. For whole-cell bioconversion, after 12 h of induction, the cells were harvested by centrifugation at 5,945 g and 4°C for 5 min. Then, the cells were washed twice with nitrogen-free M9 medium and resuspended in the modified M9 medium with 20 OD_{600}, with the addition of 0.1% (vol/vol) Triton X-100 depending on the experiment; the total volume was 20 ml. The whole-cell bioconversion was processed at different temperatures (18, 25, 30, and 37°C) for 24 h. All experiments were carried out in triplicate.

Analytical Methods

Cell density was measured at 600 nm at appropriate dilutions (Bausch & Lomb Spectronic 1001). The culture was diluted to the linear range with 0.95% (W/V) NaCl.

For extraction of FA and HFA during bioconversion, 1 ml of supernatant of the cell broth was recovered by centrifuging (13,780 g, 5 min). Then, 1.5 ml of chloroform and 1.5 ml of methanol containing 15% (vol/vol) sulfuric acid were added with 500 μL of 1 g/L undecylic acid as internal standards. The mixtures were mixed by vortexing. Then, the mixtures were exposed at 100°C for 4 h for derivatization. After the heating step, the mixtures were vortexed vigorously for 20 s, stood for 3 min, and operated three times. After centrifugation for 5 min at 1,666 g, the mixture in the tube separated into two layers. The organic layer was recovered by passing through a pipette containing 1 g of anhydrous sodium sulfate for GC analysis.

The concentrations of FFA and HFA in each sample were quantified by the GC-FID system (GC2014, Shimadzu Co., Japan)

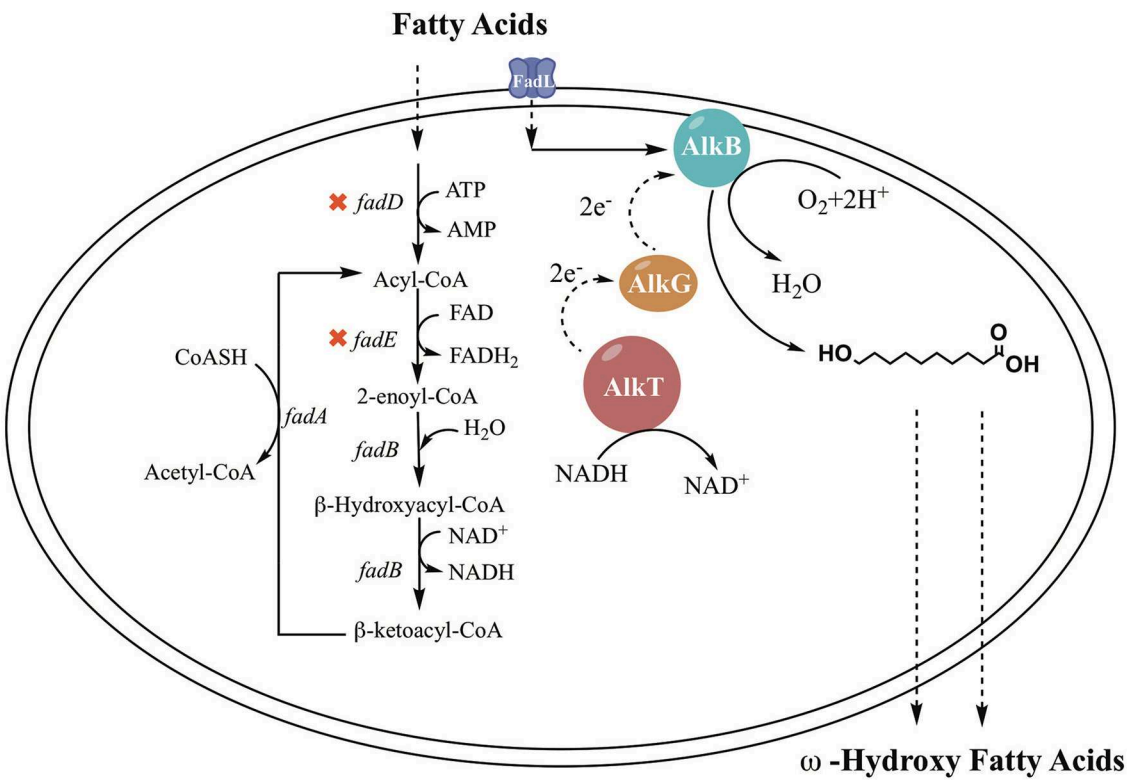

FIGURE 1 | The simplified bioconversion pathways in the engineered *E. coli* strain.

with a flame ionization detector (FID) and a 30-m DB-5 column (30 m × 0.25 mm × 1 m, Agilent Co., Palo Alto, CA). Nitrogen was used as the carrier gas, and the flow rate was set at 1 ml/min. The injector and detector temperatures were both set at 280°C. The oven temperature was initially held at 150°C for 1 min. Thereafter, the temperature was raised with a gradient of 10°C/min until the temperature reached 200°C, then raised with a gradient of 20°C/min until the temperature reached 240°C. This temperature was held for 3 min.

RESULTS AND DISCUSSION

Biosynthesis of ω-Hydroxydecanoic Acid From Decanoic Acid Using the AlkBGT System

In previous studies, it was demonstrated that the AlkBGT system took three steps to achieve ω-oxyfunctionalization of alkane (Jan et al., 2002). The efficiency of AlkBGT co-expression may affect the multistep reactions during ω-HFA biosynthesis. In general, ribosomal interactions with mRNA control translation initiation and the translation rate of proteins (Borujeni et al., 2014). Hence, in this experiment, the AlkBGT encoded by the *alkB*, *alkG*, and *alkT* genes from *P. putida* GPo1 was cloned with optimized RBS into vector pTrc99a (named pBGT) to generate the ω-HFA biosynthetic pathway (**Figure 1**).

Traditionally, the major method for performing bioconversion is to use isolated enzymes *in vitro*; however, this method usually ignores the structural characteristics and metabolic regulation of these enzymes during the overexpression process inside the host cells. *In vivo*, most oxygenases are membrane-bound proteins and have a multi-component structure (Schrewe et al., 2013). Since AlkB is membrane-bound, it seemed to be more efficient to employ whole-cell bioconversion rather than one-pot biocatalysis *in vivo*. To verify the hydroxylation of decanoic acid in the AlkBGT system, the whole-cell bioconversion of W3110(pBGT) was investigated first using W3110(pTrc99a) as a control. In this case, considering the solubility and dispersion status of decanoic acid in the medium, we chose DMSO as the co-solvent and TritonX-100 as the surfactant. Three conditions, specifically sodium fatty acids, fatty acids dissolved in dimethyl sulfoxide (DMSO) and fatty acids dissolved in DMSO containing 10% (vol/vol) Triton X-100, were tested. Approximately 0.5 g/L decanoic acid was added in the bioconversion medium. The experiment was performed at 30°C, and the IPTG concentration was 0.1 mM. The conversion rate and concentrations of ω-hydroxydecanoic acid from W3110(pBGT) in different conditions are shown in **Figure 2**. No ω-hydroxydecanoic acid accumulated in W3110(pTrc99a) (data not shown); however, the strain W3110(pBGT) expressing AlkBGT had the ability to convert decanoic acid to ω-hydroxydecanoic acid. Among these three different substrates, decanoic acid dissolved in DMSO containing 10% (vol/vol) Triton X-100 showed the best performance for ω-hydroxydecanoic acid production. The concentration and yield of ω-hydroxydecanoic acid achieved 123.15 mg/L and 0.24 mol/mol, respectively. The yield was approximately 56.6% higher than that obtained using sodium decanoic acid as the substrate

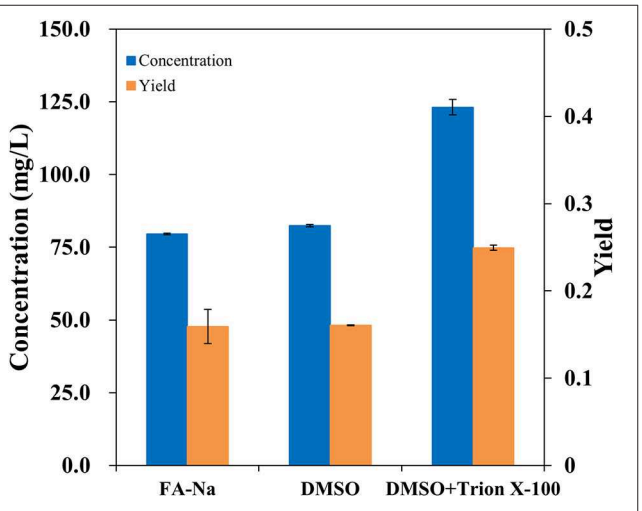

FIGURE 2 | The effects of decanoic acid with differential status in the whole-cell bioconversion of W3110(pBGT) on the concentration (blue) and yield (orange) of ω-hydroxydecanoic acid production.

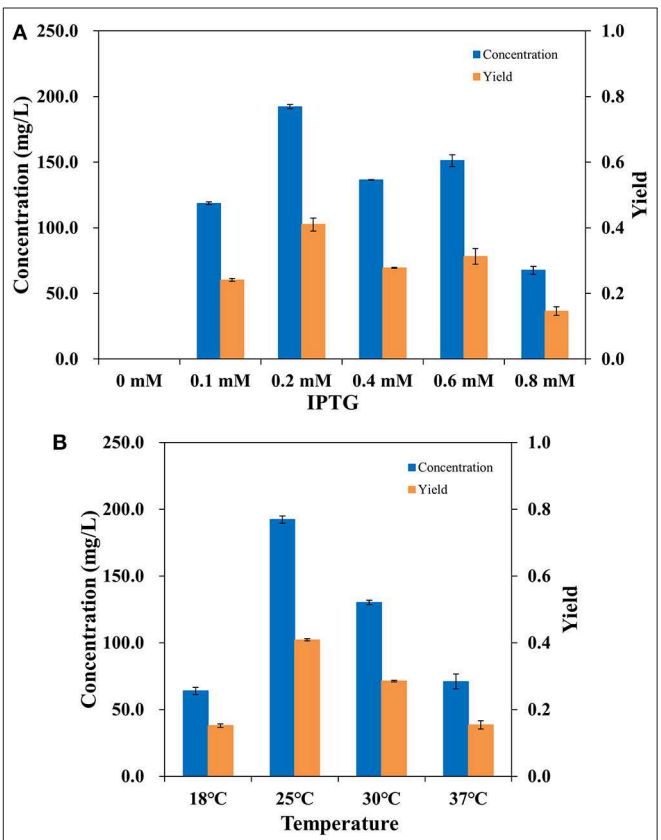

FIGURE 3 | The concentration (blue) and yield (orange) of ω-hydroxydecanoic acid produced by whole-cell conversion of W3110(pBGT) cultured with different concentrations of IPTG **(A)**. The concentration (blue) and yield (orange) of ω-hydroxydecanoic acid produced at different temperatures by the whole-cell conversion of W3110(pBGT) cultured with 0.2 mM IPTG **(B)**.

(**Figure 2**). Hence, decanoic acid dissolved in DMSO containing 10% (vol/vol) Triton X-100 was chosen in further studies. Since AlkBGT are the key enzymes of ω-hydroxydecanoic acid production in whole-cell bioconversion, the optimized expression of AlkBGT will be critical for further improvement of ω-hydroxydecanoic acid production.

Optimization of AlkBGT Expression for ω-Hydroxydecanoic Acid Production

To make the whole-cell system more efficient, the expression level of AlkBGT in W3110(pBGT) was optimized. Different concentrations of IPTG, 0.1, 0.2, 0.4, 0.6, and 0.8 mM, were tested in the cultivation conditions. The culture without the addition of IPTG was selected as the control. Whole-cell bioconversion was performed at 25°C. The yields and concentrations of ω-hydroxydecanoic acid in W3110(pBGT) collected following cultivation with different IPTG concentrations are shown in **Figure 3A**. With 0 mM IPTG addition, no ω-hydroxydecanoic acid accumulated due to the low expression of AlkBGT. The ω-hydroxydecanoic acid yields of whole cells induced by 0.1, 0.4, and 0.6 mM IPTG reached 0.24, 0.27, and 0.31 mol/mol, respectively. The highest concentration of ω-hydroxydecanoic acid was produced with the addition of 0.2 mM IPTG and reached 192.22 mg/L with the highest yield of 0.41 mol/mol (**Figure 3A**). When the concentration of IPTG increased to 0.8 mM, the yield of ω-hydroxydecanoic acid dropped dramatically to only approximately 0.15 mol/mol, which was only 36.6% of that of 0.2 mM IPTG. Hence, this result indicated that 0.2 mM IPTG was the optimum inducing concentration for AlkBGT overexpression in W3110(pBGT), and it was applied in further whole-cell bioconversion experiments.

Incubation temperature affects the catalysis of enzymes during the process of whole-cell bioconversion. To further improve the biocatalysis of AlkBGT in whole-cell bioconversion, four different temperatures, 18, 25, 30, and 37°C, were investigated during bioconversion. The yields and concentrations of ω-hydroxydecanoic acid of W3110(pBGT) in different temperatures are shown in **Figure 3B**. When whole-cell bioconversion was performed at 18 and 37°C, the concentrations of ω-hydroxydecanoic acid were similar, approximately 63.92 and 70.98 mg/L, respectively, with low yields of ω-hydroxydecanoic acid. At 30°C, the concentration and yield of ω-hydroxydecanoic acid on decanoic acid increased to 130.1 mg/L and 0.28 mol/mol, which were approximately two times

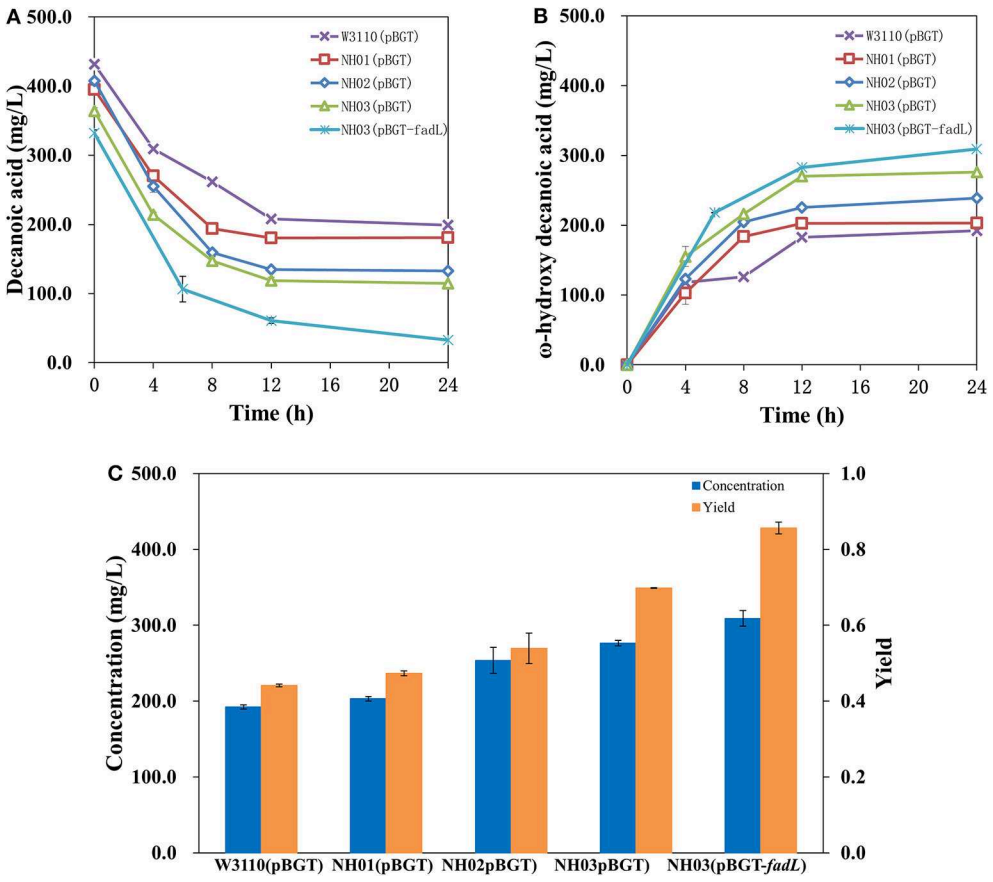

FIGURE 4 | Profiles of decanoic acid (C10FA) consumption and ω-hydroxydecanoic acid (C10HFA) accumulation in the whole-cell bioconversion of W3110(pBGT), NH01(pBGT), NH02(pBGT), NH03(pBGT), and NH03(pBGT-*fadL*). **(A)** The concentration of decanoic acid, **(B)** the concentration of ω-hydroxydecanoic acid. The summary of the concentration (blue) and yield (orange) of ω-hydroxydecanoic acid at the final time point in different engineered strains **(C)**.

higher than those at 18°C. The best result was achieved at 25°C among all of these different temperatures. The highest concentration and yield of ω-hydroxydecanoic acid on decanoic acid reached 192.22 mg/L and 0.41 mol/mol (**Figure 3B**). Therefore, 25°C was the optimum temperature for whole-cell bioconversion and was applied for further studies.

Further Genetic Modification of the FA Degradation Pathway

In a previous study, it was demonstrated that single deletion of *fadD* and *fadE* or double deletion showed high enhancement of FA accumulation (Steen et al., 2010; Li et al., 2012; Cao et al., 2016; Jawed et al., 2016). Hence, it seemed that deletion of *fadE* and *fadD* in *E. coli* might block the β-oxidation of decanoic acid, the precursor of ω-hydroxydecanoic acid, and further enhance the yield of ω-hydroxydecanoic acid. Engineered strains NH01 (Δ*fadE*), NH02 (Δ*fadD*), and NH03 (Δ*fadE* Δ*fadD*) were constructed via a CRISPR-Cas9-based approach. pBGT was transformed into NH01, NH02 and NH03 and formed NH01(pBGT), NH02(pBGT), and NH03(pBGT), respectively. The yields and concentrations of ω-hydroxydecanoic acid of these strains are shown in **Figure 4**. As a result, higher yields of ω-hydroxydecanoic acid were found in these three mutants than in W3110(pBGT). The yield of ω-hydroxydecanoic acid on decanoic acid in NH01(pBGT) achieved 0.47 mol/mol, which was 14.6% higher than that in W3110(pBGT); however, it was 13% lower than that in NH02(pBGT) (0.54 mol/mol). The deletion of *fadD* seemed to prevent decanoic acid degradation more efficiently than the deletion of *fadE*. This result was also consistent with a previous study (Bae et al., 2014). This result might be explained because NH01 with only *fadE* knockout was still able to synthesize Acyl-CoA from FA, and then Acyl-CoA might be utilized further by other metabolic pathways. The highest yield of ω-hydroxydecanoic acid was found in NH03(pBGT) with deletions of both *fadE* and *fadD*, reaching 0.70 mol/mol, which was 70.7% higher than that of W3110(pBGT). Deleting the key genes *fadE* and *fadD* related to the β-oxidation cycle showed large effects on ω-hydroxydecanoic acid accumulation during whole-cell bioconversion due to the reduction of the catabolic degradation of decanoic acid.

Effect of Native *FadI* Overexpression on Enhanced Decanoic Acid Consumption and ω-Hydroxydecanoic Acid Accumulation

Uptake of substrates, especially hydrophobic molecules, into cells through transporter proteins is critical and is one of the

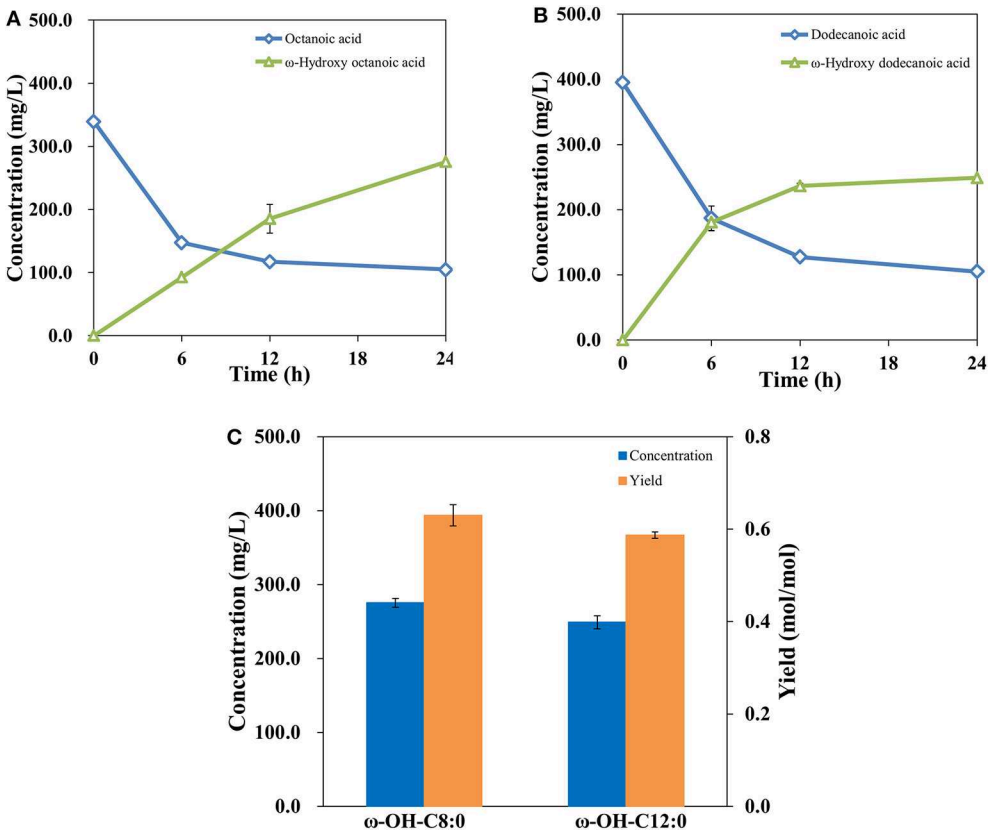

FIGURE 5 | Profiles of octanoic acid (C8FA) consumption and ω-hydroxy octanoic acid (C8HFA) accumulation in whole-cell bioconversion of NH03(pBGT-*fadL*) **(A)**. Profiles of dodecanoic acid (C12FA) consumption and ω-hydroxy dodecanoic acid (C12HFA) accumulation in whole-cell bioconversion of NH03(pBGT-*fadL*) **(B)**. Summary of the concentrations (blue) and yields (orange) of ω-hydroxyoctanoic acid and ω-hydroxydodecanoic acid at the final time point in NH03(pBGT-*fadL*) **(C)**.

limiting steps in whole-cell bioconversion. It was proven by isotopic labeling that the deletion of *fadD* decreased FA transport levels (Weimar et al., 2002). Therefore, an important aspect of enhancing catalysis is to improve transport ability. In this study, overexpression of the transporter AlkL also showed no effect on ether decanoic acid consumption or ω-hydroxydecanoic acid accumulation (data not shown). The outer membrane protein FadL of *E. coli* plays an important role in importing FAs into the cell, and FadL allows the entry of small hydrophobic molecules into the outer membrane through a hydrophobic channel (Call et al., 2016). It was reported that overexpression of *fadL* resulted in increased conversion of long-chain fatty acids to ω-hydroxy long-chain fatty acids (Bae et al., 2014). To determine whether FadL might increase catalysis for ω-hydroxydecanoic acid production, the plasmid pBGT-*fadL* was constructed. The profiles of decanoic acid consumption and ω-hydroxydecanoic acid accumulation in whole-cell bioconversion of NH03(pBGT-*fadL*) are shown in **Figure 4C**. After 24 h of whole-cell bioconversion, 308.98 mg/L ω-hydroxydecanoic acid was observed, and the yield of ω-hydroxydecanoic acid on decanoic acid reached 0.86 mol/mol. The yield of ω-hydroxydecanoic acid on decanoic acid in NH03(pBGT-*fadL*) increased by ∼22.8 and 110% relative to yields of the strains NH03(pBGT) and W3110(pBGT), respectively (**Figure 4C**). FadL overexpression increased the concentration and yield of ω-hydroxydecanoic acid, which might be because the expression of the transporter FadL enhanced the availability of decanoic acid for the AlkBGT hydroxylation system inside the cell. It was reported that a *Pseudomonas aeruginosa* outer membrane protein, ExFadLO, which belongs to the family of FadL proteins, was involved in the export of long-chain oxygenated fatty acids. According to a 3D model structure, ExFadLO had similar features and structural conformation to those described for previously crystallized FadL transporters from *E. coli* (Martínez et al., 2013). However, no conclusive evidence has been obtained for this hypothesis.

Biosynthesis of ω-Hydroxyoctanoic Acid and ω-Hydroxydodecanoic Acid

The study above suggested that a ω-hydroxydecanoic acid biosynthesis system with high efficiency has been established. It was demonstrated that AlkBGT is known to catalyze the oxyfunctionalization of medium-chain alkanes and fatty acids (Kusunose et al., 1964; Eggink et al., 1987). To further explore the substrate spectrum of this engineered whole-cell catalysis system of NH03 (pBGT-*fadL*), octanoic acid and dodecanoic acid, which are medium-chain fatty acids, were employed as substrates. The results are shown in **Figures 5A,B**. The bioconversion process of octanoic acid and dodecanoic acid was similar to that of decanoic acid. In the initial phase, highly increased product concentrations and decreased substrate levels were observed, whereas after 12 h of incubation, the rates of product accumulation and substrate consumption became slow. At 24 h, the accumulation of ω-hydroxyoctanoic acid reached 275.48 mg/L, and the yield of ω-hydroxyoctanoic acid on octanoic acid was 0.63 mol/mol. The accumulation of ω-hydroxydodecanoic acid reached 249.03 mg/L with a yield of 0.59 mol/mol (**Figure 5C**). It was noted that there are differences in efficiency among different fatty acid chain lengths. This phenomenon is consistent with a previous report, and it may be attributed to a specific amino acid position in the substrate-binding pocket of AlkB that determines the length of substrate (van Beilen et al., 2005). In the process of substrate uptake, small hydrophobic compounds can easily diffuse into the cell, but large hydrophobic molecules might be restrained by the outer membrane to some extent. However, most hydrophobic substrates are often toxic to living cells, and toxic substances that are detrimental impact bioconversion negatively, which is the major drawback in production (Scheps et al., 2013). Thereby, the lower bioconversion efficiency of octanoic acid than decanoic acid was probably caused by the variable toxicity of different chain lengths of fatty acids that accumulated in cells.

CONCLUSION

In this study, several strategies were applied to enhance the whole-cell bioconversion of strains, including optimized overexpression of *alkBGT* from *P. putida* GPo1, deletion of the FA β-oxidation-associated key enzymes FadE and FadD, and overexpression of the native FadL. The concentrations of ω-hydroxyoctanoic acid, ω-hydroxydecanoic acid and ω-hydroxydodecanoic acid in NH03(pBGT-*fadL*) reached 275.48, 308.98, and 249.03 mg/L, respectively. The yields reached 0.63, 0.86, and 0.56 mol/mol, respectively. This study demonstrated the great potential of these engineered strains for the production of ω-hydroxy medium-chain fatty acids from medium-chain fatty acids by whole-cell bioconversion.

DATA AVAILABILITY STATEMENT

All datasets generated for this study are included in the manuscript/supplementary files.

AUTHOR CONTRIBUTIONS

HW, GB, and K-YS designed the experiments. QH performed the research experiments. QH, GB, K-YS, and HW analysis the data. QH and HW wrote the manuscript. All authors read and approved the final manuscript.

FUNDING

This study was supported by the National Key Research and Development Program of China (Grant No. 2017YFB0309302), the National Natural Science Foundation of China (Grant No. 21776083), the Fok Ying-Tong Education Foundation, China (Grant No. 161017), the Fundamental Research Funds for the Central Universities (Grant No. 22221818014), and the 111 Project (B18022), the Science and Technology Commission of Shanghai Municipality (Grant No. 17JC1404800). This study was partially supported by the Open Funding Project of the State Key Laboratory of Bioreactor Engineering.

REFERENCES

Ahsan, M., Patil, M., Jeon, H., Sung, S., Chung, T., and Yun, H. (2018). Biosynthesis of nylon 12 monomer, ω-aminododecanoic acid using artificial self-sufficient P450, AlkJ and ω-TA. *Catalysts* 8:400. doi: 10.3390/catal8090400

Bae, J.H., Park, B.G., Jung, E., Lee, P.G., and Kim, B.G. (2014). *fadD* deletion and *fadL* overexpression in *Escherichia coli* increase hydroxy long-chain fatty acid productivity. *Appl. Microbiol. Biotechnol.* 98, 8917–8925. doi: 10.1007/s00253-014-5974-2

Beilen, V. J. B., Penninga, D., and Witholt, B. (1992). Topology of the membrane-bound alkane hydroxylase of *Pseudomonas oleovorans*. *J. Biol. Chem.* 267:17.

Biermann, U., Bornscheuer, U., Meier, M.A., Metzger, J.O., and Schäfer, H.J. (2011). Oils and fats as renewable raw materials in chemistry. *Angew. Chem. Int. Ed.* 50, 3854–3871. doi: 10.1002/anie.201002767

Bonen, A., Chabowski, A., Luiken, J. J., and Glatz, J.F. (2007). Is membrane transport of FFA mediated by lipid, protein, or both? Mechanisms and regulation of protein-mediated cellular fatty acid uptake: molecular, biochemical, and physiological evidence. *Physiology* 22, 15–29. doi: 10.1152/physiologyonline.2007.22.1.15

Bordeaux, M., Galarneau, A., and Drone, J. (2012). Catalytic, mild, and selective oxyfunctionalization of linear alkanes: current challenges. *Angew. Chem. Int. Ed.* 51, 10712–10723. doi: 10.1002/anie.201203280

Borujeni, E.A., Channarasappa, S.A., and Salis, M.H. (2014). Translation rate is controlled by coupled trade-offs between site accessibility, selective RNA unfolding and sliding at upstream standby sites. *Nucleic Acids Res.* 42, 2646–2659. doi: 10.1093/nar/gkt1139

Bowen, C. H., Bonin, J., Kogler, A., Barba-Ostria, C., and Zhang, F. (2016). Engineering *Escherichia coli* for conversion of glucose to medium-chain ω-hydroxy fatty acids and α,ω-dicarboxylic acids. *ACS Synth. Biol.* 18, 200–206. doi: 10.1021/acssynbio.5b00201

Bule, M., Luo, Y., Bennett, G., Karanjikar, M., Rooney, W., and San, K.-Y. (2016). Direct bioconversion of sorghum extract sugars to free fatty acids using metabolically engineered *Escherichia coli* strains: value addition to the sorghum bioenergy crop. *Biomass Bioenergy* 93, 217–226. doi: 10.1016/j.biombioe.2016.07.020

Call, T.P., Akhtar, M.K., Baganz, F., and Grant, C. (2016). Modulating the import of medium-chain alkanes in *E. coli* through tuned expression of FadL. *J. Biol. Eng.* 10:5. doi: 10.1186/s13036-016-0026-3

Cao, Y., Cheng, T., Zhao, G., Niu, W., Guo, J., Xian, M., et al. (2016). Metabolic engineering of *Escherichia coli* for the production of hydroxy fatty acids from glucose. *BMC Biotechnol.* 16:26. doi: 10.1186/s12896-016-0257-x

Cao, Y., and Zhang, X. (2013). Production of long-chain hydroxy fatty acids by microbial conversion. *Appl. Microbiol. Biotechnol.* 97, 3323–3331. doi: 10.1007/s00253-013-4815-z

Cheng, L., Miao, M., Zhang, T., Jiang, B., and Mu, W.M. (2010). Advances on research of antifungal lactic acid bacteria as a biopreservative in food industry:a review. *Food Fermentat. Ind.* 36, 129–133.

Craft, D.L., Madduri, K.M., Eshoo, M., and Wilson, C.R. (2003). Identification and characterization of the CYP52 family of *Candida tropicalis* ATCC 20336, important for the conversion of fatty acids and alkanes to α, ω-dicarboxylic acids. *Appl. Environ. Microbiol.* 69, 5983–5991. doi: 10.1128/aem.69.10.5983-5991.2003

Cross, K.C., Lionel, H., Opie, and Radda, A.G.K. (1995). Is lactate-induced myocardial ischaemic injury mediated by decreased pH or increased intracellular lactate? *J. Mol. Cell Cardiol.* 27, 1369–1381. doi: 10.1006/jmcc.1995.0130

Eggink, G., Lageveen, R.G., Altenburg, B., and Witholt, B. (1987). Controlled and functional expression of the *Pseudomonas oleovorans* alkane utilizing system in *Pseudomonas putida* and *Escherichia coli*. *J. Biol. Chem.* 262, 11712–11718.

Eschenfeldt, W.H., Zhang, Y., Samaha, H., Stols, L., Eirich, L.D., Wilson, C.R., et al. (2003). Transformation of fatty acids catalyzed by cytochrome P450 monooxygenase enzymes of *Candida tropicalis*. *Appl. Environ. Microbiol.* 69, 5992–5999. doi: 10.1128/aem.69.10.5992-5999.2003

Fer, M., Corcos, L., Dréano, Y., Plée-Gautier, E., Salaun, J.P., Berthou, F., et al. (2008). Cytochromes P450 from family 4 are the main omega hydroxylating enzymes in humans: CYP4F3B is the prominent player in PUFA metabolism. *J. Lipid Res.* 49, 2379–2389. doi: 10.1194/jlr.m800199-jlr200

Grant, C., Woodley, J.M., and Baganz, F. (2011). Whole-cell bio-oxidation of n-dodecane using the alkane hydroxylase system of *P. putida* GPo1 expressed in *E. coli*. *Enzyme Microb. Technol.* 48, 480-486. doi: 10.1016/j.enzmictec.2011.01.008

Grund, A., Shapori, J., Fennewald, M., Bacha, P., Leahy, J., Markbreiter, K., et al. (1975). Regulation of alkane oxidation in *Pseudomonas putida*. *J. Bacteriol.* 123, 546–556.

Handke, P., Lynch, S.A., and Gill, R.T. (2011). Application and engineering of fatty acid biosynthesis in *Escherichia coli* for advanced fuels and chemicals. *Metab. Eng.* 13, 28–37. doi: 10.1016/j.ymben.2010.10.007

Jan, B.N. M., Smits, T.H.M., Roth, C., Balada, S. B., and Witholt, B. (2002). Rubredoxins involved in alkane oxidation. *J. Bacteriol.* 184, 1722–1732. doi: 10.1128/jb.184.6.1722-1732.2002

Jawed, K., Mattam, A.J., Fatma, Z., Wajid, S., Abdin, M.Z., and Yazdani, S.S. (2016). Engineered production of short chain fatty acid in *Escherichia coli* using fatty acid synthesis pathway. *PLoS ONE* 11:e0160035. doi: 10.1371/journal.pone.0160035

Jeon, E.Y., Song, J.W., Cha, H.J., Lee, S.M., Lee, J., and Park, J.B. (2018). Intracellular transformation rates of fatty acids are influenced by expression of the fatty acid transporter FadL in *Escherichia coli* cell membrane. *J. Biotechnol.* 281, 161–167. doi: 10.1016/j.jbiotec.2018.07.019

Joo, S.-Y., Yoo, H.-W., Sarak, S., Kim, B.-G., and Yun, H. (2019). Enzymatic synthesis of ω-hydroxydodecanoic acid by employing a cytochrome P450 from *Limnobacter sp*. 105 MED. *Catalysts* 9:54. doi: 10.3390/catal9010054

Julsing, M.K., Schrewe, M., Cornelissen, S., Hermann, I., Schmid, A., and Buhler, B. (2012). Outer membrane protein AlkL boosts biocatalytic oxyfunctionalization of hydrophobic substrates in *Escherichia coli*. *Appl. Environ. Microbiol.* 78, 5724–5733. doi: 10.1128/aem.00949-12

Kadisch, M., Julsing, M. K., Schrewe, M., Jehmlich, N., Scheer, B., von Bergen, M., et al. (2017). Maximization of cell viability rather than biocatalyst activity improves whole-cell ω-oxyfunctionalization performance. *Biotechnol. Bioeng.* 114, 874–884. doi: 10.1002/bit.26213

Kirtz, M., Klebensberger, J., Otte, K.B., Richter, S.M., and Hauer, B. (2016). Production of -hydroxy octanoic acid with *Escherichia coli*. *J. Biotechnol.* 20, 30–33. doi: 10.1016/j.jbiotec.2016.05.017

Koay, G.F.L., Chuah, T.-G., Zainal-Abidin, S., Ahmad, S., and Choong, T.S.Y. (2011). Development, characterization and commercial application of palm based dihydroxystearic acid and its derivatives: an overview. *J. Oleo Sci.* 60, 237–265. doi: 10.5650/jos.60.237

Kusunose, M., Kusunose, E., and Coon, J. M. (1964). Enzymatic ω-oxidation of fatty acids. *J. Biol. Chem.* 239, 1374–1380. doi: 10.1201/b18138-5

Lennen, R.M., and Pfleger, B.F. (2012). Engineering *Escherichia coli* to synthesize free fatty acids. *Trends Biotechnol.* 30, 659–667. doi: 10.1016/j.tibtech.2012.09.006

Li, H., Pinot, F., Sauveplane, V., Werck-Reichhart, D., Diehl, P., Schreiber, L., et al. (2010). Cytochrome P450 family member CYP704B2 catalyzes the ω-hydroxylation of fatty acids and is required for anther cutin biosynthesis and pollen exine formation in rice. *Plant. Cell* 22, 173–190. doi: 10.1105/tpc.109.070326

Li, M., Zhang, X., Agrawal, A., and San, K.Y. (2012). Effect of acetate formation pathway and long chain fatty acid CoA-ligase on the free fatty acid production in *E. coli* expressing acy-ACP thioesterase from *Ricinus communis*. *Metab. Eng.* 14, 380–387. doi: 10.1016/j.ymben.2012.03.007

Li, Y., Lin, Z., Huang, C., Zhang, Y., Wang, Z., Tang, Y.J., et al. (2015). Metabolic engineering of *Escherichia coli* using CRISPR-Cas9 meditated genome editing. *Metab. Eng.* 31, 13–21. doi: 10.1016/j.ymben.2015.06.006

Lin, B., and Tao, Y. (2017). Whole-cell biocatalysts by design. *Microb. Cell Fact.* 16:106. doi: 10.1186/s12934-017-0724-7

Liu, C., Liu, F., Cai, J., Xie, W., Long, T.E., Turner, S.R., et al. (2011). Polymers from fatty acids: poly(ω-hydroxyl tetradecanoic acid) synthesis and physico-mechanical studies. *Biomacromolecules* 12, 3291–3298. doi: 10.1021/bk-2012-1105.ch009

Manfred, S., Magnusson, O.A., Christian, W., Bruno, B., and Andreas, S. (2011). Kinetic analysis of terminal and unactivated C-H bond oxyfunctionalization in fatty acid methyl esters by monooxygenase-based whole-cell biocatalysis. *Adv. Synth. Catal.* 353, 3485–3495. doi: 10.1002/adsc.201100440

Martínez, E., Estupiñán, M., Pastor, F. I., Busquets, M., Díaz, P., and Manresa, A. (2013). Functional characterization of ExFadLO, an outer membrane protein required for exporting oxygenated long-chain fatty acids in *Pseudomonas aeruginosa*. *Biochimie* 95, 290–298. doi: 10.1016/j.biochi.2012.09.032

Menno, K.R., Mark, P.G., Van, D.L., Philip, R., Jaap, K., Philip, H.V.L., et al. (1989). The *Pseudomonas oleovorans* alkane hydroxylase gene. Sequence and expression. *J. Biol. Chem.* 264, 5534–5541.

Picataggio, S., Rohrer, T., Deanda, K., Lanning, D., Reynolds, R., Mielenz, J., et al. (1992). Metabolic engineering of *Candida tropicalis* for the production of long-chain dicarboxylic acids. *Nature* 10:5. doi: 10.1038/nbt0892-894

Scheps, D., Honda Malca, S., Richter, S.M., Marisch, K., Nestl, B.M., and Hauer, B. (2013). Synthesis of ω-hydroxy dodecanoic acid based on an engineered CYP153A fusion construct. *Microb. Biotechnol.* 6, 694–707. doi: 10.1111/1751-7915.12073

Schrewe, M., Julsing, M.K., Buhler, B., and Schmid, A. (2013). Whole-cell biocatalysis for selective and productive C-O functional group introduction and modification. *Chem. Soc. Rev.* 42, 6346–6377. doi: 10.1039/c3cs60011d

Steen, E.J., Kang, Y., Bokinsky, G., Hu, Z., Schirmer, A., Mcclure, A., et al. (2010). Microbial production of fatty-acid-derived fuels and chemicals from plant biomass. *Nature* 463, 559–562. doi: 10.1038/nature08721

Sugiharto, Y.E.C., Lee, H., Fitriana, A.D., Lee, H., Jeon, W., Park, K., et al. (2018). Effect of decanoic acid and 10-hydroxydecanoic acid on the biotransformation of methyl decanoate to sebacic acid. *AMB Express.* 8:75. doi: 10.1186/s13568-018-0605-4

Sung, C., Jung, E., Choi, K. Y., Bae, J. H., Kim, M., Kim, J., et al. (2015). The production of ω-hydroxy palmitic acid using fatty acid metabolism and cofactor optimization in *Escherichia coli*. *Appl. Microbiol. Biotechnol.* 99, 6667–6676. doi: 10.1007/s00253-015-6630-1

Tan, Z., Black, W., Yoon, J. M., Shanks, J. V., and Jarboe, L. R. (2017). Improving *Escherichia coli* membrane integrity and fatty acid production by expression tuning of FadL and OmpF. *Microb. Cell Fact.* 16:38. doi: 10.1186/s12934-017-0650-8

Tsai, Y. F., Luo, W. I., Chang, J. L., Chang, C. W., Chuang, H. C., Ramu, R., et al. (2017). Electrochemical hydroxylation of C3-C12 n-alkanes by recombinant alkane hydroxylase (AlkB) and rubredoxin-2 (AlkG) from *Pseudomonas putida* GPo1. *Sci. Rep.* 7:8369. doi: 10.1038/s41598-017-08610-w

USDA (2018). *World Agricultural Supply and Demand Estimates*. Washington, DC: United States Department of Agriculture.

van Beilen, J. B., Smits, T. H., Roos, F. F., Brunner, T., Balada, S. B., Röthlisberger, M., et al. (2005). Identification of an amino acid position that determines the substrate range of integral membrane alkane hydroxylases. *J. Bacteriol.* 187, 85–91. doi: 10.1128/JB.187.1.85-91.2005

van den Berg, B. (2005). The FadL family: unusual transporters for unusual substrates. *Curr. Opin. Struct. Biol.* 15, 401–407. doi: 10.1016/j.sbi.2005.06.003

van Nuland, Y. M., Eggink, G., and Weusthuis, R. A. (2016). Application of AlkBGT and AlkL from *Pseudomonas putida* GPo1 for selective alkyl ester ω-oxyfunctionalization in *Escherichia coli*. *Appl. Environ. Microbiol.* 82, 3801–3807. doi: 10.1128/aem.00822-16

Wang, D., Wu, H., Thakker, C., Beyersdorf, J., Bennett, G.N., and San, K.-Y. (2015). Efficient free fatty acid production in engineered *Escherichia coli* strains using soybean oligosaccharides as feedstock. *Biotechnol. Prog.* 31, 686–694. doi: 10.1002/btpr.2092

Weimar, D. J., DiRusso, C.C., Delio, R., and Black, N.P. (2002). Functional role of fatty acyl-coenzyme A synthetase in the transmembrane movement and activation of exogenous long-chain fatty acids. *J. Biol. Chem.* 277, 29369–29376. doi: 10.1074/jbc.m107022200

Weng, P.F., and Wu, Z.F. (2008). Advances of hydroxyl fatty acids production by bioconversion of fatty acids with microbe. *J. Chin. Cereals Oil Assoc.* 23, 203–206.

Wu, H., and San, K.-Y. (2014). Efficient odd straight medium chain free fatty acid production by metabolically engineered *Escherichia coli*. *Biotechnol. Bioeng.*111, 2209–2219. doi: 10.1002/bit.25296

Wu, J., Wang, Z., Zhang, X., Zhou, P., Xia, X., and Dong, M. (2019). Improving medium chain fatty acid production in *Escherichia coli* by multiple transporter engineering. *Food Chem.* 30, 628–634. doi: 10.1016/j.foodchem.2018.08.102

Xiao, K., Yue, X.-H., Chen, W.-C., Zhou, X.-R., Wang, L., Xu, L., et al. (2018). Metabolic engineering for enhanced medium chain omega hydroxy fatty acid production in *Escherichia coli*. *Front. Bioeng. Biotechnol.* 9, 1–13. doi: 10.3389/fmicb.2018.00139

Conflict of Interest: The authors declare that the research was conducted in the absence of any commercial or financial relationships that could be construed as a potential conflict of interest.

frontiers in Bioengineering and Biotechnology

ORIGINAL RESEARCH
published: 22 October 2019
doi: 10.3389/fbioe.2019.00245

High Di-rhamnolipid Production Using *Pseudomonas aeruginosa* KT1115, Separation of Mono/Di-rhamnolipids, and Evaluation of Their Properties

Jie Zhou[1], *Rui Xue*[1], *Shixun Liu*[1], *Ning Xu*[1], *Fengxue Xin*[1,2], *Wenming Zhang*[1,2], *Min Jiang*[1,2] *and Weiliang Dong*[1,2]*

[1] State Key Laboratory of Materials-Oriented Chemical Engineering, College of Biotechnology and Pharmaceutical Engineering, Nanjing Tech University, Nanjing, China, [2] Jiangsu National Synergetic Innovation Center for Advanced Materials (SICAM), Nanjing Tech University, Nanjing, China

Rhamnolipids (RLs) are important bioproducts that are regarded as promising biosurfactant for applications in oil exploitation, cosmetics, and food industry. In this study, the newly isolated *Pseudomonas aeruginosa* KT1115 showed high production of di-RLs. The highest yield of RLs by *P. aeruginosa* KT1115, reaching 44.39 g/L after 8 days of fermentation in a 5 L bioreactor, was obtained from rapeseed oil-nitrate medium after process optimization. Furthermore, we established a new separation process that achieved up to 91.82% RLs recovery with a purity of 89% and further obtained mono/di-rhamnolipids. Finally, ESI-MS analysis showed that the RLs produced by strain KT1115 have a high proportion of di-RLs (mono-RLs: di-RLs = 11.47: 88.53), which have a lower critical micelle-forming concentration (8 mN/m) and better emulsification ability with kerosene (52.1% EI_{24}) than mono-RLs (167 mN/m and 41.4% EI_{24}, respectively). These results demonstrated that *P. aeruginosa* KT1115 is a potential industrial producer of di-RLs, which have improved applicability and offer significant commercial benefits.

Keywords: high-yielding, di-rhamnolipids, separation, CMC, emulsifying activity

OPEN ACCESS

Edited by:
Rongming Liu,
University of Colorado Boulder, United States

Reviewed by:
Ulyana Shimanovich,
Weizmann Institute of Science, Israel
Yongjun Wei,
Zhengzhou University, China

***Correspondence:**
Weiliang Dong
dwl@njtech.edu.cn

Specialty section:
This article was submitted to Industrial Biotechnology, a section of the journal Frontiers in Bioengineering and Biotechnology

Received: *10 July 2019*
Accepted: *13 September 2019*
Published: *22 October 2019*

Citation:
Zhou J, Xue R, Liu S, Xu N, Xin F, Zhang W, Jiang M and Dong W (2019) High Di-rhamnolipid Production Using Pseudomonas aeruginosa KT1115, Separation of Mono/Di-rhamnolipids, and Evaluation of Their Properties. Front. Bioeng. Biotechnol. 7:245. doi: 10.3389/fbioe.2019.00245

INTRODUCTION

Rhamnolipids (RLs), which are mainly produced by *Pseudomonas aeruginosa*, are the most intensively studied glycolipid biosurfactants (Seul Ki et al., 2011; Sodagari et al., 2013). Rhamnolipid surfactants were shown to reduce the surface tension of water from 72 to 28 mN/m, and the interfacial tension of water-oil systems from 43 to <1 mN/m (Liang-Ming et al., 2008). RLs have significant advantages in emulsification, wetting, dispersion, dissolution, and decontamination. Consequently, they have been widely used in oil exploration, cosmetics, food, and other industries owing to their high specificity, biodegradability, and biocompatibility (Mulligan, 2005).

RLs are synthesized by covalently linking one or two rhamnose moieties with one or two hydroxy fatty acids, and the corresponding types are designated as mono- or di-RLs based on the number of rhamnose units (Rendell et al., 1990). The components and properties of RLs are profoundly influenced by the producing strains and cultivation conditions (Rahman et al., 2010). For instance, the ratio of mono- and di-RLs produced by *P. aeruginosa* mainly lies between 40:60 and 30:70

(Matasandoval et al., 1999; Jadhav et al., 2018). The percentage of mono-RLs even reaches 68.35% of the total RL content produced by *P. aeruginosa* MN1 (Arino et al., 1996; Samadi et al., 2012). Compared to mono-RLs, di-RLs possess higher surface activity, and therefore show great potential in oily sludge dewatering and lignocellulose degradation (Xuwei et al., 2013; Jiang et al., 2014). However, there is little available information in terms of systematic comparative analysis of the physicochemical properties of mono- and di-RLs.

To better understand the characteristics of different RLs components, separation, and purification are the first and most important step. More than half of the cost of RLs production is due to downstream processing, and is still no economical and reliable downstream technology for the recovery and purification of RLs at the industrial scale (Roger and Banat, 2012; Rienzo et al., 2016). The most commonly employed separation techniques for the isolation of RLs from the fermentation broth include foam separation, membrane separation and adsorption (Isa et al., 2007; Rienzo et al., 2016; Jadhav et al., 2018). However, these methods are mainly used for crude RLs separation, and the lack of a quick and effective separation method is the main bottleneck holding back research on mono- and di-RLs.

In our previous study, a RLs-producing strain was successfully isolated from oil-contaminated soil, and was identified as *P. aeruginosa* KT1115. To achieve high RLs production using *P. aeruginosa* KT1115, process optimization in a rapeseed oil-nitrate medium was first conducted. Afterwards, a rapid and efficient purification and separation method for mono- and di-RLs was established. Finally, a comprehensive physicochemical characterization of the isolated mono- and di-RLs was carried out.

MATERIALS AND METHODS

Strains, Media, and Culture Conditions

Pseudomonas aeruginosa KT1115 was isolated from soil samples using CTAB screening (Varjani and Upasani, 2016). Luria-Bertani (LB) medium containing 10 g/L tryptone, 5 g/L yeast extract and 10 g/L NaCl was used for seed culture. The rapeseed oil-nitrate medium (RON) containing 60 g/L rapeseed oil (Jinlongyu, China), 6 g/L $NaNO_3$, 3 g/L yeast extract, 1 g/L KH_2PO_4, 1 g/L Na_2HPO_4, 0.1 g/L $CaCl_2{\cdot}2H_2O$, and 0.1 g/L $MgSO_4$ was used for fermentation.

All chemicals and solvents were of analytical grade and purchased from Sahn Chemical Technology Co. Ltd. (Shanghai, China). Aliquots comprising 100 mL seed and fermentation medium were dispensed into Erlenmeyer flasks (500 mL) and sterilized at 121°C for 20 min. Seed culture and bacterial fermentation were performed at 37°C and 180 rpm for 8 days. All experiments were performed in triplicates.

Single-Factor Optimization

Single factor experiments were applied to optimize the liquid fermentation conditions. The influence of different pH values (5.5, 6, 6.5, 7, 7.5, 8, and 9) concentrations of metals including calcium (0, 0.5, 1, 5, and 10 mM) and magnesium (0, 0.5, 1, 2, 5, and 10 mM), rapeseed oil concentrations (10, 20, 40, 60, 80, and 100 g/L), yeast extract concentrations (0, 3, 6, 9, and 12 g/L), $NaNO_3$ concentrations (0, 3, 6, 9, and 12 g/L), KH_2PO_4 concentrations (0, 1, 2, 5, 10, 20, and 50 g/L), Na_2HPO_4 concentrations (0, 1, 2, 5, 10, 20, and 50 g/L), and different inoculum sizes (1, 5, 10, 15, and 20%) on the production of RLs was evaluated. Quantitative analysis of rhamnolipids was conducted using anthrone colorimetry (Heyd et al., 2008).

Extraction and Purification of Rhamnolipids

RLs products were extracted based on a procedure described previously (Déziel et al., 1999), with minor modifications as follows: The bacterial cells were first removed by centrifugation (15,000 × g, 20 min), after which different concentrations of ethanol (10, 20, 30, 40, and 50%) were added to the supernatant to precipitate proteins. The samples were kept at 4°C for different times (3, 6, 9, and 18 h). The supernatants were centrifuged at 15,000 × g for 10 min, and the pH value was adjusted to 2.0 using different acids (H_3PO_4, H_4SO_4, HCl, and HNO_3). Then, the acidified supernatants were kept at 4°C for different times (3, 6, 9, and 18 h) to precipitate the RLs. The precipitates were centrifuged 15,000 × g for 10 min and the crude RLs were placed into a drying oven at 90°C for 10 h. After that, petroleum ether was added to the anhydrous precipitated RLs for purification and centrifugation (15,000 × g for 10 min) to obtain the purified rhamnolipids, which were used for further analysis.

ESI-MS Analysis

The RLs were dissolved in methanol solution, and RLs solutions with a concentration of 1 mg/mL were prepared for congener composition analysis by electrospray ionization mass spectrometry (ESI-MS). The ESI mass spectrum in negative ion mode was acquired using a capillary voltage of −3.5 kV, fragmentation voltage of 50 V and nitrogen as desolvation gas, which was heated to 325°C, at flow rate of 7 L/min. ESI tandem mass spectra were acquired by mass-selecting the target ion using the quadrupole mass analyzer followed by 20 eV collision-induced dissociation using nitrogen in the collision cell. The mass spectrometer was operated in negative ion mode scanning in the 50–1,000 m/z range.

Separation of Mono- and Di-rhamnolipids

Silica gel column chromatography was used to further separate mono-/di-RLs. The sample was loaded on top of the silica gel column and eluted with five different chloroform-methanol solvent systems of gradually increasing polarity. The five mobile phases $CHCl_3$:CH_3OH (v/v) were used in sequence: solution I was chloroform (100%), which was primarily used to remove the neutral lipids and other impurities, and solution II, solution III was chloroform/methanol (v/v) 97:3, which was primarily used to elute the mono-RLs and solution IV, solution V (chloroform/methanol = 93:7) to elute the di-RLs. Finally, the separation result was visualized by thin layer chromatography (TLC) using chloroform/methanol/H_2O (65:7:2) as mobile phase (Samadi et al., 2012).

Determination of Critical Micelle Concentrations

Aqueous solutions of the RLs at different concentrations solutions (0–1,000 mg/L) were prepared to determine the critical micelle concentration (CMC) using the break point of the surface tension vs. the log of the bulk concentration curve. For the calibration of the instrument, the surface tension of pure water was measured before each set of experiments. These experiments were conducted in triplicates and the results were presented as averages.

Analysis of Emulsifying Activity

Solutions of the extracted RLs and purified mono/di-RLs at a concentration of 100 mg/L were prepared to determine the emulsification index, and compared with SDS and Tween 80 under the same conditions. A hydrophobic phase comprising 4 mL of hydrophobic organics (kerosene, liquid paraffin, and n-hexane, respectively) was mixed with 4 mL of the RLs solutions in the test tubes. The tubes were stirred using a vortex mixer for 2 min and the height of the emulsion layer was measured after 24 h to determine the emulsification index (EI_{24}(%); Lovaglio et al., 2011).

Evaluation of the Stability of the Extracted RLs and Purified Mono/Di-RLs

The EI_{24} index were measured using liquid paraffin as emulsion phase to evaluate the stability of the extracted RLs and purified mono/di-RLs at a concentration of 100 mg/L. H_3PO_4 and NaOH at a concentration of 1 M were used to adjust the pH values. A series of solutions comprising 20 mL of RLs fraction were treated at different temperatures (4, 10, 20, 30, 40, 50, 60, 70, 80, and 90°C), different pH values (2, 4, 6, 8, 10, and 12), and different salinities (NaCl concentrations of 0, 1, 2, 4, 6, 8, 10, and 12%).

RESULTS AND DISCUSSION

Fermentation Optimization

The color change of the anthrone reagent is positively associated with the rhamnolipid concentration (100–800 mg/L). The linear correlation model between the diameters of oil spreading circle (y) and rhamnolipid concentrations (x) was described by an empirical equation as follows: $y = 330.21 \times -22.34$ ($R^2 = 0.9979$). According to the color change of the anthrone reagent, the amount of RLs in the culture was calculated using two positive linear correlation models. The single factor experiments showed that the medium composition and optimal fermentation conditions leading to the highest RLs production encompassed 60 g/L rapeseed oil, 6 g/L $NaNO_3$, 3 g/L yeast extract, 1 g/L KH_2PO_4, 1 g/L Na_2HPO_4, 0.1 g/L $CaCl_2{\cdot}2H_2O$, 0.1 g/L $MgSO_4$, and inoculation at 1% inoculum size, followed by cultivation at 37°C, pH 7.5 and 180 rpm for 8 days. The strain KT1115 produced 44.39 g/L RLs after 10 days of fermentation in a 5-L bioreactor under the optimal fermentation conditions as shown in **Figure 1**.

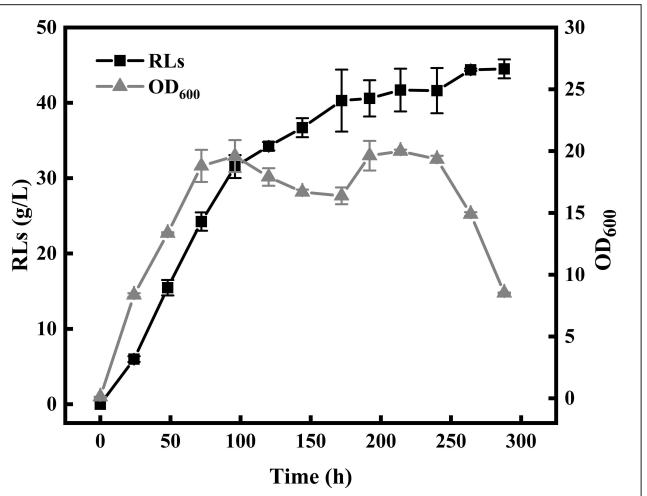

FIGURE 1 | Bioreactor fermentation for rhamnolipid production.

Extraction and Purification of the Produced RLs

Because the extraction and purification of RLs is key to any detailed study of their characteristics, we established a new separation protocol consisting of four steps including cell removal, protein removal, acid precipitation, and petroleum ether purification.

Firstly, the appearance of emulsions is a great challenge during the extraction of RLs. Large amounts of proteins were present in the RLs fermentation broth, and were identified as an essential cause of emulsification (Damodaran, 2010). Thus, after removing the cells by centrifugation, an ethanol precipitation step for eliminating as much protein as possible from the broth was applied before RLs extraction. The effects of various ethanol concentrations and treatment times on protein removal rate and RLs recovery rate were determined (**Figures 2A,B**). The protein removal rate gradually increased with the increase of the ethanol concentration, and the increase of the protein removal rate and RLs recovery rate slowed down at concentrations exceeding 20% (**Figure 2A**). The optimal treatment time was 9 h as shown in **Figure 2B**.

After removing the proteins, acid precipitation was used to further extract RLs, and the effects of different acids on RLs precipitation were investigated (**Figure 2C**). The results showed that a higher RLs recovery rate was obtained by using H_3PO_4 as the acid precipitating reagent at pH values of 2.0. Finally, petroleum ether was used to further purify the rhamnolipids, which are insoluble in petroleum ether, so that residual fats and lipid-soluble pigments in the rhamnolipid solution could be removed. Using this newly established four-step protocol, the final RLs product was separated from the fermentation broth with a high recovery rate of 91.82% and good purity of 89% (**Figure 2D**).

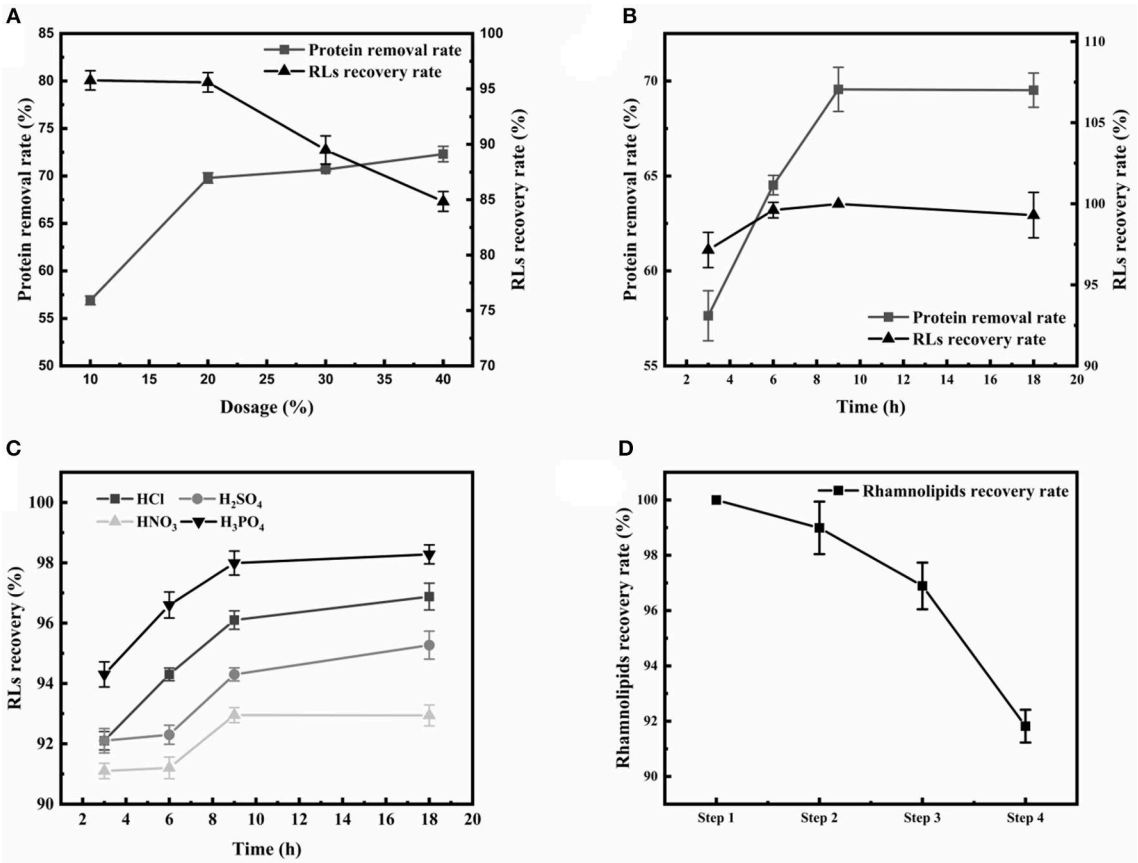

FIGURE 2 | Optimization of the crude RLs separation process. **(A)** The effects of different ethanol concentrations on the rhamnolipid recovery rate and protein removal rate; **(B)** The effects of different durations of ethanol precipitation on the rhamnolipid recovery rate and protein removal rate; **(C)** The effects of different acids on the RLs recovery rate. **(D)** Summary of purification of rhamnolipids from the fermentation broth. The rhamnolipid sample concentration was 10 g/L. The rhamnolipid recovery rate is calculated by comparing the pre- and post-treatment concentrations.

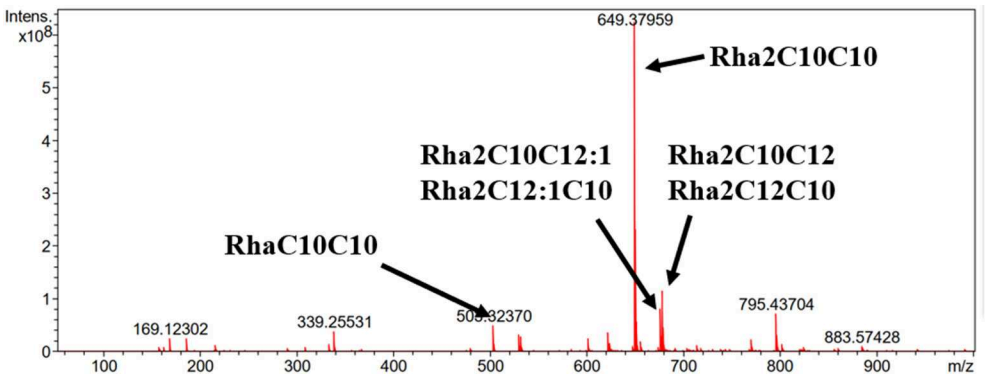

FIGURE 3 | ESI-MS analysis of the produced rhamnolipids.

Analysis of the Molecular Composition of the Produced Rhamnolipids

ESI-MS was used to analyze the molecular composition of the RLs separated by acid precipitation as shown in **Figure 3**. The results revealed the presence of many RL homologs produced by *P. aeruginosa* KT1115 during growth on RON medium, with a major ion peak at m/z 649. As shown in **Table 1**, the RLs products encompassed both mono- and di-RLs, but di-RLs such as $Rha_2C_{10}C_{10}$ at m/z 649 were detected as the major components. The results shown in **Table 2** indicate that the KT1115 strain

TABLE 1 | Structural composition of rhamnolipids produced by strain KT1115.

Homologue	Pseudomolecule ion (m/z)	Ratio (%)*
$Rha_2C_{10}C_{10}$	649	65.37
$Rha_2C_{10}C_{12}$	677	10.59
$Rha_2C_{12}C_{10}$		
$Rha_2C_{10}C_{12:1}$	675	7.40
$Rha_2C_{12:1}C_{10}$		
$RhaC_{10}C_{10}$	503	4.41

**The homologues with abundances of less than 4.41% are not listed.*

TABLE 2 | Comparison of mono/di-rhamnolipids from different RL-producing strains.

Strain	Carbon source	Mono-/di-RLs	References
P. aeruginosa UG2	Corn oil	28:72	Matasandoval et al., 1999
P. aeruginosa MTCC 2453	Sunflower oil	25.5:74.5	Jadhav et al., 2018
P. aeruginosa 47T2	Waste fried oil	21:79	Sánchez et al., 2007
P. aeruginosa MN1	Glycerol	76.48:23.52	Samadi et al., 2012
P. aeruginosa 57RP	Mannitol	31.75:68.25	Déziel et al., 1999
P. aeruginosa 57RP	Naphthalene	38.90:61.10	Déziel et al., 1999
P. aeruginosa GL1	Glycerol	69:31	Arino et al., 1996
P. aeruginosa ADMT1	Diesel	33:67	Tiwary and Dubey, 2018
P. aeruginosa MR01	Soybean oil	50.73:49.27	Lotfabad et al., 2010
***P. aeruginosa* KT1115**	**Rapeseed oil**	**11.47:88.53**	**This work**

Bold values indicates the rhamnolipid mixture, the component of the di-rhamnolipid accounted for 88.53%.

has excellent di-RLs production ability compared to previous reports. The four predominant RLs homologs were $Rha_2C_{10}C_{10}$, $Rha_2C_{10}C_{12}$, $Rha_2C_{10}C_{12:1}$, and $RhaC_{10}C_{10}$ at 63.37, 10.59, 7.40, and 4.41% of the total, respectively. In addition, all di-rhamnolipid congeners added up to 88.5% of the total congeners in the biosurfactant mixture. This result demonstrates that *P. aeruginosa* KT1115 is a high di-rhamnolipid-yielding strain.

Separation of Mono- and Di-rhamnolipids

Silica gel column chromatography was used to separate mono- and di-RLs utilizing the polarity difference between the two RLs types. The eluent solution was assessed for RLs concentration as shown in **Figure 4**. As the polarity of the eluent increased, mono- and di-RLs were eluted successively. The results of thin-layer chromatography (TLC) suggested that the mono-/di-RLs produced by *P. aeruginosa* KT1115 were completely separated. In the TLC chromatogram, the lower spots are di-rhamnolipid structures, and the higher spots contain mono-rhamnolipid molecules (**Figure 5**).

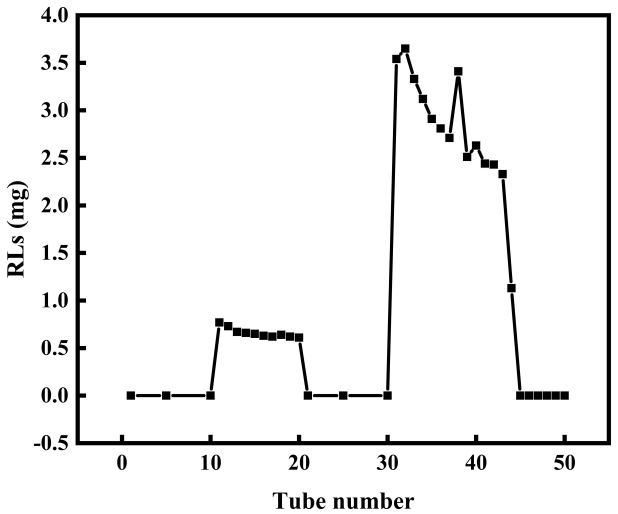

FIGURE 4 | The separation of mono- and di-RLs by silica gel column chromatography. Mono- and di-RLs were separated by gradient solvent elution. Tubes 0–10 were eluted with solvent II. Tubes 11–20 were eluted with solvent III to release mono-RLs. Tubes 21–30 tube were eluted with solvent IV, which confirmed that mono-RLs were entirely eluted because nothing was eluted in this fraction. Tubes 31–40 were eluted with solvent V to release di-RLs from the column.

Evaluation of the Surface-Active Properties of the Purified Mono- and Di-RLs

Critical Micelle Concentrations

The critical micelle concentration (CMC) is the concentration of a surfactant in a bulk phase, above which aggregates of surfactant molecules, so-called micelles, start to form. It is an important parameter for assessing the interfacial activity of surfactants (Elshikh et al., 2017). As the concentration of RLs increased, the surface tension value rapidly decreased, resulting in a sharp turn as shown in **Figures 6A,B**. And the surface tension dose not drop further above the CMC, which is extensively independent of the RLs concentration. The CMC can be calculated using the intersection between the regression straight line of the linearly dependent region and the straight line passing through the plateau. As determined by surface tension measurements, the CMC value of purified mono-RLs was 167 mN/m, whereas the value of purified di-RLs was much lower at 8 mN/m, proving that di-RLs have a better surface activity and are better biosurfactants than mono-RLs, as had been conjectured for a long time based on their respective structures. To the best of our knowledge, this is the first time that the CMC values of purified mono- and di-RLs were exactly determined.

Emulsifying Activity

The emulsifying activity of five surfactants, including RLs, mono-RLs, di-RLs, SDS, and Tween 80, was assessed using three hydrophobic organic compounds, namely, liquid paraffin, kerosene, and n-hexane. All RLs products showed a higher emulsifying activity than either SDS or Tween 80, and the EI_{24} values of RLs, mono-RLs and di-RLs with the

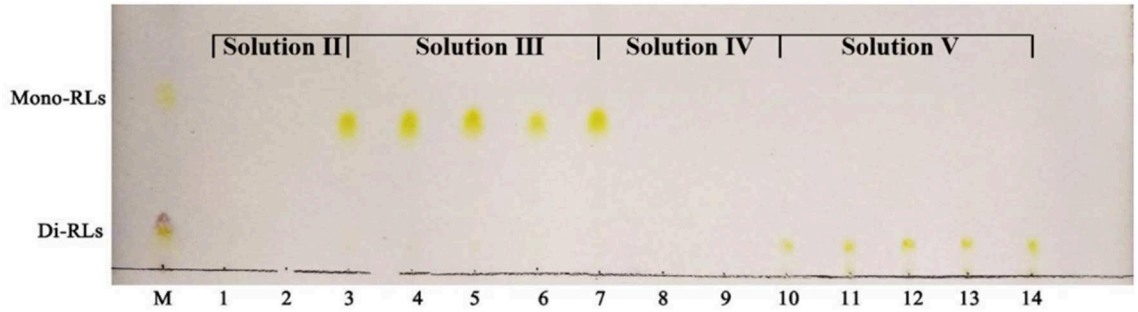

FIGURE 5 | TLC analysis of mono- and di-rhamnolipids separated by silica gel column chromatography. M, commercial rhamnolipids; Lanes 1,2, the samples eluted by solvent II; Lanes 3–7, the samples eluted by solvent III; Lanes 8,9, the samples eluted by solvent IV; Lanes 10–14, the samples eluted by solvent V.

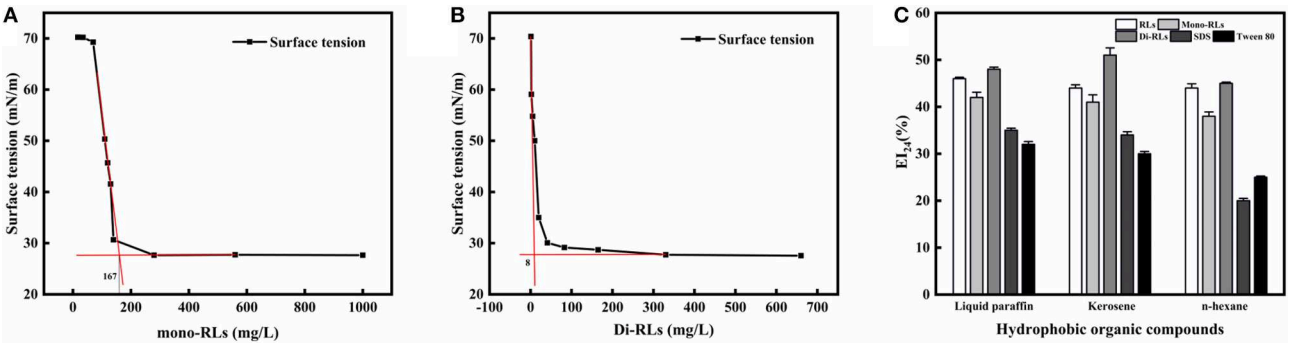

FIGURE 6 | The evaluation of surface tension and emulsifying activity. Relationship between the surface tension and concentration of mono-RLs **(A)** and di-RLs **(B)**; Emulsifying activity of five surfactants was assessed using three hydrophobic organic compounds **(C)**. The EI_{24} of the five surfactants at 100 mg/L were measured and their emulsifying activities with different substrates (kerosene, liquid paraffin, n-hexane)0020were compared.

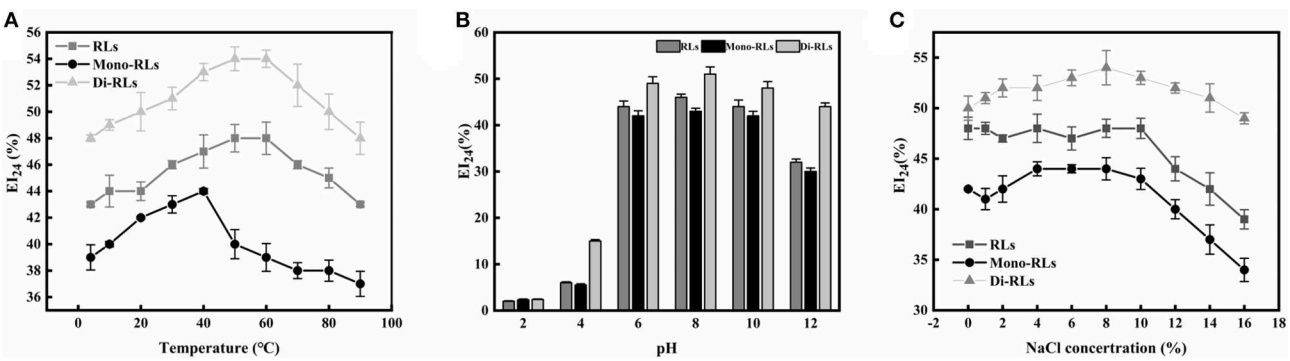

FIGURE 7 | The stability of rhamnolipids. **(A)** Thermostability; **(B)** pH stability; **(C)** salt stability.

three tested hydrophobic organic compounds were all >40% (**Figure 6C**). The high emulsifying activity of rhamnolipids makes them suitable for bioremediation of oil-polluted sites and application in microbial enhanced oil recovery (MEOR) (Wen-Jie et al., 2012).

Effects of Temperature, pH, and Ionic Strength on Biosurfactant Stability

The temperature and pH profiles of the emulsifying activity of the RLs products are shown in **Figures 7A,B**. The results indicated that temperature had little effect on the biosurfactant performance in a broad range from 20 to 80°C, whereby di-RLs had the best emulsification capacity. However, the emulsifying activity of RLs was significantly affected by the pH (**Figure 7B**). The emulsification activity of RLs was weak under strongly acidic conditions (pH 2–4). Nevertheless, the EI_{24} value of purified di-RLs was relatively stable under a wide range of pH values (4.0–12.0).

The effect of ionic strength on the emulsification capacity of different RLs products is shown in **Figure 7C**. The EI_{24} value was

strongly reduced as the ionic strength was increased up to 10% NaCl concentration. As suggested above, purified di-RLs showed a better stability than purified mono-RLs.

DISCUSSION

Rhamnolipids (RLs), which are mainly produced by *P. aeruginosa*, have attracted the attention of researcher as biosurfactants with many potential industrial applications. There are many reports underscoring the superior biosurfactant properties of RLs, with promising potential applications such as biofilm disrupting, skin damage repair and perhaps even anticancer activity (Stipcevic et al., 2006; Kamal et al., 2012; Nivedita et al., 2013). However, the RLs secreted by *P. aeruginosa*, which has been used to obtain most of the published data, constitute a heterogeneous mixture of mono- and di-RLs. Thus, it is interesting to evaluate the individual biological properties of purified mono- and di-RLs.

Pseudomonas aeruginosa KT1115 was verified as a high di-RLs-yielding strain, with di-RLs comprising a major proportion of the final product (mono-RLs: di-RLs = 11.47: 88.53). The reported rhamnolipids with different mono-/di-RLs ratios have been summarized in **Table 2**. Many studies have shown that the di-rhamnolipid proportion varied greatly, and was mostly between 23 and 79% in RLs product from various *P. aeruginosa* strains (Matasandoval et al., 1999; Jadhav et al., 2018). The *rhlC* genes, which encode the rhamnosyltransferases involved in di-rhamnolipid production in *P. aeruginosa*, may affect the distribution of mono- and di-RLs as well as different carbon sources (Nicolò et al., 2017). Thus, the mechanism of high di-rhamnolipid production in *P. aeruginosa* KT1115 merits further study.

An effective RLs purification method was established in this study and we introduced a petroleum ether purification step in the purification procedure for the first time. This is a simple and effective purification method with a RLs recovery rate as high as 91.82%, affording RLs with a good purity of 89%. Membrane separation is a good choice for continuous separation of rhamnolipids. According to the literature, membrane separation enables more than 90% rhamnolipid recovery (Isa et al., 2008; Witek-Krowiak et al., 2011). However, the method used in this study achieves efficient separation of rhamnolipids without expensive equipment foundations and cumbersome operations compared with membrane separation. Subsequently, silica gel column chromatography was used to separate mono- and di-RLs with a suitable elution protocol, and it can provide guidance for future research. However, it is worth noting that the specific purification process will be different for varying mono/di ratios. For example, Yuan et al. used chloroform: methanol at ratios of 10:1, 2:1, 1:1, and 1:2 (v/v) as mobile phase to separate mono-/di-RLs from a mixture with di-RLs constituting over 70% of the total (Yuan et al., 2007).

Based on the newly established purification and separation protocol, purified RLs, and mono-/di-RLs were obtained, and the properties of the purified mono- and di-RLs were systematically evaluated. At present, the performance of di-RLs has not been studied after mono- and di-RLs separation, and their performance was only inferred from the different ratio of the di-RLs (Wen-Jie et al., 2012; Feng et al., 2018). In this study, we systematically evaluated properties of the purified mono- and di-RLs, and it shows that di-RLs have much lower CMCs than mono-RLs and higher emulsifying activity than other chemical surfactants including to of SDS and Tween 80. Moreover, di-RLs showed better performance on the characters of temperatures, pH values, and ionic strengths, indicated that they can be used in extreme environments (Banat et al., 2000).

CONCLUSIONS

Compared to mono-RLs, di-RLs possesses higher surface activity, which show great potential in surfactant industry. In this study, the newly isolated *P. aeruginosa* KT1115 produced 44.39 g/L of RLs in a 5 L bioreactor after process optimization. Efficiently 4-step RLs recovery method was established and 91.82% RLs recovery rate with purity of 89% was obtained. The newly established separation process provided a favorable foundation for evaluation of their properties. Afterwards, the results of ESI-MS revealed that *P. aeruginosa* KT1115 is a high di-RLs-yielding strain producing a high di-RLs proportion (mono-RLs: di-RLs = 11.47: 88.53). At the same time, the properties of purified mono- and di-RLs were assessed by TLC, CMC, and EI_{24} analyses. This study provides the basic knowledge on high di-rhamnolipid-yielding *P. aeruginosa* KT1115 and surfactant characteristics of mono/di-RLs. Further genome and transcriptome analysis of the genes involved RLs production may help us to understand the molecular mechanism and genetics of high di-RLs production of strain KT1115.

DATA AVAILABILITY STATEMENT

All datasets generated for this study are included in the manuscript/supplementary files.

AUTHOR CONTRIBUTIONS

JZ, RX, and SL designed and did all experiments, analyzed data, and wrote the paper. NX, FX, WZ, MJ, and WD contributed to the conception of the experiments and supervise the overall project.

FUNDING

This work was supported by the National Natural Science Foundation of China (Nos. 31961133017, 31700092, 21978129, and 21908102), National Key Research and Development Program of China (2018YFA0902200), the Jiangsu Province Natural Science Foundation for Youths (BK20170997, BK20170993), National Postdoctoral Program for Innovative Talents (BX20180140), China Postdoctoral Science Foundation (2018M642238), Jiangsu Synergetic Innovation Center for Advanced Bio-Manufacture of China, Project of State Key Laboratory of Materials-Oriented Chemical Engineering (ZK201601), Huaian Science Foundation HAB201702.

REFERENCES

Arino, S., Marchal, R., and Vandecasteele, J. P. (1996). Identification and production of a rhamnolipidic biosurfactant by a *Pseudomonas* species. *Appl. Microbiol. Biotechnol.* 45, 162–168. doi: 10.1007/s002530050665

Banat, I. M., Makkar, R. S., and Cameotra, S. S. (2000). Potential commercial applications of microbial surfactants. *Appl. Microbiol. Biotechnol.* 53, 495–508. doi: 10.1007/s002530051648

Damodaran, S. (2010). Protein stabilization of emulsions and foams. *J. Food Sci.* 70, 54–66. doi: 10.1111/j.1365-2621.2005.tb07150.x

Déziel, E., Lépine, F., Dennie, D., Boismenu, D., Mamer, O. A., and Villemur, R. (1999). Liquid chromatography/mass spectrometry analysis of mixtures of rhamnolipids produced by *Pseudomonas aeruginosa* strain 57RP grown on mannitol or naphthalene. *Biochim. Biophys. Acta* 1440, 244–252. doi: 10.1016/s1388-1981(99)00129-8

Elshikh, M., Funston, S., Chebbi, A., Ahmed, S., Marchant, R., and Banat, I. M. (2017). Rhamnolipids from non-pathogenic Burkholderia thailandensis E264: physicochemical characterization, antimicrobial and antibiofilm efficacy against oral hygiene related pathogens. *Nat. Biotechnol.* 36, 26–36. doi: 10.1016/j.nbt.2016.12.009

Feng, Z., Shi, R., Fang, M., Han, S., and Ying, Z. (2018). Oxygen effects on rhamnolipids production by *Pseudomonas aeruginosa*. *Microb. Cell Fact.* 17:39. doi: 10.1186/s12934-018-0888-9

Heyd, M., Kohnert, A., Tan, T. H., Nusser, M., Kirschhöfer, F., Brenner-Weiss, G., et al. (2008). Development and trends of biosurfactant analysis and purification using rhamnolipids as an example. *Anal. Bioanalyt. Chem.* 391, 1579–1590. doi: 10.1007/s00216-007-1828-4

Isa, M. H. M., Coraglia, D. E., Frazier, R. A., and Jauregi, P. (2007). Recovery and purification of surfactin from fermentation broth by a two-step ultrafiltration process. *J. Membr. Sci.* 296, 51–57. doi: 10.1016/j.memsci.2007.03.023

Isa, M. H. M., Frazier, R. A., and Jauregi, P. (2008). A further study of the recovery and purification of surfactin from fermentation broth by membrane filtration. *Separ. Purif. Technol.* 64, 176–182. doi: 10.1016/j.seppur.2008.09.008

Jadhav, J., Dutta, S., Kale, S., and Pratap, A. (2018). Fermentative production of rhamnolipid and purification by adsorption chromatography. *Prep. Biochem. Biotechnol.* 48, 234–241. doi: 10.1080/10826068.2017.1421967

Jiang, L., Shen, C., Long, X., Zhang, G., and Meng, Q. (2014). Rhamnolipids elicit the same cytotoxic sensitivity between cancer cell and normal cell by reducing surface tension of culture medium. *Appl. Microbiol. Biotechnol.* 98, 10187–10196. doi: 10.1007/s00253-014-6065-0

Kamal, A., Shaik, A. B., Kumar, C. G., Mongolla, P., Rani, P. U., Krishna, K. V., et al. (2012). Metabolic profiling and biological activities of bioactive compounds produced by *Pseudomonas sp.* strain ICTB-745 isolated from Ladakh, India. *J. Microbiol. Biotechnol.* 22, 69–79. doi: 10.4014/jmb.1105.05008

Liang-Ming, W., Liu, P. W. G., Chih-Chung, M., and Sheng-Shung, C. (2008). Application of biosurfactants, rhamnolipid, and surfactin, for enhanced biodegradation of diesel-contaminated water and soil. *J. Hazardous Mater.* 151, 155–163. doi: 10.1016/j.jhazmat.2007.05.063

Lotfabad, T. B., Abassi, H., Ahmadkhaniha, R., Roostaazad, R., Masoomi, F., Zahiri, H. S., et al. (2010). Structural characterization of a rhamnolipid-type biosurfactant produced by *Pseudomonas aeruginosa* MR01: enhancement of di-rhamnolipid proportion using gamma irradiation. *Colloids Surf. B Biointerfaces* 81, 397–405. doi: 10.1016/j.colsurfb.2010.06.026

Lovaglio, R. B., Santos, F. J. D., Junior, M. J., and Contiero, J. (2011). Rhamnolipid emulsifying activity and emulsion stability: pH rules. *Colloids Surf. B Biointerfaces* 85, 301–305. doi: 10.1016/j.colsurfb.2011.03.001

Matasandoval, J., C., Karns, J., and Torrents, A. (1999). High-performance liquid chromatography method for the characterization of rhamnolipid mixtures produced by *Pseudomonas aeruginosa* UG2 on corn oil. *J. Chromatogr. A* 864, 211–220. doi: 10.1016/s0021-9673(99)00979-6

Mulligan, C. N. (2005). Environmental applications for biosurfactants. *Environ. Pollut.* 133, 183–198. doi: 10.1016/j.envpol.2004.06.009

Nicolò, M. S., Cambria, M. G., Impallomeni, G., Rizzo, M. G., Pellicorio, C., Ballistreri, A., et al. (2017). Carbon source effects on the mono/dirhamnolipid ratio produced by *Pseudomonas aeruginosa* L05, a new human respiratory isolate. *New Biotechnol.* 39, 36–41. doi: 10.1016/j.nbt.2017.05.013

Nivedita, S., Pemmaraju, S. C., Pruthi, P. A., Cameotra, S. S., and Vikas, P. (2013). Candida biofilm disrupting ability of di-rhamnolipid (RL-2) produced from *Pseudomonas aeruginosa* DSVP20. *Appl. Biochem. Biotechnol.* 169, 2374–2391. doi: 10.1007/s12010-013-0149-7

Rahman, K. S., Rahman, T. J., Mcclean, S., Marchant, R., and Banat, I. M. (2010). Rhamnolipid biosurfactant production by strains of *Pseudomonas aeruginosa* using low-cost raw materials. *Biotechnol. Prog.* 18, 1277–1281. doi: 10.1021/bp020071x

Rendell, N. B., Taylor, G. W., Somerville, M., Todd, H., Wilson, R., and Cole, P. J. (1990). Characterisation of *Pseudomonas* rhamnolipids. *Biochim. Biophys. Acta* 1045, 189–193. doi: 10.1016/0005-2760(90)90150-V

Rienzo, M. A. D. D., Kamalanathan, I. D., and Martin, P. J. (2016). Comparative study of the production of rhamnolipid biosurfactants by *B. thailandensis* E264 and *P. aeruginosa* ATCC 9027 using foam fractionation. *Process Biochem.* 51, 820–827. doi: 10.1016/j.procbio.2016.04.007

Roger, M., and Banat, I. M. (2012). Microbial biosurfactants: challenges and opportunities for future exploitation. *Trends Biotechnol.* 30, 558–565. doi: 10.1016/j.tibtech.2012.07.003

Samadi, N., Abadian, N., Ahmadkhaniha, R., Amini, F., Dalili, D., Rastkari, N., et al. (2012). Structural characterization and surface activities of biogenic rhamnolipid surfactants from *Pseudomonas aeruginosa* isolate MN1 and synergistic effects against methicillin-resistant *Staphylococcus aureus*. *Folia Microbiol.* 57, 501–508. doi: 10.1007/s12223-012-0164-z

Sánchez, M., Aranda, F. J., Espuny, M. J., Marqués, A., Teruel, J. A., Manresa, Á., et al. (2007). Aggregation behaviour of a dirhamnolipid biosurfactant secreted by *Pseudomonas aeruginosa* in aqueous media. *J. Colloid Interface Sci.* 307, 246–253. doi: 10.1016/j.jcis.2006.11.041

Seul Ki, K., Young Cheol, K., Sunwoo, L., Cheol, K. J., Young, Y. M., and In Seon, K. (2011). Insecticidal activity of rhamnolipid isolated from *Pseudomonas* sp. EP-3 against green peach aphid (*Myzus persicae*). *J. Agric. Food Chem.* 59, 934–938. doi: 10.1021/jf104027x

Sodagari, M., Wang, H., Newby, B. M. Z., and Ju, L. K. (2013). Effect of rhamnolipids on initial attachment of bacteria on glass and octadecyltrichlorosilane-modified glass. *Colloid Surf. B Biointerfaces* 103, 121–128. doi: 10.1016/j.colsurfb.2012.10.004

Stipcevic, T., Piljac, A., and Piljac, G. (2006). Enhanced healing of full-thickness burn wounds using di-rhamnolipid. *Burns* 32, 24–34. doi: 10.1016/j.burns.2005.07.004

Tiwary, M., and Dubey, A. K. (2018). Characterization of biosurfactant produced by a novel strain of *Pseudomonas aeruginosa*, isolate ADMT1. *J. Surfactants Deterg.* doi: 10.1002/jsde.12021

Varjani, S. J., and Upasani,V. N. (2016). Core flood study for enhanced oil recovery through *ex-situ* bioaugmentation with thermo-and halo-tolerant rhamnolipid produced by *Pseudomonas aeruginosa* NCIM 5514. *Bioresour. Technol.* 220, 175–182. doi: 10.1016/j.biortech.2016.08.060

Wen-Jie, X., Zhi-Bin, L., Han-Ping, D., Li, Y., Qing-Feng, C., Yong-Qiang, B. (2012). Synthesis, characterization, and oil recovery application of biosurfactant produced by indigenous Pseudomonas aeruginosa WJ-1 using waste vegetable oils. *Appl. Biochem. Biotech.* 166, 1148–1166. doi: 10.1007/s12010-011-9501-y

Witek-Krowiak, A., Witek, J., Gruszczynska, A., Szafran, R. G., Kozlecki, T., and Modelski, S. (2011). Ultrafiltrative separation of rhamnolipid from culture medium. *World J. Microbiol. Biotechnol.* 27, 1961–1964. doi: 10.1007/s11274-011-0655-0

Xuwei, L., Guoliang, Z., Li, H., and Qin, M. (2013). Dewatering of floated oily sludge by treatment with rhamnolipid. *Water Res.* 47, 4303–4311. doi: 10.1016/j.watres.2013.04.058

Yuan, X. Z., Ren, F. Y., Zeng, G. M., Zhong, H., Fu, H. Y., Liu, J., et al. (2007). Adsorption of surfactants on a *Pseudomonas aeruginosa* strain and the effect on cell surface lypohydrophilic property. *Appl. Biochem. Biotechnol.* 76, 1189–1198. doi: 10.1007/s00253-007-1080-z

Conflict of Interest: The authors declare that the research was conducted in the absence of any commercial or financial relationships that could be construed as a potential conflict of interest.

frontiers in Bioengineering and Biotechnology

ORIGINAL RESEARCH
published: 27 November 2019
doi: 10.3389/fbioe.2019.00361

Engineering Oleaginous Yeast as the Host for Fermentative Succinic Acid Production From Glucose

Mahsa Babaei[1], Kanchana Rueksomtawin Kildegaard[2], Aligholi Niaei[1], Maryam Hosseini[3], Sirous Ebrahimi[4], Suresh Sudarsan[2], Irini Angelidaki[5] and Irina Borodina[2]**

[1] Department of Chemical & Petroleum Engineering, University of Tabriz, Tabriz, Iran, [2] The Novo Nordisk Foundation Center for Biosustainability, Technical University of Denmark, Lyngby, Denmark, [3] Department of Chemical Engineering, Faculty of Engineering, Azarbaijan Shahid Madani University, Tabriz, Iran, [4] Biotechnology Research Center, Faculty of Chemical Engineering, Sahand University of Technology, Tabriz, Iran, [5] Department of Environmental Engineering, Technical University of Denmark, Lyngby, Denmark

OPEN ACCESS

Edited by:
Hui Wu,
East China University of Science and Technology, China

Reviewed by:
Jiangfeng Ma,
Nanjing Tech University, China
Chong Li,
Chinese Academy of Agricultural Sciences, China

***Correspondence:**
Irina Borodina
irbo@biosustain.dtu.dk
Irini Angelidaki
iria@env.dtu.dk

Specialty section:
This article was submitted to Industrial Biotechnology, a section of the journal Frontiers in Bioengineering and Biotechnology

Received: *15 September 2019*
Accepted: *12 November 2019*
Published: *27 November 2019*

Citation:
Babaei M, Rueksomtawin Kildegaard K, Niaei A, Hosseini M, Ebrahimi S, Sudarsan S, Angelidaki I and Borodina I (2019) Engineering Oleaginous Yeast as the Host for Fermentative Succinic Acid Production From Glucose. Front. Bioeng. Biotechnol. 7:361. doi: 10.3389/fbioe.2019.00361

Oleaginous yeast *Yarrowia lipolytica* is a prospective host for production of succinic acid. The interruption of tricarboxylic acid cycle through succinate dehydrogenase gene (*SDH*) deletion was reported to result in strains incapable of glucose utilization and this ability had to be restored by chemical mutation or long adaptive laboratory evolution. In this study, a succinate producing strain of *Y. lipolytica* was engineered by truncating the promoter of *SDH1* gene, which resulted in 77% reduction in *SDH* activity but did not impair the ability of the strain to grow on glucose. The flux toward succinic acid was further improved by overexpressing the genes in the glyoxylate pathway and the oxidative TCA branch, and expressing phosphoenolpyruvate carboxykinase from *Actinobacillus succinogenes*. A short adaptation on glucose reduced the lag phase of the strain and increased its tolerance to high glucose concentrations. The resulting strain produced 7.8 ± 0.0 g/L succinic acid with a yield of 0.105 g/g glucose in shake flasks without pH control, while mannitol (11.8 ± 0.8 g/L) was the main by-product. Further investigations showed that mannitol accumulation was caused by low pH stress and buffering the fermentation medium eliminated mannitol formation. In a fed-batch bioreactor in mineral medium at pH 5, at which point according to K_a values of succinic acid, the major fraction of product was in acidic form rather than dissociated form, the strain produced 35.3 ± 1.5 g/L succinic acid with 0.26 ± 0.00 g/g glucose yield.

Keywords: metabolic engineering, succinic acid, *SDH1*, *Yarrowia lipolytica*, fed-batch fermentation

INTRODUCTION

Succinic acid ($C_4H_6O_4$) is a potential platform chemical with a wide range of applications in food, pharmacy, biopolymers, coatings, green solvents, and plasticizers (Ahn et al., 2016). Succinic acid can be chemically converted into other value-added products, as 1,4-butanediol, γ-butyrolactone, *N*-methyl-2-pyrrolidone, tetrahydrofurane, and 2-pyrrolidone (Pateraki et al., 2016). Succinic acid market demand comprised 50,000 metric tons in 2016 and is expected to double by 2025 (Chinthapalli et al., 2018). The total plant capacity for production of succinic acid by fermentation is about 64,000 tons per year (BioAmber, Myriant—now GC Innovation America, Reverdia and Succinctly).

Various microbes have been engineered for production of succinate by fermentation. The highest volumetric rates have been reported for rumen bacterium *Mannheimia succiniciproducens*. The group of Sang Yup Lee reported titer of 78.4 g/L with yield of 1.64 mol/mol glucose and overall volumetric productivity of 6.02 g/L/h on a mixed feed of glycerol and sucrose (Lee et al., 2016). Bacterial fermentations typically require neutral pH and result in succinate salt. In the downstream processing, succinate must be acidified into succinic acid, generating large amounts of by-product, such as gypsum (Sauer et al., 2008). This can be avoided if the fermentation is to be carried out at low pH.

Many yeasts are tolerant to low pH, some species as *Y. lipolytica* can grow at pH as low as 3.5 (Mironczuk et al., 2016). Considering the pKa of succinic acid of 4.2 and 5.6 at 25°C (Dean, 1999), at pH 3.5 more than 80% of succinic acid would be in protonated form. *Saccharomyces cerevisiae* has been engineered for succinic acid production by Reverdia (joint venture of DSM and Roquette), which required, among other modifications, a deletion of pyruvate decarboxylases to prevent ethanol fermentation. In 2013, BioAmber/Mitsui switched from *Escherichia coli* as host microorganism to the yeast *Candida krusei*, a low pH-tolerant strain discovered by Cargill (Jansen and van Gulik, 2014).

In the past decade, non-conventional yeast *Y. lipolytica* has become relatively well-amenable for genetic manipulation and it has been engineered for commercial production of polyunsaturated fatty acids (DuPont) and lipids (Novogy, acquired by Total). This yeast has a long record of safe use, since it's been used as food additive and supplement in 80's and has undergone extensive toxicity tests for this purpose (Zinjarde, 2014). Some strains of *Y. lipolytica* are native overproducers of tricarboxylic acid (TCA) cycle acids: citric (Cavallo et al., 2017), isocitric (Kamzolova et al., 2013) and α-ketoglutaric (Guo et al., 2016), which renders the species a potentially attractive host for the production of another TCA cycle acid, namely succinic acid. Kamzolova et al have utilized the capability of this yeast to secrete high titers of α-ketoglutaric acid for succinic acid production in a two-step process. The strain VKMY-2412 was engineered to produce 88.7 g/L α-ketoglutaric acid, which was subsequently decarboxylized chemically to succinic acid in the presence of H_2O_2 (Kamzolova et al., 2014a,b).

A number of studies on engineering *Y. lipolytica* for direct succinic acid production have been published (**Table 1**).The common feature of all the reported strains is reduced succinate dehydrogenase activity, to decrease the succinate conversion into fumarate in the TCA cycle. The succinate dehydrogenase (*SDH*) complex in *Y. lipolytica* includes five subunits, flavoprotein subunit *YALI0D11374g* (*SDH1*), iron-sulfur subunit *YALI0D23397g* (*SDH2*), cytochrome b560 subunit *YALI0E29667g* (*SDH3*), membrane anchor subunit *YALI0A14784g* (*SDH4*), and succinate dehydrogenase assembly factor 2 *YALI0F11957g* (*SDH5*). The early study from Yuzbashev et al. (2010) reported a *Y. lipolytica* strain with deletion of *SDH2* gene. The deletion of *SDH2* gene impaired the utilization of glucose, while glycerol utilization was intact. The disruption of TCA cycle through inhibition of the conversion of succinate to fumarate by *SDH* gene deletion leads to insufficient regeneration of reducing equivalents (FADH2) that results in less ATP synthesis through oxidative phosphorylation in yeast cells. In addition, the export of produced succinic acid is an energy dependent process that aggravates the ATP deficiency in the *SDH*-deleted mutants. The inadequate ATP is considered as the reason for observed loss of the ability of cells to grow on glucose after *SDH* deletion. However, switching the carbon source from glucose to glycerol metabolism, on the other hand, generates 3 ATP molecules more than glucose that makes the cell growth and succinic acid production feasible even at low pH (Yuzbashev et al., 2011).

A high viability mutant of the knock-out strain Y-3314 produced 17.4 g/L succinic acid from glycerol in shake flasks. The strain was further improved by chemical mutation and selection, a better performing mutant Y-4215 was identified, producing 50.2 g/L succinic acid on glucose (Yuzbashev et al., 2016). Sineokii et al. patented a strain of *Y. lipolytica* VKPM Y-3753, obtained by multistage mutagenesis using nitrosoguanidine and subsequent two-stage selection. The strain produced up to 60 g/L succinic acid in test tubes from glucose at low pH of 3 in rich medium (Sineokii et al., 2012). Optimization of the cultivation mode of this strain in bioreactor resulted in 55.3 g/L in 48 h produced on mineral medium with glucose without pH control (Bondarenko et al., 2017).

Jost et al. constructed a *Y. lipolytica* strain H222-AZ2 with a 64% reduction in *SDH* activity by replacing the indigenous endogenous promoter of gene *SDH2* with the inducible promoter of 3-ketoacyl-CoA thiolase encoding gene (*POT1*) from *Y. lipolytica*, which is almost inactive in *Y. lipolytica* grown on glucose or glycerol (Jost et al., 2014). When strain H222-AZ2 was fermented in controlled bioreactors with oxygen limitation, succinic acid was produced at 25 g/L titer and 0.26 g/g glycerol yield with 0.152 g/L/h productivity.

A different approach was undertaken by the research group of Qingsheng Qi, who deleted *SDH5* gene in PO1f strain (derivative of W29), obtaining PGC01003. This strain produced 198.2 g/L succinate on complex medium with glycerol in an *in situ* fibrous bed bioreactor (*is*FBB) with pH controlled at 6.0 (Li et al., 2017, 2018b). The yield was calculated at 0.42 g/g glycerol, however for complex media the yield numbers can be misleading because other media components are used as carbon sources as well. We will further only discuss the yields measured on mineral media with a single carbon source. The strain PGC01003 also had an impaired glucose metabolism, consuming <6 g/L glucose after 120 h in shake flask (Gao et al., 2016). The strain underwent adaptive laboratory evolution on glucose for 21 days to result in strain PSA02004, which produced 65.7 g/L succinate in complex medium with glucose at pH 6.0 (Yang et al., 2017). The strain was further evolved in an *is*FBB for around 60 days to give strain PSA3.0, which produced 18.4 g/L succinic acid at pH 3.0 (Li et al., 2018a). The authors also tried a rational approach, where the Δ*sdh5* strain PGC01003 was further engineered by deleting acetyl-CoA hydrolase (*ACH1*) and expressing phosphoenolpyruvate carboxykinase (*PCK*) from *S. cerevisiae* and endogenous succinyl-CoA synthase beta-subunit (*SCS2*) (Cui et al., 2017). The resulting strain PGC202 produced

TABLE 1 | Overview of production of succinic acid by *Yarrowia lipolytica*.

Strain	Genotype	Cultivation	Medium and carbon source	Succinic acid performance metrics	Reference
Y-3314	High viability mutant of [a]PO1f [b] Δ*SDH2*::[c]*URA3*	Shake flask	Complex with glycerol ([d]YPG) without pH control. Final pH 3.2	17.4 g/L in 7 days 0.87 g/g glycerol*	Yuzbashev et al., 2010
Y-4215	Chemical mutagenesis and adaptive evolution of Y-3314 in low pH chemostat (840 h)	Bioreactor	Mineral with glucose, without pH control. Final pH 2.7	50.2 g/L in 54 h, 0.43 g/g glucose	Yuzbashev et al., 2016
VKPM Y-3753	Multistage mutation including chemical mutagenesis and selection	Test Tube (5 mL)	Complex with glucose ([e]YPD), without pH control. Final pH 3.	60 g/L in 96 h, 0.57 g/g glucose*	Sineokii et al., 2012
		Bioreactor	Mineral with glucose, without pH control. Final pH 3.65	55.3 g/L in 48 h, 0.34 g/g glucose	Bondarenko et al., 2017
H222-AZ2	[f]H222 [g]*POT1-SDH2 URA3*	Bioreactor	Mineral with glycerol, pH controlled at 5.0	25 g/L in 165 h, 0.26 g/g glycerol	Jost et al., 2014
PGC01003	PO1f Δ*SDH5::URA3*	Bioreactor	Complex with crude glycerol (YPG), pH controlled at 6.0	160 g/L in 400 h, 0.40 g/g glycerol*	Gao et al., 2016
		[h]isFB Bioreactor	Complex with glycerol (YPG), with pH controlled at 6.0	198.2 g/L in 238 h, 0.42 g/g glycerol*	Li et al., 2017
PSA02004	Evolutionary adapted mutant of PGC01003 (21 days)	Bioreactor	Complex with glucose (YPD), pH controlled at 6.0	65.7 g/L in 96 h, 0.50 g/g glucose*	Yang et al., 2017
PSA3.0	Evolutionary adapted (62 days) mutant of PSA02004	[h]isFB Bioreactor	Complex with glucose (YPD), pH controlled at 3.0.	18.4 g/L, 0.23 g/g glucose*	Li et al., 2018a
PGC202	PGC01003 [i](Δ*ACH1::loxP ScPCK SCS2*)	Bioreactor	Complex with glycerol (YPG), without pH control. Final pH 3.4	110.7 g/L in 138 h, 0.53 g/g glycerol*	Cui et al., 2017
			Complex with glucose (YPD), without pH control. Final pH 5	53.6 g/L in 110 h, 0.61 g/g glucose*	Yu et al., 2018
ST8578	Short adaptation (5 days) of W29 [i](*SpMAE1* Δ*ACH1 tPSDH1_95bp SCS2 KGDH MLS MDH ICL AsPCK*)	Bioreactor	Mineral with glucose, pH controlled at 5.0	35.3 g/L in 58 h, 0.26 g /g glucose	This study

[a]*PO1f, W29 MatA, leu2-270, ura3-302, xpr2-322, axp-2, auxotrophic for Leu and Ura.*
[b]*SDH, Succinate dehydrogenase gene, subunit indicated after the name of the gene.*
[c]*URA3, Uracil requiring Orotidine-5′-phosphate decarboxylase.*
[d]*YPG, Medium with 10 g/L yeast extract, 20 g/L peptone, and glycerol.*
[e]*YPD, Medium with 10 g/L yeast extract, 20 g/L peptone, and glucose.*
[f]*H222, W29 MATA ura3-302 ku70Δ-1572.*
[g]*POT1, 3-ketoacyl-CoA thiolase encoding gene from Y. lipolytica.*
[h]*isFB, in situ fibrous bed reactor.*
[i]*ACH1, acetyl-CoA hydrolase, ScPCK: phosphoenolpyruvate carboxykinase from S. cerevisiae, SCS2: succinyl-CoA synthase beta-subunit.*
[j]*SpMAE1, dicarboxylic acid transporter from Schizosaccharomyces pombe; tPSDH1_95bp, truncated promoter of SDH1 gene to 95 bp; KGDH, α-ketoglutarate dehydrogenase; MLS, malate synthase; MDH, malate dehydrogenase; ICL, isocitrate lyase; AsPCK, phosphoenolpyruvate carboxykinase from Actinobacillus succinogenes.*
**Yield numbers for complex media can be misleading because other media components are used as carbon sources as well.*

110.7 g/L succinic acid on complex medium with glycerol without pH control (Cui et al., 2017); the authors did not report whether the ability to utilize glucose was restored in this strain. A year later, Yu et al. reported that the strain PGC202 was able to produce 53.6 g/L succinate in complex medium in bioreactors (Yu et al., 2018). However, in this study, the pH of the fermentation was not controlled and it dropped from 6.5 to only 5.1, which is contradictory to the theoretical pH drop that would occur at the concentration of succinic acid above 50 g/L (the final pH should be below 3, see also final pH values in fermentation without pH control in **Table 1**). The comparison of final succinic acid titer by all the developed strain so far (**Table 1**) shows that even the highest producer from glucose (about 50 g/L) is still far below the acceptable range of titer and productivity required for implementing in large-scale production. For commercial production of bulk chemicals using fermentation, the titers above 100–150 g/L are typically required and hence all the *Y. lipolytica* strains reported in literature so far are still far away from this goal.

In the current study, we engineered *Y. lipolytica* to produce succinic acid in mineral medium with glucose as the sole carbon source. The main aim was to construct the strain through rational metabolic engineering approach, rather than mutagenesis, to have the final strain fully genetically defined. The strain was engineered rationally by downregulating the expression of *SDH1*, which unlike *SDH* deletion, had no inhibitory effect on cell growth on glucose. The succinic acid production in this strain was further improved by optimizing the flux toward succinate through manipulation of the glyoxylate pathway, oxidative TCA branch, and reductive carboxylation pathways. The strain carries nine specific genome edits and presents a platform for further rational engineering toward succinic acid production.

MATERIALS AND METHODS

Strains, Culture Conditions, and Chemicals

Escherichia coli strain DH5α was used for cloning and plasmid propagation. Lysogeny Broth (LB) liquid medium or LB solid medium supplemented with 20 g/L agar containing 100 mg/L ampicillin was used for *E.coli* cultivation at 37°C.

Yarrowia lipolytica ST6512 with the genotype ku70Δ cas9::DsdA MatA was used as the parental strain. To construct this strain, simultaneous ku70 disruption and Cas9 insertion were performed by transforming linearized pCfB6364 into *Y. lipolytica* W29. The plasmid bears dsdAMX selection marker (Stovicek et al., 2015), which enables growth on D-serine as the sole nitrogen source (Vorachek-Warren and McCusker, 2004). All the strains are listed in **Supplementary Table 1**. The media used for growth of *Y. lipolytica* strains contained 10 g/L yeast extract, 20 g/L peptone (YP media), supplemented with 5% v/v glycerol (YPG media) or 2% w/v D-glucose monohydrate (YPD media), unless other concentrations are stated. Antibiotics were also supplemented when needed at following concentrations: hygromycin B (Thermo Fisher Scientific) at 400 mg/L and nourseothricin (Jena Bioscience GmbH) at 250 mg/L. The chemicals were all obtained from Sigma-Aldrich, unless otherwise mentioned.

Plasmid Construction

All plasmids and BioBricks used are listed in **Supplementary Tables 2, 3**, respectively. BioBricks were amplified by PCR using Phusion U polymerase (Thermo Fisher Scientific) with following thermal program: 98°C for 30 s, 30 cycles of (98°C for 10 s, 51°C for 30 s, 72°C for 30 s/kb), and 72°C for 5 min. BioBricks were then resolved on 1% agarose gels and purified using NucleoSpin®Gel and PCR Clean-up kit (Macherey-Nagel). The assembly of BioBricks into vectors was conducted by USER cloning (Holkenbrink et al., 2017). The parental vectors were digested with FastDigest SfaAl (Thermo Fisher Scientific) at 37°C for 60 min and nicked with Nb.BsmI (New England BioLabs) at 65°C for 60 min. BioBricks with compatible overhangs and SfaAl/Nb.BsmI-treated parental vectors prepared as above were incubated in CutSmart® buffer with USER enzyme (New England BioLabs) for 25 min at 37°C, followed by 10 min at 25°C, and transformation into *E. coli*. The colonies were tested by colony PCR and correct assembly was verified by DNA sequencing.

Construction of *Y. lipolytica* Strains

All the integrative vectors together with gRNA vectors are listed in **Supplementary Table 2**. Plasmids and BioBricks were transformed into parental strains by standard lithium acetate protocol (Chen et al., 1997) described in detail elsewhere (Holkenbrink et al., 2017). All the integration vectors were linearized with endonuclease NotI (Thermo Fisher Scientific) and gel purified for yeast transformation.

Genome editing of the strains, including gene knockout, and integration of single or multiple genes, were all performed according to the EasyCloneYALI Toolbox (Holkenbrink et al., 2017). Briefly, strain ST8218 with deleted gene *YALI0E30965g* (*ACH1*) was constructed by transforming 500–1,000 ng gRNA helper vector together with 500–1,000 ng of the repair template, which encodes 500 up- and 500 bp downstream sequences around the *ACH1* open reading frame. The required repair templates were made according to EasyCloneYALI Toolbox (Holkenbrink et al., 2017). The right colonies were selected by colony PCR using OneTaq Master Mix (New England Biolabs) using the sequencing primers listed in **Supplementary Table 4**. For strain ST8507 with down-regulated *SDH1* expression, crRNA sequence of gRNA vector was found by identifying the promoter region of gene *YALI0D11374g* (*SDH1*) as the target site on the online tool "CHOPCHOP" (http://chopchop.cbu.uib.no).

Screening of *Y. lipolytica* strains was carried out in 24-deep-well plates with air-penetrable metal lids (EnzyScreen, The Netherlands) containing 3 mL of YPG media with 60 g/L glycerol. A pre-culture of each *Y. lipolytica* strain was grown in 5 mL YPG medium (60 g/L glycerol) in 13-mL tubes overnight at 30°C and 250 rpm. The inoculation of all strains was done with an adequate amount of pre-culture to obtain the starting OD_{600} =0.1. The plates were incubated at 30°C with shaking at 300 rpm at 5 cm orbit cast. Samples were taken after 4 days and analyzed for cell growth and succinic acid titer. All the experiments were run in triplicates, the average and standard deviation values are reported. All the measured standard deviations were below 20%.

Shake Flask Fermentation

The shake flask cultivations were carried out in either 250 or 500 mL shake flasks containing YPG or YPD media at the volume of 10 or 20% of the total flask volume. The flasks were inoculated with overnight pre-culture (described in section 0) to a starting OD_{600} of 0.1, and incubated at 30°C with shaking at 250 rpm. In the case of fermentation at neutral pH, solid $CaCO_3$ corresponding to final concentration of 10 g/L was sterilized together with the shake flask, and the sterile medium was then added aseptically. Samples of 200 μL were taken aseptically at specific time intervals. All the experiments were run in triplicates, the average and standard deviation values are reported. All the measured standard deviations were below 20%.

Adaptation on Glucose

Adaptation of succinic acid producing *Y. lipolytica* strain on glucose was conducted in 250 mL shake flasks containing 50 mL of YPD medium with subsequently increasing initial glucose concentration. The adaptation was carried out in 3 independent lines and the transfer to new media was performed separately for each line. In first step, named as "transfer 1," the shake flasks containing YPD with 20 g/L glucose were inoculated from overnight growing cells in YPG with 60 g/L glycerol to get an OD_{600} = 0.1. The cells were then grown at 30°C and 250 rpm up to OD_{600} 5, after which an adequate amount was transferred to new medium to get an initial OD_{600} = 0.1. This process was repeated with increasing glucose concentrations in the medium.

To separate and purify the adapted isolates, the exponentially growing cells of the final transfer were serially diluted and

cultivated on YPD plates containing 20 g/L glucose for 72 h at 30°C. Single isolates were tested for succinic acid production.

Fed-Batch Fermentation in Bioreactors

Fed-batch fermentation for succinate production was carried out in 1 L bioreactors (BIOSTAT® Q plus, Sartorius, Goettingen, Germany). The bioreactors were equipped with measurement probes for pH, dissolved oxygen (DO), temperature and cell density. During the fermentation, off-gas CO_2 and O_2 concentration was monitored continuously (Thermo Scientific Prima BT MS). Data acquisition was achieved with Lucullus software (Securecell AG, Switzerland). The seed culture was prepared by cultivating the adapted strain in 100 mL of mineral medium described by Maury et al. (2018) containing 20 g/L glucose, and incubating overnight at 30°C and 250 rpm. The seed culture was then centrifuged, washed twice and resuspended in 10 mL media and inoculated to the bioreactors containing 400 mL mineral medium (Maury et al., 2018) to a starting OD_{600} of 1.0. Fermentation was carried out at 30°C, with 1 vvm aeration and pH controlled at 5.0 by addition of 2M KOH. During the cultivation, the dissolved oxygen (DO) level was kept above 40% by cascaded control of stirrer speed and air input flow rate. For repeated fed-batch, sterile glucose was pulsed to a final concentration of 25–50 g/L in the reactor after observing a significant drop in CO_2 levels.

Analytical Methods

In shake flask and deep well-plate experiments, cell growth was monitored by measuring the optical density at 600 nm (OD_{600}) using NanoPhotometer (Implen GmbH, Germany). In the case of buffered fermentation, the samples were diluted with 1 M HCl to dissolve carbonate salts. To conversion of OD_{600} values to dry cell weight (DCW) was done by following empirical correlation:

$$DCW(g/L) = 0.1394 \times OD_{600} - 0.0029$$

The activity of *SDH* enzyme in the strains was measured by using calorimetric assay kit (Sigma Aldrich, Denmark). Cell-free samples were prepared by homogenizing 1×10^6 cells in 100 µL of ice cold *SDH* Assay Buffer (provided by manufacturer) and centrifuging at 10,000 $\times g$ for 5 min. *SDH* activity was determined by generating dichlorophenolindophenol (DCIP) as product with absorbance at 600 nm, which is proportional to the enzymatic activity present. One unit of succinate dehydrogenase was defined as the amount of enzyme that generated 1.0 µmole of dichlorophenolindophenol (DCIP) per minute at pH 7.2 at 25°C.

Glucose, glycerol, succinic acid, and mannitol were all detected and quantified using high performance liquid chromatography (HPLC) Agilent 1,100 series with a refractive index detector and a Bio-Rad Aminex HPX-87H column (300 × 7.8 mm) with 5 mM H_2SO_4 as an eluent at a flow rate of 0.6 mL/min with column oven temperature set to 30°C. To protect the HPX-87H column from contamination and foreign particles, a guard column was fitted to the system. In repeated fed-batch fermentations in bioreactor, glucose concentration of the samples was measured enzymatically by YSI 2900 Biochemistry Analyzer (USA). The yield of succinic acid was defined as the amount of final succinic acid/succinate produced from 1 g of carbon source consumed.

RESULTS AND DISCUSSION

Metabolic Engineering of *Y. lipolytica* for Succinate Production

The cells synthesize succinate as an intermediate of the TCA cycle in mitochondria and as a product of glyoxylate cycle in the cytosol and peroxisomes. Succinate produced in glyoxylate pathway is transported into mitochondria, where it enters the TCA cycle. If succinate dehydrogenase *SDH* that converts succinate to fumarate were inactivated, then TCA and glycoxylate pathways would function in the linear mode with succinate as the product. However, succinate dehydrogenase is an essential enzyme in the obligatory aerobic *Y. lipolytica* and this enzymatic activity cannot be completely eliminated, but only attenuated. Hence, our strategy was to reduce the activity of *SDH* by decreasing gene expression.

To ease the strain engineering, we deleted *KU70* gene that participates in non-homologous end-joining and introduced *Y. lipolytica* codon-optimized *cas9* gene from *Streptococcus pyogenes* into the genome of *Y. lipolytica* strain W29. The resulting strain ST6512 had only a slightly lower maximum specific growth rate ($0.43 \pm 0.04\ h^{-1}$) in comparison to the parental W29 strain ($0.46 \pm 0.03\ h^{-1}$) (**Supplementary Figure 1**).

Further strain metabolic engineering was to interrupt TCA cycle, by trying to knock out the *SDH5* gene, however this was not possible to do in our strain. In parallel, we continued with inactivation of the mitochondrial acetate production in ST6512, which would occur upon interruption of the TCA cycle and would cause growth inhibition (Gao et al., 2016; Cui et al., 2017). For this, we deleted *YALI0E30965g* gene, encoding the mitochondrial acetyl-CoA hydrolase (*ACH1*). The resulting strain (ST8218) and all the derived strains produced no acetate in fermentation experiments. Next step was the introduction of dicarboxylic acid transporter *SpMae1* from *Schizosaccharomyces pombe* in order to improve the secretion of succinic acid. This transporter has been proven to increase malic acid titer significantly in *S. cerevisiae* (Zelle et al., 2008). We also recently showed that *SpMae1* transporter is likely a *SLAC1* voltage-dependent anion channel and is thus very energetically efficient (Darbani et al., 2019). Hence, we expressed transporter gene *SpMae1* in Δ*ACH1* ST8218, to obtain strain ST8413.

Then we proceeded with downregulating the activity of succinate dehydrogenase, as an alternative method for *SDH* deletion. The enzyme consists of five protein subunits, each encoded by a separate gene (*SDH1* to *SDH5*). *SDH5* has been reported to be knocked out in *Y. lipolytica* W29 strain before (Gao et al., 2016). However, all our attempts to knock out this gene in the same background strain W29 with four different designed crRNAs (assembled to plasmids pCfB8032, pCfB8033, pCfB8114, and pCfB8115, **Supplementary Table 2**) were unsuccessful. We also tried to delete this gene using dominant selection marker (hygromycin B resistance) and

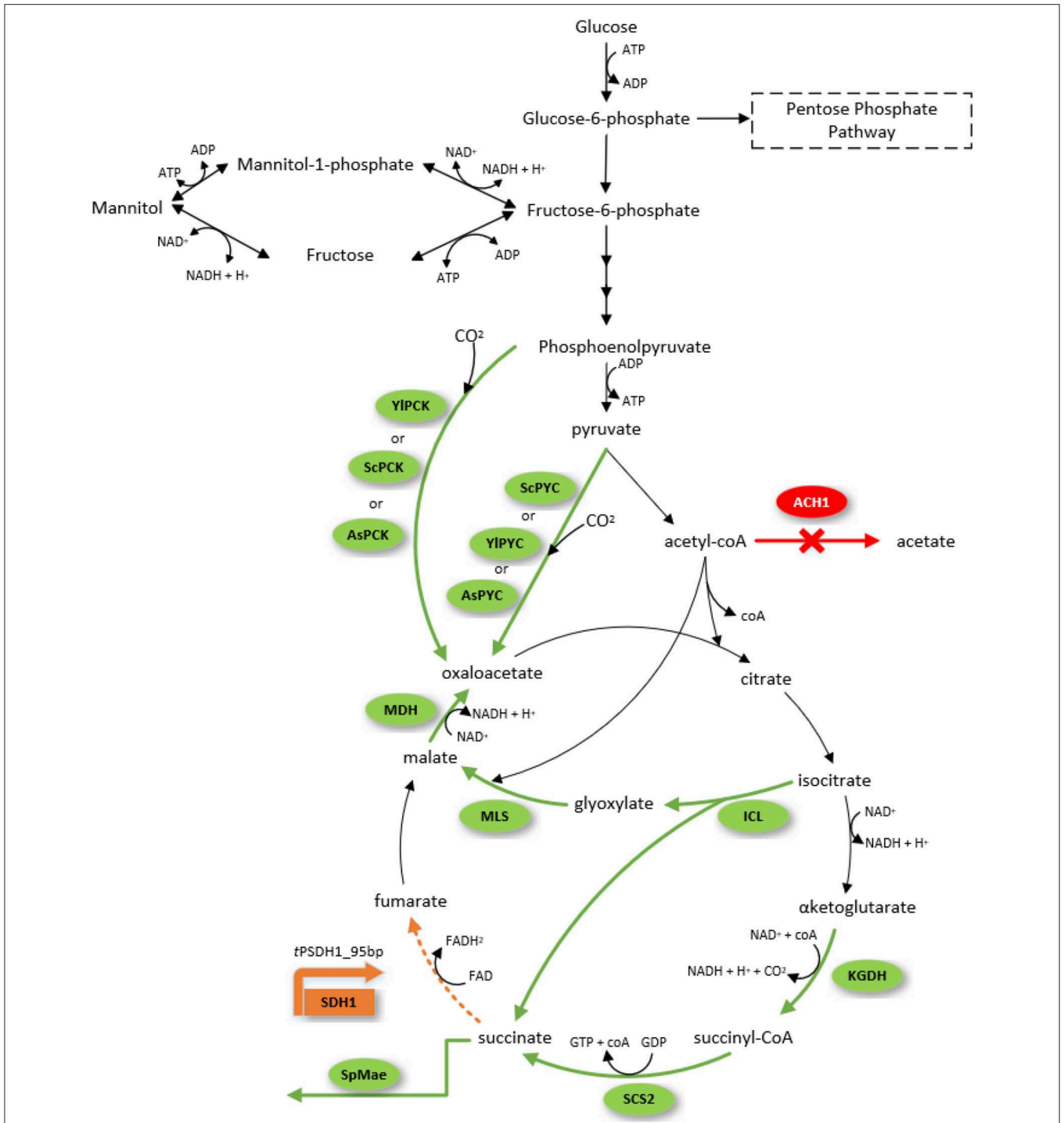

FIGURE 1 | Succinic acid and mannitol biosynthesis pathway from glucose as the sole carbon source in *Yarrowia lipolytica.* The engineered route for overexpression of genes in this study is highlighted with green arrows, deleted pathways highlighted in red, and downregulated pathway in orange. Gene nomenclature: Acetyl-CoA hydrolase (*ACH1*), phosphoenolpyruvate carboxykinase from *A. succinogenes* (*AsPCK*), pyruvate carboxylase from *A. succinogenes* (*AsPYC*), Isocitrate lyase (*ICL*), α-ketoglutarate dehydrogenase (*KGDH*), malate dehydrogenase (*MDH*), malate synthase (*MLS*), pyruvate carboxylase from *S. cerevisiae* (*ScPYC*), phosphoenolpyruvate carboxykinase from *S. cerevisiae* (*ScPCK*), succinyl-CoA synthase beta-subunit (*SCS2*), dicarboxylic acid transporter from *S. pombe* (*SpMae1*), pyruvate carboxylase from *Y.lipolytica* (*YlPYC*), phosphoenolpyruvate carboxykinase (*YlPCK*), succinate dehydrogenase subunit 1 under the control of truncated promoter (*tPSDH1*).

large 500 bp homologous arms. This method typically works very well in *Y. lipolytica*, but we still could not obtain any colonies for *SDH5* deletion mutants on either glycerol- or glucose-based media. This indicates that *SDH5* is an essential gene. Two other subunits of succinate dehydrogenase *SDH1* and *SDH2* were reported to be essential previously (Yuzbashev et al., 2010). Hence, we decided to downregulate the *SDH1* gene like following. The endogenous promoter of *SDH1* gene was truncated to 95 bp upstream of the start codon (*t*P*SDH1*) in strain ST8413. The resulting strain ST8507 accumulated 1.2 ± 0.1 g/L succinate in 4 days in deep-well plate cultivation, while no succinate was produced by the parental strain ST8413 (**Figure 2**). The comparison between *SDH* activity in the parental strain ST8413 (0.012 ± 0.001 milliunits/μL) and in *SDH1* promoter truncation strain ST8507 (0.003 ± 0.000 milliunits/μL) confirmed a significant reduction of *SDH* activity by 77% (**Supplementary Figure 1**). Further, the strain ST8507 had a lower growth with μ_{max} decreasing from 0.49 ± 0.01 h^{-1} to 0.33 ± 0.02 h^{-1} and an 8-h longer lag phase (**Supplementary Figure 2**). This indicates the significant role of this gene in the cell growth and metabolism.

The strain was further engineered to improve succinic acid production through three different strategies (**Figure 1**). The first strategy was to enhance the carboxylation of reactions that generate oxaloacetate for the TCA cycle. Here, we expressed pyruvate carboxylase encoding genes: native (*PYC*), from *S. cerevisiae* (*ScPYC1* and *ScPYC2*) or from *A. succinogenes* (*AsPYC*). We also tested the expression of phosphoenolpyruvate carboxykinase gene: native (*PCK*), from *S. cerevisiae* (*ScPCK*), or from *A. succinogenes* (*AsPCK*), to investigate whether *PYC* or *PCK* pathways were more effective on improving succinic acid titer. The second strategy was directed to increasing the flux through glyoxylate pathway, where additional copies of the native isocitrate lyase (*ICL*), malate synthase (*MLS*), and malate dehydrogenase (*MDH*) genes were expressed from

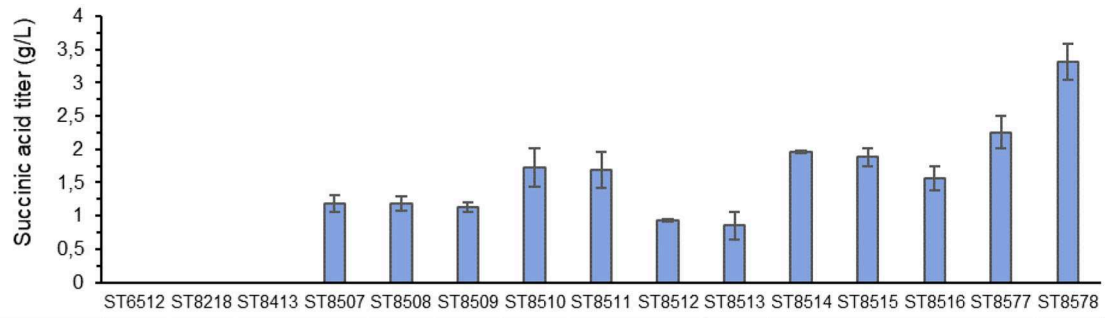

	ST6512	ST8218	ST8413	ST8507	ST8508	ST8509	ST8510	ST8511	ST8512	ST8513	ST8514	ST8515	ST8516	ST8577	ST8578
Δ*ACH1*	-	+	+	+	+	+	+	+	+	+	+	+	+	+	+
SpMae1	-	-	+	+	+	+	+	+	+	+	+	+	+	+	+
*t*P*SDH1*	-	-	-	+	+	+	+	+	+	+	+	+	+	+	+
ScPYC1	-	-	-	-	+	-	-	-	-	-	-	-	-	-	-
ScPYC2	-	-	-	-	+	-	-	-	-	-	-	-	-	-	-
ScPCK	-	-	-	-	-	+	-	-	-	-	-	-	-	-	-
AsPCK	-	-	-	-	-	-	+	-	-	-	-	-	-	-	+
AsPYC	-	-	-	-	-	-	-	+	-	-	-	-	-	-	-
YlPCK	-	-	-	-	-	-	-	-	+	-	-	-	-	-	-
YlPYC	-	-	-	-	-	-	-	-	-	+	-	-	-	-	-
MLS	-	-	-	-	-	-	-	-	-	-	+	+	-	+	+
ICL	-	-	-	-	-	-	-	-	-	-	+	+	-	+	+
MDH	-	-	-	-	-	-	-	-	-	-	-	+	-	+	+
SCS2	-	-	-	-	-	-	-	-	-	-	-	-	+	+	+
KGDH	-	-	-	-	-	-	-	-	-	-	-	-	+	+	+

FIGURE 2 | Succinic acid production by engineered strains of *Y. lipolytica*. The strains were cultivated on YP medium with 5% v/v of glycerol as carbon source in deep-well plates for 4 days. The highest producing strain ST8578 was selected for further study. The values are averages from three biological replicates, the error bars show the standard deviation.

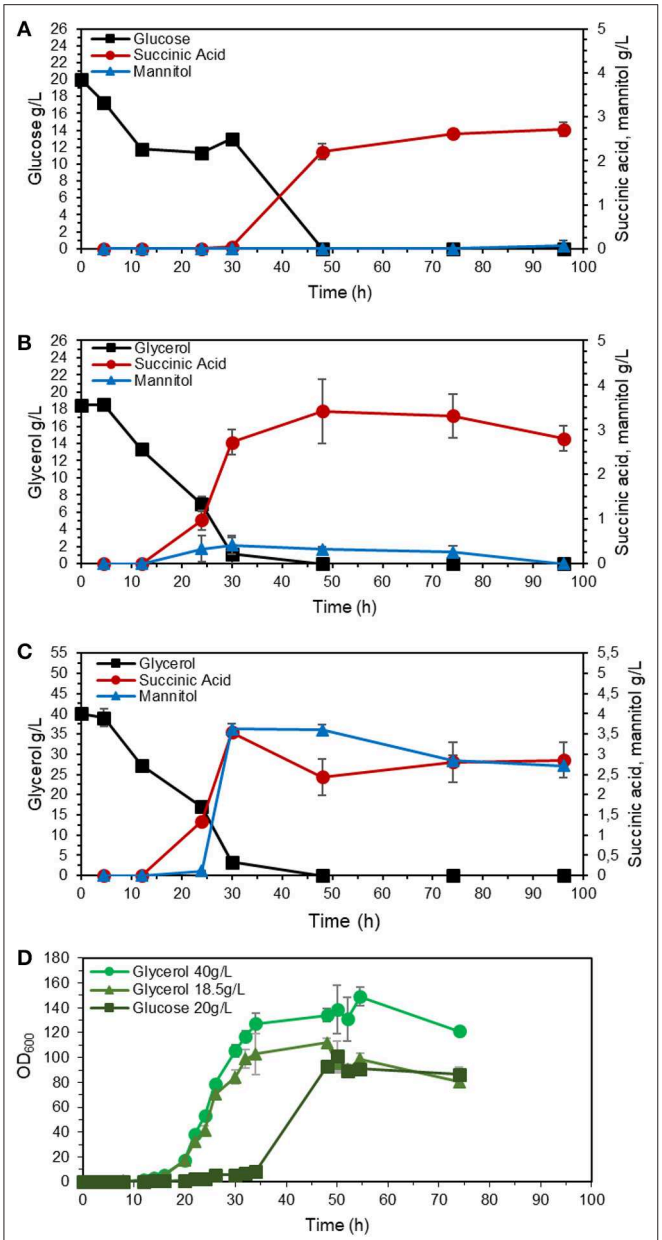

FIGURE 3 | Performance of succinate-producing strain (ST8578) on glucose or glycerol as carbon source. The strains were cultivated in shake flasks on YP medium with 20 g/L glucose monohydrate **(A)**, 18.5 g/L glycerol **(B)**, or 40 g/L glycerol **(C)**, with OD_{600} profile showing the ability of the cells to grow on glucose with longer lag phase compared to glycerol **(D)**. The values are averages from three biological replicates, the error bars show the standard deviation.

strong constitutive promoters. The third strategy aimed to increase the flux through the oxidative TCA branch. For this, we expressed additional copies of succinyl-CoA synthase beta subunit (*SCS2*) and α-ketoglutarate dehydrogenase (*KGDH*) genes, again driven by strong constitutive promoters. A total of 11 strains were constructed and tested for succinate production on complex medium with glycerol as carbon source in deep-well plates (**Figure 2**).

TABLE 2 | Shake flask fermentation results of ST8578 on YP media supplemented with 1.3 C-mol/L glycerol (40 g/L), 0.6 C-mol/L glycerol (18.5 g/L), and 0.6 C-mol/L D-glucose (20 g/L) after 48 h of cultivation.

Parameter	Glucose 0.6 C-mol/L	Glycerol 0.6 C-mol/L	Glycerol 1.3 C-mol/L
Succinic Acid titer (g/L)	2.2 ± 0.1	3.4 ± 0.7	2.8 ± 0.4
Yield ($C\text{-}mol_{SA}/C\text{-}mol_{substrate}$)	0.13 ± 0.01	0.20 ± 0.04	0.07 ± 0.01
Mannitol titer (g/L)	0	0.3 ± 0.0	3.6 ± 0.1

For the carboxylation strategy, we saw a 42 and 45% improvement of succinate titer upon expression of pyruvate carboxylase and PEP carboxykinase from *A. succinogenes*, respectively (**Figure 2**). The expression of *Yarrowia* native or *S. cerevisiae* enzyme variants did not improve succinate production.

The glyoxylate pathway strategy, where *ICL*, *MLS*, and *MDH* genes were overexpressed resulted in 58% improvement of the succinate titer. The native glyoxylate pathway genes are repressed during the growth on glucose (Juretzek et al., 2001), while we used strong constitutive TEF promoter with its intron (pTEFin) for *ICL* expression (Tai and Stephanopoulos, 2013) and thus activated the pathway. These results can be compared with the results obtained by Cui et al., who expressed *ICL* gene under the control of *HP4D* promoter and could not see any improvement in succinate titer (Cui et al., 2017). In this study, we overexperessed *ICL* gene from *TEF1* promoter with intron and we observed a positive effect on succinic acid production. The TEF1 promoter was shown to be 5-fold stronger than *HP4D* promoter in *Y. lipolytica* (Tai and Stephanopoulos, 2013).

Overexpression of the oxidative branch of the TCA cycle genes (*SCS2* and *KDGH*) alone did not give an improvement of succinate production, but when combined with glyoxylate strategy, an improvement of 90% was obtained in comparison to the reference strain ST8507. These results shows the synergic and additive effect of genes in glyoxylate shunt and oxidative branch of TCA cycle, on succinic acid titer. Finally, we combined all three strategies (from the first strategy, we chose *AsPCK* expression, as both *AsPCK* and *AsPYC* showed similar effect on succinic acid titer) into strain ST8578 that gave 3.3 ± 0.2 g/L succinic acid, a 280% increase in comparison to the reference ST8507.

Growth and Succinic Acid Production of the Engineered Strain

The strains with inactivated *SDH5* were previously reported to lose the ability to grow on glucose (Yang et al., 2017). To investigate the effect of reduced expression of *SDH1*, we studied the growth and product formation profile of the engineered strain ST8578 on complex medium, as shown in **Figure 3**, with glucose or glycerol as carbon source (0.6 C-mol substrate/L). The strain grew on glucose medium, however, the lag phase was longer compared to growth on glycerol (16 vs. 6 h). There were also distinct differences between the metabolites production on two media. Succinic acid was

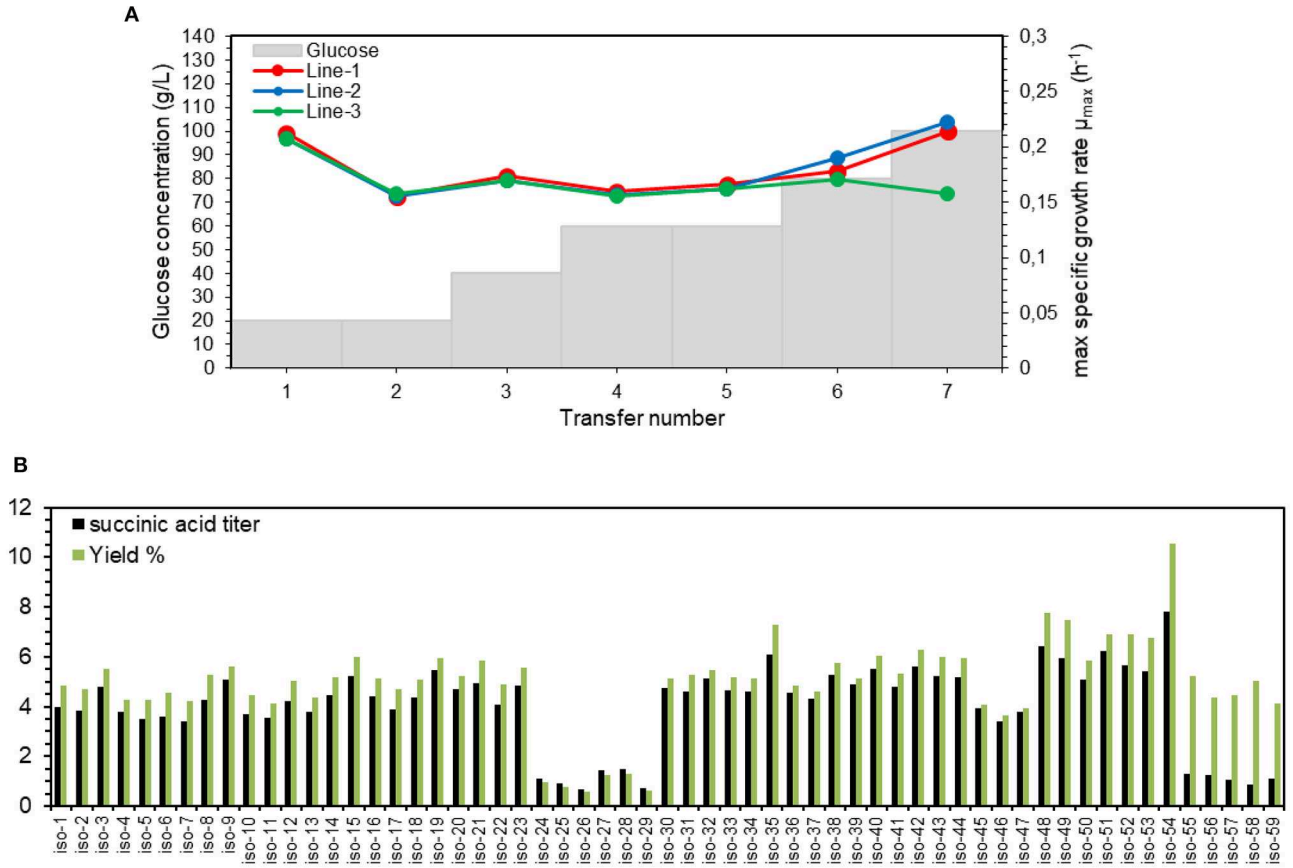

FIGURE 4 | Adaptation of succinate-producing strain ST8578 to high concentrations of glucose. **(A)** Maximum specific growth rates (μ_{max}) are shown as the strains are serially transferred to media with higher glucose concentrations. **(B)** Succinate titer and yield of multiple adapted isolates of ST8578 was assessed in deep-well plates on YP medium with 100 g/L glucose after 48 h incubation **(B)**. The isolate nr. 54 (iso-54) was chosen as the best producer.

produced at a higher titer in glycerol medium compared to glucose medium, 3.4 ± 0.7 vs. 2.2 ± 0.1 g/L and with a higher yield, 0.20 ± 0.04 C-mol/C-mol glycerol vs. 0.13 ± 0.01 C-mol/C-mol glucose (**Table 2**). While succinic acid titer was higher on glycerol, there was also a by-product mannitol produced at 0.30 ± 0.04 g/L mannitol, which was not detected in glucose fermentation. When we used higher starting glycerol concentration, succinic acid titer decreased slightly, while mannitol increased to 3.6 ± 0.1 g/L. This presents a problem for using glycerol as carbon source for succinic acid production, because a large fraction of carbon is channeled to mannitol.

Glycerol is a more reduced substrate than glucose and generates an additional mol of NADH during the catabolism. If the culture is oxygen limited (as may happen at higher cell densities), the rate of NAD^+ regeneration via oxidative phosphorylation will be slower than NADH generation (Diano et al., 2006). To manage the redox co-factor imbalance, *Y. lipolytica* begins synthesizing mannitol regenerating NAD^+ in the process (Workman et al., 2013). Additionally, polyols as mannitol function as osmoprotectants, and their synthesis may be further induced by exposure to high concentrations of the substrate.

Adaptation of Final Engineered Strain on Glucose

While the strain engineered through downregulation of *SDH1* preserved the ability to metabolize glucose, it had a longer lag phase on glucose than on glycerol and grew slower. We then carried out a short adaptation to shorten the lag phase and to increase the tolerance of the cells to high glucose concentrations.

For this purpose, a series of experiments in shake flasks with YP media containing initially 20 g/L glucose was started in 3 separate lines. The cells were transferred to the new medium when OD_{600} reached 5. If this OD value was reached within <20 h, then a serial transfer was done into a medium with a higher glucose concentration, otherwise glucose concentration in the next transfer was kept the same. The initial decrease in μ_{max} from transfer number 1–2 is due to the presence of glycerol in the 1st transfer, which was inoculated with YPG-grown preculture (**Figure 4A**). The average μ_{max} of all the three lines of transfers

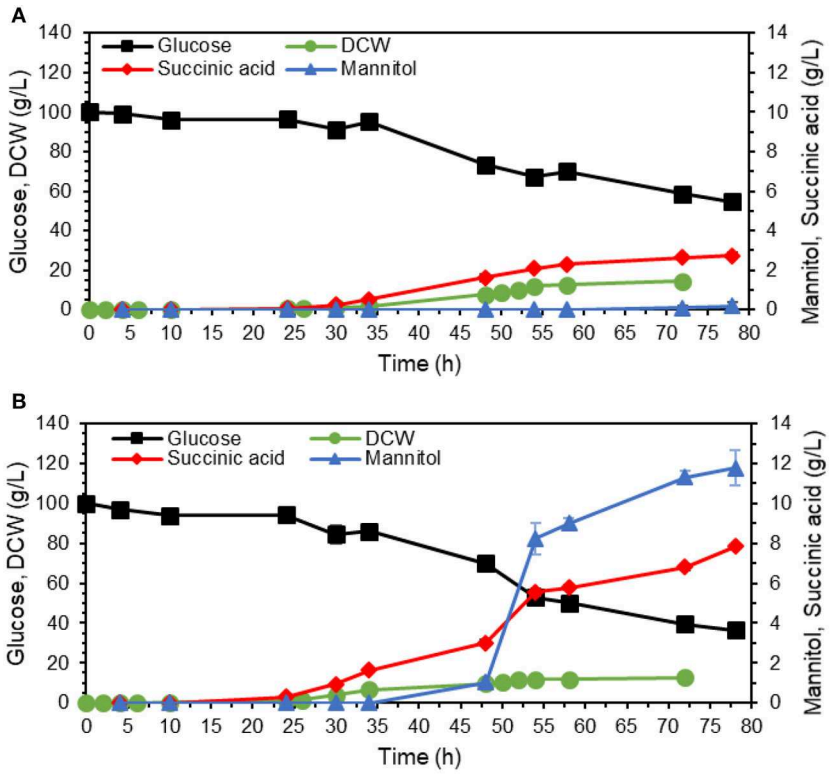

FIGURE 5 | Comparison of the succinate-producing strain ST8578 **(A)** and its adapted isolate (iso-54) **(B)**. The strains were cultivated in shake flasks with YP medium containing 100 g/L glucose as carbon source. The values are averages from three biological replicates, the error bars show the standard deviation.

2–5 was 0.16 ± 0.00 h^{-1}, which is close to that on YPD with 20 g/L glucose (**Table 2**). This implies that with 5 transfers, the cells were adapted to utilize 60 g/L of glucose with no change in the maximum specific growth rate. For transfers 6 and 7 (80 and 100 g/L glucose), μ_{max} value increased for lines 1&2 to 0.21 h^{-1}, while it decreased for line 3 to 0.15 h^{-1}.

As the adapted culture likely is a mixed population of different clones, we isolated single clones. A total of 59 single colonies were isolated from transfer 7 of **Figure 4B**, where 23 colonies were from line 1 (iso-1 to 23), 18 colonies from line 2 (iso-24 to 41), and 18 colonies from line 3 (iso-42 to 59). The results of deep-well plate fermentation of these 59 isolates in the medium containing 100 g/L glucose (**Figure 4B**) showed that isolates 48–54 from the slower growing line 3 had the highest succinic acid titer. Also from **Figure 4B**, it can be seen that the isolates 24–29 had improved growth on glucose through adaptation process, but had lost succinic acid production ability during this time course. The highest titer of succinic acid was for isolate 54, with 7.8 ± 0.0 g/L succinic acid after 48 h, corresponding to 0.105 g/g glucose yield, which was also the highest among the isolates. Therefore, after only 7 transfers, the isolate 54 (named adapted-ST8578) was obtained that was able to grow on YPD containing 100 g/L glucose.

The adapted strain was compared to the parental strain in 250 mL shake flasks containing YPD with 100 g/L glucose. The adaptation has shortened the lag phase for ∼6 h (**Figure 5**), with the final biomass concentrations of 14.5 ± 0.5 g DCW/L and 12.8 ± 0.1 g DCW/L for non-adapted and adapted strains, respectively. The μ_{max} increased from 0.14 ± 0.01 to 0.18 ± 0.00 h^{-1}. The final titer of succinic acid increased 2.8-fold, from 2.7 ± 0.2 g/L succinic acid for the non-adapted strain to 7.8 ± 0.0 g/L for the adapted strain (**Figure 5**). Furthermore, the adapted strain utilized a higher fraction of the added glucose (63.6 ± 2.9 g/L of glucose vs. 45.5 ± 3.6 g/L of glucose for the non-adapted strain). Interestingly, the adapted strain produced large amount of mannitol, 11.8 ± 0.9 g/L vs. 0.2 ± 0.1 g/l for the non-adapted strain.

Suppression of Mannitol Production in the Adapted Strain

Mannitol is a sugar alcohol that is involved in carbohydrate storage, redox co-factor balancing, osmoprotection, and oxidative stress protection (Patel and Williamson, 2016). The pathway, also shown in **Figure 1**, is known to be activated under oxygen limitation (Diano et al., 2006). We tested whether higher aeration would decrease mannitol production by filling up the flasks with medium up to 10% instead of 20% of the total volume (**Figures 6A,B**). Based on results from **Figure 5**, the adapted cells were cultivated in YPD media containing 70 g/L, corresponding

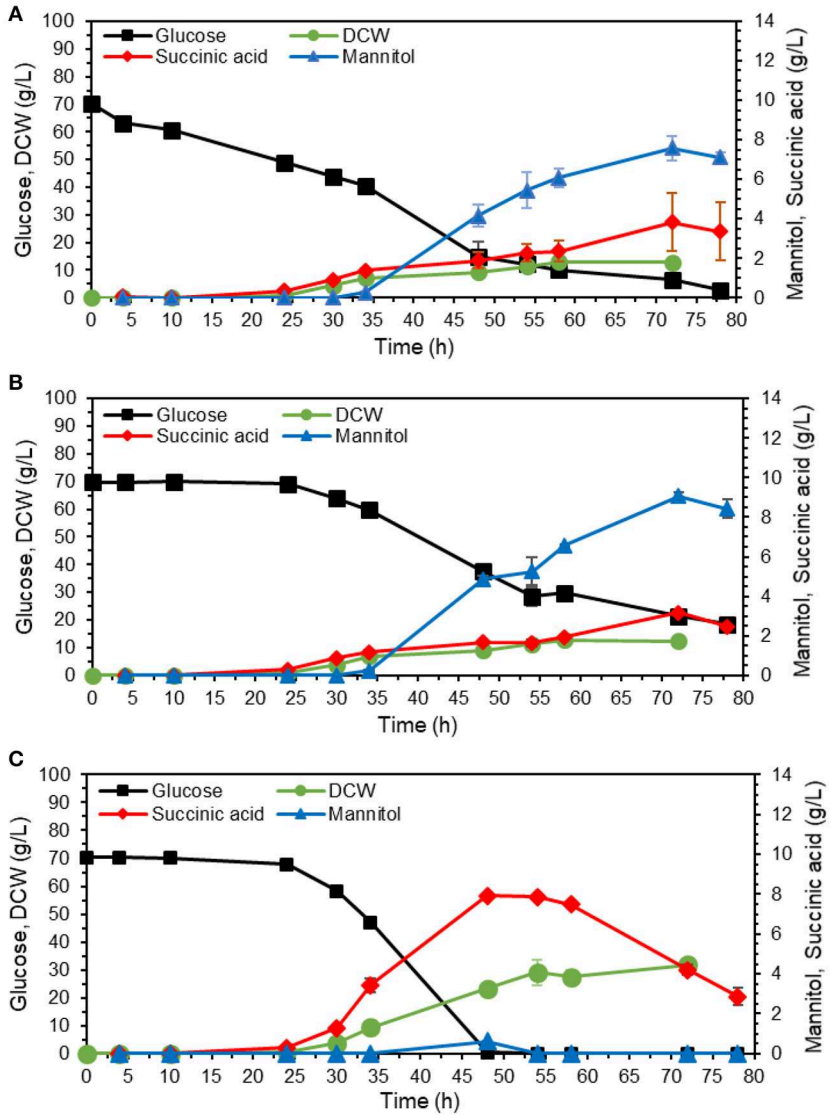

FIGURE 6 | Effect of aeration rate and medium buffering on mannitol production. The adapted isolate 54 was cultivated in shake flasks on YP with 70 g/L glucose. **(A)** Cultivation volume was 20% of the total flask volume. **(B)** Cultivation volume was 10% of the total flask volume to obtain better aeration. **(C)** Cultivation volume was as in A, medium was buffered with 10 g/L calcium carbonate. The values are averages from three biological replicates, the error bars show the standard deviation.

to glucose amount that could be utilized by the strain in 80 h (**Figure 5B**).

Contrary to our hypothesis, the final mannitol titer was actually higher in the flask with better aeration (10% working volume), 8.4 ± 0.5 vs. 7.6 ± 0.6 g/L in the flask with normal aeration (20% working volume). The final biomass was similar for both conditions, 12.8 ± 1.1 g DCW/L for normal aeration (**Figure 6A**) and 12.4 ± 0.3 g DCW/L for high aeration (**Figure 6B**). These results imply that mannitol overproduction by the adapted strain was not caused by oxygen limitation. We then hypothesized that mannitol production could instead be caused by acidic pH stress. To investigate the effect of pH, we supplemented YPD medium containing 70 g/L glucose with 10 g/L $CaCO_3$ for buffering (**Figure 6C**) and indeed this supplementation abolished mannitol production. Moreover, the glucose was depleted already at 48 h in contrast to 78 h in unbuffered fermentation. After glucose depletion, the cells started using succinate as the substrate. The final biomass at glucose depletion point was nearly double for the buffered fermentation, 23.3 ± 0.7 g DCW/L compared to 12.8 ± 1.1 g DCW/L. With no carbon wasted on mannitol synthesis, buffered fermentation also resulted in more succinate, 7.9 ± 0.1 g/L with a yield of 0.11 ± 0.00 g/g glucose (**Figure 6C**) compared to 3.3 ± 1.5 g/L and 0.05 ± 0.02 g/g glucose for unbuffered fermentation (**Figure 6A**). The secretion of mannitol started nearly at the same time as succinate

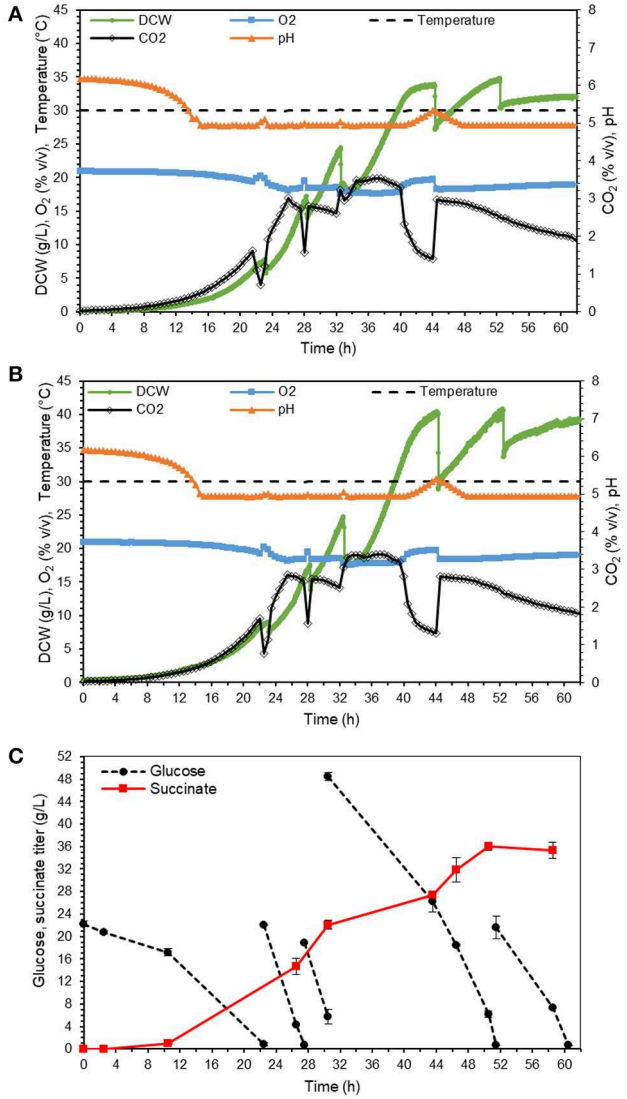

FIGURE 7 | Bioreactor fermentation results of adapted strain in minimal medium in two 1 L fermenters, with online data for individual reactors **(A,B)**, and offline measurements as average for both reactors **(C)**, error bars indicate standard deviation calculated from the two independent bioreactor experiments.

production (**Figures 5**, **6**), which confirms our hypothesis that mannitol production may be a cellular response to the acidic pH.

Fed-Batch Fermentation in Bioreactors

Finally, we tested the production of succinic acid in mineral medium at pH 5 in two controlled repeated fed-batch mode operated bioreactors. At this pH, the major fraction of product is in acidic form rather than dissociated form (according to calculations based on K_a values of succinic acid 6.2×10^{-5} and 2.3×10^{-6}), which means that no succinic acid recovery is needed in the downstream process. The feeding was aimed to provide 25–50 g/L glucose to the culture on the time points of glucose depletion, which was indicated by CO_2 production drop or pH increase. The batch phase with exponential growth was completed at around 22 h, after which the first pulse of feeding was spiked. As shown in **Figures 7A,B** for individual bioreactors, the process was highly reproducible with 32 and 39 g DCW/L and final succinate titer of 35.3 ± 1.5 g/L in 59 h of fermentation (**Figure 7C**). The yield 0.26 ± 0.00 g/g glucose was almost double as high as in the shake flask cultivations (section Suppression of mannitol production in the adapted strain). The productivity was 0.60 ± 0.03 g/L/h. The maximum uptake rate of glucose for adapted strain was 1.0 ± 0.03 g/L.h during batch phase. With similar growth condition and biomass concentration of 11 g/L, Moeller et al. reported a maximum glucose uptake rate of 1.1 ± 0.14 g/L.h for *Y. lipolytica* (Moeller et al., 2012). Comparison of these two values shows that the adapted strain has almost recovered all its capability of glucose utilization. However, the glucose consumption rate of Y. lipolytica is still much lower than other yeast species. For instance, the glucose uptake rate for succinate producer *S. cerevisiae* strain AH22ura3 (Raab et al., 2010) is more than two times higher than that of *Y. lipolytica*.

The comparison of the results in our study with the titer of highest succinate producer of *Y. lipolytica* strain VKPM Y-3753 from glucose (Bondarenko et al., 2017, **Table 1**) shows that the later produces about 20 g/L higher than our strain. However, the titer for both processes is at least 100 g/L away from where it should be for commercial implementation. Hence a lot of future work is needed on both strains to bring them to the performance level required for production of a bulk chemical as succinic acid. The main advantage of adapted-ST8578 constructed in this study is that it has been developed through rational metabolic engineering approach and it is fully genetically defined. In contrast, VKPM Y-3753, strain was created by multiple rounds of mutagenesis and selection. The adapted-ST8578 can be further genetically modified or evolved/mutagenized following similar strategies as described by Bondarenko et al. and will likely reach higher performance. Eventually, the commercial process will need to be carried out at a lower pH, possibly even avoiding base addition altogether. For this, further strain and process optimizations are needed that go beyond the scope of this study.

CONCLUSION

The main aim of the study was to construct a variant of *Y. lipolytica* yeast capable of producing succinic acid from glucose through rational engineering. The successful engineering strategies included overexpression of glyoxylate pathway, oxidative TCA cycle branch, and reductive carboxylation, as well as expression of dicarboxylic acid transporter from *S. pombe*. A short adaptation of this strain on glucose reduced the lag phase and improved the growth rate at high glucose concentrations. The production of mannitol as by-product could be eliminated by maintaining a neutral pH. In fed-batch fermentation at pH 5, the succinic acid titer was 35.3 ± 1.5 g/L

with the yield on glucose of 0.26 ± 0.00 g/g and volumetric productivity of 0.60 ± 0.03 g/L/h. At pH 5.0, the major fraction of product is in acidic form rather than dissociated form (according to calculations based on K_a values of succinic acid 6.2×10^{-5} and 2.3×10^{-6}). Hence the ultimate goal of producing succinic acid from glucose was accomplished in the current work.

DATA AVAILABILITY STATEMENT

All datasets generated for this study are included in the article/**Supplementary Material**.

AUTHOR CONTRIBUTIONS

MB, KR, and IB conceived the study and designed the experiments and analyzed the data. MB performed the experiments. The fed-batch fermentation was performed by MB and SS. MB, KR, MH, SE, AN, and IB wrote the manuscript. IB and IA secured the funding and supervised the project.

ACKNOWLEDGMENTS

The authors acknowledge the financial support from the Novo Nordisk Foundation (Grant Agreement No. NNF10CC1016517 and No. NNF15OC0016592), from the European Research Council under the European Union's Horizon 2020 research and innovation programme (YEAST-TRANS project, Grant Agreement No. 757384) and from Iranian Ministry of Science and Technology.

The authors acknowledge ARS culture collection (NRRL, USA) for providing *Y. lipolytica* W29 strain. We also thank Eko Roy Marella for developing W29 strain with Cas9.

SUPPLEMENTARY MATERIAL

The Supplementary Material for this article can be found online at: https://www.frontiersin.org/articles/10.3389/fbioe.2019.00361/full#supplementary-material

REFERENCES

Ahn, J. H., Jang, Y. S., and Lee, S. Y. (2016). Production of succinic acid by metabolically engineered microorganisms. *Curr. Opin. Biotechnol.* 42, 54–66. doi: 10.1016/j.copbio.2016.02.034

Bondarenko, P. Y., Fedorov, A. S., and Sineoky, S. P. (2017). Optimization of repeated-batch fermentation of a recombinant strain of the yeast *Yarrowia lipolytica* for succinic acid production at low pH. *Appl. Biochem. Micro.* 53, 882–887. doi: 10.1134/S0003683817090022

Cavallo, E., Charreau, H., Cerrutti, P., and Foresti, M. L. (2017). *Yarrowia lipolytica*: a model yeast for citric acid production. *FEMS Yeast Res.* 17:fox084 doi: 10.1093/femsyr/fox084

Chen, D. C., Beckerich, J. M., and Gaillardin, C. (1997). One-step transformation of the dimorphic yeast *Yarrowia lipolytica*. *Appl. Microbiol. Biotechnol.* 48, 232–235. doi: 10.1007/s002530051043

Chinthapalli, R., Iffland, K., Aeschelmann, F., Raschka, A., and Carus, M. (2018). *Succinic acid: New Bio-Based Building Block With a Huge Market and Environmental Potential?* Nova-Institut GmbH. Retrieved from: http://www.bio-based.eu/reports/ (accessed April, 2019).

Cui, Z., Gao, C., Li, J., Hou, J., Lin, C. S. K., and Qi, Q. (2017). Engineering of unconventional yeast *Yarrowia lipolytica* for efficient succinic acid production from glycerol at low pH. *Metab. Eng.* 42, 126–133. doi: 10.1016/j.ymben.2017.06.007

Darbani, B., Stovicek, V., van der Hoek, S. A., and Borodina, I. (2019). Engineering energetically efficient transport of dicarboxylic acids in yeast *Saccharomyces cerevisiae*. *Proc. Nat. Acad. Sci.* 116, 19415–20. doi: 10.1073/pnas.1900287116

Dean, J. A. (1999). *Lange's Handbook of Chemistry*. New York, NY; London: McGraw-Hill, Inc.

Diano, A., Bekker-Jensen, S., Dynesen, J., and Nielsen, J. (2006). Polyol synthesis in *Aspergillus niger*: influence of oxygen availability, carbon and nitrogen sources on the metabolism. *Biotechnol. Bioeng.* 94, 899–908. doi: 10.1002/bit.20915

Gao, C., Yang, X., Wang, H., Rivero, C. P., Li, C., Cui, Z., et al. (2016). Robust succinic acid production from crude glycerol using engineered *Yarrowia lipolytica*. *Biotechnol. Biofuels* 9:179. doi: 10.1186/s13068-016-0597-8

Guo, H., Su, S., Madzak, C., Zhou, J., Chen, H., and Chen, G. (2016). Applying pathway engineering to enhance production of alpha-ketoglutarate in *Yarrowia lipolytica*. *Appl. Microbiol. Biotechnol.* 100, 9875–9884. doi: 10.1007/s00253-016-7913-x

Holkenbrink, C., Dam, M. I., Kildegaard, K. R., Beder, J., Dahlin, J., Doménech Belda, D., et al. (2017). EasyCloneYALI: CRISPR/Cas9-based synthetic toolbox for engineering of the yeast *Yarrowia lipolytica*. *Biotechnol. J.* 13:9. doi: 10.1002/biot.201700543

Jansen, M. L., and van Gulik, W. M. (2014). Towards large scale fermentative production of succinic acid. *Curr. Opin. Biotechnol.* 30, 190–197. doi: 10.1016/j.copbio.2014.07.003

Jost, B., Holz, M., Aurich, A., Barth, G., Bley, T., and Müller, R. A. (2014). The influence of oxygen limitation for the production of succinic acid with recombinant strains of *Yarrowia lipolytica*. *Appl. Microbiol. Biotechnol.* 99, 1675–1686. doi: 10.1007/s00253-014-6252-z

Juretzek, T., Le Dall, M., Mauersberger, S., Gaillardin, C., Barth, G., and Nicaud, J. (2001). Vectors for gene expression and amplification in the yeast Yarrowia lipolytica. *Yeast* 18, 97–113. doi: 10.1002/1097-0061(20010130)18:2<97::AID-YEA652>3.0.CO;2-U

Kamzolova, S. V., Dedyukhina, E. G., Samoilenko, V. A., Lunina, J. N., Puntus, I. F., Allayarov, R. L., et al. (2013). Isocitric acid production from rapeseed oil by *Yarrowia lipolytica* yeast. *Appl. Microbiol. Biotechnol.* 97, 9133–9144. doi: 10.1007/s00253-013-5182-5

Kamzolova, S. V., Vinokurova, N. G., Dedyukhina, E. G., Samoilenko, V. A., Lunina, J. N., Mironov, A. A., et al. (2014a). The peculiarities of succinic acid production from rapeseed oil by *Yarrowia lipolytica* yeast. *Appl. Microbiol. Biotechnol.* 98, 4149–4157. doi: 10.1007/s00253-014-5585-y

Kamzolova, S. V., Vinokurova, N. G., Shemshura, O. N., Bekmakhanova, N. E., Lunina, J. N., Samoilenko, V. A., et al. (2014b). The production of succinic acid by yeast *Yarrowia lipolytica* through a two-step process. *Appl. Microbiol. Biotechnol.* 98, 7959–7969. doi: 10.1007/s00253-014-5887-0

Lee, J. W., Yi, J., Kim, T. Y., Choi, S., Ahn, J. H., Song, H., et al. (2016). Homo-succinic acid production by metabolically engineered *Mannheimia succiniciproducens*. *Metab. Eng.* 38, 409–417. doi: 10.1016/j.ymben.2016.10.004

Li, C., Gao, S., Li, X., Yang, X., and Lin, C. S. K. (2018a). Efficient metabolic evolution of engineered *Yarrowia lipolytica* for succinic acid production using a glucose-based medium in an *in situ* fibrous bioreactor under low-pH condition. *Biotechnol. Biofuels* 11:236. doi: 10.1186/s13068-018-1233-6

Li, C., Gao, S., Yang, X., and Lin, C. S. K. (2018b). Green and sustainable succinic acid production from crude glycerol by engineered *Yarrowia lipolytica* via agricultural residue based *in situ* fibrous bed bioreactor. *Bioresour. Technol.* 249, 612–619. doi: 10.1016/j.biortech.2017.10.011

Li, C., Yang, X., Gao, S., Wang, H., and Lin, C. S. K. (2017). High efficiency succinic acid production from glycerol via *in situ* fibrous bed bioreactor with an engineered *Yarrowia lipolytica*. *Bioresour. Technol.* 225, 9–16. doi: 10.1016/j.biortech.2016.11.016

Maury, J., Kannan, S., Jensen, N. B., Öberg, F. K., and Kildegaard, K. R., Forster, J., et al. (2018). Glucose-dependent promoters for dynamic regulation of metabolic pathways. *Front. Bioeng. Biotechnol*. 6:63. doi: 10.3389/fbioe.2018.00063

Mironczuk, A. M., Rzechonek, D. A., Biegalska, A., Rakicka, M., and Dobrowolski, A. (2016). A novel strain of *Yarrowia lipolytica* as a platform for value-added product synthesis from glycerol. *Biotechnol. Biofuels*. 9:180. doi: 10.1186/s13068-016-0593-z

Moeller, L., Zehnsdorf, A., Aurich, A., Bley, T., and Strehlitz, B. (2012). Substrate utilization by recombinant *Yarrowia lipolytica* growing on sucrose. *Appl. Microbiol. Biotechnol*. 93:1695. doi: 10.1007/s00253-011-3681-9

Patel, T. K., and Williamson, J. D. (2016). Mannitol in plants, fungi, and plant–fungal interactions. *Trends Plant Sci*. 21, 486–497. doi: 10.1016/j.tplants.2016.01.006

Pateraki, C., Patsalou, M., Vlysidis, A., Kopsahelis, N., Webb, C., Koutinas, A. A., et al. (2016). *Actinobacillus succinogenes*: advances on succinic acid production and prospects for development of integrated biorefineries. *Biochem. Eng. J*. 112, 285–303. doi: 10.1016/j.bej.2016.04.005

Raab, A. M., Gebhardt, G., Bolotina, N., Weuster-Botz, D., and Lang, C. (2010). Metabolic engineering of *Saccharomyces cerevisiae* for the biotechnological production of succinic acid. *Metab. Eng*. 12, 518–525. doi: 10.1016/j.ymben.2010.08.005

Sauer, M., Porro, D., Mattanovich, D., and Branduardi, P. (2008). Microbial production of organic acids: expanding the markets. *Trends Biotechnol*. 26, 100–108. doi: 10.1016/j.tibtech.2007.11.006

Sineokii, S. P., Sobolevskaya, T. N., and Lukina, G. P. (2012). *Yeast Strain Yarrowia Lipolytica VKPM Y-3753 Is A Succinic Acid Producer. RF Patents* 46.

Stovicek, V., Borja, G. M., Forster, J., and Borodina, I. (2015). EasyClone 2.0: expanded toolkit of integrative vectors for stable gene expression in industrial *Saccharomyces cerevisiae* strains. *J. Ind. Microbiol. Biotechnol*. 42, 1519–1531. doi: 10.1007/s10295-015-1684-8

Tai, M., and Stephanopoulos, G. (2013). Engineering the push and pull of lipid biosynthesis in oleaginous yeast *Yarrowia lipolytica* for biofuel production. *Met. Eng*. 15, 1–9. doi: 10.1016/j.ymben.2012.08.007

Vorachek-Warren, M. K., and McCusker, J. H. (2004). DsdA (D-serine deaminase): a new heterologous MX cassette for gene disruption and selection in *Saccharomyces cerevisiae*. *Yeast* 21, 163–171. doi: 10.1002/yea.1074

Workman, M., Holt, P., and Thykaer, J. (2013). Comparing cellular performance of *Yarrowia lipolytica* during growth on glucose and glycerol in submerged cultivations. *AMB Express* 3, 1–9. doi: 10.1186/2191-0855-3-58

Yang, X., Wang, H., Li, C., and Lin, C. S. K. (2017). Restoring of glucose metabolism of engineered *Yarrowia lipolytica* for succinic acid production via a simple and efficient adaptive evolution strategy. *J. Agric. Food Chem*. 65, 4133–4139. doi: 10.1021/acs.jafc.7b00519

Yu, Q., Cui, Z., Zheng, Y., Huo, H., Meng, L., Xu, J., et al. (2018). Exploring succinic acid production by engineered *Yarrowia lipolytica* strains using glucose at low pH. *Biochem. Eng. J*. 139, 51–56. doi: 10.1016/j.bej.2018.08.001

Yuzbashev, T. V., Bondarenko, P. Y., Sobolevskaya, T. I., Yuzbasheva, E. Y., Laptev, I. A., Kachala, V., et al. (2016). Metabolic evolution and 13C flux analysis of a succinate dehydrogenase deficient strain of *Yarrowia lipolytica*. *Biotechnol. Bioeng*. 113, 2425–2432. doi: 10.1002/bit.26007

Yuzbashev, T. V., Yuzbasheva, E. Y., Laptev, I. A., Sobolevskaya, T. I., Vybornaya, T. V., Larina, A. S., et al. (2011). Is it possible to produce succinic acid at a low pH? *Bioeng. Bugs* 2, 115–119. doi: 10.4161/bbug.2.2.14433

Yuzbashev, T. V., Yuzbasheva, E. Y., Sobolevskaya, T. I., Laptev, I. A., Vybornaya, T. V., Larina, A. S., et al. (2010). Production of succinic acid at low pH by a recombinant strain of the aerobic yeast *Yarrowia lipolytica*. *Biotechnol. Bioeng.* 107, 673–682. doi: 10.1002/bit.22859

Zelle, R. M., De Hulster, E., Van Winden, W. A., De Waard, P., Dijkema, C., Winkler, A. A., et al. (2008). Malic acid production by *Saccharomyces cerevisiae*: engineering of pyruvate carboxylation, oxaloacetate reduction, and malate export. *Appl. Environ. Microbiol*. 74, 2766–2777. doi: 10.1128/AEM.02591-07

Zinjarde, S. S. (2014). Food-related applications of *Yarrowia lipolytica*. *Food Chem*. 152, 1–10. doi: 10.1016/j.foodchem.2013.11.117

Conflict of Interest: The authors declare that the research was conducted in the absence of any commercial or financial relationships that could be construed as a potential conflict of interest.

frontiers in Bioengineering and Biotechnology

REVIEW
published: 09 January 2020
doi: 10.3389/fbioe.2019.00440

Recent Advances of L-ornithine Biosynthesis in Metabolically Engineered *Corynebacterium glutamicum*

Xiao-Yu Wu[1], *Xiao-Yan Guo*[1], *Bin Zhang*[1]*, *Yan Jiang*[1] and *Bang-Ce Ye*[2]

[1] *Jiangxi Engineering Laboratory for the Development and Utilization of Agricultural Microbial Resources, College of Bioscience and Engineering, Jiangxi Agricultural University, Nanchang, China,* [2] *Laboratory of Biosystems and Microanalysis, State Key Laboratory of Bioreactor Engineering, East China University of Science and Technology, Shanghai, China*

L-ornithine, a valuable non-protein amino acid, has a wide range of applications in the pharmaceutical and food industries. Currently, microbial fermentation is a promising, sustainable, and environment-friendly method to produce L-ornithine. However, the industrial production capacity of L-ornithine by microbial fermentation is low and rarely meets the market demands. Various strategies have been employed to improve the L-ornithine production titers in the model strain, *Corynebacterium glutamicum*, which serves as a major indicator for improving the cost-effectiveness of L-ornithine production by microbial fermentation. This review focuses on the development of high L-ornithine-producing strains by metabolic engineering and reviews the recent advances in breeding strategies, such as reducing by-product formation, improving the supplementation of precursor glutamate, releasing negative regulation and negative feedback inhibition, increasing the supply of intracellular cofactors, modulating the central metabolic pathway, enhancing the transport system, and adaptive evolution for improving L-ornithine production.

Keywords: L-ornithine, *Corynebacterium glutamicum*, metabolic engineering, genetic engineering, fermentation

OPEN ACCESS

Edited by:
Hui Wu,
East China University of Science and Technology, China

Reviewed by:
Xixian Xie,
Tianjin University of Science and Technology, China
Tsutomu Tanaka,
Kobe University, Japan

***Correspondence:**
Bin Zhang
zhangbin2919@163.com

Specialty section:
This article was submitted to Industrial Biotechnology, a section of the journal Frontiers in Bioengineering and Biotechnology

Received: *16 October 2019*
Accepted: *11 December 2019*
Published: *09 January 2020*

Citation:
Wu X-Y, Guo X-Y, Zhang B, Jiang Y and Ye B-C (2020) Recent Advances of L-ornithine Biosynthesis in Metabolically Engineered Corynebacterium glutamicum. Front. Bioeng. Biotechnol. 7:440. doi: 10.3389/fbioe.2019.00440

INTRODUCTION

The amino acid market is worth several billion dollars. Hence, the production of amino acids has been an active field of biotechnology research in recent years (Lee and Wendisch, 2017; Li et al., 2017; D'Este et al., 2018). Currently, most amino acids are produced by microbial fermentation, a technique adopted in Japan several decades ago. Microbial fermentation is an eco-friendly technology, which can address the growing concerns about environmental issues and can be used to establish a sustainable economy independent of fossil fuels (Becker et al., 2018; Kogure and Inui, 2018). L-ornithine, a non-protein amino acid, is widely used to improve human health as it is reported to have beneficial effects on the liver and the heart (Acharya et al., 2009; Rathi and Taneja, 2018; Butterworth and McPhail, 2019). L-ornithine is also produced by microbial fermentation using *Escherichia coli*, *Saccharomyces cerevisiae*, or *Corynebacterium glutamicum* as the microbial cell factory (Mitsuhashi, 2014; Becker and Wittmann, 2015). *E. coli* is a widely used microbe for the development of engineered strains to produce chemicals as it has several advantages, such as rapid propagation, availability of a completely sequenced genome, and ease of genetic manipulation (Sarria et al., 2017; Li et al., 2018). *E. coli* could be engineered for producing L-ornithine

by rational modulation of the urea cycle and optimizing the fermentation process (Lee and Cho, 2006). However, *E. coli* synthesizes endotoxin, which is banned in the food and pharmaceutical industries (Okuda et al., 2016). This limits the application of *E. coli* as an ideal host to produce L-ornithine. *S. cerevisiae*, an alternative host, has been identified as a generally recognized as safe (GRAS) strain. *S. cerevisiae* exhibits strong robustness or tolerance to harsh growing conditions and is used for the production of various food and pharmaceutical compounds (Guo et al., 2018; Yu et al., 2018; Luo et al., 2019). Modular metabolic engineering strategies were used to engineer the carbon source transport system, central metabolic pathway, ammonia metabolism, energy supply, and transport of small molecular weight compounds in *S. cerevisiae* to produce L-ornithine (Qin et al., 2015). However, the production titer of L-ornithine was low when *S. cerevisiae* was used as a chassis microorganism and hence, the process could not be scaled up to industrial production. As shown in **Table 1**, *C. glutamicum* is predominantly used to produce L-ornithine. *C. glutamicum,* a gram positive bacterium, was intensively engineered by mutation breeding to enable utilization of a broad spectrum of carbon sources to produce desired chemical compounds (Jeandet et al., 2018; Becker and Wittmann, 2019; Kim et al., 2019). Recent developments in genetic manipulation tools have enabled further genetic modifications, which can further improve L-ornithine production in *C. glutamicum* by metabolic engineering. In this review, we have summarized the current advances in the metabolic engineering strategies for *C. glutamicum*. Comprehensive information on the modification of *C. glutamicum* metabolic pathways has been provided to improve the production of L-ornithine.

MAIN BIOSYNTHESIS PATHWAYS OF L-ORNITHINE

In *C. glutamicum*, the biosynthesis of L-ornithine occurs through the urea cycle coupled with the tricarboxylic acid cycle. As described in **Figure 1**, α-oxoglutarate, an intermediate metabolite in the tricarboxylic acid cycle pathway, can be converted to glutamate by the reversible enzyme, glutamate dehydrogenase (encoded by *gdh*/*NCgl0181*). Further, glutamate is converted to L-ornithine through the enzymatic activities of N-acetylglutamate synthase (encoded by *cg3035*/*NCgl2644*), N-acetylglutamate kinase (encoded by *argB*/*NCgl1342*), N-acetyl-gamma-glutamyl-phosphate reductase (encoded by *argC*/*NCgl1340*), acetylornithine aminotransferase (encoded by *argD*/*NCgl1343*), and ornithine acetyltransferase (encoded by *argJ*/*NCgl1341*). Additionally, L-ornithine can be converted to L-citrulline and L-arginine through the enzymatic activities of ornithine carbamoyltransferase (encoded by *argF*/*NCgl1344*), argininosuccinate synthase (encoded by *argG*/*NCgl1346*), and argininosuccinate lyase (encoded by *argH*/*NCgl1347*). The genes encoding these enzymes are arranged in two operons, *argCJBDFR* and *argGH*. The two operons are repressed by a negative regulatory protein, ArgR/NCgl1345 (Ikeda et al., 2009; Stäbler et al., 2011). The generation of 1 mole of L-ornithine requires 2 moles of NADPH during the conversion of α-oxoglutarate to glutamate and N-acetyl-γ-glutamyl-phosphate to N-acetylglutamate semialdehyde. The enzyme activity of N-acetylglutamate kinase is regulated by L-arginine and L-citrulline via a feedback regulation mechanism. To select and engineer high L-ornithine-producing *C. glutamicum* strains, it is necessary to release the feedback regulation, improve supplementation of cofactor NADPH, and modulate metabolic pathways (**Figure 2**).

BLOCKING THE BY-PRODUCT PATHWAYS VIA GENE DISRUPTION

Under anaerobic conditions, *C. glutamicum* strains are reported to exhibit enhanced glutamate production and decreased L-ornithine production (Gourdon and Lindley, 1999; Lapujade et al., 1999; Hirasawa and Wachi, 2017; Tuyishime et al., 2018). L-ornithine, an intermediate compound in the L-arginine biosynthetic pathway, was synthesized using glutamate as a precursor, which was tightly regulated by feedback inhibition of the terminal metabolites, such as L-arginine and L-citrulline (Ikeda et al., 2009). The enzymatic activity of N-acetylglutamate kinase, which is involved in the main synthetic pathway of L-ornithine, was inhibited by L-arginine and L-citrulline at a concentration of <1 mM (Xu et al., 2012a,b). Thus, the biosynthetic pathways of L-arginine and L-citrulline not only consume L-ornithine, but also hinder its production. To promote the accumulation of L-ornithine, *argF* (encodes ornithine carbamoyltransferase) was disrupted to block the metabolic pathway that converts L-ornithine to L-citrulline and L-arginine. This markedly inhibited the production of L-citrulline and L-arginine in all the L-ornithine-producing *C. glutamicum* strains. However, the deletion of *argF* also resulted in a major hindrance in cell growth as the cells lacked the ability to synthesize arginine. To address this limitation, L-arginine was added to the fermentation medium to meet the demand for cell growth. However, the supplementation of L-arginine increases the cost and the operational complexity. Therefore, it is necessary to adopt appropriate strategies to attenuate the expression of *argF*. Metabolic engineering strategies, such as changing the ribosome binding site (Xiao et al., 2019), replacing the promoter (Xu et al., 2019), changing the translation initiation codon (Otten et al., 2015), and transcription interference by clustered regular interspaced short palindromic repeats (CRISPR) (Cleto et al., 2016; Yoon and Woo, 2018; Park et al., 2019) were successfully applied to optimize the flux of the metabolic pathway. The expression of *argF* was attenuated by changing the ribosome binding site and the translation initiation codon. It was difficult to attenuate the catabolism of L-ornithine owing to the enhanced transcription level of the *argCJBDF* operon. Additionally, the expression of *argF* was attenuated by introducing a strong terminator in the upstream region of *argF*. The L-ornithine titer in the engineered *C. glutamicum* was 6.1 g/L, which was 11-fold higher than that in the original strain and 42.8% higher than that in the mutant strain with *argF* deletion (Zhang et al., 2018c). It must be noted that insertion of a strong terminator in the

TABLE 1 | Characteristic of L-ornithine producing strains developed by metabolic engineered strategies.

Strains	Substrate	L-ornithine titer (g/L)	yield (g/g substrate)	Cultivation	Modulations	References
E. coli SJ7055	Glucose	0.052*	ND	Shake flask; batch	Inactivation of *argF*, *argR*, *argI*, *proB*, and *speF*; overexpression of *argA214*	Lee and Cho, 2006
S. cerevisiae M1dM2qM3e	Glucose	5.1	ND	Bioreactor; fed-batch	Modular pathway rewiring	Qin et al., 2015
C. glutamicum SJC8514 (pEC-*argCJBD*mut)	Glucose	12.48	ND	Shake flask; batch	Overexpression of NCgl0462 and *argCJBD*mut	Kim D. J. et al., 2015
Cc-QF-4	Glucose	40.4	0.27*	Bioreactor; batch	Deletion of *proB* and *argF*; positive mutation E19Y of ArgB; heterologous expression of *argA* and *argE*	Shu et al., 2018
SO26	Glucose	43.6	0.34	Bioreactor; fed-batch	Deletion of *argF*, *NCgl1221*, *argR*, *putP*, *mscCG2*, and *iolR*; attenuation of *odhA*, *proB, ncgl2228*, *pta*, *cat*, and *pgi*; overexpression of *lysE*, *gdh*, *cg3035, pfkA, tkt*, *argCJBD*, *glt*, and *gdh2*	Zhang B. et al., 2019
SO29	Xylose	18.9	0.4	Shake flask; batch	heterologous expression of *xylAB* operon from *Xanthomonas campestris*	Zhang B. et al., 2019
CO-9	Glucose	6.1	ND	Shake flask; batch	Attenuate expression of *argF* by insertion of a T4 terminator in the upstream region	Zhang et al., 2018c
YW06 (pSY223)	Glucose	51.5	0.24	Bioreactor; fed-batch	Deletion of *argF*, *argR*, and *proB*; Reinforcement of the PPP pathway flux; The use of a feedback-resistant enzyme	Kim S. Y. et al., 2015
ΔAPE6937R42	Sucrose/ molasses	22/27	ND	Shake flask; batch	Heterologous expression of *sacC* from *Mannheimia succiniciproducens*	Zhang et al., 2015
ORN6	Glucose	20.96*	0.524	Shake flask; batch	Deletion of *argF*, *argR*, and *argG*; overexpression of $argB^{M}$; attenuation of *pgi*.	Jensen et al., 2015
SJC 8260	Glucose	14*	ND	Shake flask; batch	Deletion of *argF*, *argR*, and *proB*; Blocking gluconate biosynthesis	Hwang and Cho, 2014
ORN1(pVWEx1-$glpFKD^{Eco}$)	Glycerol	2.24*	0.11	Shake flask; batch	Heterologous expression of *glpF*, *glpK*, and *glpD* from *E. coli*	Meiswinkel et al., 2013b
ΔAPE6937R42	Glucose	24.1	0.298	Bioreactor; batch	Deletion of *argF*, *argR*, and *proB*; Adaptive evolution in presence of L-ornithine	Jiang et al., 2013a
ORN1(pEKEx3-$xylA_{Xc}$-$xylB_{Cg}$)	Xylose	2.59	ND	Shake flask; batch	Overexpression of *xylA* from *X. campestris* and endogenous *xylB*	Meiswinkel et al., 2013a
SJC 8399	Glucose	13.16	ND	Shake flask; batch	Inactivation of the gluconate kinase gene (*gntK*)	Hwang and Cho, 2012
ORN1 (pVWEx1-*araBAD*)	Arabinose	11.7	0.32	Shake flask; batch	Overexpression of *araBAD* from *E. coli* MG1655	Schneider et al., 2011
SJ8074(pEK-P_{trc}::1469)	Glucose	0.32	ND	Shake flask; batch	Overexpression of *NCgl1469*	Hwang and Cho, 2010
1006Δ*argR-argJ*	Glucose	31.6	0.396	Shake flask; batch	Deletion of *argR*; overexpression of *argJ*;	Hao et al., 2016
SJC8043	Glucose	3.3	ND	Shake flask; batch	Supplement of L-proline	Lee et al., 2010

**These values were not described in the main text of the original reference and thus estimated from the figure or graph.*

upstream region of *argF* can not only attenuate the expression of *argF*, but also stimulate the expression of *argCJBD* gene clusters, which are required for the synthesis of ornithine. Therefore, attenuation of *argF* expression is a promising strategy for constructing an efficient L-ornithine-producing *C. glutamicum*.

Glutamate is also utilized to form L-proline via three steps of enzymatic reactions (Lee et al., 2010). The biosynthesis of a compete metabolite of L-proline not only consumes carbon sources, but also the NADPH cofactor, which limits L-ornithine production (Wendisch et al., 2016). In various studies, the *proB*/*NCgl2274* (encodes γ-glutamyl kinase) gene has been deleted to construct high L-ornithine-producing strains by blocking the L-proline biosynthetic pathway. The engineered L-ornithine-producing strains that exhibit enhanced L-ornithine production include YW06 (pSY223) (Kim S. Y. et al., 2015) and Cc-QF-1 (Shu et al., 2018). However, the deletion of *argF* in *C. glutamicum* and inactivation of *proB* negatively affected cell growth due to L-proline deficiency. Thus, proline

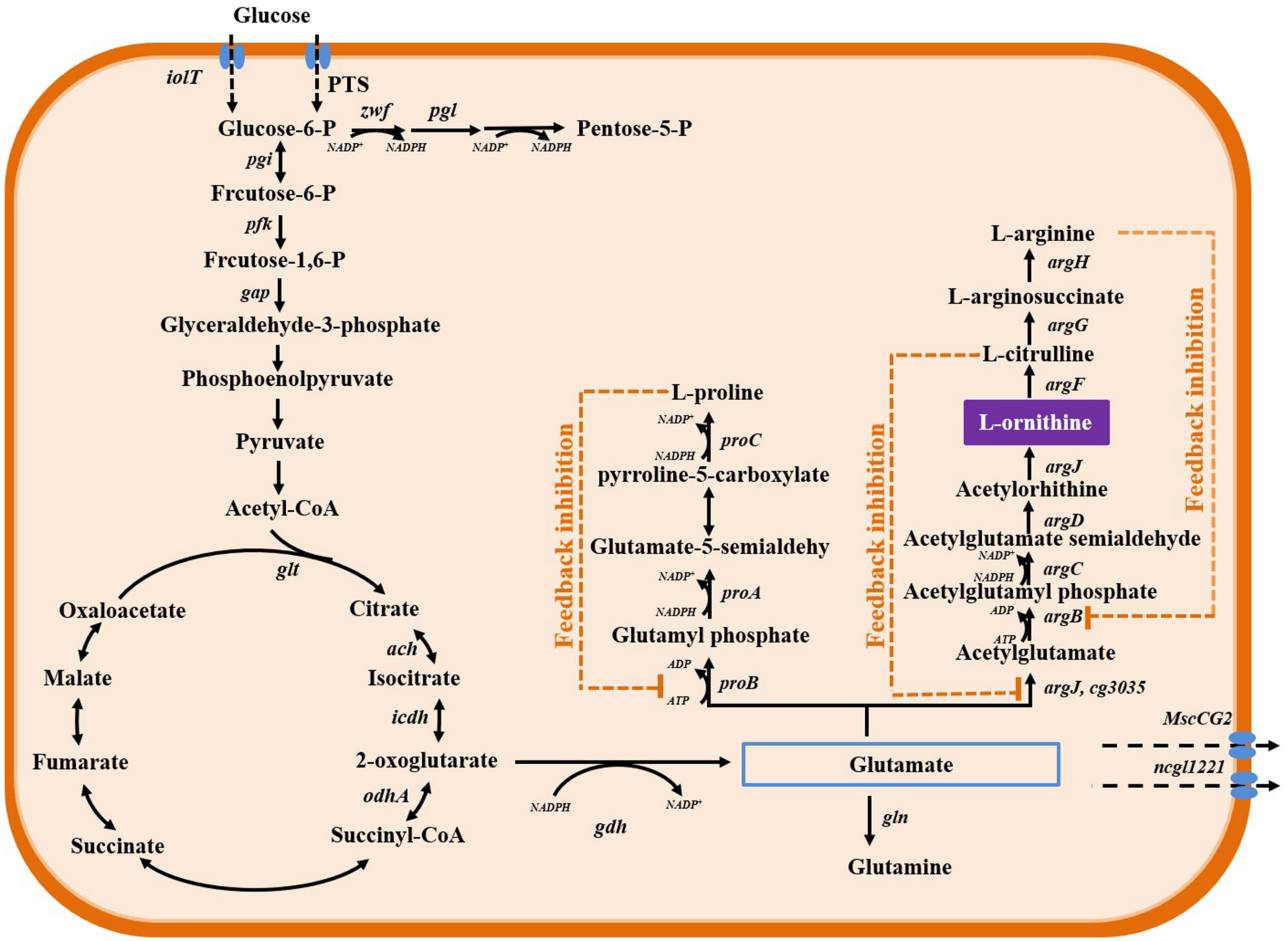

FIGURE 1 | L-ornithine biosynthesis metabolic pathways in *C. glutamicum*. The genes annotation of enzymes as describe in previous study (Zhang B. et al., 2019). The dotted orange line represents feedback inhibition.

must be added to the culture medium to maintain normal cell growth. However, the addition of proline to the culture medium increases the operational cost and complexity. To address these limitations, recent studies have attenuated the expression of *proB* by inserting a terminator, which improved L-ornithine production without disturbing the cell growth (Zhang et al., 2018a). As suggested in the modulation of *argF*, attenuating the expression of *proB* by inserting a terminator is an efficient strategy for constructing a L-ornithine-producing *C. glutamicum* strain. In addition to the biosynthetic pathway of proline, the biosynthetic pathways of other amino acids, such as valine, isoleucine, and leucine also consume carbon sources, which limits L-ornithine production. Therefore, a recent study reported that deleting the *ncgl2228* gene (encodes a putative branched amino acid transporter) in the engineered *C. glutamicum* orn8 strain decreased the yield of L-leucine (from 1.90 to 0.13 g/L), L-valine (from 2.16 to 0.22 g/L), and L-isoleucine (from 1.60 to 0.04 g/L) and increased the yield of L-ornithine (from 19 to 22 g/L) (Zhang et al., 2018a). Since the accumulation of by-products in the fermentation prevents the utilization of carbon source and cofactors for producing valuable compounds, it has been concluded that the inactivation of a corresponding transporter is an efficient strategy to reduce accumulation of by-products and increase production of the desired compound.

REMOVAL OF FEEDBACK REPRESSION AND FEEDBACK INHIBITION

In the *C. glutamicum* genome, the genes encoding the enzymes involved in the biosynthesis of L-ornithine are present in the *argCJBD* operon, which is repressed by the negative regulatory protein, ArgR. The expression of *argCJBD* operon is repressed at low level, which is an important rate-limiting factor for the biosynthesis of L-ornithine. Hence, the *argR* gene was deleted in all the engineered L-ornithine-producing *C. glutamicum* strains, which provided a powerful strategy for improving the L-ornithine production titer. Inactivation of *argR* in the *C. glutamicum* 1006 strain improved the yield of L-ornithine (from 20.5 to 28.3 g/L) and yield from 0.256 to 0.354 g/g glucose (Hao et al., 2016). However, the yield of L-ornithine did not

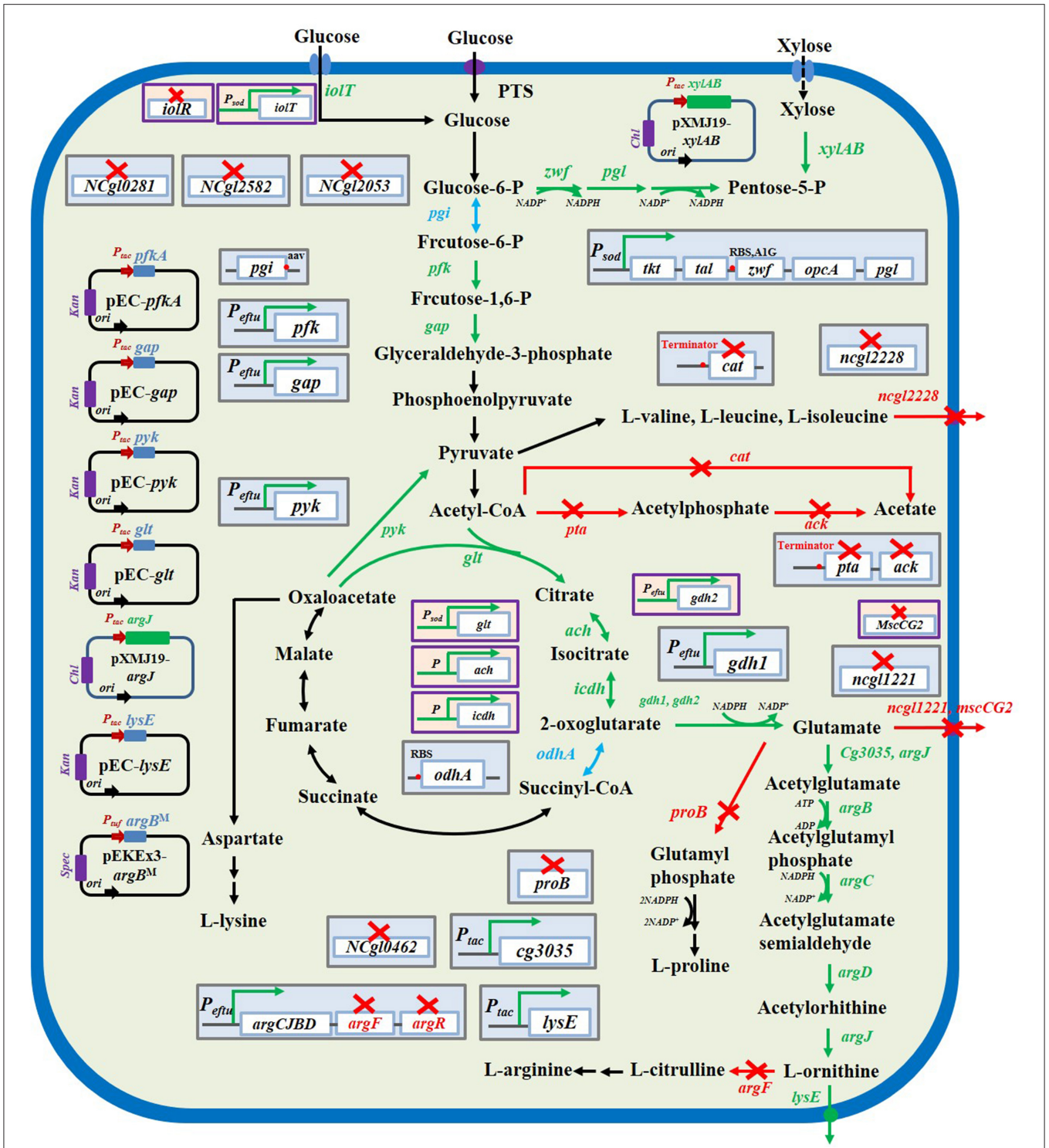

FIGURE 2 | L-ornithine biosynthesis metabolic pathways in *C. glutamicum* and strategies to improve L-ornithine accumulation. The red× represented this pathway were inactivated. The blue font and arrows represented that pathways were attenuated. The green font and arrows indicated that pathways were overexpressed. The genes encoding enzymes involved in catalytically relevant reactions.

improve further upon overexpression of the *argCJBD* operon by employing a plasmid or by inserting a strong promoter as the ArgR repressor was absent (Zhang B. et al., 2017; Zhang et al., 2018a). This suggested that the production of L-ornithine limited by the low expression of the *argCJBD* operon can be addressed by removing the ArgR repressor, which concurred with the results

described in the construction of the L-arginine-producing strain (Chen et al., 2014; Park et al., 2014).

As described above, the deletion of *argR* removed the transcription control on the main biosynthetic pathway of L-ornithine in *C. glutamicum*. However, stimulation of the *argCJBD* operon expression is not enough for releasing the negative control of the L-ornithine biosynthetic pathway. This is because of the presence of dual control systems in *C. glutamicum*: feedback repression and feedback inhibition. For feedback inhibition of L-ornithine, the enzyme activity of ornithine acetyltransferase (encoded by *argJ*) was inhibited by 50% by using 5 mM L-ornithine. The overexpression of *argJ* increased the yield of L-ornithine from 28.3 to 31.6 g/L in the engineered *C. glutamicum* 1006 strain (Hao et al., 2016). However, the mechanism underlying the inhibition of ornithine acetyltransferase by L-ornithine has not been elucidated. This mechanism can be an effective target for improving L-ornithine production. The gene encoding the ornithine acetyltransferase enzyme was subjected to site-directed mutagenesis, which did not result in the generation of valuable mutants (Shu et al., 2018). Additionally, the fermentation medium for producing L-ornithine was manually supplemented with a certain amount of arginine that resulted in the feedback inhibition of the rate-limiting enzyme, N-acetylglutamate kinase (encoded by *argB*), which is unfavorable for the accumulation of L-ornithine. Several studies have extensively evaluated the release of the negative effect mediated by the addition of L-arginine. The heterologous expression of *argCJBD* derived from the L-arginine-producing strain, *C. glutamicum* ATCC 21831, in the engineered *C. glutamicum* YW03 strain resulted in the production of 7.2 g/L L-ornithine, which was 2.6-fold higher than the L-ornithine titer produced upon expression of *argCJBD* operon derived from *C. glutamicum* ATCC 13032 in the *C. glutamicum* YW03 strain (2.0 g/L) (Kim S. Y. et al., 2015). These results suggest that the *argB* sequences are inconsistent between *C. glutamicum* ATCC 21831 and *C. glutamicum* ATCC 13032, which resulted in differential L-ornithine production. Furthermore, several studies have been performed recently to discover arginine-insensitive N-acetylglutamate kinase in the engineered L-arginine-producing strains (Ikeda et al., 2009; Xu et al., 2012a,b; Zhang J. et al., 2017). The production of L-ornithine was markedly improved upon overexpression of mutant *argB*, such as $argB^{E19R}$, $argB^{H268N}$, $argB^{G287D}$, $argB^{A49V,M54V}$, $argB^{A49V,M54V,G287D}$, $argB_{E.coli}$ in the engineered *C. glutamicum* ORN2B strain. The L-ornithine titers in the *C. glutamicum* ORN2B (pEKEx3-$argB^{E19R}$), ORN2B (pEKEx3-$argB^{A49V,M54V}$), and ORN2B (pEKEx3$argB_{E.col}$) strains were 0.307, 0.3, and 0.3 g/g glucose, respectively. These titers were higher than those in the *C. glutamicum* ORN2B (pEKEx3-*argB*) strain (0.257 g/g glucose) (Jensen et al., 2015).

IMPROVING THE SUPPLEMENTATION OF GLUTAMATE BY OVEREXPRESSION OF *gdh* AND BLOCKING GLUTAMATE SECRETION

In addition to the optimization of L-ornithine biosynthetic pathway by blocking other competitive metabolic pathways and releasing feedback regulation, adequate supply of precursor glutamate was reported to be another key factor for developing high L-ornithine-producing strains. Currently, many powerful strategies, such as overexpression of the endogenous or exogenous glutamate dehydrogenase, inhibition of the glutamate secretion system, and attenuation of α-ketoglutarate dehydrogenase, have been employed to engineer *C. glutamicum* for improving the flux of glutamate supplementation. The plasmid-based overexpression of *gdh* (encodes glutamate dehydrogenase) in the *C. glutamicum* ΔAP strain increased L-ornithine production by 16% (from 8.6 to 10.0 g/L). Simultaneously, individual chromosomal integration of the *rocG/BSU37790* gene (encodes NADH-coupled glutamate dehydrogenase) derived from *Bacillus subtilis* improved L-ornithine concentration from 12.12 ± 0.57 to 14.84 ± 0.57 g/L in the engineered *C. glutamicum* ΔAPER strain (Jiang et al., 2013b). Additionally, glutamate was synthesized from α-ketoglutarate, which is an intermediate metabolite of the tricarboxylic acid cycle. However, the tricarboxylic acid cycle is closely related to cell growth and cannot be blocked. To balance the cell growth and L-ornithine production, the expression of *odhA* (*NCgl1084*), which encodes an enzyme component of the α-ketoglutarate dehydrogenase complex, was attenuated to reduce the metabolic flux of the tricarboxylic acid cycle and provide more glutamate for the biosynthesis of L-ornithine. When the native ribosome binding site (predicted translation initial intensity was 1,613 au) of *odhA* was replaced with a synthetic ribosome binding site with a predicted translation initial intensity of 837 au on the chromosome, the L-ornithine production titer increased from 13.7 to 16 g/L in the engineered *C. glutamicum* Sorn4 strain (Zhang B. et al., 2017). Furthermore, the overexpression of pyruvate carboxylase and deletion of phosphoenolpyruvate carboxykinase also improved glutamate concentration in the fermentation medium, but did not promote the accumulation of L-ornithine (Hwang et al., 2008). The authors claimed that the supply of glutamate is not a rate-limiting step for L-ornithine production. However, the major reason for the unchanged concentration of L-ornithine may be the extracellular secretion of glutamate, which increased the cost of downstream reaction and precursor wastage. The secretion of glutamate can be inhibited by deleting the *NCgl1221* gene (encodes a glutamate transporter). This was first discovered for developing the L-arginine-producing *C. glutamicum* strain. The deletion of *NCgl1221* markedly improved the L-arginine production titer (Park et al., 2014; Chen M. et al., 2015). Inspired by these reports, inactivation of *NCgl1221* was introduced into the *C. glutamicum* Sorn1 strain, which dramatically decreased the secretion of glutamate and improved L-ornithine production by 22.7% (from 7.97 to 9.8 g/L). However, the deletion of *NCgl1221* is not enough to interrupt the glutamate secretion due to the presence of another glutamate transporter MscCG2 (encoded by *mscCG2*) in *C. glutamicum*. Hence, both *NCgl1221* and *mscCG2* genes were deleted in the engineered *C. glutamicum* S9114 strain, which exhibited negligible glutamate production and enhanced L-ornithine accumulation (Zhang B. et al., 2019). Hence, improving the glutamate availability is an efficient strategy for L-ornithine accumulation in *C. glutamicum*.

MODULATING THE CENTRAL METABOLIC PATHWAY

Upon consumption of glucose for L-ornithine production by *C. glutamicum* strains, the metabolic flux of central metabolic pathways, including the glycolytic pathway and the tricarboxylic acid cycle pathway, may be a limiting factor as these pathways provide the carbon skeleton. Various strategies have been explored for increasing the metabolic flux of central metabolic pathways for producing L-ornithine. Proteomic studies indicated differential proteomes in the parent strain and L-ornithine-producing strain. The effect of individual plasmid-based overexpression of *pgi* (*NCgl0817*), *pfkA* (*NCgl1202*), *gap* (*NCgl0900*), *pyk* (*NCgl2008*), *pyc* (*NCgl0659*), and *glt* (*NCgl0795*) on L-ornithine production was investigated in the *C. glutamicum* ΔAP strain. Modulating the expression of enzymes involved in the glycolytic pathway, such as Pgi, PfkA, GapA, and Pyk, improved L-ornithine production (Jiang et al., 2013b). A common feature in the enhanced expression of these genes is the improved metabolic flux of glycolysis. Additionally, a recent study focused on strengthening the glycolytic pathway by inserting a strong P_{eftu} promoter in the upstream region of *pfkA* in the engineered *C. glutamicum* SO1 strain, which improved the yield of L-ornithine from 23.8 to 26.5 g/L (Zhang et al., 2018b). These results suggested the importance of the glycolytic pathway in L-ornithine production.

The tricarboxylic acid cycle is a source of the carbon skeleton for the biosynthesis of amino acids, such as L-lysine, L-isoline, L-threonine, L-glutamate, L-arginine, L-proline, L-ornithine, and L-citrulline. A recent study reported that rationally engineering the tricarboxylic acid cycle by overexpressing the *pyc*, *ppc* (*NCgl1523*), and *gdh* genes (encoding pyruvate carboxylase, phosphoenolpyruvate carboxylase, and glutamate dehydrogenase, respectively) and deleting the P1 promoter of *glt* (encodes citrate synthase) improved the lysine yield (from 14.47 ± 0.41 to 23.86 ± 2.16 g/L) and carbon yield (from 36.18 to 59.65%) in the *C. glutamicum* JL68 strain (Xu et al., 2018a). Hence, the tricarboxylic acid cycle pathway was also modulated by overexpressing the *glt*, *icdh* (*NCgl0634*), and *ach* (*NCgl1482*) genes in the L-ornithine-producing *C. glutamicum* SO16 strain. The insertion of a strong P_{sod} promoter in the upstream region of *glt* improved the yield of L-ornithine from 30.8 to 34.1 g/L. Simultaneously, rational modulation of the tricarboxylic acid cycle pathway by overexpressing the *glt* gene improved the glucose consumption in the *C. glutamicum* SO16 strain (Zhang B. et al., 2019).

ENHANCED SUPPLY OF INTRACELLULAR COFACTOR NADPH AND ACETYL-CoA

Efficient supply of the cofactor is important in preventing obstruction of the metabolic pathways to enable production of valuable chemicals using the microbial cell factory (Xu et al., 2018b). NADPH, an important cofactor, is widely used in the biosynthesis of various amino acids, such as lysine (Wu et al., 2019), valine (Zhang H. et al., 2018), methionine (Li et al., 2016), ornithine (Hwang and Cho, 2012), and arginine (Chen M. et al., 2015). Intracellular supplementation of NADPH can be increased by various strategies, such as improving the metabolic flux of the pentose phosphate pathway (Siedler et al., 2013), overexpression of NAD kinase (Lindner et al., 2010; Xu et al., 2016), and developing a NADP-dependent glyceraldehyde 3-phosphate dehydrogenase (Takeno et al., 2010, 2016; Hoffmann et al., 2018). NADPH is a rate-limiting factor in the biosynthesis of metabolites in *C. glutamicum*. In the metabolic pathway of L-ornithine, 2 moles of NADPH are consumed in two steps of enzymatic reactions: conversion from α-oxoglutarate to glutamate catalyzed by glutamate dehydrogenase and from N-acetyl-glutamyl-phosphate to N-acetyl-glutamyl-semialdehyde catalyzed by N-acetyl-γ-glutamyl-phosphate reductase. Ornithine production is frequently limited by the supply of NADPH. Hence, the metabolic flux was redirected toward the pentose phosphate pathway by attenuating *pgi*, replacing the native promoter of *tkt* operon with a strong P_{sod} promoter, and changing the translation initiation codon (G1A) of *zwf* (*NCgl1514*) in the YW03 strain, which improved the yield of L-ornithine from 261.3 to 417.2 mg/L (Kim S. Y. et al., 2015). Additionally, the carbon flux of the pentose phosphate pathway was enhanced by deleting the gluconate kinase gene in the *C. glutamicum* SJC8039 strain, which increased the intracellular NADPH concentration by 51.8%. L-Ornithine production yield in the engineered *C. glutamicum* SJC8399 strain with double deletion of *NCgl2399* and *NCgl2905* was 13.16 g/L, which is higher than that (8.78 g/L) in the parent *C. glutamicum* SJC8039 strain (Hwang and Cho, 2012). Furthermore, inactivation of *NCgl0281*, *NCgl2582*, and *NCgl2053* genes, which encode putative $NADP^+$-dependent oxidoreductases, enhanced the intracellular NADPH content by 72.4%. Inactivation of these genes inhibited glucose dehydrogenase activity and improved L-ornithine yield by 66.3% in the engineered SJC8039 strain (Hwang and Cho, 2014). Moreover, NADPH availability for L-ornithine production in the *C. glutamicum* ΔAPER strain was improved by heterologous expression of NADP-dependent glyceraldehyde-3-phosphate dehydrogenase derived from *Clostridium acetobutylicum*, which improved L-ornithine production (Jiang et al., 2013b). Therefore, increased intracellular NADPH supply is a major limiting factor for developing high L-ornithine-producing *C. glutamicum* strains.

In addition to NADPH, the supply of acetyl-CoA cofactor is required to produce L-ornithine. The acetyl-CoA co-factor is consumed during the conversion of oxaloacetate to citrate and glutamate to N-acetylglutamate. Recently, overexpression of *cg3035* (encodes an N-acetylglutamate synthetase) was reported to be an efficient strategy for improving L-ornithine accumulation. This was the first study to report the role of acetyl-CoA in L-ornithine production. The intracellular concentration of acetyl-CoA was improved by attenuating the acetate biosynthesis pathway through insertion of a terminator in the upstream region of *pta-ack* (*NCgl2657-NCgl2656*) operon or *cat* (*NCgl2480*) in the *C. glutamicum* SO1 strain. Modulation of the acetate biosynthesis pathway improved the yield of L-ornithine from 23.8 to 26 g/L (Zhang et al., 2018b).

ENHANCED TRANSPORT SYSTEM

One of the efficient strategies for developing engineered strains to produce amino acids is overexpression of a specific transport system, such as Ncgl1221 (Nakamura et al., 2007; Nakayama et al., 2012) and MscCG2 (Wang Y. et al., 2018) glutamate transporters, lysine transporter (LysE/NCgl1214) (Vrljic et al., 1996; Kind et al., 2011), phenylalanine transporter (AroP) (Shang et al., 2013), and branched chain amino acid transporters (BrnFE) (Kennerknecht et al., 2002; Chen C. et al., 2015). Currently, there are no reported ornithine-specific transporters. The effect of plasmid-based overexpression of *lysE* (encodes a lysine transporter) on L-ornithine production was investigated in an engineered *C. glutamicum* ATCC 13032 strain containing inactivated *argF*. The intracellular and extracellular concentrations of L-ornithine were measured in short-term fermentation. The analysis indicated that LysE is not an ornithine transporter (Bellmann et al., 2001). However, there was not much progress on the ornithine transport system until the overexpression of *lysE* was studied in the L-ornithine-producing *C. glutamicum* Sorn8 strain. In this strain, the yield of L-ornithine increased by 21.8% when compared to the parent strain after 72 h of fermentation (Zhang B. et al., 2017). Subsequently, the effect of LysE on L-ornithine production was evaluated by deleting the *lysE* gene in the engineered *C. glutamicum* orn1 strain, which reduced the L-ornithine yield by 41.7%. Furthermore, overexpression of LysE by insertion of a strong P_{tac} promoter in the upstream region of *lysE* also improved the L-ornithine production titer from 15.3 to 19 g/L. This suggested that LysE promotes L-ornithine production (Zhang et al., 2018a). Although the direct transporter of L-ornithine is not known, the LysE transporter may contribute to developing high L-ornithine-producing strains.

ADAPTIVE EVOLUTION

The strategies discussed so far for increasing the L-ornithine production titer were based on genetic modifications. However, direct manipulations of one or more genes may negatively affect cell growth or metabolism. Therefore, the combination of irrational metabolic engineering methods, such as adaptive laboratory evolution (Stella et al., 2019) and genetic modification strategies will facilitate the development of high L-ornithine-producing strains. Adaptive laboratory evolution is widely applied for the construction of microbial strains, which not only stimulate latent metabolic pathways but also promote the phenotype and environmental adaptation of engineered strains (Garst et al., 2017; Yu et al., 2018). Compared to rational genetic modifications, adaptive laboratory evolution has provided extensive genetic manipulation targets to improve the strain phenotype. Adaptive laboratory evolution was applied for improving the strain phenotype of *C. glutamicum* ΔAPE. The L-ornithine production titer in the resultant *C. glutamicum* ΔAPE6937 strain was 13.6 ± 0.5 g/L, which was 20% higher than that in the parent strain (11.3 ± 0.3 g/L) (Jiang et al., 2013a). The accelerated cell growth caused by adaptive laboratory evolution was the main factor that contributed to the enhanced L-ornithine production titer in the *C. glutamicum* ΔAPE strain.

ALTERNATIVE SUBSTRATES

Currently, majority of L-ornithine is produced from glucose, which is also used for human nutrition and animal feed industries. To minimize the competition for glucose between food security and industrial biotechnology, several studies have investigated the production of L-ornithine using non-edible feedstocks, such as xylose and arabinose.

Xylose is the second most abundant sustainable raw material for fermentation. Xylose is obtained from the hydrolysis of lignocellulosic biomasses and is widely used for the production of valuable chemicals, such as succinate (Mao et al., 2018), sarcosine (Mindt et al., 2019), 5-aminovalerate (Jorge et al., 2017b), L-pipecolic acid (Perez-Garcia et al., 2017), 3-hydroxypropionic acid (Chen et al., 2017), and γ-aminobutyric acid (Jorge et al., 2017a) in engineered *C. glutamicum* strains. The utilization of xylose can be improved by heterologous expression of xylose isomerase (Jo et al., 2017), overexpression of myo-inositol/proton symporter IolT1 (Brusseler et al., 2018), and adaptive laboratory evolution (Radek et al., 2017) of *C. glutamicum*. Previously, L-ornithine was produced from xylose by engineering the xylose metabolic pathways in the *C. glutamicum* ORN1 strain. The yield of L-ornithine was further enhanced by overexpressing *xylA* (encodes xylose isomerase) derived from *Xanthomonas campestris* and endogenous *xylB* (encodes xylulokinase) in the *C. glutamicum* ORN1 strain, which improved the L-ornithine yield from 9.4 ± 1.4 to 19.6 ± 1.9 mM (Meiswinkel et al., 2013a). Recently, heterologous expression of *xylAB* operon derived from *X. campestris* in the engineered *C. glutamicum* SO26 strain resulted in the production of 16.32 g/L L-ornithine with a yield of 0.14 g/g xylose. The production titer of L-ornithine was further improved to 18.9 g/L by optimizing the concentration of the inducer, isopropyl β-D-1-thiogalactopyranoside (IPTG) (Zhang B. et al., 2019). Arabinose is another component of lignocellulosic biomass hydrolysate and is widely used for producing valuable compounds (Zahoor et al., 2012; Zhao et al., 2018). Several studies have developed superior microbial cell factories, such as *C. glutamicum* that can efficiently utilize arabinose (Henke et al., 2018; Kawaguchi et al., 2018; Mindt et al., 2019). The heterologous expression of *araBAD* operon derived from *E. coli* enabled the *C. glutamicum* ORN1 strain to utilize arabinose. This engineered strain produced 89 ± 3 mM L-ornithine with a yield of 0.37 M/M arabinose (Schneider et al., 2011).

CONCLUSIONS AND PERSPECTIVES

Currently, several comprehensive and rational genetic strategies have been employed for engineering *C. glutamicum* strains to produce L-ornithine. There is rapid progress in improving strain performance by combining the optimization of the metabolic pathways in *C. glutamicum*. For example, Kim S. Y. et al. (2015) reported the construction of a recombinant *C. glutamicum* by disrupting *proB*, *argR*, and *argF*, and overexpressing the

operon of *argCJBD* from *C. glutamicum* ATCC 21831. Fed-batch culture of the engineered strain in a 6.6-L fermenter yielded 51.5 g/L of L-ornithine production titer from glucose. In our previous work, a recombinant *C. glutamicum* with modulation in the deletion of *argF*, *NCgl1221*, *argR*, *putP*, *mscCG2*, and *iolR*, attenuation of *odhA*, *proB*, *ncgl2228*, *pta*, *cat*, and *pgi*, and overexpression of *lysE*, *gdh*, *cg3035*, *pfkA*, *tkt*, *argCJBD*, *glt*, and *gdh2* produced 43.6 g/L of L-ornithine during a 72 h fed-batch cultivation (Zhang B. et al., 2019). Although the production of L-ornithine by microbial fermentation is a promising and attractive strategy, very few microbes have been used for industrial production due to low yield and low productivity. Metabolic engineering of *C. glutamicum* is an efficient strategy to improve L-ornithine production. The mechanisms underlying the transportation of L-ornithine must be further investigated by new engineering techniques, such as genomics (Teusink and Smid, 2006), transcriptomics (Kim et al., 2017), and proteomics (Shen et al., 2016; Varela et al., 2018) to aid the development of high L-ornithine-producing strains. CRISPR/Cas9, a novel gene-editing technology, is a rapid and efficient method that can be applied for genetic modifications, such as gene deletion, large fragment DNA assembly, or site-directed gene mutation (Cho et al., 2017; Jiang et al., 2017; Wang B. et al., 2018; Zhang J. et al., 2019) in *C. glutamicum*, which can accelerate the pathway engineering in *C. glutamicum* strains. Irrational breeding strategies such as induced mutation breeding, or adaptive evolution have enabled rapid progress in improving the yield of L-ornithine. However, random mutations and labor-intensive screening methods remain as bottleneck issues. Recently, high-throughput screening of mutant strains was developed using a metabolite biosensor, which can measure the metabolite concentrations based on the fluorescence signals or antibiotic selective pressure (Hammer and Avalos, 2016; Lin et al., 2017; Yeom et al., 2018). Due to an improvement in the screening efficiency using a metabolite biosensor, the traditional irrational breeding strategy is considered a promising method for the construction of engineered strains (Zheng et al., 2018). Future studies must focus on developing an efficient intracellular L-ornithine biosensor, which can activate the irrational breeding of high L-ornithine-producing strain.

AUTHOR CONTRIBUTIONS

X-YW planned and wrote the first manuscript. X-YG, YJ, and B-CY modified this manuscript. BZ supervised and finalized the manuscript. All authors read and approved the final manuscript.

FUNDING

This work was supported by grants from the National Natural Science Foundation of China (Grant No. 31730004) and Jiangxi Key R&D Program (Grant No. 20171ACF60006).

ACKNOWLEDGMENTS

We thank Dr. Xue-Lan Chen for providing pk18*mobsacB*. We also thank Dr. Zhong-Gui Mao and Dr. Li-Ming Liu for providing *Corynebacterium glutamicum* S9114. We would like to thank Editage (www.editage.cn) for English language editing.

REFERENCES

Acharya, S. K., Bhatia, V., Sreenivas, V., Khanal, S., and Panda, S. K. (2009). Efficacy of L-ornithine L-aspartate in acute liver failure: a double-blind, randomized, placebo-controlled study. *Gastroenterology* 136, 2159–2168. doi: 10.1053/j.gastro.2009.02.050

Becker, J., Rohles, C. M., and Wittmann, C. (2018). Metabolically engineered *Corynebacterium glutamicum* for bio-based production of chemicals, fuels, materials, and healthcare products. *Metab. Eng.* 50, 122–141. doi: 10.1016/j.ymben.2018.07.008

Becker, J., and Wittmann, C. (2015). Advanced biotechnology: metabolically engineered cells for the bio-based production of chemicals and fuels, materials, and health-care products. *Angew. Chem. Int. Ed. Engl.* 54, 3328–3350. doi: 10.1002/anie.201409033

Becker, J., and Wittmann, C. (2019). A field of dreams: lignin valorization into chemicals, materials, fuels, and health-care products. *Biotechnol. Adv.* 37:107360. doi: 10.1016/j.biotechadv.2019.02.016

Bellmann, A., Vrljic, M., Patek, M., Sahm, H., Kramer, R., and Eggeling, L. (2001). Expression control and specificity of the basic amino acid exporter LysE of *Corynebacterium glutamicum*. *Microbiology* 147, 1765–1774. doi: 10.1099/00221287-147-7-1765

Brusseler, C., Radek, A., Tenhaef, N., Krumbach, K., Noack, S., and Marienhagen, J. (2018). The myo-inositol/proton symporter IolT1 contributes to d-xylose uptake in *Corynebacterium glutamicum*. *Bioresour. Technol.* 249, 953–961. doi: 10.1016/j.biortech.2017.10.098

Butterworth, R. F., and McPhail, M. J. W. (2019). L-Ornithine L-Aspartate (LOLA) for hepatic encephalopathy in cirrhosis: results of randomized controlled trials and meta-analyses. *Drugs* 79, 31–37. doi: 10.1007/s40265-018-1024-1

Chen, C., Li, Y., Hu, J., Dong, X., and Wang, X. (2015). Metabolic engineering of *Corynebacterium glutamicum* ATCC13869 for L-valine production. *Metab. Eng.* 29, 66–75. doi: 10.1016/j.ymben.2015.03.004

Chen, M., Chen, X., Wan, F., Zhang, B., Chen, J., and Xiong, Y. (2015). Effect of tween 40 and dtsR1 on L-arginine overproduction in *Corynebacterium crenatum*. *Microb. Cell. Fact.* 14:119. doi: 10.1186/s12934-015-0310-9

Chen, X. L., Zhang, B., Tang, L., Jiao, H. T., Xu, H. Y., Xu, F., et al. (2014). Expression and characterization of ArgR, an arginine regulatory protein in *Corynebacterium crenatum*. *Biomed. Environ. Sci.* 27, 436–443. doi: 10.3967/bes2014.072

Chen, Z., Huang, J., Wu, Y., Wu, W., Zhang, Y., and Liu, D. (2017). Metabolic engineering of *Corynebacterium glutamicum* for the production of 3-hydroxypropionic acid from glucose and xylose. *Metab. Eng.* 39, 151–158. doi: 10.1016/j.ymben.2016.11.009

Cho, J. S., Choi, K. R., Prabowo, C. P. S., Shin, J. H., Yang, D., Jang, J., et al. (2017). CRISPR/Cas9-coupled recombineering for metabolic engineering of *Corynebacterium glutamicum*. *Metab. Eng.* 42, 157–167. doi: 10.1016/j.ymben.2017.06.010

Cleto, S., Jensen, J. V., Wendisch, V. F., and Lu, T. K. (2016). *Corynebacterium glutamicum* metabolic engineering with CRISPR interference (CRISPRi). *ACS Synth. Biol.* 5, 375–385. doi: 10.1021/acssynbio.5b00216

D'Este, M., Alvarado-Morales, M., and Angelidaki, I. (2018). Amino acids production focusing on fermentation technologies - a review. *Biotechnol. Adv.* 36, 14–25. doi: 10.1016/j.biotechadv.2017.09.001

Garst, A. D., Bassalo, M. C., Pines, G., Lynch, S. A., Halweg-Edwards, A. L., Liu, R., et al. (2017). Genome-wide mapping of mutations at single-nucleotide resolution for protein, metabolic and genome engineering. *Nat. Biotechnol.* 35, 48–55. doi: 10.1038/nbt.3718

Gourdon, P., and Lindley, N. D. (1999). Metabolic analysis of glutamate production by *Corynebacterium glutamicum*. *Metab. Eng.* 1, 224–231. doi: 10.1006/mben.1999.0122

Guo, J., Suastegui, M., Sakimoto, K. K., Moody, V. M., Xiao, G., Nocera, D. G., et al. (2018). Light-driven fine chemical production in yeast biohybrids. *Science* 362, 813–816. doi: 10.1126/science.aat9777

Hammer, S. K., and Avalos, J. L. (2016). Metabolic engineering: biosensors get the green light. *Nat. Chem. Biol.* 12, 894–895. doi: 10.1038/nchembio.2214

Hao, N., Mu, J., Hu, N., Xu, S., Shen, P., Yan, M., et al. (2016). Implication of ornithine acetyltransferase activity on l-ornithine production in *Corynebacterium glutamicum*. *Biotechnol. Appl. Biochem.* 63, 15–21. doi: 10.1002/bab.1353

Henke, N. A., Wiebe, D., Perez-Garcia, F., Peters-Wendisch, P., and Wendisch, V. F. (2018). Coproduction of cell-bound and secreted value-added compounds: simultaneous production of carotenoids and amino acids by *Corynebacterium glutamicum*. *Bioresour. Technol.* 247, 744–752. doi: 10.1016/j.biortech.2017.09.167

Hirasawa, T., and Wachi, M. (2017). Glutamate fermentation-2: mechanism of L-glutamate overproduction in *Corynebacterium glutamicum*. *Adv. Biochem. Eng. Biotechnol.* 159, 57–72. doi: 10.1007/10_2016_26

Hoffmann, S. L., Jungmann, L., Schiefelbein, S., Peyriga, L., Cahoreau, E., Portais, J. C., et al. (2018). Lysine production from the sugar alcohol mannitol: design of the cell factory *Corynebacterium glutamicum* SEA-3 through integrated analysis and engineering of metabolic pathway fluxes. *Metab. Eng.* 47, 475–487. doi: 10.1016/j.ymben.2018.04.019

Hwang, G. H., and Cho, J. Y. (2010). Identification of a suppressor gene for the arginine-auxotrophic argJ mutation in *Corynebacterium glutamicum*. *J. Ind. Microbiol. Biotechnol.* 37, 1131–1136. doi: 10.1007/s10295-010-0760-3

Hwang, G. H., and Cho, J. Y. (2012). Implication of gluconate kinase activity in L-ornithine biosynthesis in *Corynebacterium glutamicum*. *J. Ind. Microbiol. Biotechnol.* 39, 1869–1874. doi: 10.1007/s10295-012-1197-7

Hwang, G. H., and Cho, J. Y. (2014). Enhancement of L-ornithine production by disruption of three genes encoding putative oxidoreductases in *Corynebacterium glutamicum*. *J. Ind. Microbiol. Biotechnol.* 41, 573–578. doi: 10.1007/s10295-013-1398-8

Hwang, J. H., Hwang, G. H., and Cho, J. Y. (2008). Effect of increased glutamate availability on L-ornithine production in *Corynebacterium glutamicum*. *J. Microbiol. Biotechnol.* 18, 704–710.

Ikeda, M., Mitsuhashi, S., Tanaka, K., and Hayashi, M. (2009). Reengineering of a *Corynebacterium glutamicum* L-arginine and L-citrulline producer. *Appl. Environ. Microbiol.* 75, 1635–1641. doi: 10.1128/AEM.02027-08

Jeandet, P., Sobarzo-Sanchez, E., Clement, C., Nabavi, S. F., Habtemariam, S., Nabavi, S. M., et al. (2018). Engineering stilbene metabolic pathways in microbial cells. *Biotechnol. Adv.* 36, 2264–2283. doi: 10.1016/j.biotechadv.2018.11.002

Jensen, J. V., Eberhardt, D., and Wendisch, V. F. (2015). Modular pathway engineering of *Corynebacterium glutamicum* for production of the glutamate-derived compounds ornithine, proline, putrescine, citrulline, and arginine. *J. Biotechnol.* 214, 85–94. doi: 10.1016/j.jbiotec.2015.09.017

Jiang, L. Y., Chen, S. G., Zhang, Y. Y., and Liu, J. Z. (2013a). Metabolic evolution of *Corynebacterium glutamicum* for increased production of L-ornithine. *BMC Biotechnol.* 13:47. doi: 10.1186/1472-6750-13-47

Jiang, L. Y., Zhang, Y. Y., Li, Z., and Liu, J. Z. (2013b). Metabolic engineering of *Corynebacterium glutamicum* for increasing the production of L-ornithine by increasing NADPH availability. *J. Ind. Microbiol. Biotechnol.* 40, 1143–1151. doi: 10.1007/s10295-013-1306-2

Jiang, Y., Qian, F., Yang, J., Liu, Y., Dong, F., Xu, C., et al. (2017). CRISPR-Cpf1 assisted genome editing of *Corynebacterium glutamicum*. *Nat. Commun.* 8:15179. doi: 10.1038/ncomms15179

Jo, S., Yoon, J., Lee, S. M., Um, Y., Han, S. O., and Woo, H. M. (2017). Modular pathway engineering of *Corynebacterium glutamicum* to improve xylose utilization and succinate production. *J. Biotechnol.* 258, 69–78. doi: 10.1016/j.jbiotec.2017.01.015

Jorge, J. M., Nguyen, A. Q., Perez-Garcia, F., Kind, S., and Wendisch, V. F. (2017a). Improved fermentative production of gamma-aminobutyric acid via the putrescine route: Systems metabolic engineering for production from glucose, amino sugars, and xylose. *Biotechnol. Bioeng.* 114, 862–873. doi: 10.1002/bit.26211

Jorge, J. M. P., Perez-Garcia, F., and Wendisch, V. F. (2017b). A new metabolic route for the fermentative production of 5-aminovalerate from glucose and alternative carbon sources. *Bioresour. Technol.* 245, 1701–1709. doi: 10.1016/j.biortech.2017.04.108

Kawaguchi, H., Yoshihara, K., Hara, K. Y., Hasunuma, T., Ogino, C., and Kondo, A. (2018). Metabolome analysis-based design and engineering of a metabolic pathway in *Corynebacterium glutamicum* to match rates of simultaneous utilization of D-glucose and L-arabinose. *Microb. Cell. Fact.* 17:76. doi: 10.1186/s12934-018-0927-6

Kennerknecht, N., Sahm, H., Yen, M. R., Patek, M., Saier, M. H. Jr., and Eggeling, L. (2002). Export of L-isoleucine from *Corynebacterium glutamicum*: a two-gene-encoded member of a new translocator family. *J. Bacteriol.* 184, 3947–3956. doi: 10.1128/JB.184.14.3947-3956.2002

Kim, D. J., Hwang, G. H., Um, J. N., and Cho, J. Y. (2015). Increased L-ornithine production in *Corynebacterium glutamicum* by overexpression of a gene encoding a putative aminotransferase. *J. Mol. Microbiol. Biotechnol.* 25, 45–50. doi: 10.1159/000375124

Kim, H. T., Khang, T. U., Baritugo, K. A., Hyun, S. M., Kang, K. H., Jung, S. H., et al. (2019). Metabolic engineering of *Corynebacterium glutamicum* for the production of glutaric acid, a C5 dicarboxylic acid platform chemical. *Metab. Eng.* 51, 99–109. doi: 10.1016/j.ymben.2018.08.007

Kim, S., Jeong, H., Kim, E. Y., Kim, J. F., Lee, S. Y., and Yoon, S. H. (2017). Genomic and transcriptomic landscape of *Escherichia coli* BL21(DE3). *Nucleic. Acids Res.* 45, 5285–5293. doi: 10.1093/nar/gkx228

Kim, S. Y., Lee, J., and Lee, S. Y. (2015). Metabolic engineering of *Corynebacterium glutamicum* for the production of L-ornithine. *Biotechnol. Bioeng.* 112, 416–421. doi: 10.1002/bit.25440

Kind, S., Kreye, S., and Wittmann, C. (2011). Metabolic engineering of cellular transport for overproduction of the platform chemical 1,5-diaminopentane in *Corynebacterium glutamicum*. *Metab. Eng.* 13, 617–627. doi: 10.1016/j.ymben.2011.07.006

Kogure, T., and Inui, M. (2018). Recent advances in metabolic engineering of *Corynebacterium glutamicum* for bioproduction of value-added aromatic chemicals and natural products. *Appl. Microbiol. Biotechnol.* 102, 8685–8705. doi: 10.1007/s00253-018-9289-6

Lapujade, P., Goergen, J. L., and Engasser, J. M. (1999). Glutamate excretion as a major kinetic bottleneck for the thermally triggered production of glutamic acid by *Corynebacterium glutamicum*. *Metab. Eng.* 1, 255–261. doi: 10.1006/mben.1999.0129

Lee, J. H., and Wendisch, V. F. (2017). Production of amino acids-genetic and metabolic engineering approaches. *Bioresour. Technol.* 245, 1575–1587. doi: 10.1016/j.biortech.2017.05.065

Lee, S. Y., Cho, J. Y., Lee, H. J., Kim, Y. H., and Min, J. (2010). Enhancement of ornithine production in proline-supplemented *Corynebacterium glutamicum* by ornithine cyclodeaminase. *J. Microbiol. Biotechnol.* 20, 127–131. doi: 10.4014/jmb.0907.07034

Lee, Y. J., and Cho, J. Y. (2006). Genetic manipulation of a primary metabolic pathway for L-ornithine production in *Escherichia coli*. *Biotechnol. Lett.* 28, 1849–1856. doi: 10.1007/s10529-006-9163-y

Li, S., Li, Y., and Smolke, C. D. (2018). Strategies for microbial synthesis of high-value phytochemicals. *Nat. Chem.* 10, 395–404. doi: 10.1038/s41557-018-0013-z

Li, Y., Cong, H., Liu, B., Song, J., Sun, X., Zhang, J., et al. (2016). Metabolic engineering of *Corynebacterium glutamicum* for methionine production by removing feedback inhibition and increasing NADPH level. *Antonie Van Leeuwenhoek* 109, 1185–1197. doi: 10.1007/s10482-016-0719-0

Li, Y., Wei, H., Wang, T., Xu, Q., Zhang, C., Fan, X., et al. (2017). Current status on metabolic engineering for the production of l-aspartate family amino acids and derivatives. *Bioresour. Technol.* 245, 1588–1602. doi: 10.1016/j.biortech.2017.05.145

Lin, J. L., Wagner, J. M., and Alper, H. S. (2017). Enabling tools for high-throughput detection of metabolites: metabolic engineering and directed evolution applications. *Biotechnol. Adv.* 35, 950–970. doi: 10.1016/j.biotechadv.2017.07.005

Lindner, S. N., Niederholtmeyer, H., Schmitz, K., Schoberth, S. M., and Wendisch, V. F. (2010). Polyphosphate/ATP-dependent NAD kinase of *Corynebacterium glutamicum*: biochemical properties and impact of *ppnK* overexpression on lysine production. *Appl. Microbiol. Biotechnol.* 87, 583–593. doi: 10.1007/s00253-010-2481-y

Luo, X., Reiter, M. A., d'Espaux, L., Wong, J., Denby, C. M., Lechner, A., et al. (2019). Complete biosynthesis of cannabinoids and their unnatural analogues in yeast. *Nature* 567, 123–126. doi: 10.1038/s41586-019-0978-9

Mao, Y., Li, G., Chang, Z., Tao, R., Cui, Z., Wang, Z., et al. (2018). Metabolic engineering of *Corynebacterium glutamicum* for efficient production of succinate from lignocellulosic hydrolysate. *Biotechnol. Biofuels* 11:95. doi: 10.1186/s13068-018-1094-z

Meiswinkel, T. M., Gopinath, V., Lindner, S. N., Nampoothiri, K. M., and Wendisch, V. F. (2013a). Accelerated pentose utilization by *Corynebacterium glutamicum* for accelerated production of lysine, glutamate, ornithine and putrescine. *Microb. Biotechnol.* 6, 131–140. doi: 10.1111/1751-7915.12001

Meiswinkel, T. M., Rittmann, D., Lindner, S. N., and Wendisch, V. F. (2013b). Crude glycerol-based production of amino acids and putrescine by *Corynebacterium glutamicum*. *Bioresour. Technol.* 145, 254–258. doi: 10.1016/j.biortech.2013.02.053

Mindt, M., Heuser, M., and Wendisch, V. F. (2019). Xylose as preferred substrate for sarcosine production by recombinant *Corynebacterium glutamicum*. *Bioresour. Technol.* 281, 135–142. doi: 10.1016/j.biortech.2019.02.084

Mitsuhashi, S. (2014). Current topics in the biotechnological production of essential amino acids, functional amino acids, and dipeptides. *Curr. Opin. Biotechnol.* 26, 38–44. doi: 10.1016/j.copbio.2013.08.020

Nakamura, J., Hirano, S., Ito, H., and Wachi, M. (2007). Mutations of the *Corynebacterium glutamicum NCgl1221* gene, encoding a mechanosensitive channel homolog, induce L-glutamic acid production. *Appl. Environ. Microbiol.* 73, 4491–4498. doi: 10.1128/AEM.02446-06

Nakayama, Y., Yoshimura, K., and Iida, H. (2012). A gain-of-function mutation in gating of *Corynebacterium glutamicum* NCgl1221 causes constitutive glutamate secretion. *Appl. Environ. Microbiol.* 78, 5432–5434. doi: 10.1128/AEM.01310-12

Okuda, S., Sherman, D. J., Silhavy, T. J., Ruiz, N., and Kahne, D. (2016). Lipopolysaccharide transport and assembly at the outer membrane: the PEZ model. *Nat. Rev. Microbiol.* 14, 337–345. doi: 10.1038/nrmicro.2016.25

Otten, A., Brocker, M., and Bott, M. (2015). Metabolic engineering of *Corynebacterium glutamicum* for the production of itaconate. *Metab. Eng.* 30, 156–165. doi: 10.1016/j.ymben.2015.06.003

Park, J., Yu, B. J., Choi, J. I., and Woo, H. M. (2019). Heterologous production of squalene from glucose in engineered *Corynebacterium glutamicum* using multiplex CRISPR interference and high-throughput fermentation. *J. Agric. Food. Chem.* 67, 308–319. doi: 10.1021/acs.jafc.8b05818

Park, S. H., Kim, H. U., Kim, T. Y., Park, J. S., Kim, S. S., and Lee, S. Y. (2014). Metabolic engineering of *Corynebacterium glutamicum* for L-arginine production. *Nat. Commun.* 5:4618. doi: 10.1038/ncomms5618

Perez-Garcia, F., Max Risse, J., Friehs, K., and Wendisch, V. F. (2017). Fermentative production of L-pipecolic acid from glucose and alternative carbon sources. *Biotechnol. J.* 12:1600646. doi: 10.1002/biot.201600646

Qin, J., Zhou, Y. J., Krivoruchko, A., Huang, M., Liu, L., Khoomrung, S., et al. (2015). Modular pathway rewiring of *Saccharomyces cerevisiae* enables high-level production of L-ornithine. *Nat. Commun.* 6:8224. doi: 10.1038/ncomms9224

Radek, A., Tenhaef, N., Muller, M. F., Brusseler, C., Wiechert, W., Marienhagen, J., et al. (2017). Miniaturized and automated adaptive laboratory evolution: Evolving *Corynebacterium glutamicum* towards an improved d-xylose utilization. *Bioresour. Technol.* 245, 1377–1385. doi: 10.1016/j.biortech.2017.05.055

Rathi, S., and Taneja, S. (2018). Terminating and episode of overt hepatic encephalopathy: L-ornithine-L-aspartate may have some role. *Hepatology* 67:797. doi: 10.1002/hep.29570

Sarria, S., Kruyer, N. S., and Peralta-Yahya, P. (2017). Microbial synthesis of medium-chain chemicals from renewables. *Nat. Biotechnol.* 35, 1158–1166. doi: 10.1038/nbt.4022

Schneider, J., Niermann, K., and Wendisch, V. F. (2011). Production of the amino acids l-glutamate, l-lysine, l-ornithine and l-arginine from arabinose by recombinant *Corynebacterium glutamicum*. *J. Biotechnol.* 154, 191–198. doi: 10.1016/j.jbiotec.2010.07.009

Shang, X., Zhang, Y., Zhang, G., Chai, X., Deng, A., Liang, Y., et al. (2013). Characterization and molecular mechanism of AroP as an aromatic amino acid and histidine transporter in *Corynebacterium glutamicum*. *J.Bacteriol.* 195, 5334–5342. doi: 10.1128/JB.00971-13

Shen, H. J., Cheng, B. Y., Zhang, Y. M., Tang, L., Li, Z., Bu, Y. F., et al. (2016). Dynamic control of the mevalonate pathway expression for improved zeaxanthin production in *Escherichia coli* and comparative proteome analysis. *Metab. Eng.* 38, 180–190. doi: 10.1016/j.ymben.2016.07.012

Shu, Q., Xu, M., Li, J., Yang, T., Zhang, X., Xu, Z., et al. (2018). Improved L-ornithine production in *Corynebacterium crenatum* by introducing an artificial linear transacetylation pathway. *J. Ind. Microbiol. Biotechnol.* 45, 393–404. doi: 10.1007/s10295-018-2037-1

Siedler, S., Lindner, S. N., Bringer, S., Wendisch, V. F., and Bott, M. (2013). Reductive whole-cell biotransformation with *Corynebacterium glutamicum*: improvement of NADPH generation from glucose by a cyclized pentose phosphate pathway using *pfkA* and *gapA* deletion mutants. *Appl. Microbiol. Biotechnol.* 97, 143–152. doi: 10.1007/s00253-012-4314-7

Stäbler, N., Oikawa, T., Bott, M., and Eggeling, L. (2011). *Corynebacterium glutamicum* as a host for synthesis and export of D-amino acids. *J. Bacteriol.* 193, 1702–1709. doi: 10.1128/JB.01295-10

Stella, R. G., Wiechert, J., Noack, S., and Frunzke, J. (2019). Evolutionary engineering of *Corynebacterium glutamicum*. *Biotechnol. J.* 14:e1800444. doi: 10.1002/biot.201800444

Takeno, S., Hori, K., Ohtani, S., Mimura, A., Mitsuhashi, S., and Ikeda, M. (2016). l-Lysine production independent of the oxidative pentose phosphate pathway by *Corynebacterium glutamicum* with the *Streptococcus mutans* gapN gene. *Metab. Eng.* 37, 1–10. doi: 10.1016/j.ymben.2016.03.007

Takeno, S., Murata, R., Kobayashi, R., Mitsuhashi, S., and Ikeda, M. (2010). Engineering of *Corynebacterium glutamicum* with an NADPH-generating glycolytic pathway for L-lysine production. *Appl. Environ. Microbiol.* 76, 7154–7160. doi: 10.1128/AEM.01464-10

Teusink, B., and Smid, E. J. (2006). Modelling strategies for the industrial exploitation of lactic acid bacteria. *Nat. Rev. Microbiol.* 4, 46–56. doi: 10.1038/nrmicro1319

Tuyishime, P., Wang, Y., Fan, L., Zhang, Q., Li, Q., Zheng, P., et al. (2018). Engineering *Corynebacterium glutamicum* for methanol-dependent growth and glutamate production. *Metab. Eng.* 49, 220–231. doi: 10.1016/j.ymben.2018.07.011

Varela, C., Schmidt, S. A., Borneman, A. R., Pang, C. N. I., Krömerx, J. O., Khan, A., et al. (2018). Systems-based approaches enable identification of gene targets which improve the flavour profile of low-ethanol wine yeast strains. *Metab. Eng.* 49, 178–191. doi: 10.1016/j.ymben.2018.08.006

Vrljic, M., Sahm, H., and Eggeling, L. (1996). A new type of transporter with a new type of cellular function: L-lysine export from *Corynebacterium glutamicum*. *Mol. Microbiol.* 22, 815–826. doi: 10.1046/j.1365-2958.1996.01527.x

Wang, B., Hu, Q., Zhang, Y., Shi, R., Chai, X., Liu, Z., et al. (2018). A RecET-assisted CRISPR-Cas9 genome editing in *Corynebacterium glutamicum*. *Microb. Cell. Fact.* 17:63. doi: 10.1186/s12934-018-0910-2

Wang, Y., Cao, G., Xu, D., Fan, L., Wu, X., Ni, X., et al. (2018). A novel *Corynebacterium glutamicum* l-glutamate exporter. *Appl. Environ. Microbiol.* 84:e02691-17. doi: 10.1128/AEM.02691-17

Wendisch, V. F., Jorge, J. M., Pérez-García, F., and Sgobba, E. (2016). Updates on industrial production of amino acids using *Corynebacterium glutamicum*. *World J. Microbiol. Biotechnol.* 32:105. doi: 10.1007/s11274-016-2060-1

Wu, W., Zhang, Y., Liu, D., and Chen, Z. (2019). Efficient mining of natural NADH-utilizing dehydrogenases enables systematic cofactor engineering of lysine synthesis pathway of *Corynebacterium glutamicum*. *Metab. Eng.* 52, 77–86. doi: 10.1016/j.ymben.2018.11.006

Xiao, F., Wang, H., Shi, Z., Huang, Q., Huang, L., Lian, J., et al. (2019). Multi-level metabolic engineering of *Pseudomonas mutabilis* ATCC31014 for efficient production of biotin. *Metab. Eng.* doi: 10.1016/j.ymben.2019.05.005. [Epub ahead of print].

Xu, J. Z., Wu, Z. H., Gao, S. J., and Zhang, W. (2018a). Rational modification of tricarboxylic acid cycle for improving L-lysine production in *Corynebacterium glutamicum*. *Microb. Cell. Fact.* 17:105. doi: 10.1186/s12934-018-0958-z

Xu, J. Z., Yang, H. K., and Zhang, W. G. (2018b). NADPH metabolism: a survey of its theoretical characteristics and manipulation strategies in amino acid biosynthesis. *Crit. Rev. Biotechnol.* 38, 1061–1076. doi: 10.1080/07388551.2018.1437387

Xu, M., Qin, J., Rao, Z., You, H., Zhang, X., Yang, T., et al. (2016). Effect of Polyhydroxybutyrate (PHB) storage on L-arginine production in recombinant

Corynebacterium crenatum using coenzyme regulation. *Microb. Cell. Fact.* 15:15. doi: 10.1186/s12934-016-0414-x

Xu, M., Rao, Z., Dou, W., Jin, J., and Xu, Z. (2012a). Site-directed mutagenesis studies on the L-arginine-binding sites of feedback inhibition in N-acetyl-L-glutamate kinase (NAGK) from *Corynebacterium glutamicum*. *Curr. Microbiol.* 64, 164–172. doi: 10.1007/s00284-011-0042-y

Xu, M., Rao, Z., Dou, W., Yang, J., Jin, J., and Xu, Z. (2012b). Site-directed mutagenesis and feedback-resistant N-acetyl-L-glutamate kinase (NAGK) increase *Corynebacterium crenatum* L-arginine production. *Amino Acids* 43, 255–266. doi: 10.1007/s00726-011-1069-x

Xu, N., Wei, L., and Liu, J. (2019). Recent advances in the applications of promoter engineering for the optimization of metabolite biosynthesis. *World J. Microbiol. Biotechnol.* 35:33. doi: 10.1007/s11274-019-2606-0

Yeom, S. J., Kim, M., Kwon, K. K., Fu, Y., Rha, E., Park, S. H., et al. (2018). A synthetic microbial biosensor for high-throughput screening of lactam biocatalysts. *Nat. Commun.* 9:5053. doi: 10.1038/s41467-018-07488-0

Yoon, J., and Woo, H. M. (2018). CRISPR interference-mediated metabolic engineering of *Corynebacterium glutamicum* for homo-butyrate production. *Biotechnol. Bioeng.* 115, 2067–2074. doi: 10.1002/bit.26720

Yu, T., Zhou, Y. J., Huang, M., Liu, Q., Pereira, R., David, F., et al. (2018). Reprogramming yeast metabolism from alcoholic fermentation to lipogenesis. *Cell* 174, 1549–1558. doi: 10.1016/j.cell.2018.07.013

Zahoor, A., Lindner, S. N., and Wendisch, V. F. (2012). Metabolic engineering of *Corynebacterium glutamicum* aimed at alternative carbon sources and new products. *Comput. Struct. Biotechnol. J.* 3:e201210004. doi: 10.5936/csbj.201210004

Zhang, B., Gao, G., Chu, X. H., and Ye, B. C. (2019). Metabolic engineering of *Corynebacterium glutamicum* S9114 to enhance the production of l-ornithine driven by glucose and xylose. *Bioresour. Technol.* 284, 204–213. doi: 10.1016/j.biortech.2019.03.122

Zhang, B., Ren, L. Q., Yu, M., Zhou, Y., and Ye, B. C. (2018a). Enhanced l-ornithine production by systematic manipulation of l-ornithine metabolism in engineered *Corynebacterium glutamicum* S9114. *Bioresour. Technol.* 250, 60–68. doi: 10.1016/j.biortech.2017.11.017

Zhang, B., Yu, M., Wei, W. P., and Ye, B. C. (2018b). Optimization of L-ornithine production in recombinant *Corynebacterium glutamicum* S9114 by *cg3035* overexpression and manipulating the central metabolic pathway. *Microb. Cell. Fact.* 17:91. doi: 10.1186/s12934-018-0940-9

Zhang, B., Yu, M., Zhou, Y., Li, Y., and Ye, B. C. (2017). Systematic pathway engineering of *Corynebacterium glutamicum* S9114 for L-ornithine production. *Microb. Cell. Fact.* 16:158. doi: 10.1186/s12934-017-0776-8

Zhang, B., Yu, M., Zhou, Y., and Ye, B. C. (2018c). Improvement of L-ornithine production by attenuation of argF in engineered *Corynebacterium glutamicum* S9114. *AMB Express* 8:26. doi: 10.1186/s13568-018-0557-8

Zhang, H., Li, Y., Wang, C., and Wang, X. (2018). Understanding the high L-valine production in *Corynebacterium glutamicum* VWB-1 using transcriptomics and proteomics. *Sci. Rep.* 8:3632. doi: 10.1038/s41598-018-21926-5

Zhang, J., Xu, M., Ge, X., Zhang, X., Yang, T., Xu, Z., et al. (2017). Reengineering of the feedback-inhibition enzyme N-acetyl-L-glutamate kinase to enhance L-arginine production in *Corynebacterium crenatum*. *J. Ind. Microbiol. Biotechnol.* 44, 271–283. doi: 10.1007/s10295-016-1885-9

Zhang, J., Yang, F., Yang, Y., Jiang, Y., and Huo, Y. X. (2019). Optimizing a CRISPR-Cpf1-based genome engineering system for *Corynebacterium glutamicum*. *Microb. Cell. Fact.* 18:60. doi: 10.1186/s12934-019-1109-x

Zhang, Y. Y., Bu, Y. F., and Liu, J. Z. (2015). Production of L-ornithine from sucrose and molasses by recombinant *Corynebacterium glutamicum*. *Folia Microbiol.* 60, 393–398. doi: 10.1007/s12223-014-0371-x

Zhao, N., Qian, L., Luo, G., and Zheng, S. (2018). Synthetic biology approaches to access renewable carbon source utilization in *Corynebacterium glutamicum*. *Appl. Microbiol. Biotechnol.* 102, 9517–9529. doi: 10.1007/s00253-018-9358-x

Zheng, B., Ma, X., Wang, N., Ding, T., Guo, L., Zhang, X., et al. (2018). Utilization of rare codon-rich markers for screening amino acid overproducers. *Nat. Commun.* 9:3616. doi: 10.1038/s41467-018-05830-0

Conflict of Interest: The authors declare that the research was conducted in the absence of any commercial or financial relationships that could be construed as a potential conflict of interest.

The handling Editor declared a shared affiliation, though no other collaboration, with one of the authors B-CY.

frontiers in Bioengineering and Biotechnology

ORIGINAL RESEARCH
published: 15 January 2020
doi: 10.3389/fbioe.2019.00471

Two-Stage Crystallization Combining Direct Succinimide Synthesis for the Recovery of Succinic Acid From Fermentation Broth

Yiwen Xiao[1,2], *Zhibin Zhang*[1], *Ya Wang*[2], *Boliang Gao*[2], *Jun Chang*[2] *and Du Zhu*[1,2]*

[1] *Key Laboratory of Protection and Utilization of Subtropic Plant Resources of Jiangxi Province, Jiangxi Normal University, Nanchang, China,* [2] *Key Laboratory of Bioprocess Engineering of Jiangxi Province, College of Life Sciences, Jiangxi Science and Technology Normal University, Nanchang, China*

OPEN ACCESS

Edited by:
Hui Wu,
East China University of Science and Technology, China

Reviewed by:
Liya Liang,
University of Colorado Boulder, United States
Jianmin Xing,
Institute of Process Engineering (CAS), China
Kequan Chen,
Nanjing Tech University, China

***Correspondence:**
Du Zhu
zhudu12@163.com

Specialty section:
This article was submitted to Industrial Biotechnology, a section of the journal Frontiers in Bioengineering and Biotechnology

Received: *25 October 2019*
Accepted: *23 December 2019*
Published: *15 January 2020*

Citation:
Xiao Y, Zhang Z, Wang Y, Gao B, Chang J and Zhu D (2020) Two-Stage Crystallization Combining Direct Succinimide Synthesis for the Recovery of Succinic Acid From Fermentation Broth. Front. Bioeng. Biotechnol. 7:471. doi: 10.3389/fbioe.2019.00471

Succinic acid is an important chemical and raw material widely used in medicine, food, biodegradable materials, fine chemicals, and other industrial fields. However, traditional methods for purifying succinic acid from fermentation broth are costly, poorly efficient, and harmful to the environment. In this study, an efficient method for purifying succinic acid from the fermentation broth of *Escherichia coli* NZN111 was developed through crystallization and co-crystallization with urea. First, the filtrate was collected by filtering the fermentation broth, and pH was adjusted to 2.0 by supplementing sulfuric acid. Crystallization was carried out at 8°C for 4 h to obtain succinic acid crystals. The recovery rate and purity of succinic acid were 73.4% and over 99%, respectively. Then, urea was added to the remaining solution with a mass ratio of urea to residual succinic acid of 4:1 (m_{urea}/m_{SA}). The second crystallization was carried out at pH 2 and 4°C for 12 h to obtain succinic acid-urea co-crystal. The recovery rate of succinic acid residue was 92.0%. The succinic acid-urea crystal was further mixed with phosphorous acid (4.2% of the mass of succinic acid co-crystal) and maintained at 195°C for 6 h to synthesize succinimide, and the yield was >80%. This novel and efficient purification process was characterized by the significantly reduced urea consumption, and high succinic acid recovery (totally 95%), and high succinimide synthesis yield (80%). Thus, this study potentially provided a novel and efficient strategy for the industrial production of succinic acid and succinimide.

Keywords: succinimide, recovery, co-crystals, succinic acid, urea

INTRODUCTION

Succinic acid is an important renewable four-carbon building block chemical that is prevalent in humans, animals, plants, and microorganisms (Li et al., 2010; Alexandri et al., 2019). Succinic acid has been widely used in medicine, food, the chemical industry, and agriculture (Delhomme et al., 2009). Presently, the market demand for succinic acid has increased dramatically owing to its application in green solvents and biodegradable polymers (Jansen and van Gulik, 2014). Succinic acid is primarily produced via chemical synthesis using maleic anhydride as a raw material, which causes serious environmental and economic concerns such as increased pollution

and energy consumption, thereby rendering this process unsustainable (Cukalovic and Stevens, 2008; Pinazo et al., 2015). Thus, a novel and green strategy for producing succinic acid through the biotransformation of cheap, renewable materials has been suggested (Sheldon and Sanders, 2015). For example, succinic acid can be produced via the fermentation of cassava, straw, and waste biomass by microorganisms, such as engineered *Escherichia coli* (Zhang et al., 2018), *Actinobacillus succinogenes* (Gunnarsson et al., 2014; Dessie et al., 2018), and *Anaerobiospirillum succiniciproducens* (Akhtar et al., 2013; Lee et al., 2015), respectively. However, an efficient method of purifying succinic acid from these fermentation broths remains unavailable.

Generally, the bio-production of succinic acid involves four steps: right raw material selection, pretreatment, fermentation, and purification. The separation and purification procedures account for 50–80% of the total production costs (Cheng et al., 2012; López-Garzón and Straathof, 2014). Therefore, the costs involved in these steps must be reduced to promote the industrialization of biologically synthesized succinic acid. Conventional methods for separating succinic acid from the fermentation broth include calcium salt precipitation, solvent extraction, ion exchange, electrodialysis, and membrane separation (Khunnonkwao et al., 2018; Prochaska et al., 2018; Antczak et al., 2019). However, these methods have many disadvantages, including high cost, low efficiency, and environmentally hazardous elements, which impede their use in industrial applications. For example, the yield of isolated succinic acid using calcium salt precipitation is only 52% (Li et al., 2010); meanwhile, a large amount of calcium sulfate waste is produced. Succinic acid can also be separated using a two-phase system. This process is simple and energy saving but cannot be used to remove heteroacids; therefore, a large amount of solvent is wasted (Matsumoto and Tatsumi, 2018). Previous reports have shown that increasing the yield of succinic acid from residual solvent is difficult, costly, and polluting. Thus, a strategy is required to transform the succinic acid that is available in residues solvent into an easily purified and valuable product, such as succinimide (Deng et al., 2014), Diethyl succinate (Kolah et al., 2008; López-Garzón et al., 2012; Orjuela et al., 2012), poly (butylene succinate), γ-butyrolactone (Hong et al., 2012a), and tetrahydrofuran (Hong et al., 2012b). Amongst them, succinimide is an important intermediate used as for medicine, pesticides, and silver-plating industry (Liu et al., 2018). Therefore, a simple, highly efficient, and green method for separating succinic acid from a microorganism fermentation broth is needed.

In the present study, a simple and inexpensive method involving crystallization and urea co-crystallization was developed to separate succinic acid from fermentation broth efficiently. This study also focused on the feasibility of succinimide synthesis following succinic acid–urea co-crystallization. The established method is not only simple and highly efficient in separating succinic acid with high purity and yield, but also selective for succinic acid among various carboxylic acids. More importantly, the method provides a novel strategy for the full recovery of residual succinic acid following the purification process.

MATERIALS AND METHODS

Materials

Succinic acid and succinimide standards were purchased from Sigma-Aldrich (Shanghai, China). Urea, phosphorous acid, pyruvic acid, and acetic acid were acquired from Aladdin (Shanghai, China). Methanol and acetonitrile were HPLC graded and acquired from Merck (Darmstadt, Germany). Actual succinic acid fermentation broth was provided by Professor Zhimin Li (East China University of Science and Technology). The glucose standard was procured from Xilong Chemical Co., Ltd. (Guangzhou, China).

The succinic acid fermentation broth was used as a raw material in accordance with previously described methods (Chen et al., 2014). The concentrations of succinic acid, acetic acid, pyruvic acid, glucose, and protein were 106.17, 3.37, 0.99, 4.15, and 0.043 g/L, respectively.

Pretreatment

The broth was centrifuged at 8,000 rpm for 30 min to remove bacteria, macromolecular impurities, and insoluble substances. Then, activated carbon was added to decolorize the broth under 30°C, pH 6.8, and 250 rpm for 40 min.

Crystallization

The schematic diagram was shown in **Figure 1**. At stage I, the decolorized broth was cooled and then crystallized directly at various temperatures (4, 8, 12, 16, 20, 28, 32, 36, and 40°C) and pH 2.0 for 4 h. During crystallization, the succinic acid, pyruvate, and acetic acid concentrations were determined. The broth volume was measured before and after the experiment to enable the recovery rate of succinic acid to be calculated. The experimental processes for measuring time and pH were similar to for measuring temperature.

At stage II, after direct crystallization, the pH of the broth was adjusted to 2.0. Then, urea was added to 50 mL of the broth at mass ratios of urea to succinic acid of 1:1, 2:1, 3:1, 4:1, 5:1, and 6:1, respectively. The mixtures were maintained at 4°C for 12 h for crystallization to occur. The concentration and the recovery rate of succinic acid were measured using ultra-performance liquid chromatography UPLC (Acquity H-class, Waters, USA).

Succinimide Synthesis

In this procedure, 11.81 g of succinic acid, 3.07 g of urea, 10 mL of water, and 1.0 g phosphite solid were mixed and dissolved at 80°C. Succinimide was synthesized at 195°C for 5 h. The reaction system was cooled to 80°C, and 8 mL of water and 1 g of activated carbon were added. Thereafter, the mixture was filtered with hot water, and crystallized at 25°C for 12 h to obtain crude succinimide, which was further recrystallized with ethanol. The effects of the mass ratio of succinic acid to urea, reaction temperature, reaction time, and amount of catalyst on the reaction process were investigated on the basis of the experimental operation above. Succinimide was synthesized with succinic acid-urea co-crystals under optimal reaction conditions. The mass ratio of succinic acid to urea was adjusted to 2:1 using the condensed succinic acid as a raw material, adding ∼4.2% solid phosphorite, stirring, heating to 195°C, and reacting

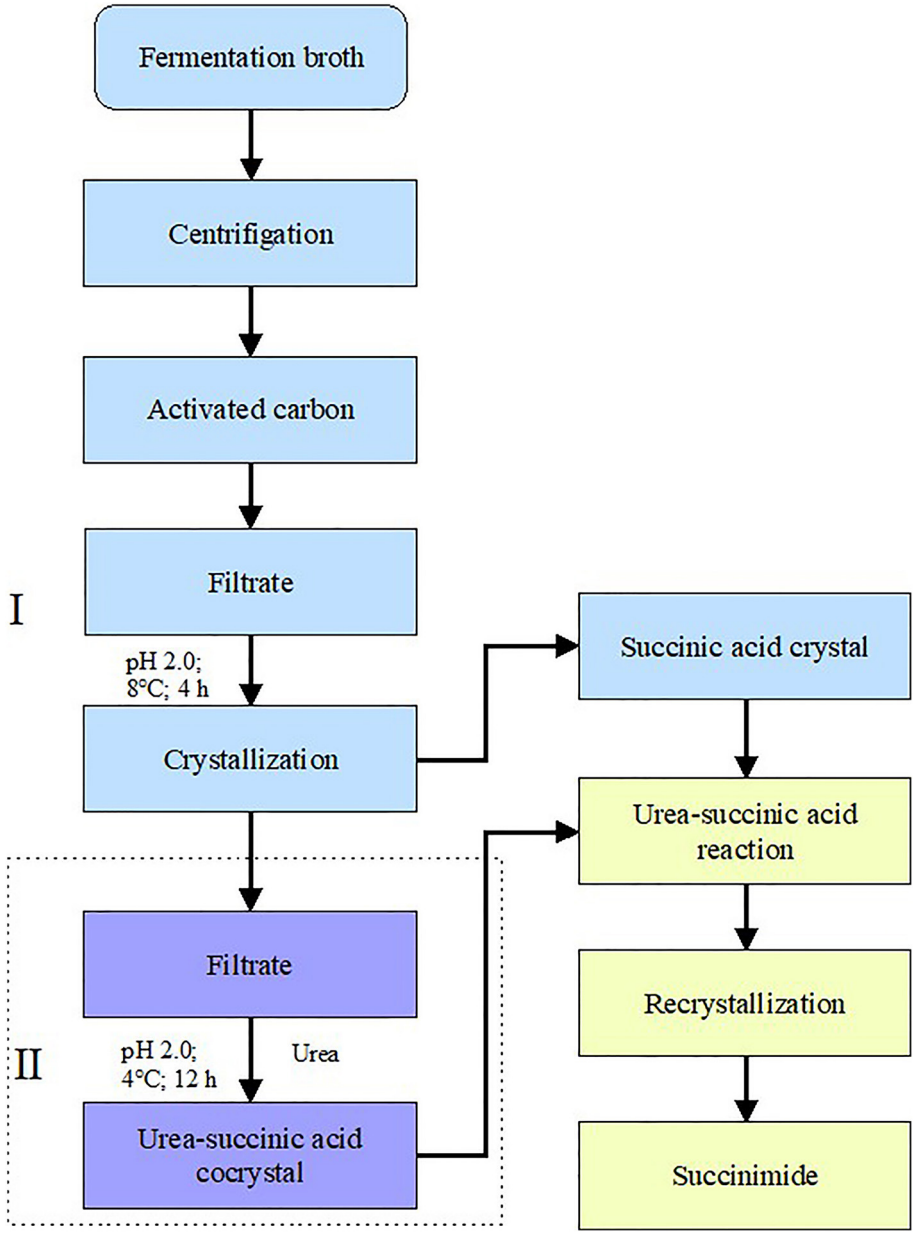

FIGURE 1 | Schematic diagrams of two-stage crystallization combining direct succinimide synthesis for succinic acid recovery. (I) Direct crystallization and (II) co-crystallization of succinic acid with urea.

at a constant temperature for 6 h. The succinimide yield was subsequently calculated.

All experiments were conducted in triplicate.

Methods of Analysis

Organic acids were analyzed using UPLC equipped with an Acquity UPLC BEH, a C_{18}, and 1.7 μm, 2.1 × 100 mm chromatography column (Waters, USA). The mobile phase consisted of acetonitrile and 3 mM H_2SO_4 (CH_3CN:3 mM H_2SO_4 = 3:97, v/v). The flow rate was 0.2 mL/min, and the wavelength was set at 210 nm. Protein contents were determined using the Bradford (Bradford, 1976), with bovine serum albumin (Sigma Chemical Co.) used as a standard. Yield and purity were calculated as followed:

Yield (%) = [dry weight of succinic acid in the recovered crystals (g)/weight of succinic acid in the initial fermentation broth (g)] × 100%.

Purity (%) = [dry weight of succinic acid in crystals recovered (g)/dry weight of the recovered crystals (g)] × 100%.

Succinimide yield was obtained as follows:

Succinimide yield (%) = actual product quality (g)/theoretical product quality (g) × 100%.

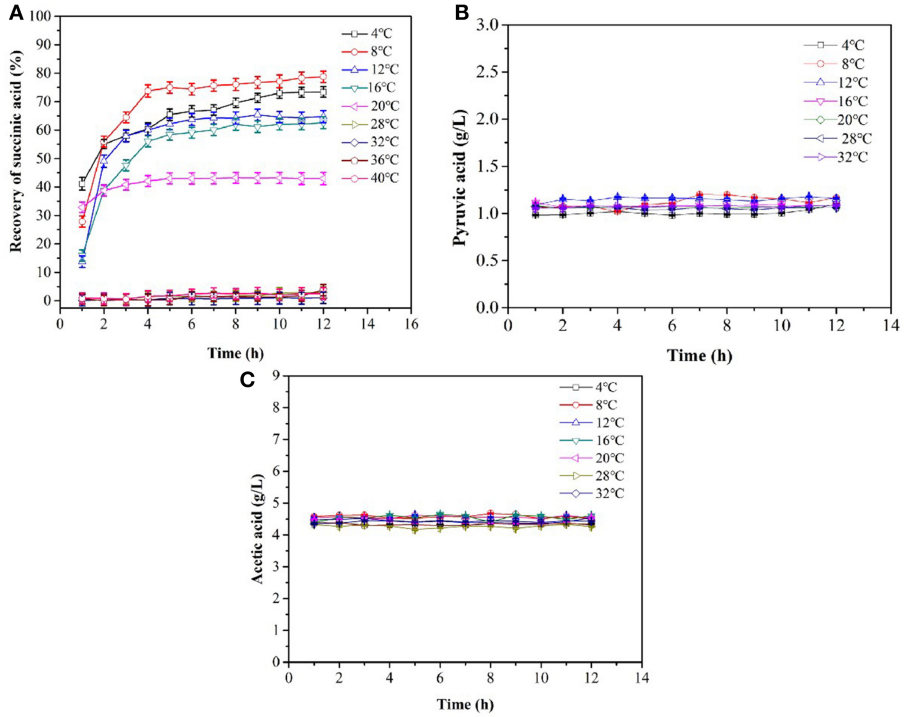

FIGURE 2 | Cooling crystallization of the simulated fermentation broth. **(A)** Yield of succinic acid during the crystallization, **(B)** the concentration of pyruvic acid, **(C)** the concentration of acetic acid.

RESULTS

Optimization of Succinic Acid Crystallization From Fermentation Broth

Crystallization From Simulated Fermentation Broth

No succinic acid crystals were observed within 12 h from 32 to 40°C (**Figures 2A**, **4B**). The maximum amount of succinic acid crystal was obtained at 8°C. The number of crystals increased drastically within 120 min and the succinic acid yield was 55.9%. The increase in crystals yield at 20°C was not significant after 3 h. At 4°C, the crystallization increased with time, and the yield of succinic acid was stable at 73.0% after 10 h. The pyruvic acid and acetic acid concentrations remained at initial values during the whole period of crystallization (**Figures 2B,C**). This result indicated that pyruvic acid and acetic acid were not crystallized. **Figure 2A** shows that temperatures significantly affected succinic acid crystallization. The optimal temperature and time value for the crystallization of succinic acid from the fermentation broth were 8°C and 4 h, respectively. In addition, the largest amount of crystals in powder form was obtained at <20°C. Prismatic and flaky crystals would be obtained when the broth was slowly cooled at room temperature.

Impurities such as acetic acid and pyruvate could not be crystallized from the fermentation broth during crystallization (**Figures 2B,C**). Therefore, the influence of these impurities on the recovery rate of succinic acid could be not considered in the subsequent co-crystallization of succinic acid with urea.

When the succinic acid concentration of succinic acid was <100 g/L, the yield of cooling succinic acid crystallization increased as the succinic acid concentration increased (**Figure 3A**). Glucose and protein were noted to have no influence on the recovery rate of succinic acid (**Figures 3B,C**), consistent with the results of Wang et al. (2014). The average recovery rate of the succinic acid fermentation broth was above 75.0%.

Effect of pH on Succinic Acid Crystallization

Increases in pH lead to decreases in the succinic acid recovery rate (**Figure 4A**). A pH of <2 resulted in a recovery rate of >76.4% succinic acid, possibly because the compound was in a free molecular state and had low solubility at low pH. A high pH would result in the partial dissociation of succinate molecules, thereby increasing solubility. Thus, extracting succinate from a solution at pH >2.0 was difficult, leading to a decreased recovery rate.

Effect of Time on Succinic Acid Crystallization

Figure 4C shows that the recovery rate of succinic acid increases with time over a period of 1–2 h. Crystal growth was slowed down after 2 h and ceased after 4 h. Therefore, the optimal period for cooling and crystallization was 4 h.

Effect of Temperature on Succinic Acid Crystallization

When the temperature was <10°C, the recovery rate of succinic acid was >70% (**Figure 4B**). The recovery rate of succinic acid at

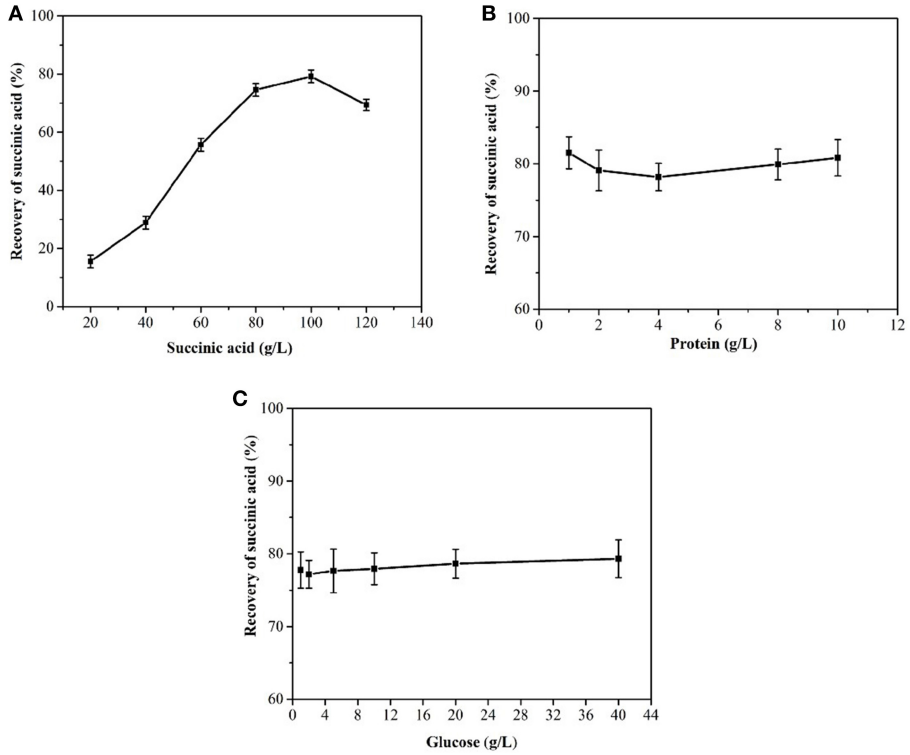

FIGURE 3 | Effects of succinic acid **(A)**, protein **(B)**, and glucose concentration **(C)** on the cooling crystallization of the simulated fermentation broth.

8°C was higher than that at 4°C. Possibly because the lower the temperature, the slower the molecules diffuse. This condition led to the slow crystal growth after nucleation. Therefore, the optimal temperature of succinic acid crystallization was determined to be 8°C. Following the first crystallization step, the succinic acid concentration in the broth was 28 g/L.

Co-crystallization of Succinic Acid With Urea

Influence of the Mass Ratio of Urea to Succinic Acid on the Urea Co-crystallization Process

The influence of a range of urea to succinic acid mass ratios from 1:1 to 6:1 on the yield of succinic acid was also investigated. **Figure 5A** shows that no urea and succinic acid were precipitated into crystals at mass ratio of 1:1. When the ratio was increased to 2:1, 70% of succinic acid could be co-crystallized. With the addition of urea, the succinic acid content in the fermentation broth was reduced. The optimal mass ratio of urea to succinic acid was determined to be 4:1.

Effect of pH on Co-crystallization With Urea

The pH of the feed solution significantly affected co-crystallization with urea (**Figure 5B**). At pH 2.0, the largest number of co-crystallites was obtained. As succinic acid was present in ionic form in the solution, the formation of hydrogen bonds between succinic acid and urea was difficult and a pH > 5.0 resulted in low succinic acid recovery. Therefore, the optimal pH was determined to be 2.0.

Effect of Time on Co-crystallization With Urea

The co-crystallites of succinic acid and urea grew rapidly into nucleation within 5 h (**Figure 5C**) and stopped at 12 h. This result indicated that the optimal total crystallization time was 12 h.

Effect of Temperature on Co-crystallization With Urea

Temperature was inversely related to the number of succinic acid and urea co-crystallites (**Figure 5D**). The maximum number of co-crystallites was obtained at 4°C.

Feasibility of Succinimide Synthesis

At an initial mass ratio of succinic acid to urea of 3.9:1, the succinic acid was slightly excessive, and the succinimide yield was 75% (**Figure 6A**). In terms of cost, excess urea shifted the balance toward production. However, excessive urea, would result in the formation of the byproduct, that is, succinamide. The selected mass ratio of succinic acid to urea was therefore 2:1 (Charville et al., 2010).

The reaction of succinic acid and urea is endothermic; hence, increasing the temperature helps to shift the reaction in an endothermic direction and increase the amount of succinimide produced (Pavelka and Grmela, 2019). However, when the temperature is too high, carbonization occurs easily and energy consumption is high. In this study, the reaction temperature was 195°C (**Figure 6B**).

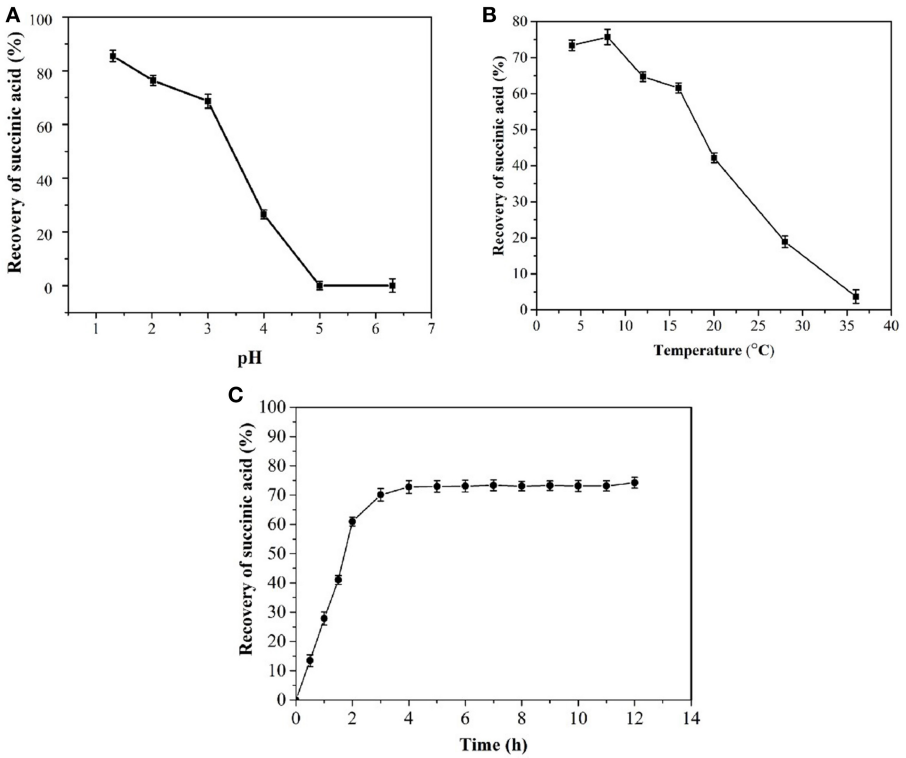

FIGURE 4 | Effects of pH **(A)**, temperature **(B)**, and time **(C)** on the crystallization of succinic acid from fermentation broth.

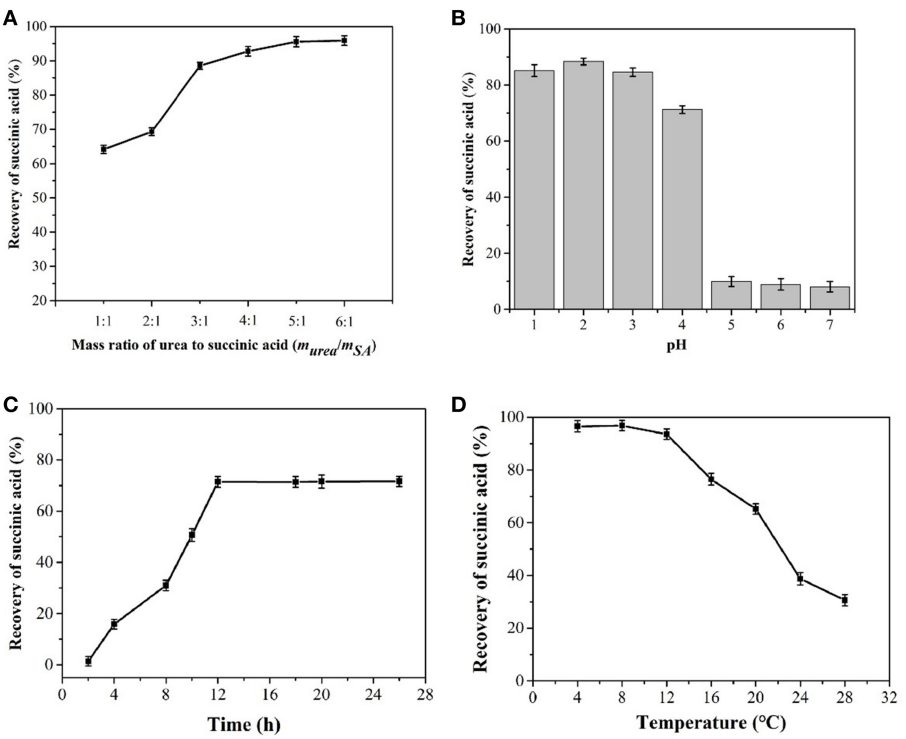

FIGURE 5 | Influence of the mass ratio of urea to succinic acid **(A)**, pH **(B)**, time **(C)**, and temperature **(D)** on co-crystallization process from fermentation broth after cooling crystallization.

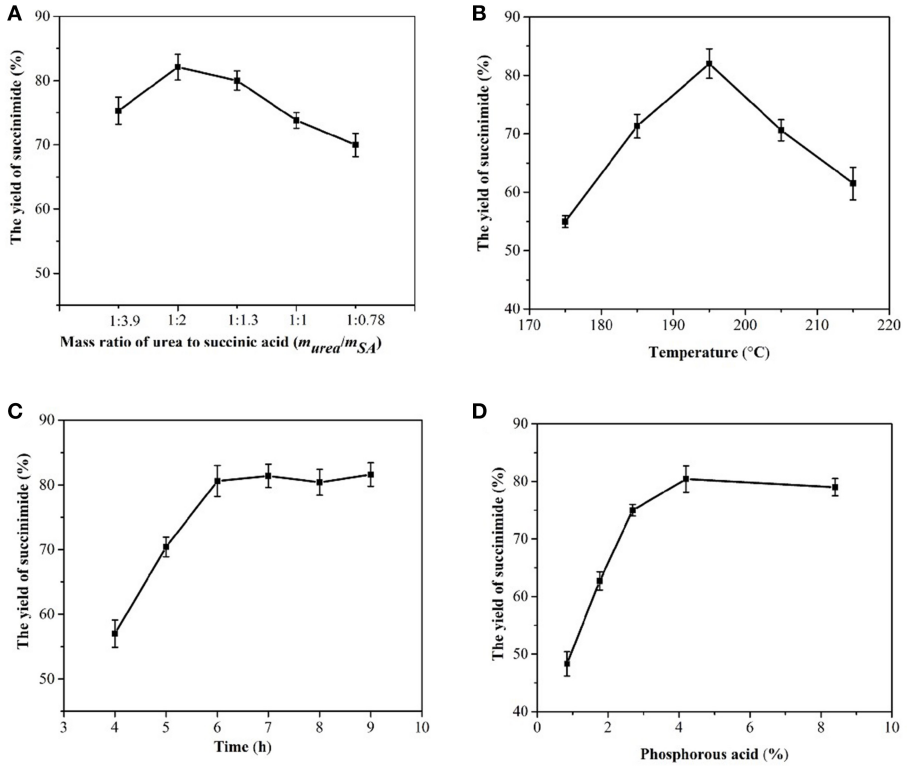

FIGURE 6 | Effects of the mass ratio of succinic acid to urea **(A)**, temperature **(B)**, time **(C)**, and phosphorous acid **(D)** on succinimide yield.

The maximum amount of succinimide was synthesized during a reaction period of 4-6 h (**Figure 6C**). Therefore, the optimal reaction time was determined to be 6 h, and the yield of succinimide was 80.6%.

Phosphorous acid can accelerate a reaction to reach its equilibrium and shorten the reaction time. In the reactions with 11.81 g of succinic acid and 3.07 g urea, 0.5 g phosphorous acid, e.g., 4.2% of the mass of succinic acid was found to be an appropriate addition to the reaction system (**Figure 6D**).

The yield of 80% succinimide was obtained by adjusting the mass ratio of succinic acid and urea to 2:1 using condensed succinic acid as a raw material, adding ∼4.2% solid phosphorite, stirring, heating to 195°C, and reacting at a constant temperature for 6 h. Succinimide standards and succinimide synthesized from succinic acid–urea samples were compared using UPLC. The results revealed that succinimide synthesis by succinic acid–urea co-crystallization was successful (**Figure 7**).

DISCUSSION

Using a simple process at a low cost, succinic acid was separated from a complex fermentation broth by cooling crystallization and urea co-crystallization, with a high rate of recovery. So far, other reports on crystallization have shown that cooling crystallization is usually combined with vacuum distillation, ion exchange adsorption, and salting-out extraction. Li et al. (2010) analyzed one-step crystallization and obtained yield and purity of 70% and 90%, respectively. Luque et al. (2009) applied direct vacuum distillation-crystallization, and obtained yield and purity of 75% and 97% for the simulated broth, respectively. In the present study, the yield and purity of succinic acid recovered from fermentation broth were 73.4% and 99%, respectively, which were the same as those obtained using one-step crystallization and direct vacuum distillation-crystallization, as stated above. However, the purity of succinic acid obtained using our newly defined method was better than that obtained through one-step crystallization and direct vacuum distillation-crystallization, even though the yields were almost the same. Vacuum distillation as a unit operation was required, but this process consumed high energy and the impurity of fermentation was also concentrated. Therefore, the high succinic acid titer of 106.17 g/L in this study could be helpful for crystallization.

The results obtained from other technologies are listed in **Table 1**. Sun et al. (2014) developed salting-out extraction combined with crystallization to recover succinic acid from simulated and actual fermentation broth. They obtained an identical total yield (65%) and a higher purity (97%) of succinic acid by using a synthetic fermentation broth rather than by using the actual fermentation broth (65 and 91%, respectively). Furthermore, Sun et al. (2019) also reported two other methods. One of these methods is sugaring-out

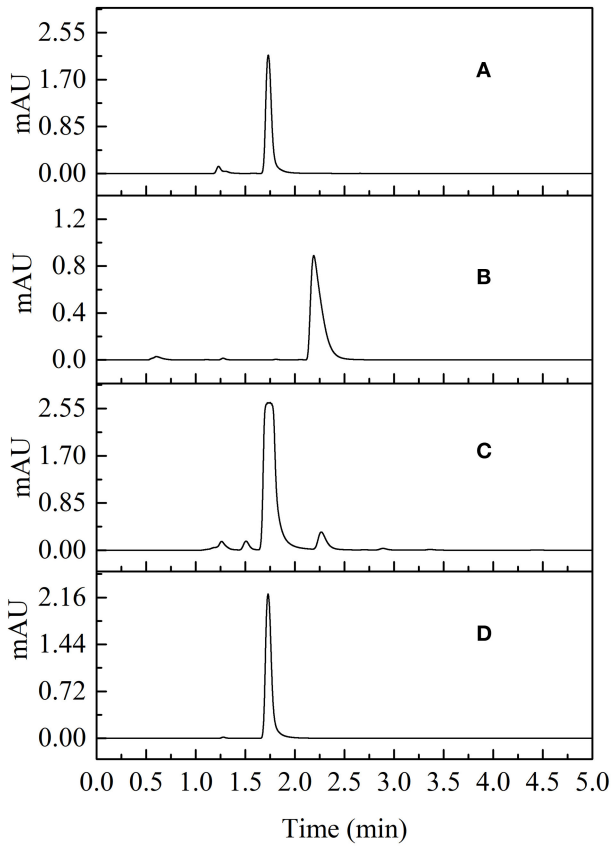

FIGURE 7 | Chromatographic comparisons of succinimide standards and succinimide synthesis from succinic acid-urea samples at 210 nm (**A** succinimide standard; **B** succinic acid-urea; **C** succinimide synthesis from succinic acid-urea; **D** recrystallization of succinimide synthesis from succinic acid-urea).

extraction combined with crystallization for the recovery of succinic acid with a total yield of 73% and a higher purity of 98%. However, a salt-assisted technique should be used for the sugaring-out extraction of succinic acid in a t-butanol/glucose system. The drawback of this method is the high energy consumption of cyclic t-butanol utilization via vacuum distillation. The other method is ionic liquid-based sugaring-out and salting-out extraction of succinic acid with a total yield of 75% for simulated fermentation broth and a total yield of 72% for actual fermentation broth (Sun et al., 2018). These types of extraction are, however, not achieved easily in industrial production settings because the ionic liquids are expensive and cyclic utilization is complex. Lin et al. (2010) reported used resin-based vacuum distillation-crystallization and obtained succinic acid at a purity of 99% and yield of 89.5%. Furthermore, Thuy et al. (2017) applied the seeded batch cooling crystallization after pretreatment via nanofiltration and obtained succinic acid with 99% purity and 93.5% yield from high seeding experiments.

Owing to the problems of low concentration and difficulty in recovering the remaining succinic acid from the fermentation broth after cooling crystallization, if concentrated, solvent extraction and ion exchange chromatography are used, high amounts of energy are consumed, and a great deal of wastewater is produced. Currently, research on co-crystallization is mainly focused on wastewater treatment to recover organic acids and crystalline products (Zhang et al., 2017). In this study, urea co-crystallization was used to separate succinic acid from the fermentation broth, which was achieved with a high yield, i.e., 92%.

Succinic acid must be subsequently separated from the co-crystallization of urea and succinic acid, which is a hard nut to crack. Succinic acid is usually extracted from the co-crystallization products with ether-based organic solvents and exchanged with resin. A considerable amount of energy is also required to recycle the organic solvent and water but high-value-added succinic acid derivatives, such as polybutylene succinate (Bechthold et al., 2008; Wang et al., 2014) and succinimide. According to previous reports, succinimide can be synthesized using succinic acid and urea or NH_3 as a raw material (Fischer et al., 2011; Liu et al., 2018). Succinimide synthesis occurs by controlling the initial ratio of succinic acid to urea from the co-crystalline product of urea. In this study, the synthesis of succinimide from succinic acid and urea was investigated and the appropriate mass ratio of succinic acid to urea, reaction temperature, reaction time, amount of catalyst (phosphorous acid) were determined. The optimum reaction mass ratio of succinic acid to urea was 2:1, the most suitable amount of added phosphorous acid was 4.2% of the mass of succinic acid, and the reaction performed best at 195°C for 6 h. Finally, high-purity succinimide was obtained by recrystallization.

Urea is widely used to design and synthesize solid structures and functional materials in crystal engineering and supermolecular chemistry (Alhalaweh et al., 2010). Urea and solvents can be recycled through rectification to reduce the damage caused by solvents to the environment. Methods of synthesis involve the use of biological products as starting materials, which cause little pollution. The residual fermentation broth is harmless to organisms during preparation, and a certain amount of residual succinic acid is present in the fermentation broth. As a result, urea can be used as a biological fertilizer in the fermentation broth to promote crop growth (Shi et al., 2019). CO_2 produced by synthesizing succinimide can be used for microbial cultivation in the pre-succinic acid fermentation (Wu et al., 2012).

CONCLUSIONS

An efficient and environment-friendly method was developed to produce succinimide from biomass-derived succinic acid through succinic acid–urea co-crystallization. This innovative strategy could reduce production costs, recycle materials, and protect the environment from the harmful chemicals used in a conventional succinic acid purification methods. Cooling crystallization was first applied to separate the decolorized fermentation broth. The optimal conditions for

TABLE 1 | Summary of succinic acid purification.

Method of downstream process of SA	Product	Purity (%)	Total yield (%)	Solution	Advantage	Drawbacks	References
Sugaring-out extraction combining crystallization	Succinic acid	98%	73%	Synthetic fermentation broth	Coupling with upstream fermentation technology	t-Butanol recovering by vacuum distillation and high energy consumption	Sun et al., 2019
Two-step membrane process	Succinic acid	85–99.5%	92%	Synthetic fermentation broth	–	–	Khunnonkwao et al., 2018
Ionic liquid-based sugaring-out and salting-out extraction	Succinic acid	– –	75%; 72%	Simulated fermentation broth; Actual fermentation broth	A sound basis for developing green, cost-effective strategies	Expensive Ionic liquids	Sun et al., 2018
Membrane separation and reactive extraction	Succinic acid	–	90%	Broth	–	Not selective enough to separate succinic acid from other acids in the broth	Prochaska et al., 2018
Pretreatment using nanofiltration Seeded batch cooling crystallization	Succinic acid	99.35%	93.47%	Fermentation broth	High purity and yield	Membrane pollution and high operation cost	Thuy et al., 2017
Salting-out extraction, vacuum distillation, crystallization, and drying; Salting-out extraction, vacuum distillation, activate carbon absorption, crystallization, and drying	Succinic acid	97%; 91%	65%; 65%	Synthetic fermentation broth; Actual fermentation broth	Low energy consumption and easy amplification	Low yield	Sun et al., 2014
Bipolar membrane electrodialysis	Succinic acid	–	90%	Synthetic broth	Suitable for continuous separation	High energy consumption, high membranes cost, and low succinate selectivity	Fu et al., 2014
Extraction	Succinic acid	–	78–85%	Fermentation broth	High output and low energy consumption	Requirement of broth pretreatment and expensive agents for reactive extraction	Kurzrock and Weuster-Botz, 2011
Centrifugation, filtration, resin-based vacuum distillation-crystallization	Succinic acid	99%	89.5%	Actual fermentation broths	High recovery yield	High energy consumption	Lin et al., 2010
One-step crystallization	Succinic acid	90%	70%	Fermentation broth	Simple process	Low succinic acid purity	Li et al., 2010
Direct vacuum distillation-crystallization	Succinic acid	97% 45%	75% 28%	Fermentation broth Synthetic broth	Easy operation and absence of additional reagents	Low succinate yield and purity, requirement of other unit operations	Luque et al., 2009
Traditional calcium precipitation coupled ion-exchange adsorption	Succinic acid	92%	52%	Fermentation broth	Easy scaling up and operation, low technical barriers, and low-priced precipitants	Water consumption, requirement of large quantities of precipitants, useless byproducts, and regeneration and cleaning of adsorbents	Li et al., 2009
Direct crystallization, co-crystallization with urea, and succinimide synthesis	Succinic acid Succinimide	99.0%	95% 80%	Fermentation broth	High Recovery, Simple Process, and low Cost	–	This study

cooling crystallization were determined to be 8°C, 4 h, and pH 2.0. Glucose and protein concentrations had no significant effect on the cooling crystallization process. The residue from cooling crystallization was further used for co-crystallization with urea, resulting in a recovery rate of >90% at 4°C for 12 h. This purification process was simple and cost effective. The succinimide yield could reach 80% by adjusting the mass ratio of succinic acid to urea to 2:1, adding ∼4.2% solid phosphorous acid, stirring, and heating the obtained solution to 195°C via a constant temperature reaction for 6 h. This process may be remarkably advantageous in preventing environmental pollution by utilizing succinic acid for value-added chemical production and reducing the dependency on petroleum-based chemical production. In conclusion, the method established in this study not only integrates the separation of succinic acid with the synthesis of succinimide but also produced valuable intermediate products that may increase the added value of the method by improving the separation efficiency and helping the system to meet environmental requirements.

DATA AVAILABILITY STATEMENT

All datasets generated for this study are included in the article/supplementary material.

AUTHOR CONTRIBUTIONS

YX designed and performed all experiments under the supervision of DZ, and developed the manuscript draft. JC and ZZ supervised studies on the crystallization and co-crystallization of succinic acid from fermentation broth. BG and YW analyzed the experimental data and discussed the results with the coauthors and revised this manuscript.

FUNDING

This research was supported by the National High Technology Research and Development Program of China (Grant No. 2012AA021205), the Foundation of Jiangxi Provincial Department of Education (No. GJJ180636), and Funds of Jiangxi Science and Technology Normal University (2017XJZD004).

REFERENCES

Akhtar, J., Idris, A., and Aziz, R. A. (2013). Recent advances in production of succinic acid from lignocellulosic biomass. *Appl. Microbiol. Biotechnol.* 98, 987–1000. doi: 10.1007/s00253-013-5319-6

Alexandri, M., Schneider, R., Papapostolou, H., Ladakis, D., Koutinas, A., and Venus, J. (2019). Restructuring the conventional sugar beet industry into a novel biorefinery: fractionation and bioconversion of sugar beet pulp into succinic acid and value-added coproducts. *ACS Sustain. Chem. Eng.* 7, 6569–6579. doi: 10.1021/acssuschemeng.8b04874

Alhalaweh, A., George, S., Boström, D., and Velaga, S. P. (2010). 1:1 and 2:1 urea-succinic acid cocrystals: structural diversity, solution chemistry, and thermodynamic stability. *Cryst. Growth Des.* 10, 4847–4855. doi: 10.1021/cg100823p

Antczak, J., Szczygiełda, M., and Prochaska, K. (2019). Nanofiltration separation of succinic acid from post fermentation broth: impact of process conditions and fouling analysis. *J. Ind. Eng. Chem.* 77, 253–261. doi: 10.1016/j.jiec.2019.04.046

Bechthold, I., Bretz, K., Kabasci, S., Kopitzky, R., and Springer, A. (2008). Succinic acid: a new platform chemical for biobased polymers from renewable resources. *Chem. Eng. Technol.* 31, 647–654. doi: 10.1002/ceat.200800063

Bradford, M. M. (1976). A rapid and sensitive method for the quantitation of microgram quantities of protein utilizing the principle of protein-dye binding. *Anal. Biochem.* 72, 248–254. doi: 10.1016/0003-2697(76)90527-3

Charville, H., Jackson, D., Hodges, G., and Whiting, A. (2010). The thermal and boron-catalysed direct amide formation reactions: mechanistically understudied yet important processes. *Chem. Commun.* 46, 1813–1823. doi: 10.1039/b923093a

Chen, C. X., Ding, S. P., Wang, D. Z., Li, Z. M., and Ye, Q. (2014). Simultaneous saccharification and fermentation of cassava to succinic acid by *Escherichia coli* NZN111. *Bioresour. Technol.* 163, 100–105. doi: 10.1016/j.biortech.2014.04.020

Cheng, K. K., Zhao, X. B., Zeng, J., Wu, R. C., Xu, Y. Z., and Liu, D. H., et al. (2012). Downstream processing of biotechnological produced succinic acid. *Appl. Microbiol. Biotechnol.* 95, 841–850. doi: 10.1007/s00253-012-4214-x

Cukalovic, A., and Stevens, C. V. (2008). Feasibility of production methods for succinic acid derivatives: a marriage of renewable resources and chemical technology. *Biofuels Bioprod. Bioref.* 2, 505–529. doi: 10.1002/bbb.105

Delhomme, C., Weuster-Botz, D., and Kühn, Fritz, E. (2009). Succinic acid from renewable resources as a C4 building-block chemical—a review of the catalytic possibilities in aqueous media. *Green Chem.* 11, 13–26. doi: 10.1039/B810684C

Deng, J., Zhang, Q. G., Pan, T., Xu, Q., Guo, Q. X., and Fu, Y. (2014). Synthesis of biobased succinimide from glutamic acid via silver-catalyzed decarboxylation. *RSC Adv.* 4, 27541–27544. doi: 10.1039/C4RA04567J

Dessie, W., Xin, F., Zhang, W., Jiang, Y., Wu, H., Ma, J., et al. (2018). Opportunities, challenges, and future perspectives of succinic acid production by *Actinobacillus succinogenes*. *Appl. Microbiol. Biotechnol.* 102, 9893–9910. doi: 10.1007/s00253-018-9379-5

Fischer, W., Klein, D., Künkel, A., Pinkos, R., and Scholten, E. (2011). *Method for Producing Pyrrolidones From Succinates From Fermentation Broths*. U. S. Patent No. 8, 017, 790. Washington, DC: U.S. Patent and Trademark Office.

Fu, L., Gao, X., Yang, Y., Aiyong, F., Hao, H., and Gao, C. (2014). Preparation of succinic acid using bipolar membrane electrodialysis. *Sep. Purif. Technol.* 127, 212–218. doi: 10.1016/j.seppur.2014.02.028

Gunnarsson, I. B., Karakashev, D., and Angelidaki, I. (2014). Succinic acid production by fermentation of Jerusalem artichoke tuber hydrolysate with *Actinobacillus succinogenes* 130Z. *Ind. Crop. Prod.* 62, 125–129. doi: 10.1016/j.indcrop.2014.08.023

Hong, U. G., Park, H. W., Lee, J., Hwang, S., and Song, I. K. (2012a). Hydrogenation of succinic acid to γ-butyrolactone (GBL) over ruthenium catalyst supported on surfactant-templated mesoporous carbon. *J. Ind. Eng. Chem.* 18, 462–468. doi: 10.1016/j.jiec.2011.11.054

Hong, U. G., Park, H. W., Lee, J., Hwang, S., Yi, J., and Song, I. K. (2012b). Hydrogenation of succinic acid to tetrahydrofuran (THF) over rhenium catalyst supported on H_2SO_4-treated mesoporous carbon. *Appl. Catal. A Gen.* 415–416, 141–148. doi: 10.1016/j.apcata.2011.12.022

Jansen, M. L., and van Gulik, W. M. (2014). Towards large scale fermentative production of succinic acid. *Curr. Opin. Biotechnol.* 30, 190–197. doi: 10.1016/j.copbio.2014.07.003

Khunnonkwao, P., Jantama, K., Kanchanatawee, S., Galier, S., and Roux-de Balmann, H. (2018). A two steps membrane process for the recovery of succinic acid from fermentation broth. *Sep. Purif. Technol.* 207, 451–460. doi: 10.1016/j.seppur.2018.06.056

Kolah, A. K., Asthana, N. S., Vu, D. T., Lira, C. T., and Miller, D. J. (2008). Reaction kinetics for the heterogeneously catalyzed esterification of succinic acid with ethanol. *Ind. Eng. Chem. Res.* 47, 5313–5317. doi: 10.1021/ie0706616

Kurzrock, T., and Weuster-Botz, D. (2011). New reactive extraction systems for separation of bio-succinic acid. *Bioprocess Biosyst. Eng.* 34, 779–787. doi: 10.1007/s00449-011-0526-y

Lee, P. C., Lee, W. G., Lee, S. Y., and Chang, H. N. (2015). Succinic acid production with reduced by-product formation in the fermentation of *Anaerobiospirillum succiniciproducens* using glycerol as a carbon source. *Biotechnol. Bioeng.* 72, 41–48. doi: 10.1002/1097-0290(20010105)72:1;41::AID-BIT6;3.0.CO;2-N

Li, Q., Wang, D., Wu, Y., Li, W., Zhang, Y., Xing, J., et al. (2010). One step recovery of succinic acid from fermentation broths by crystallization. *Sep. Purif. Technol.* 72, 294–300. doi: 10.1016/j.seppur.2010.02.021

Li, Q., Xing, J., Li, W., Liu, Q., and Su, Z. (2009). Separation of succinic acid from fermentation broth using weak alkaline anion exchange adsorbents. *Ind. Eng. Chem. Res.* 48, 3595–3599. doi: 10.1021/ie801304k

Lin, S. K. C., Du, C., Blaga, A. C., Camarut, M., Webb, C., Stevens, C. V., et al. (2010). Novel resin-based vacuum distillation-crystallisation method for recovery of succinic acid crystals from fermentation broths. *Green Chem.* 12, 666–671. doi: 10.1039/b913021g

Liu, Y., Fu, J., Ren, D., Song, Z., Jin, F., and Huo, Z. (2018). Efficient synthesis of succinimide from succinic anhydride in water over unsupported nanoporous nickel material. *Chem. Select.* 3, 724–728. doi: 10.1002/slct.201703154

López-Garzón, C. S., Ottens, M., van der Wielen, L. A., and Straathof, A. J. (2012). Direct downstream catalysis: from succinate to its diethyl ester without intermediate acidification. *Chem. Eng. J.* 200, 637–644. doi: 10.1016/j.cej.2012.06.079

López-Garzón, C. S., and Straathof, A. J. (2014). Recovery of carboxylic acids produced by fermentation. *Biotechnol. Adv.* 32, 873–904. doi: 10.1016/j.biotechadv.2014.04.002

Luque, R., Lin, C. S., Du, C., Macquarrie, D. J., Koutinas, A., and Wang, R., et al. (2009). Chemical transformations of succinic acid recovered from fermentation broths by a novel direct vacuum distillation-crystallisation method. *Green Chem.* 11, 193–200. doi: 10.1039/B813409J

Matsumoto, M., and Tatsumi, M. (2018). Extraction and esterification of succinic acid using aqueous two-phase systems composed of ethanol and salts. *Solvent Extr. Res. Dev.* 25, 101–107. doi: 10.15261/serdj.25.101.

Orjuela, A., Kolah, A., Hong, X., Lira, C. T., and Miller, D. J. (2012). Diethyl succinate synthesis by reactive distillation. *Sep. Purif. Technol.* 88, 151–162. doi: 10.1016/j.seppur.2011.11.033

Pavelka, M., and Grmela, M. (2019). Braun-Le Chatelier principle in dissipative thermodynamics. *Atti Accad. Pelorit. Pericol. Cl. Sci. Fis. Mat. Nat.* 97:22. doi: 10.1478/AAPP.97S1A22

Pinazo, J. M., Domine, M. E., Parvulescu, V., and Petru, F. (2015). Sustainability metrics for succinic acid production: a comparison between biomass-based and petrochemical routes. *Catal. Today* 239, 17–24. doi: 10.1016/j.cattod.2014.05.035

Prochaska, K., Antczak, J., Regel-Rosocka, M., and Szczygiełda, M. (2018). Removal of succinic acid from fermentation broth by multistage process (membrane separation and reactive extraction). *Sep. Purif. Technol.* 192, 360–368. doi: 10.1016/j.seppur.2017.10.043

Sheldon, R. A., and Sanders, J. P. (2015). Toward concise metrics for the production of chemicals from renewable biomass. *Catal. Today* 239, 3–6. doi: 10.1016/j.cattod.2014.03.032

Shi, W., Ju, Y., Bian, R., Li, L., Joseph, S., and Mitchell, D. R. (2019). Biochar bound urea boosts plant growth and reduces nitrogen leaching. *Sci. Total Environ.* 2019:134424. doi: 10.1016/j.scitotenv.2019.134424

Sun, Y., Yan, L., Fu, H., and Xiu, Z. (2014). Salting-out extraction and crystallization of succinic acid from fermentation broths. *Process Biochem.* 49, 506–511. doi: 10.1016/j.procbio.2013.12.016

Sun, Y., Zhang, S., Zhang, X., Zheng, Y., and Xiu, Z. (2018). Ionic liquid-based sugaring-out and salting-out extraction of succinic acid. *Sep. Purif. Technol.* 204, 133–140. doi: 10.1016/j.seppur.2018.04.064

Sun, Y., Zhang, X., Zheng, Y., Yan, L., and Xiu, Z. (2019). Sugaring-out extraction combining crystallization for recovery of succinic acid. *Sep. Purif. Technol.* 209, 972–983. doi: 10.1016/j.seppur.2018.09.049

Thuy, N. T. H., Kongkaew, A., Flood, A., and Boontawan, A. (2017). Fermentation and crystallization of succinic acid from *Actinobacillus succinogenes* ATCC55618 using fresh cassava root as the main substrate. *Bioresour. Technol.* 233, 342–352. doi: 10.1016/j.biortech.2017.02.114

Wang, C., Ming, W., Yan, D., Zhang, C., Yang, M., and Liu, Y., et al. (2014). Novel membrane-based biotechnological alternative process for succinic acid production and chemical synthesis of bio-based poly (butylene succinate). *Bioresour. Technol.* 156, 6–13. doi: 10.1016/j.biortech.2013.12.043

Wu, H., Li, Q., Li, Z. M., and Ye, Q. (2012). Succinic acid production and CO_2 fixation using a metabolically engineered *Escherichia coli* in a bioreactor equipped with a self-inducing agitator. *Bioresour. Technol.* 107, 376–384. doi: 10.1016/j.biortech.2011.12.043

Zhang, T., Yu, Q., Li, X., and Ma, X. (2017). Preparation of 2: 1 urea-succinic acid cocrystals by sublimation. *J. Cryst. Growth* 469, 114–118. doi: 10.1016/j.jcrysgro.2016.09.025

Zhang, W., Zhang, T., Song, M., Dai, Z., Zhang, S., and Xin, F. (2018). Metabolic engineering of *Escherichia coli* for high yield production of succinic acid driven by methanol. *ACS Synth. Biol.* 7, 2803–2811. doi: 10.1021/acssynbio.8b00109

Conflict of Interest: The authors declare that the research was conducted in the absence of any commercial or financial relationships that could be construed as a potential conflict of interest.

frontiers in Bioengineering and Biotechnology

REVIEW
published: 19 February 2020
doi: 10.3389/fbioe.2020.00098

Transcription Factor Engineering for High-Throughput Strain Evolution and Organic Acid Bioproduction: A Review

*Jia-Wei Li, Xiao-Yan Zhang, Hui Wu and Yun-Peng Bai**

State Key Laboratory of Bioreactor Engineering, East China University of Science and Technology, Shanghai, China

Metabolic regulation of gene expression for the microbial production of fine chemicals, such as organic acids, is an important research topic in post-genomic metabolic engineering. In particular, the ability of transcription factors (TFs) to respond precisely in time and space to various small molecules, signals and stimuli from the internal and external environment is essential for metabolic pathway engineering and strain development. As a key component, TFs are used to construct many biosensors *in vivo* using synthetic biology methods, which can be used to monitor the concentration of intracellular metabolites in organic acid production that would otherwise remain "invisible" within the intracellular environment. TF-based biosensors also provide a high-throughput screening method for rapid strain evolution. Furthermore, TFs are important global regulators that control the expression levels of key enzymes in organic acid biosynthesis pathways, therefore determining the outcome of metabolic networks. Here we review recent advances in TF identification, engineering, and applications for metabolic engineering, with an emphasis on metabolite monitoring and high-throughput strain evolution for the organic acid bioproduction.

Keywords: transcription factor, biosensor, metabolic engineering, synthetic biology, organic acid, high-throughput screening

OPEN ACCESS

Edited by:
Xiao-Jun Ji,
Nanjing Tech University, China

Reviewed by:
Zongjie Dai,
Chalmers University of Technology, Sweden
Xiulai Chen,
Jiangnan University, China

***Correspondence:**
Yun-Peng Bai
ybai@ecust.edu.cn

Specialty section:
This article was submitted to Industrial Biotechnology, a section of the journal Frontiers in Bioengineering and Biotechnology

Received: *30 October 2019*
Accepted: *03 February 2020*
Published: *19 February 2020*

Citation:
Li J-W, Zhang X-Y, Wu H and Bai Y-P (2020) Transcription Factor Engineering for High-Throughput Strain Evolution and Organic Acid Bioproduction: A Review. Front. Bioeng. Biotechnol. 8:98. doi: 10.3389/fbioe.2020.00098

INTRODUCTION

In nature, transcription factors (TFs) control the rate of gene transcription by recognizing specific DNA sequences, thus regulating expression of the genome. In addition to the normal biological and physiological roles that TFs play in human cells, they can be used as building blocks and regulatory tools in metabolic engineering and synthetic biology (Yadav et al., 2012; Shi et al., 2018; Yang et al., 2019). For example, in one study 55 TFs and 750 metabolic genes were used to construct a regulatory network for controlling metabolism in *Saccharomyces cerevisiae* (*S. cerevisiae*) (Herrgård et al., 2006). There are a wide range of TFs available from diverse microbes, and TF engineering is a very flexible approach, which makes TFs a particularly useful resource for biotechnology. Functional screening is used to identify novel TFs that can then be engineered in host cells to control the expression of key enzymes in biosynthetic gene clusters (BGCs) (Liu et al., 2013). In past decades, researchers have designed and optimized many biosynthetic pathways for natural products (Yadav et al., 2012), such as artemisinin (Paddon and Keasling, 2014). When constructing such pathways, over-expressing positive regulators or knocking down/out negative

regulators are two important ways of activating BGCs (Xie et al., 2015; Thanapipatsiri et al., 2016). As an example, over-expressing the global TF AdpA in *Streptomyces hygroscopicus* enhances gene cluster transcription and antibiotic synthesis (Tan et al., 2013). Novel genomic editing and protein engineering tools have been applied to synthesize target products via TF-mediated activation of silent BGCs (Tong et al., 2015; Zhang et al., 2017; Grau et al., 2018). Because TFs are sensitive to their corresponding signal molecules, they can also be used to construct highly sensitive biosensors for use in high-throughput screening for improved strains (Yu et al., 2019). Protein engineering can be used to alter the ligand specificity of TFs such that they can detect new signaling molecules (Machado et al., 2019), furthering expanding their applications in metabolic engineering.

With the rapid development of bioinformatics and genomic editing tools, TFs are playing more important roles in improving the microbial production of valuable chemicals. In this paper, we will briefly review recent advances in the use of microbial TFs to regulate metabolic production of valuable chemical products, with a particular focus on the production of organic acids. We will also summarize strategies for identifying new TFs and review the use of TFs as biosensors for monitoring metabolites *in vivo* and performing high-throughput screening for overproducers, which are important methods used to obtain a strain with the desired phenotype from a library of mutants containing a wide variety of genomic alterations.

METHODS FOR IDENTIFYING TFs

Transcription factors are sequence-specific DNA-binding proteins that bind to promoters to either activate or repress transcription (**Figure 1**). So far, TFs in prokaryotes can be grouped into a dozen families identified on the basis of sequence analysis, with the LacI, AraC, LysR, CRP, TetR, and OmpR families being characterized best (Browning and Busby, 2004). New TFs continue to be identified by experimental methods such as transcriptome analysis (Raghavan et al., 2019), one-hybrid assays (Reece-Hoyes and Walhout, 2012), electrophoretic mobility shift assay (EMSA, Hellman and Fried, 2007), DNA affinity purification-mass spectrometry (AP-MS, Tacheny et al., 2013), and protein microarrays (Hu et al., 2009).

In general, TFs have a DNA-binding domain (DBD) and a regulatory domain (RD). Knowledge of binding sites, ligand-protein interaction and binding affinity can help identify an unknown DNA-binding protein. DBDs have been widely characterized both experimentally and bioinformatically, so today, most newly discovered and putative TFs can be identified and grouped by sequence homology to a previously characterized DBD. Now, information on the DBD structures in complex with DNA can be found in the Protein Data Bank[1]. Bacterial TF binding sites and related information are also available in some open databases such as CollecTF (Kilic et al., 2014). RD, also called "effector binding domain," performs many tasks including ligand binding, protein-protein interactions and modulating the DNA-binding affinity of TFs. The diversity, abundance and structure variability of RD have been identified and investigated systematically for transcription regulation (Perez-Rueda et al., 2018; Sanchez et al., 2020). In particular, the high variability of RDs and recognition promiscuity may have evolutionary implications that they can be targeted for engineering to change the ligand specificity and/or improve the sensing dynamics.

[1]https://www.rcsb.org

USING TFs AS BIOSENSORS IN METABOLIC ENGINEERING

Monitoring Metabolites *in vivo*

Due to the inherent complexity of biological systems, it is desirable to quantitatively or semi-quantitatively evaluate metabolites of interest *in vivo*. By binding metabolites of interest, TFs can either activate the expression of reporter genes in a genetic circuit as an activator (**Figure 2A**), or induce the downstream gene expression by reducing the repression of RNA polymerase-promoter binding (**Figure 2B**), resulting in a detectable signal that can be easily assayed (Dietrich et al., 2010; Mahr and Frunzke, 2016; D'Ambrosio and Jensen, 2017; Liu Y. et al., 2017). TFs can be used to detect small molecules, ion accumulation, and changes in physiological parameters. A wide variety of TF-based biosensors have been constructed and characterized that recognize different small molecules, including but not limited to glutarate (Thompson et al., 2019), 3-hydroxypropionic acid (Rogers and Church, 2016; Seok et al., 2018; Nguyen et al., 2019), itaconic acid (Hanko et al., 2018), flavonoids (Siedler et al., 2014a; Trabelsi et al., 2018), anhydrotetracycline (Lutz and Bujard, 1997), arabinose (Lee and Keasling, 2006), lactam (Zhang et al., 2016), mevalonate (Tang and Cirino, 2011), L-methionine (Mustafi et al., 2012), amino acids (Binder et al., 2012; Mustafi et al., 2012; Leavitt et al., 2016), acrylic acid (Raghavan et al., 2019), isoprene (Kim et al., 2018), shikimate (Liu C. et al., 2017), and aromatic compounds (Willardson et al., 1998; Kim et al., 2005; Jha et al., 2016). Some typical biosensors with sensing kinetics are listed in **Table 1**.

Although wild-type TFs are sensitive to their corresponding metabolites, they have narrow dynamic ranges, which limits their practical applications. Thus, TFs are often engineered to increase their dynamic ranges (**Figure 2C**). LuxR, a TF that is involved in quorum sensing in many bacteria, has been engineered to respond to butanoyl-homoserine lactone at concentrations as low as 10 nM (Hawkins et al., 2007). Structural analysis and site-directed mutagenesis were used to engineer a BmoR mutant that has a wider detection range (0–100 mM) for intracellular isobutanol than the wild-type protein (Yu et al., 2019). Promoter binding sites can also influence the dynamic range of TFs. The maximum dynamic range of a bacterial TF-based biosensor in *S. cerevisiae* was expanded by modifying promoter sequences (Dabirian et al., 2019a). Leavitt et al. (2016) engineered both wild-type TFs and promoters involved in aromatic amino acid induction and regulation in S. cerevisiae to obtain a transcriptional output 15-fold greater than the off-state. Similarly, TyrR, a TF that is activated in response to increased intracellular L-Phe concentrations in *E. coli*, exhibited higher

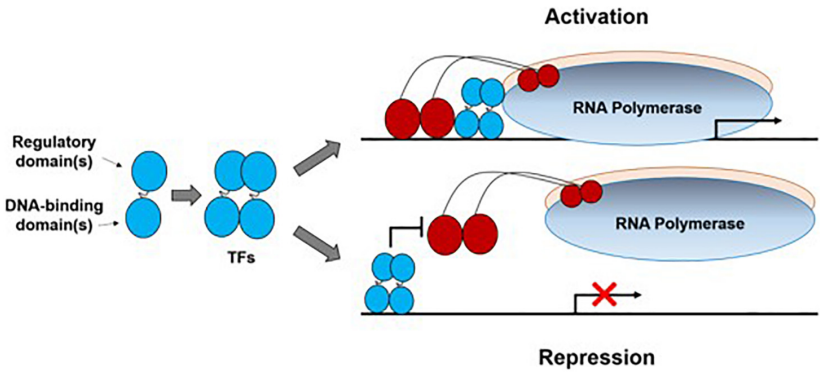

FIGURE 1 | Illustration of bacterial transcription factors (TFs). A transcription factor subunit (denoted as a dumbbell shape) usually contains a regulatory domain and a DNA-binding domain. Normally two subunits dimerize to form a TF which interacts with a bacterial promoter region to either activate or repress transcription initiation. Here, only one activation mode (TF contacts domain 4 of the RNA polymerase σ subunit) and one repression mode (via steric hindrance) were shown to illustrate this process.

sensitivity when combined with optimized promoters, with a dynamic range up to 15 times greater than when it was used in a strain with wild-type promoter sequences (Liu Y.F. et al., 2017).

In addition to naturally occurring metabolite-responsive biosensors, there are many metabolites for which a natural TF does not exist, or for which the detection limit is too high. To address this problem, a known TF, such as PcaV (Machado et al., 2019), can be engineered by directed evolution to expand is sensing profile (**Figure 2D**). Another example is the switch in the effector specificity of an *L*-arabinose-responsive TF, AraC, which was modified by molecular evolution to respond to D-arabinose concentrations as low as 1 mM (Tang et al., 2008). Biosensor engineering by random domain insertion (BERDI) is another technique that can be used to generate new metabolite-responsive TFs. In this case, *in vitro* transposon-mediated mutagenesis was used to construct a TF library, followed by fluorescence-activated cell sorting (FACS) to isolate functional biosensors (Younger et al., 2017). Recently, MphR was found to bind promiscuously to macrolides, and was then engineered to improve its sensitivity, specificity, and selectivity for these small molecules (Kasey et al., 2017). The tailored MphR biosensors provide a useful means of screening key enzymes involved in complex macrolide biosynthesis, demonstrating the power of protein engineering in creating new metabolite-responsive TFs. Similarly, an *Acinetobacter* TF, PobR, was engineered to switch its specificity from the native effector 4-hydroxybenzoate to p-nitrophenol (pNP) (Jha et al., 2016). Given the significant similarity between the two effectors, the high specificity of this engineered TF for pNP (detection limit of 2 μM) demonstrates the importance of engineering TFs by directed evolution.

TF-Biosensor Based Strain Screening

Since only a few metabolites are natural chromophores or fluorophores, high-throughput screening (HTS) methods are needed to identify engineered microorganisms that produce the desired products. The application of TF-based biosensors to high-throughput screening has recently been reviewed in detail (Bott, 2015; Mahr and Frunzke, 2016; Cheng et al., 2018). Here, we focus on combining random genomic mutation with high-throughput screening to obtain high-yield strains. Cells contain sophisticated metabolic networks, which can make it challenging to rationally engineer metabolic pathways that produce large amounts of target compounds. Although genomic editing tools enable the rapid and precise tuning of gene expression, our ability to rewire cellular metabolism is still limited (Yadav et al., 2012). Therefore, genome-wide approaches for introducing random mutations, followed by high-throughput screening, provide an efficient way to evolve strains (**Figure 2E**). Chou and Keasling (2013) developed a feedback-controlled system that contains different TFs for sensing isopentenyl diphosphate in bacteria and yeast. Several rounds of adaptive laboratory evolution (ALE) resulted in a strain that produces more tyrosine and isoprenoid than the original strain (Chou and Keasling, 2013). Recently, a cooperative two-factor ALE was developed to enhance lipid production in *Schizochytrium sp.* by 57.5% relative to the parent strain after 30 adaption cycles (Sun et al., 2018).

Transcription factor-based biosensors turn a chemical input, which normally does not have an observable phenotype, into a detectable output, such as fluorescence, which can be easily coupled to FACS, an ultra-throughput method capable of screening of more than 50,000 cells per second, thereby greatly accelerating the optimization of production strains. The power of TF sensor–based FACS screening is clear. For example, using an L-lysine sensor, a library of 10 million mutated *E. coli* cells was screened by FACS in 30 min (Wang Y. et al., 2016). The best mutant was selected and evaluated in a 5-L fermenter within 2 weeks after one round of HTS, which is 10^4–10^5 times faster than traditional selection methods. The number of studies that have applied this strategy is increasing rapidly (Binder et al., 2012, 2013; Mustafi et al., 2012; Siedler et al., 2014b, 2017; Jha et al., 2016; Wang Y. et al., 2016; Liu Y.F. et al., 2017; Schulte et al., 2017; Flachbart et al., 2019; Kortmann et al., 2019). In practice, cross-talk between cells should be noted, as it may lead to false positive results, decreasing the screening efficiency; this can be

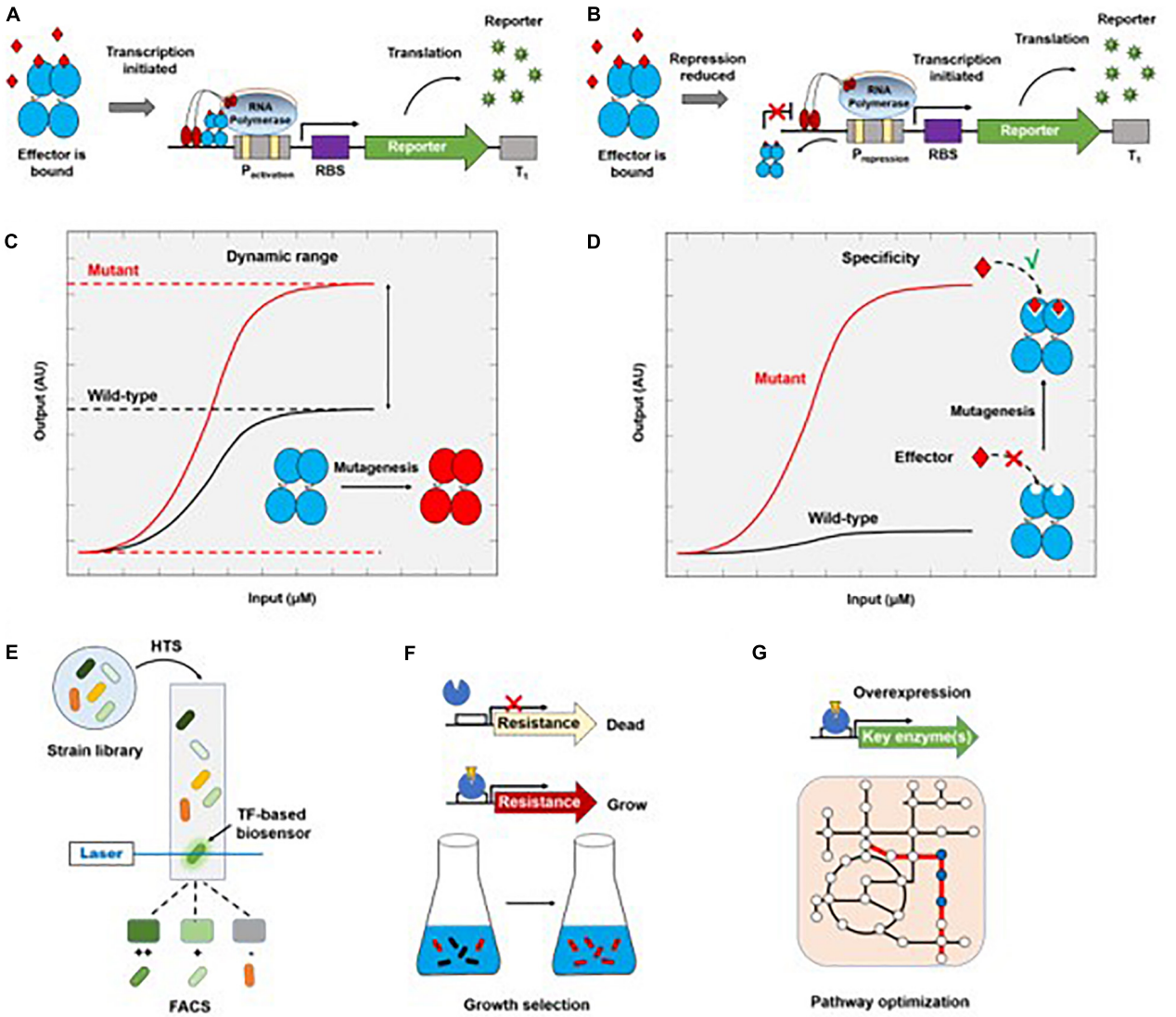

FIGURE 2 | Genetically encoded TF-based biosensors and their applications in metabolic engineering. Metabolic molecules can be transformed into a detectable reporter molecule through the initiation of reporter transcription by an activator **(A)** or a repressor **(B)**. The correlation between input (product concentration) and output (AU, arbitrary reporter units) provides the dynamic range **(C)** and ligand specificity of transfer function **(D)**. The wild-type TFs can be engineered so that the mutant can have a higher dynamic range **(C)** or sense a new type of molecule **(D)**. TF-based biosensors can be coupled to HTS methods such as FACS **(E)** or to growth **(F)** for screening overproducers. TFs can also be engineered to optimize biosynthetic pathways of target products **(G)**.

minimized by optimizing expression and cultivation conditions (Flachbart et al., 2019).

In contrast to the use of fluorescence-coupled biosensors, growth-coupled screening is a high-throughput method that can be performed without expensive equipment (**Figure 2F**; Dietrich et al., 2010). Lee and Oh (2015) developed a suicide riboswitch, *glmS*, for the high-throughput screening of metabolites in *S. cerevisiae*. Growth of the strain harboring the suicide riboswitch was restored when the level of the metabolite of interest level increased. An N-acetyl glucosamine producer strain was isolated after screening. Liu S.D. et al. (2017) coupled the microbial production of L-tryptophan (L-Trp) to cell growth with maltose as the sole carbon source. The selection of mutated producers led to a strain with up to 65% increased L-Trp production. An approach combining growth recovery with a fluorescent reporter protein has also been developed for enzyme-directed evolution (Michener and Smolke, 2012).

TF ENGINEERING FOR THE MICROBIAL PRODUCTION OF ORGANIC ACIDS

Organic acids and their derivatives have a wide range of industrial applications, and can be used as food additives, pharmaceuticals, antimicrobial agents, biomaterials, biofuels,

TABLE 1 | Overview of some TF-based biosensors with sensing kinetics.

Host chassis	TFs	Analyte	Detection range	Reporter	References
E. coli	LuxR	Butanoyl-homoserine lactone	10 nM-1 μm	GFP	Hawkins et al., 2007
E. coli XL1-Blue	BmoR	Isobutanol	0–100 mM	GFP	Yu et al., 2019
Saccharomyces cerevisiae	FapR	Glucose	95-fold to 2.4-fold	GFP	Dabirian et al., 2019a
E. coli	AraC	D-Arabinose	100 mM	GFP	Tang et al., 2008
E. coli	PobR	p-Nitrophenol	<2 μM	GFP	Jha et al., 2016
Pseudomonas putida	GcdR	Glutarate	2.5 mM	RFP	Thompson et al., 2019
E. coli	HucR	Shikimic Acid	3–20 mM	RFP	Li et al., 2017
E. coli	LysR	3-Hydroxypropionic acid	0.01–100 mM	GFP	Seok et al., 2018
E. coli	YpItcR	Itaconic acid	0.07–0.7 nM	RFP	Hanko et al., 2018
E. coli DH5	FdeR	Naringenin	100 μM	RFP	Trabelsi et al., 2018
E. coli DH10B	ChnR	Lactams	3–12.5 mM	RFP	Zhang et al., 2016
E. coli	AraC	Mevalonate	<1 mM	GFP	Tang and Cirino, 2011
E. coli	Lrp	L-Methionine	>0.2–23.5 mM	eYFP	Mustafi et al., 2012
E. coli	LysR	L-Lysine	<5 mM	eYFP	Binder et al., 2012
E. coli	PyHCN	Acrylic acid	500 μM	eGFP	Raghavan et al., 2019
E. coli	TbuT	Isoprene	0.1 mM	eGFP	Kim et al., 2018
Corynebacterium glutamicum	LysR	Shikimic acid	19.5–120.9 mM	eGFP	Liu C. et al., 2017

TABLE 2 | Strain evolution for the enhanced production of organic acids.

Host chassis	TF	Screening/ Analysis	Method	Product	Enhancement	References
E. coli	LysR	Growth selection	Enzyme directed evolution	3-HP	2.79-fold in catalytic efficiency of α-ketoglutaric semialdehyde dehydrogenase	Seok et al., 2018
E. coli	SoxR	FACS	Genome-wide mutagenesis by CRISPR	3-HP	7- and 8-fold increase in productivity	Liu et al., 2018
E. coli	PyHCN	FACS	Enzyme directed evolution	Acrylic acid	50% increase in catalytic efficiency of an amidase	Raghavan et al., 2019
E. coli JM109	HIF-1	HPLC	TF engineering	Pyruvic acid	Titer increased to 53.1 g/L	Luo et al., 2020
E. coli	LysR	HPLC	TF engineering	Itaconic acid	215-fold in itaconic acid detection	Hanko et al., 2018
E. coli	ARO1	FACS	Combined ALE and metabolic engineering	Muconic acid	Titer increased to 2.1 g/L	Leavitt et al., 2017
Corynebacterium glutamicum	ShiR	FACS	RBS engineering	Shikimic acid	Titer increased to 3.72 mM	Liu C. et al., 2017
E. coli	pfkA	HPLC	Dynamic control of metabolic fluxes	D-Glucaric acid	Titer improved by up to 42%	Reizman et al., 2015
E. coli	acuR/prpR	FACS	Design–build–test cycle	3-HP	Titer increased to 4.2 g/L	Rogers and Church, 2016
S. cerevisiae	FadR	FACS	Gene library	Fatty acid	30% increased fatty acid level observed	Dabirian et al., 2019b

and more (reviewed in Chen and Nielsen, 2016; Liu J.J. et al., 2017). Due to recent concerns about climate change and limited fossil reserves, the use of renewable biomass for the biological production of fuels and chemicals has received increasing attention as an alternative to chemical production (Sarria et al., 2017). Large-scale production using microorganisms requires the development of HTS tools for strain engineering and techniques for analyzing strain performance and the efficiency of biological processes. Many TF-based biosensors for measuring the intracellular concentrations of organic acids are currently available (Sint Fiet et al., 2006; Uchiyama and Miyazaki, 2010; Dietrich et al., 2013; Tang et al., 2013; Raman et al., 2014; Chen et al., 2015; Zhou et al., 2015; Leavitt et al., 2017; Liu C. et al., 2017; Hanko et al., 2018; Nguyen et al., 2019; Raghavan et al., 2019; Thompson et al., 2019) that provide a HTS method when combined with FACS. Alternatively, TFs can activate or repress the expression of target genes, which can be used to rewire microbial metabolic pathways, thus leading to an increase in the production of organic acids (**Figure 2G**). Compared with HTS-based strain evolution, engineering TFs for pathway reconstruction requires extensive knowledge of cellular metabolic machinery. Here, we discuss some recent examples of studies that have improved organic acid production using the above two strategies, with an emphasis on the role TFs play in this process (**Table 2**).

3-Hydroxypropionic Acid (3-HP)

3-Hydroxypropionic acid is a platform molecule for the production of 3-carbon chemicals; in particular, it can easily be converted to acrylic acid upon dehydration. However, it is difficult to detect intracellular 3-HP. To address this problem, Rogers and co-workers developed a system that uses the TF CdaR to generate a fluorescent readout in proportion to the intracellular concentration of a target metabolite (Rogers and Church, 2016). Using this sensor, the authors were able to identify a strain that produced 4.2 g/L 3-HP, a level that is 23-fold higher than any previously reported. Liu et al. (2018) introduced genome-wide mutations to target 30 genes including a TF SoxR that plays important roles in genome-level transcription. The mutant $SoxR_{S26G,E32V}$ conferred high furfural and acetate resistance to the engineered strain, leading to a 7- and 8-fold increase in 3-HP productivity relative to the parent strain under high furfural and high acetate hydrolyzate fermentation, respectively, demonstrating the importance of the TF-mediated global regulation of gene expression.

Acrylic Acid (AA)

As mentioned above, AA biosynthesis via enzymatic dehydration of 3-HP has been demonstrated in engineered *E. coli* (Chu et al., 2015; Liu and Liu, 2016). However, the yields are low, which led Raghavan et al. (2019) to apply HTS to identify strains the exhibited greater activity of key enzymes in the AA synthesis pathway. By identifying *E. coli* genes that were selectively up-regulated in the presence of AA, this group found that the gene *yhcN* encodes a protein that can respond specifically to AA at low concentrations when it was coupled to an eGFP reporter (Raghavan et al., 2019). This biosensor was used to find an amidase variant that converted acrylamide to AA with 1.6-fold improvement in catalytic efficiency, which is important to enhance AA production.

Pyruvic Acid (PA)

Pyruvic acid is widely used as additive in food and cosmetics, and as a starting material for the biosynthesis of pharmaceuticals such as L-tyrosine and (*R*)-phenylacetylcarbinol (Song et al., 2016). Currently, the microbial production of PA from renewable biomass requires high levels of dissolved oxygen (DO). To remove this restriction, hypoxia-inducible factor 1 (H1F-1) was engineered to increase the transcription of key enzymes involved in PA synthesis under low DO levels (Luo et al., 2020). The stability of H1F1 was further optimized, resulting in a titer of 53.1 g/L for PA production in a 5-L bioreactor under 10% DO.

Itaconic Acid (IA)

As an unsaturated 5-carbon dicarboxylic acid, IA is a useful monomer for constructing synthetic polymers. IA can also be used as a precursor for the production of high-value chemicals (Thakker et al., 2015). Variants of a number of microorganisms, such as *Aspergillus terreus*, *E. coli*, and *S. cerevisiae*, have been developed that produce IA. To further improve production titers, it is important to be able to quantify intracellular levels of IA. Recently, Hanko et al. (2018) reported the development of the first IA biosensor based on identifying LysR-type TFs and their promoters in *Yersinia pseudotuberculosis* and *Pseudomonas aeruginosa*. The *Yp*ItcR/P_{ccl} inducible system was used in *E. coli* to identify the optimum expression level of a key enzyme in the IA synthesis pathway. The dynamic range was 5–100 μM, which could be improved further by protein engineering. This biosensor displayed the potential to facilitate improved IA biosynthesis through high-throughput strain development.

Muconic Acid (MA)

Microbial production of MA was first demonstrated in *E. coli* (Niu et al., 2002), and achieved a level of 18 g/L. Later, to simplify downstream separations and reduce high alkali loads, *S. cerevisiae* was used to produce MA at a low pH, although the titers were low (Weber et al., 2012; Curran et al., 2013). By combining metabolic engineering and electrocatalysis, Suastegui et al. (2016) were able to engineer a strain that produces an MA titer of nearly 560 mg/L. To further improve the productivity, Leavitt et al. (2016, 2017) applied a combined ALE and rational engineering strategy, in which an aromatic amino acid (AAA) biosensor was coupled to anti-metabolite selection to increase the activity of the AAA biosynthetic pathway. Activating this pathway led to a significant improvement in MA production titer to 2.1 g/L in a fed-batch bioreactor, representing the highest titer obtained to date.

Shikimic Acid (SA)

Shikimic acid is an important metabolic intermediate of the shikimate pathway. Various microorganisms have been engineered to produce SA (Licona-Cassani et al., 2014; Martínez et al., 2015; Kogure et al., 2016). Liu C. et al. (2017) developed an SA biosensor constructed from a LysR-type transcriptional regulator ShiR to monitor the SA production of different *Corynebacterium glutamicum* strains (Schulte et al., 2017). This biosensor was used to identify a high-yield SA-producing strain with 2.4-fold improvement in titer over low-yield strains identified by FACS. Taking another approach, Li et al. (2017) performed directed evolution of a uric acid–responsive regulatory protein, HucR, to switch its specificity to SA, which the mutant sensor can detect in the range of 3–20 mM. The biosensor was used to monitor metabolic flux and improve the specific activity of a key enzyme in the SA biosynthetic pathway.

Glucaric Acid (GA)

Glucaric acid is a promising platform molecule for making synthetic polymers such as nylons and plastics. The microbial production of GA was first demonstrated in *E. coli,* and subsequently developed strains produce titers of up to 4.85 g/L (B strain) and 2 g/L (K strain) (Moon et al., 2009, 2010; Shiue and Prather, 2014; Reizman et al., 2015; Doong et al., 2018; Qu et al., 2018). More recently, to overcome the limitation of acid-induced toxicity, an *S. cerevisiae* strain was engineered to produce GA (Gupta et al., 2016; Chen et al., 2018). Raman et al. (2014) described the development of a selection system that uses a biosensor to couple metabolite concentrations to cell fitness. A negative selection scheme was also developed to rule out false positives. After four rounds of evolution, GA production was increased 22-fold, although the absolute titer was lower

than that produced by the *E. coli* K strain. Later, another group developed a general GA-responsive biosensor (Rogers and Church, 2016). Recently, Zheng et al. (2018) employed this biosensor to construct a two-strain system for rapid screening of myo-inositol oxygenase mutants, which play a key role in the GA synthesis pathway (Zheng et al., 2018), and found that fine-tuning the cofactor balance resulted in an increase in GA production in yeast.

Fatty Acid (FA)

Due to the lack of techniques available for monitoring fatty acyl-CoA levels *in vivo*, historically it has been very challenging to design rational approaches to identifying genes that modulate the production of these compounds. Recently, a FadR-based biosensor was developed to screen for *S. cerevisiae* genes that increase the fatty acyl-CoA pool using FACS (Dabirian et al., 2019b). Using this biosensor, this group found that the overexpression of *GGA2* could increase fatty acid levels by 30 and 24% at 8 and 24 h after inoculation, respectively, which was mainly due to a significant increase in the $C_{16:1}$ and $C_{16:0}$ fatty acid levels. In addition, Bergman et al. (2019) used to HTS to find that overexpressing the TF Stb5 can enhance FA production in *S. cerevisiae*. This increase in FA production could be because of the consumption of excess NADPH, which would alleviate a potential redox imbalance.

CONCLUSION AND PERSPECTIVE

In a context of growing concerns regarding climate change, environmental protection, and sustainable development, the biological production of chemicals, pharmaceutical products, fuels, and materials through microbial fermentation of renewable biomass has developed rapidly in the past decade, providing promising solutions for these issues. To make this approach economically feasible in practice, however, the titer, yield, and productivity of organic acid bioproduction, for example, need to be improved further (Chen and Nielsen, 2016). As a metabolite sensor and gene expression regulator, TFs play an important role in determining the end-product productivity in a cell factory. Therefore, the importance of TFs engineering is that it is a critical tool in optimizing phenotypes. In particular, the explosive development of genomic editing tools in a wide variety of prokaryotic and eukaryotic microorganisms since 2012 (reviewed in Csörgő et al., 2016; Wang H.F. et al., 2016; Tian et al., 2017; Shapiro et al., 2018), together with various high-throughput strategies for mutagenesis, screening, sorting, and sequencing, has facilitated and accelerated the strain improvement significantly. Researchers have begun to engineer TFs systematically to improve bioproduction efficiency. TFs are key components used to construct synthetic genetic circuits *in vivo*, and can be used to detect intracellular metabolites and even the activity of entire pathways that would otherwise remain "invisible." TF-based biosensors also provide a HTS method for use in rapid strain evolution, as they enable overproducers to be identified quickly from a genome-wide mutant library using FACS and other technologies (e.g., microfluidics). The combination of genome-wide genomic editing and HTS technologies has drawn increasing attention in the field of strain development. In addition, TFs are also important global regulators that control the expression levels of key enzymes in biosynthesis pathways, therefore determining the direction, flux, balance, and outcome of metabolic networks. Identifying, engineering, and using TFs for applications such as biosensors can help fine-tune gene expression, improve the activity and stability of key enzymes, and direct metabolic flux, thus providing flexible tools for metabolic engineering, as has been demonstrated in the many works reviewed above.

Although there are many examples of successful TF engineering in metabolic engineering and synthetic biology, some challenges remain. To date, the majority of TF-based biosensors have been demonstrated in "proof-of-concept" experiments, with few examples showing real improvement in bioproduction. This is because the type, function, performance, specificity and number of TFs are still limited compared with the large number of host cells, pathways, and metabolites that need to be engineered. The development of novel, high-quality TFs with more functions relies on the further utilization of advanced bioinformatics, computational biology, and protein engineering. In addition, the molecular mechanism, compatibility, robustness, interaction, and quantification of heterogeneous TFs in regulating metabolic networks in host cells need to be understood and thoroughly elucidated to enhance the efficiency of TF-based strain development.

AUTHOR CONTRIBUTIONS

J-WL, X-YZ, HW, and Y-PB participated in searching and analyzing literature for this review, as well as writing and critical reviewing the manuscript.

FUNDING

We are grateful to China's National Key Research and Development Program (2016YFA0204300), the Shanghai Natural Science Foundation (No. 18ZR1409900), and the Key Project of the Shanghai Science and Technology Committee (18DZ1112703) for supporting this work.

REFERENCES

Bergman, A., Vitay, D., Hellgren, J., Chen, Y., Nielsen, J., and Siewers, V. (2019). Effects of overexpression of STB5 in *Saccharomyces cerevisiae* on fatty acid biosynthesis, physiology and transcriptome. *FEMS Yeast Res.* 19:foz027. doi: 10.1093/femsyr/foz027

Binder, S., Schendzielorz, G., Stäbler, N., Krumbach, K., Hoffmann, K., Bott, M., et al. (2012). A high-throughput approach to identify genomic variants of bacterial metabolite producers at the single-cell level. *Genome Biol.* 13:R40. doi: 10.1186/gb-2012-13-5-r40

Binder, S., Siedler, S., Marienhagen, J., Bott, M., and Eggeling, L. (2013). Recombineering in corynebacterium glutamicum combined with optical

nanosensors: a general strategy for fast producer strain generation. *Nucleic Acids Res.* 41, 6360–6369. doi: 10.1093/nar/gkt312

Bott, M. (2015). Need for speed-finding productive mutations using transcription factor-based biosensors, fluorescence-activated cell sorting and recombineering. *Microb. Biotechnol.* 8, 8–10. doi: 10.1111/1751-7915.12248

Browning, D., and Busby, S. (2004). The regulation of bacterial transcription initiation. *Nat. Rev. Microbiol.* 2, 57–65. doi: 10.1038/nrmicro787

Chen, N., Wang, J. Y., Zhao, Y. Y., and Deng, Y. (2018). Metabolic engineering of *Saccharomyces cerevisiae* for efficient production of glucaric acid at high titer. *Microb. Cell Fact.* 17:67. doi: 10.1186/s12934-018-0914-y

Chen, W., Zhang, S., Jiang, P., Yao, J., He, Y. Z., Chen, L. C., et al. (2015). Design of an ectoine-responsive AraC mutant and its application in metabolic engineering of ectoine biosynthesis. *Metab. Eng.* 30, 149–155. doi: 10.1016/j.ymben.2015.05.004

Chen, Y., and Nielsen, J. (2016). Biobased organic acids production by metabolically engineered microorganisms. *Curr. Opin. Biotechnol.* 37, 165–172. doi: 10.1016/j.copbio.2015.11.004

Cheng, F., Tang, X. L., and Kardashliev, T. (2018). Transcription factor-based biosensors in high-throughput screening: advances and applications. *Biotechnol. J.* 13:1700648. doi: 10.1002/biot.201700648

Chou, H. H., and Keasling, J. D. (2013). Programming adaptive control to evolve increased metabolite production. *Nat. Commun.* 4:2595. doi: 10.1038/ncomms3595

Chu, H. S., Ahn, J. H., Yun, J., Choi, I. S., Nam, T. W., and Cho, K. M. (2015). Direct fermentation route for the production of acrylic acid. *Metab. Eng.* 32, 23–29. doi: 10.1016/j.ymben.2015.08.005

Csörgő, B., Nyerges, A., Posfai, G., and Feher, T. (2016). System-level genome editing in microbes. *Curr. Opin. Microbiol.* 33, 113–122. doi: 10.1016/j.mib.2016.07.00

Curran, K. A., Leavitt, J. M., Karim, A. S., and Alper, H. S. (2013). Metabolic engineering of muconic acid production in *Saccharomyces cerevisiae*. *Metab. Eng.* 15, 55–66. doi: 10.1016/j.ymben.2012.10.003

Dabirian, Y., Li, X. W., Chen, Y., David, F., Nielsen, J., and Siewers, V. (2019a). Expanding the dynamic range of a transcription factor-based biosensor in Saccharomyces cerevisiae. *ACS Synth. Biol.* 8, 1968–1975. doi: 10.1021/acssynbio.9b00144

Dabirian, Y., Teixeira, P. G., Nielsen, J., Siewers, V., and David, F. (2019b). FadR-based biosensor-assisted screening for genes enhancing fatty Acyl-CoA pools in *Saccharomyces cerevisiae*. *ACS Synth. Biol.* 8, 1788–1800. doi: 10.1021/acssynbio.9b00118

D'Ambrosio, V., and Jensen, M. K. (2017). Lighting up yeast cell factories by transcription factor-based biosensors. *FEMS Yeast Res.* 17:fox076. doi: 10.1093/femsyr/fox076

Dietrich, J. A., McKee, A. E., and Keasling, J. D. (2010). High-throughput metabolic engineering: advances in small-molecule screening and selection. *Annu. Rev. Biochem.* 79, 563–590. doi: 10.1146/annurev-biochem-062608-095938

Dietrich, J. A., Shis, D. L., Alikhani, A., and Keasling, J. D. (2013). Transcription factor-based screens and synthetic selections for microbial small-molecule biosynthesis. *ACS Synth. Biol.* 2, 47–58. doi: 10.1021/sb300091d

Doong, S. J., Gupta, A., and Prather, K. L. J. (2018). Layered dynamic regulation for improving metabolic pathway productivity in *Escherichia coli*. *Proc. Natl. Acad. Sci. U.S.A.* 115, 2964–2969. doi: 10.1073/pnas.1716920115

Flachbart, L. K., Sokolowsky, S., and Marienhagen, J. (2019). Displaced by deceivers: prevention of biosensor cross-talk is pivotal for successful biosensor-based high-throughput screening campaigns. *ACS Synth. Biol.* 8, 1847–1857. doi: 10.1021/acssynbio.9b00149

Grau, M. F., Entwistle, R., Chiang, Y. M., Ahuja, M., Elizabeth Oakley, C., Akashi, T., et al. (2018). Hybrid transcription factor engineering activates the silent secondary metabolite gene cluster for (+)-Asperlin in *Aspergillus nidulans*. *ACS Chem. Biol.* 13, 3193–3205. doi: 10.1021/acschembio.8b00679

Gupta, A., Hicks, M. A., Manchester, S. P., and Prather, K. L. J. (2016). Porting the synthetic D-glucaric acid pathway from *Escherichia coli* to *Saccharomyces cerevisiae*. *Biotechnol. J.* 11, 1201–1208. doi: 10.1002/biot.201500563

Hanko, E. K. R., Minton, N. P., and Malys, N. (2018). A transcription factor-based biosensor for detection of itaconic acid. *ACS Synth. Biol.* 7, 1436–1446. doi: 10.1021/acssynbio.8b00057

Hawkins, A. C., Arnold, F. H., Stuermer, R., Hauer, B., and Leadbetter, J. R. (2007). Directed evolution of *Vibrio fischeri* LuxR for improved response to butanoyl-homoserine lactone. *Appl. Environ. Microbiol.* 73, 5775–5781. doi: 10.1128/AEM.00060-07

Hellman, L. M., and Fried, M. G. (2007). Electrophoretic mobility shift assay (EMSA) for detecting protein-nucleic acid interactions. *Nat. Protoc.* 2, 1849–1861. doi: 10.1038/nprot.2007.249

Herrgård, M. J., Lee, B. S., Portnoy, V., and Palsson, B. (2006). Integrated analysis of regulatory and metabolic networks reveals novel regulatory mechanisms in *Saccharomyces cerevisiae*. *Genome Res.* 16, 627–635. doi: 10.1101/gr.4083206

Hu, S., Xie, Z., Onishi, A., Yu, X., Jiang, L., Lin, J., et al. (2009). Profiling the human protein-DNA interactome reveals ERK2 as a transcriptional repressor of interferon signaling. *Cell* 139, 610–622. doi: 10.1016/j.cell.2009.08.037

Jha, R. K., Kern, T. L., Kim, Y., Tesar, C., Jedrzejczak, R., Joachimiak, A., et al. (2016). A microbial sensor for organophosphate hydrolysis exploiting an engineered specificity switch in a transcription factor. *Nucleic Acids Res.* 17, 8490–8500. doi: 10.1093/nar/gkw687

Kasey, C. M., Zerrad, M., Li, Y. W., Cropp, T. A., and Williams, G. J. (2017). Development of transcription factor-based designer macrolide biosensors for metabolic engineering and synthetic biology. *ACS Synth. Biol.* 7, 227–239. doi: 10.1021/acssynbio.7b00287

Kilic, S., White, E. R., Sagitova, D. M., Cornish, J. P., and Erill, I. (2014). CollecTF: a database of experimentally validated transcription factor-binding sites in bacteria. *Nucleic Acids Res.* 42, 156–160. doi: 10.1093/nar/gkt1123

Kim, M. N., Park, H. H., Lim, W. K., and Shin, H. J. (2005). Construction and comparison of *Escherichia coli* whole-cell biosensors capable of detecting aromatic compounds. *J. Microbiol. Method* 60, 235–245. doi: 10.1016/j.mimet.2004.09.018

Kim, S. K., Kim, S. H., Subhadra, B., Woo, S. G., Rha, E., Kim, S. W., et al. (2018). A genetically encoded biosensor for monitoring isoprene production in engineered *Escherichia coli*. *ACS Synth. Biol.* 7, 2379–2390. doi: 10.1021/acssynbio.8b00164

Kogure, T., Kubota, T., Suda, M., Hiraga, K., and Inui, M. (2016). Metabolic engineering of *Corynebacterium glutamicum* for shikimate overproduction by growth-arrested cell reaction. *Metab. Eng.* 38, 204–216. doi: 10.1016/j.ymben.2016.08.005

Kortmann, M., Mack, C., Baumgart, M., and Bott, M. (2019). Pyruvate carboxylase variants enabling improved lysine production from glucose identified by biosensor-based high- throughput fluorescence-activated cell sorting screening. *ACS Synth. Biol.* 8, 274–281. doi: 10.1021/acssynbio.8b00510

Leavitt, J. M., Tong, A., Tong, J., Pattie, J., and Alper, H. S. (2016). Coordinated transcription factor and promoter engineering to establish strong expression elements in *Saccharomyces cerevisiae*. *Biotechnol. J.* 11, 866–876. doi: 10.1002/biot.201600029

Leavitt, J. M., Wagner, J. M., Tu, C. C., Tong, A., Liu, Y. Y., and Alper, H. S. (2017). Biosensor-enabled directed evolution to improve muconic acid production in *Saccharomyces cerevisiae*. *Biotechnol. J.* 12:1600687. doi: 10.1002/biot.201600687

Lee, S. K., and Keasling, J. D. (2006). Effect of glucose or glycerol as the sole carbon source on gene expression from the *Salmonella* prpBCDE promoter in *Escherichia coli*. *Biotechnol. Prog.* 22, 1547–1551. doi: 10.1021/bp060193f

Lee, S. W., and Oh, M. K. (2015). A synthetic suicide riboswitch for the high-throughput screening of metabolite production in *Saccharomyces cerevisiae*. *Metab. Eng.* 28, 143–150. doi: 10.1016/j.ymben.2015.01.004

Li, H., Liang, C. N., Chen, W., Jin, J. M., Tang, S. Y., and Tao, Y. (2017). Monitoring *in vivo* metabolic flux with a designed whole-cell metabolite biosensor of shikimic acid. *Biosens. Bioelectron.* 98, 457–465. doi: 10.1016/j.bios.2017.07.022

Licona-Cassani, C., Lara, A. R., Cabrera-Valladares, N., Escalante, A., Hernández-Chávez, G., Martinez, A., et al. (2014). Inactivation of pyruvate kinase or the phosphoenolpyruvate: sugar phosphotransferase system increases shikimic and dehydroshikimic acid yields from glucose in Bacillus subtilis. *J. Mol. Microbiol. Biotechnol.* 24, 37–45. doi: 10.1159/000355264

Liu, C., Zhang, B., Liu, Y. M., Yang, K. Q., and Liu, S. J. (2017). New intracellular shikimic acid biosensor for monitoring shikimate synthesis in *Corynebacterium glutamicum*. *ACS Synth. Biol.* 7, 591–600. doi: 10.1021/acssynbio.7b00339

Liu, G., Chater, K. F., Chandra, G., Niu, G. Q., and Tan, H. R. (2013). Molecular regulation of antibiotic biosynthesis in *Streptomyces*. *Microbiol. Mol. Biol. Rev.* 1, 112–143. doi: 10.1128/MMBR.00054-12

Liu, J. J., Li, J. H., Shin, H. D., Liu, L., Du, G. C., and Chen, J. (2017). Protein and metabolic engineering for the production of organic acids. *Bioresource Technol.* 239, 412–421. doi: 10.1016/j.biortech.2017.04.052

Liu, R. M., Liang, L. Y., Garst, A. D., Choudhury, A., Nogué, V. S., Beckham, G. T., et al. (2018). Directed combinatorial mutagenesis of *Escherichia coli* for complex phenotype engineering. *Metab. Eng.* 47, 10–20. doi: 10.1016/j.ymben.2018.02.007

Liu, S. D., Wu, Y. N., Wang, T. M., Zhang, C., and Xing, X. H. (2017). Maltose utilization as a novel selection strategy for continuous evolution of microbes with enhanced metabolite production. *ACS Synth. Biol.* 6, 2326–2338. doi: 10.1021/acssynbio.7b00247

Liu, Y., Liu, Y., and Wang, M. (2017). Design, optimization and application of small molecule biosensor in metabolic engineering. *Front. Microbiol.* 8:2012. doi: 10.3389/fmicb.2017.02012

Liu, Y. F., Zhuang, Y. Y., Ding, D. Q., Xu, Y. R., Sun, J. B., and Zhang, D. W. (2017). Biosensor-based evolution and elucidation of a biosynthetic pathway in *Escherichia coli*. *ACS Synth. Biol.* 6, 837–848. doi: 10.1021/acssynbio.6b00328

Liu, Z. J., and Liu, T. G. (2016). Production of acrylic acid and propionic acid by constructing a portion of the 3-hydroxypropionate/4-hydroxybutyrate cycle from *Metallosphaera sedula* in *Escherichia coli*. *J. Ind. Microbiol. Biotechnol.* 43, 1659–1670. doi: 10.1007/s10295-016-1843-6

Luo, Z. S., Zeng, W. Z., Du, G. C., Chen, J., and Zhou, J. W. (2020). Enhancement of pyruvic acid production in *Candida glabrata* by engineering hypoxia-inducible factor 1. *Bioresource Technol.* 295:12224. doi: 10.1016/j.biortech.2019.122248

Lutz, R., and Bujard, H. (1997). Independent and tight regulation of transcriptional units in *Escherichia coli* via the LacR/O, the TetR/O and AraC/I1-I2 regulatory elements. *Nucleic Acids Res.* 25, 1203–1210. doi: 10.1093/nar/25.6.1203

Machado, L. F. M., Currin, A., and Dixon, N. (2019). Directed evolution of the PcaV allosteric transcription factor to generate a biosensor for aromatic aldehydes. *J. Biol. Eng.* 13:91. doi: 10.1186/s13036-019-0214-z

Mahr, R., and Frunzke, J. (2016). Transcription factor-based biosensors in biotechnology: current state and future prospects. *Appl. Microbiol. Biotechnol.* 100, 79–90. doi: 10.1007/s00253-015-7090-3

Martínez, J. A., Bolívar, F., and Escalante, A. (2015). Shikimic acid production in *Escherichia coli*: from classical metabolic engineering strategies to omics applied to improve its production. *Front. Bioeng. Biotechnol.* 3:145. doi: 10.3389/fbioe.2015.00145

Michener, J. K., and Smolke, C. D. (2012). High-throughput enzyme evolution in *Saccharomyces cerevisiae* using a synthetic RNA switch. *Metab. Eng.* 14, 306–316. doi: 10.1016/j.ymben.2012.04.004

Moon, T. S., Dueber, J. E., Shiue, E., and Jones, P. K. L. (2010). Use of modular, synthetic scaffolds for improved production of glucaric acid in engineered *E. coli*. *Metab. Eng.* 12, 298–305. doi: 10.1016/j.ymben.2010.01.003

Moon, T. S., Yoon, S. H., Lanza, A. M., Roy-Mayhew, J. D., and Prather, K. L. J. (2009). Production of glucaric acid from a synthetic pathway in recombinant *Escherichia coli*. *Appl. Environ. Microbiol.* 75, 589–595. doi: 10.1128/AEM.00973-08

Mustafi, N., Grünberger, A., Kohlheyer, D., Bott, M., and Frunzke, J. (2012). The development and application of a single-cell biosensor for the detection of L-methionine and branched-chain amino acids. *Metab. Eng.* 14, 449–457. doi: 10.1016/j.ymben.2012.02.002

Nguyen, N. H., Kim, J. R., and Park, S. (2019). Development of biosensor for 3-hydroxypropionic acid. *Biotechnol. Bioproc. Eng.* 24, 109–118. doi: 10.1007/s12257-018-0380-8

Niu, W., Draths, K. M., and Frost, J. W. (2002). Benzene-free synthesis of adipic acid. *Biotechnol. Prog.* 18, 201–211. doi: 10.1021/bp010179x

Paddon, C. J., and Keasling, J. D. (2014). Semi-synthetic artemisinin: a model for the use of synthetic biology in pharmaceutical development. *Nat. Rev. Microbiol.* 12, 355–367. doi: 10.1038/nrmicro3240

Perez-Rueda, E., Hernandez-Guerrero, R., Martinez-Nuñez, M. A., Armenta-Medina, D., Sanchez, I., Ibarra, J. A., et al. (2018). Abundance, diversity and domain architecture variability in prokaryotic DNA-binding transcription factors. *PLoS One* 13:e0195332. doi: 10.1371/journal.pone.0195332

Qu, Y. N., Yan, H. J., Guo, Q., Li, J. L., Ruan, Y. C., Yue, X. Z., et al. (2018). Biosynthesis of D-glucaric acid from sucrose with routed carbon distribution in metabolically engineered *Escherichia coli*. *Metab. Eng.* 47, 393–400. doi: 10.1016/j.ymben.2018.04.020

Raghavan, S. S., Chee, S., Li, J. T., Poschmann, J., Nagarajan, N., Wei, S. J., et al. (2019). Development and application of a transcriptional sensor for detection of heterologous acrylic acid production in *E. coli*. *Microb. Cell Fact.* 18:139. doi: 10.1186/s12934-019-1185-y

Raman, S., Rogers, J. K., Taylor, N. D., and Church, G. M. (2014). Evolution-guided optimization of biosynthetic pathways. *Proc. Natl. Acad. Sci. U.S.A.* 111, 17803–17808. doi: 10.1073/pnas.1409523111

Reece-Hoyes, J. S., and Walhout, A. J. M. (2012). Yeast one-hybrid assays: a historical and technical perspective. *Methods* 57, 441–447. doi: 10.1016/j.ymeth.2012.07.027

Reizman, I. M. B., Stenger, A. R., Reisch, C. R., Gupta, A., Connors, N. C., and Prather, K. L. J. (2015). Improvement of glucaric acid production in *E. coli* via dynamic control of metabolic fluxes. *Metab. Eng. Commun.* 2, 109–116. doi: 10.1016/j.meteno.2015.09.002

Rogers, J. K., and Church, G. M. (2016). Genetically encoded sensors enable real-time observation of metabolite production. *Proc. Natl. Acad. Sci. U.S.A.* 113, 2388–2393. doi: 10.1073/pnas.1600375113

Sanchez, I., Hernandez-Guerrero, R., Mendez-Monroy, P. E., Martínez Núñez, M. A., Antonio Ibarra, J., Pérez-Rueda, E., et al. (2020). Evaluation of the abundance of DNA-binding transcription factors in prokaryotes. *Genes* 11:52. doi: 10.3390/genes11010052

Sarria, S., Kruyer, N. S., and Peralta-Yahya, P. (2017). Microbial synthesis of medium-chain chemicals from renewables. *Nat. Biotechnol.* 12, 1158–1166. doi: 10.1038/nbt.4022

Schulte, J., Baumgart, M., and Bott, M. (2017). Development of a single-cell GlxR-based cAMP biosensor for *Corynebacterium glutamicum*. *J. Biotechnol.* 258, 33–40. doi: 10.1016/j.jbiotec.2017.07.004

Seok, J. Y., Yang, J., Choi, S. J., Lim, H. G., Choi, U. J., Kim, K. J., et al. (2018). Directed evolution of the 3-hydroxypropionic acid production pathway by engineering aldehyde dehydrogenase using a synthetic selection device. *Metab. Eng.* 47, 113–120. doi: 10.1016/j.ymben.2018.03.009

Shapiro, R. S., Chavez, A., and Collins, J. J. (2018). CRISPR technologies: a toolkit for making genetically intractable microbes tractable. *Nat. Rev. Microbiol.* 6, 333–339. doi: 10.1038/s41579-018-0002-7

Shi, T., Han, P. P., You, C., and Zhang, Y. H. (2018). An in vitro synthetic biology platform for emerging industrial biomanufacturing: bottom-up pathway design. *Synth. Syst. Biotechnol.* 3, 186–195. doi: 10.1016/j.synbio.2018.05.002

Shiue, E., and Prather, K. L. J. (2014). Improving D -glucaric acid production from *myo*-inositol in *E. coli* by increasing MIOX stability and myo-inositol transport. *Metab. Eng.* 22, 22–31. doi: 10.1016/j.ymben.2013.12.002

Siedler, S., Khatri, N. K., Zsohaìr, A., Kjærbølling, I., Vogt, M., Hammar, P., et al. (2017). Development of a bacterial biosensor for rapid screening of yeast *p*-coumaric acid production. *ACS Synth. Biol.* 6, 1860–1869. doi: 10.1021/acssynbio.7b00009

Siedler, S., Schendzielorz, G., Binder, S., Eggeling, L., Bringer, S., and Bott, M. (2014a). SoxR as a single-cell biosensor for NADPH-consuming enzymes in *Escherichia coli*. *ACS Synth. Biol.* 3, 41–47. doi: 10.1021/sb400110j

Siedler, S., Stahlhut, S. G., Malla, S., Mauryn, J., and Neves, A. R. (2014b). Novel biosensors based on flavonoid-responsive transcriptional regulators introduced into *Escherichia coli*. *Metab. Eng.* 21, 2–8. doi: 10.1016/j.ymben.2013.10.011

Sint Fiet, S. V., Beilen, J. B. V., and Witholt, B. (2006). Selection of biocatalysts for chemical synthesis. *Proc. Natl. Acad. Sci. U.S.A.* 103, 1693–1698. doi: 10.1073/pnas.0504733102

Song, Y., Li, J. H., Shin, H. D., Liu, L., Du, G. C., and Chen, J. (2016). Biotechnological production of alpha-keto acids: current status and perspectives. *Bioresour. Technol.* 219, 716–724. doi: 10.1016/j.biortech.2016.08.015

Suastegui, M., Matthiesen, J. E., Carraher, J. M., Hernandez, N., Quiroz, N. R., Okerlund, A., et al. (2016). Combining metabolic engineering and electrocatalysis: application to the production of polyamides from sugar. *Angew. Chem. Int. Ed.* 55, 2368–2373. doi: 10.1002/anie.201509653

Sun, X. M., Ren, L. J., Bi, Z. Q., Ji, X. J., Zhao, Q. Y., Jiang, L., et al. (2018). Development of a cooperative two-factor adaptive-evolution method to enhance lipid production and prevent lipid peroxidation in *Schizochytrium* sp. *Biotechnol. Biofuels* 11:65. doi: 10.1186/s13068-018-1065-4

Tacheny, A., Dieu, M., Arnould, T., and Renard, P. (2013). Mass spectrometry-based identification of proteins interacting with nucleic acids. *J. Proteom.* 6, 89–109. doi: 10.1016/j.jprot.2013.09.011

Tan, G. Y., Bai, L. Q., and Zhong, J. J. (2013). Exogenous 1,4-butyrolactone stimulates A-factor-like cascade and validamycin biosynthesis in *Streptomyces hygroscopicus* 5008. *Biotechnol. Bioeng.* 110, 2984–2993. doi: 10.1002/bit.24965

Tang, S. Y., and Cirino, P. C. (2011). Design and application of a mevalonate-responsive regulatory protein. *Angew. Chem. Int. Ed.* 50, 1084–1086. doi: 10.1002/anie.201006083

Tang, S. Y., Fazelinia, H., and Cirino, P. C. (2008). AraC regulatory protein mutants with altered effector specificity. *J. Am. Chem. Soc.* 130, 5267–5271. doi: 10.1021/ja7109053

Tang, S. Y., Qian, S., Akinterinwa, O., Frei, C. S., Gredell, J. A., and Cirino, P. C. (2013). Screening for enhanced triacetic acid lactone production by recombinant *Escherichia coli* expressing a designed triacetic acid lactone reporter. *J. Am. Chem. Soc.* 135, 10099–10103. doi: 10.1021/ja402654z

Thakker, C., Martínez, I., Li, W., San, K. Y., and Bennett, G. N. (2015). Metabolic engineering of carbon and redox flow in the production of small organic acids. *J. Ind. Microbiol. Biotechnol.* 42, 403–422. doi: 10.1007/s10295-014-1560-y

Thanapipatsiri, A., Gomez-Escribano, J. P., Song, L. J., Bibb, M. J., Al-Bassam, M., Chandra, G., et al. (2016). Discovery of unusual biaryl polyketides by activation of a silent *Streptomyces venezuelae* biosynthetic gene cluster. *Chembiochem* 17, 2189–2198. doi: 10.1002/cbic.201600396

Thompson, M. G., Costello, Z., Hummel, N. F. C., Cruz-Morales, P., Blake-Hedges, J. M., Krishna, R. N., et al. (2019). Robust characterization of two distinct glutarate sensing transcription factors of *Pseudomonas putida* L-lysine metabolism. *ACS Synth. Biol.* 8, 2385–2396. doi: 10.1021/acssynbio.9b00255

Tian, P. F., Wang, J., Shen, X. L., Rey, J. F., Yuan, Q. P., Yan, Y. J., et al. (2017). Fundamental CRISPR-Cas9 tools and current applications in microbial systems. *Synth. Syst. Biotechnol.* 2, 219–225. doi: 10.1016/j.synbio.2017.08.006

Tong, Y. J., Charusanti, P., Zhang, L. X., Weber, T., and Lee, S. Y. (2015). CRISPR-Cas9 based engineering of actinomycetal genomes. *ACS Synth. Biol.* 4, 1020–1029. doi: 10.1021/acssynbio.5b00038

Trabelsi, H., Koch, M., and Faulon, J. L. (2018). Building a minimal and generalizable model of transcription factor–based biosensors: showcasing flavonoids. *Biotechnol. Bioeng.* 115, 2292–2304. doi: 10.1002/bit.26726

Uchiyama, T., and Miyazaki, K. (2010). Product-induced gene expression, a product-responsive reporter assay used to screen metagenomic libraries for enzyme-encoding genes. *Appl. Environ. Microbiol.* 76, 7029–7035. doi: 10.1128/AEM.00464-10

Wang, H. F., Russa, M. L., and Qi, L. S. (2016). CRISPR/Cas9 in genome editing and beyond. *Annu. Rev. Biochem.* 85, 227–264. doi: 10.1146/annurev-biochem-060815-014607

Wang, Y., Li, Q. G., Zheng, P., Guo, Y. M., Wang, L. X., Zhang, T. C., et al. (2016). Evolving the L-lysine high-producing strain of *Escherichia coli* using a newly developed high-throughput screening method. *J. Ind. Microbiol. Biotechnol.* 43, 1227–1235. doi: 10.1007/s10295-016-1803-1

Weber, C., Brückner, C., Weinreb, S., Lehr, C., Essl, C., and Boles, E. (2012). Biosynthesis of *cis, cis*-muconic acid and its aromatic precursors, catechol and protocatechuic acid from renewable feedstocks by *Saccharomyces cerevisiae*. *Appl. Environ. Microbiol.* 78, 8421–8430. doi: 10.1128/AEM.01983-12

Willardson, B. M., Wilkins, J. F., Rand, T. A., Schupp, J. M., Hill, K. K., Keim, P., et al. (1998). Development and testing of a bacterial biosensor for toluene-based environmental contaminants. *Appl. Environ. Microbiol.* 64, 1006–1012. doi: 10.1128/aem.64.3.1006-1012.1998

Xie, C., Deng, J. J., and Wang, H. X. (2015). Identification of AstG1, a LAL family regulator that positively controls ansatrienins production in *Streptomyces* sp. *XZQH*13. *Curr. Microbiol.* 70, 859–864. doi: 10.1007/s00284-015-0798-6

Yadav, V. G., Mey, M. D., Lim, C. G., Ajikumar, P. K., and Stephanopoulos, G. (2012). The future of metabolic engineering and synthetic biology: towards a systematic practice. *Metab. Eng.* 14, 233–241. doi: 10.1016/j.ymben.2012.02.001

Yang, J., Kim, B., Kim, G. Y., Jung, G. Y., and Seo, S. W. (2019). Synthetic biology for evolutionary engineering: from perturbation of genotype to acquisition of desired phenotype. *Biotechnol. Biofuels* 12:113. doi: 10.1186/s13068-019-1460-5

Younger, A. K. D., Su, P. Y., Shepard, A. J., Udani, S. V., Cybulski, T. R., Tyo, K. E. J., et al. (2017). Development of novel metabolite-responsive transcription factors via transposon-mediated protein fusion. *Protein Eng. Des. Sel.* 31, 55–63. doi: 10.1093/protein/gzy001

Yu, H., Chen, Z. Y., Wang, N., Yu, S. Z., Yan, Y. J., and Huo, Y. X. (2019). Engineering transcription factor BmoR for screening butanol overproducers. *Metab. Eng.* 56, 28–38. doi: 10.1016/j.ymben.2019.08.015

Zhang, J. W., Barajas, J. F., Burdu, M., Ruegg, T. L., Dias, B., and Keasling, J. D. (2016). Development of a transcription factor-based lactam biosensor. *ACS Synth. Biol.* 6, 439–445. doi: 10.1021/acssynbio.6b00136

Zhang, M., Wong, F. T., Wang, Y., Luo, S., Lim, Y. H., Heng, E., et al. (2017). CRISPR-Cas9 strategy for activation of silent *Streptomyces* biosynthetic gene clusters. *Nat. Chem. Biol.* 13, 607–609. doi: 10.1038/nchembio.2341

Zheng, S., Hou, J., Zhou, Y., Fang, H., Wang, T. T., Liu, F., et al. (2018). One-pot two-strain system based on glucaric acid biosensor for rapid screening of myo-inositol oxygenase mutations and glucaric acid production in recombinant cells. *Metab. Eng.* 49, 212–219. doi: 10.1016/j.ymben.2018.08.005

Zhou, S. F., Ainala, S. K., Seol, E., Nguyen, T. T., and Park, S. (2015). Inducible gene expression system by 3-hydroxypropionic acid. *Biotechnol. Biofuels* 8:169. doi: 10.1186/s13068-015-0353-5

Conflict of Interest: The authors declare that the research was conducted in the absence of any commercial or financial relationships that could be construed as a potential conflict of interest.

frontiers in Bioengineering and Biotechnology

ORIGINAL RESEARCH
published: 28 February 2020
doi: 10.3389/fbioe.2020.00120

Two-Stage Semi-Continuous 2-Keto-Gluconic Acid (2KGA) Production by *Pseudomonas plecoglossicida* JUIM01 From Rice Starch Hydrolyzate

Lei Sun[1†], Da-Ming Wang[1,2†], Wen-Jing Sun[2], Feng-Jie Cui[2], Jin-Song Gong[1], Xiao-Mei Zhang[1], Jin-Song Shi[1] and Zheng-Hong Xu[1*]*

[1] The Key Laboratory of Industrial Biotechnology, National Engineering Laboratory for Cereal Fermentation Technology, School of Biotechnology, Jiangnan University, Ministry of Education, Wuxi, China, [2] School of Food and Biological Engineering, Jiangsu University, Zhenjiang, China

A two-stage semi-continuous strategy for producing 2-keto-gluconic acid (2KGA) by *Pseudomonas plecoglossicida* JUIM01 from rice starch hydrolyzate (RSH) has been developed. The initial glucose concentration (140 g/L) was selected for first-stage fermentation due to its highest 2KGA productivity of 7.58 g/(L · h), cell weight of 3.91 g/L, and residual glucose concentration of 25.00 g/L. Followed by removing 70.0% (v/v) of the first-stage broth and feeding 400.0 g/L of glucose to the second-stage fermentor, a total of 50680.0 g glucose was consumed, and 50005.20 g 2KGA was obtained with a yield of 0.9867 g/g by *P. plecoglossicida* JUIM01 after a 3-cycle two-stage semi-continuous fermentation. Our results indicated that the developed two-stage semi-continuous fermentation could be industrially applied due to its high 2KGA concentration, 2KGA yield and operation efficiency.

Keywords: 2-Keto-gluconic acid, *Pseudomonas plecoglossicida*, two-stage semi-continuous fermentation, rice starch hydrolyzate, fermentation performance

OPEN ACCESS

Edited by:
Hui Wu,
East China University of Science and Technology, China

Reviewed by:
Liya Liang,
University of Colorado Boulder, United States
Elisabeth Jacobsen,
Norwegian University of Science and Technology, Norway
Mingjie Jin,
Nanjing University of Science and Technology, China

***Correspondence:**
Wen-Jing Sun
juswj@163.com;
juswj@ujs.edu.cn
Zheng-Hong Xu
zhenghxu@jiangnan.edu.cn

† These authors have contributed equally to this work and share first authorship

Specialty section:
This article was submitted to Industrial Biotechnology, a section of the journal Frontiers in Bioengineering and Biotechnology

Received: *25 November 2019*
Accepted: *07 February 2020*
Published: *28 February 2020*

Citation:
Sun L, Wang D-M, Sun W-J, Cui F-J, Gong J-S, Zhang X-M, Shi J-S and Xu Z-H (2020) Two-Stage Semi-Continuous 2-Keto-Gluconic Acid (2KGA) Production by Pseudomonas plecoglossicida JUIM01 From Rice Starch Hydrolyzate. Front. Bioeng. Biotechnol. 8:120. doi: 10.3389/fbioe.2020.00120

INTRODUCTION

Erythorbic acid, also known as D-isoascorbic acid, is a stereoisomer of ascorbic acid. Its global market demand is approximately 40,000 tons/year due to its significant applications in preventing food oxidation, inhibiting the decrease of color, flavors and aroma, and blocking the formation of carcinogenic ammonium nitrite during food processing (Walker, 1991; Wei et al., 2008). Erythorbic acid and its salts are generally recognized as safe (GRAS) by the US Food and Drug Administration (FDA) and approved as food ingredients E315 (free acid) and E316 (sodium salt) in Europe with no safety concern (Aguilar et al., 2016). Recently, erythorbic acid and its salts have seen their applications extended to include roles in mushroom post-harvesting as an oxygen scavenger, in

the oil and gas industry as an oxygen scavenger, in feed industries as a calcium-rich additive and as acidulates, and in the florescent materials field to promote the synthesis of CdS quantum dots (Liang et al., 2014; Joven et al., 2015; Al Helal et al., 2018; Ping et al., 2018).

2-Keto-D-gluconic acid (2KGA) is a key intermediate for erythorbic acid and erythorbate production. It is also a versatile chemical applied in the cosmetics and pharmaceutical industries (Li et al., 2016). For 2KGA preparation, at least three methods including chemical synthesis, enzymatic conversion, and microbial fermentation have been proposed. However, chemical and enzymatic methods had limits to large-scale production due to their critical reaction conditions, low yield and/or high process costs (Elseviers et al., 2000; Tanimura et al., 2003). Microbial fermentation is the main industrial 2KGA production method with two consecutive oxidations by glucose dehydrogenase and gluconate dehydrogenase.

$$\text{Glucose} \xrightarrow{\text{Glucose}-1-\text{dehydrogenase}} \text{Gluconic Acid} \xrightarrow{\text{Gluconate dehydrogenase}} 2-\text{Keto}-\text{Gluconic Acid}$$

Gluconobacter, *Pseudogluconobacter*, *Pseudomonas*, *Serratia,* and *Klebsiella* are the potential genera for 2KGA production with various fermentation performances. For example, *Serratia marcescens* NRRL B-486 yielded 2KGA ranging from 0.85 g/g to 1.0 g/g glucose using continuous fermentation (Minisenhermer et al., 1965). Since 1998, our group has screened several 2KGA producing strains, such as *Pseudomonas fluorescens* AR4, *Arthrobacter globiformis* C224, and *Pseudomonas plecoglossicida* JUIM01. Among them, *P. fluorescens* AR4 showed a high substrate tolerance (>120 g/L glucose) and a low susceptibility to phage infection (Sun et al., 2006). Other engineered strains have also been constructed by overexpressing the *ga2dh* gene of *Gluconobacter oxidans* which produced approximately 486 g/L 2KGA from 480 g/L gluconic acid (Shi et al., 2015).

In order to overcome the inhibitory effects of substrate and/or product in the conventional batch processes, various culture systems, e.g., fed-batch, semi-continuous and continuous fermentation, have been developed. Three-cycle DO-stat repeated fed batch fermentation was developed to yield 72 g of 2KGA from 110 g of cassava by the immobilized *Pseudomonas aeruginosa* with a maximum productivity and cell concentration of 0.55 g/(L · h) and 35 g/L, respectively (Chia et al., 2008). Our group has also proposed a semi-continuous process, continuous process and direct conversion of glucose to 2KGA by *P. fluorescens* AR4 or *A. globiformis* C224 in an unsterile and buffer-free system with the purpose to increase its final concentration and improve the handling process (Teng et al., 2013; Sun et al., 2015). A production of 195 g/L 2KGA, 3.05 g/(L · h) productivity and a yield of 1.07 g/g were achieved in a non-sterile and buffer-free system by *P. fluorescens* AR4 (Sun et al., 2015). Our previous results also showed that the semi-continuous fermentation of *P. fluorescens* AR4 was able to produce 444.96 g/L of 2KGA, with a productivity of 6.74 g/L · h and a yield of 0.93 g/g, the values of which reached the industrially acceptable levels for 2KGA production (Sun et al., 2012). However, the industrial application of the 2KGA semi-continuous process highlighted some disadvantages including a lot of time spent on equipment sterilization to avoid contamination after reactor turnover. Recently, a two-stage fed-batch operation was proven to favor a significant increase of DHA threshold values by culturing the viable microbial cells in the first stage and converting a high concentration of glycerol to DHA in the second stage (Bauer et al., 2005). The present study therefore aimed to develop a two−stage semi-continuous fermentation system with the potential to improve the industrial 2KGA fermentation performance by *P. plecoglossicida* JUIM01, through improving its working efficiency and increasing the utilization ratio of equipment with the aim to substitute the current 2KGA batch or semi-continuous production process.

MATERIALS AND METHODS

Microorganism and Media

Pseudomonas plecoglossicida JUIM01 was screened and stocked in our laboratory (Wang et al., 2018; Sun et al., 2019). The media for the stocking strain consisted of (g/L): peptone 10.0, NaCl 5.0, beef extract 5.0 and agar 20.0. Media for preparing the seed contained (g/L, pH 7.0): glucose 20.0, urea 2.0, corn syrup powder 5.0, $MgSO_4 \cdot 7H_2O$ 0.5 and KH_2PO_4 2.0.

The concentrated rice starch hydrolyzate (RSH) containing 450 g/L of glucose and 3.5 g/L of protein was prepared by Parchn Sodium Isovitamin C Co. Ltd (Dexing, Jiangxi, China), and diluted to specific glucose concentrations for two-stage fermentation. Media for the first-stage fermentation contained (g/L, pH 6.7): glucose 140.0, corn syrup powder 7.5, $CaCO_3$ 39.0. Glyceryl polyether at 0.02% (*v/v*) was added as defoamer. The feeding media for the first-stage was (g/L, pH 6.7): glucose 140.0, corn syrup powder 7.5, urea 0.15, KH_2PO_4 0.1 and $CaCO_3$ 39.0. The feeding media for the second-stage was (g/L, pH 6.7): glucose 300.0 and $CaCO_3$ 82.5.

Cultivation and Two-Stage Fermentation

The seed of *P. plecoglossicida* JUIM01 used for 50-L scale fermentation was prepared by activating the stock cells in 50 mL of seed media at 30°C for 20 h and cultivating the activated cells in a 5-L fermentor with working a volume of 3.5 L. The agitation speed and aeration rate of the 5-L fermentor (Green Bio-engineering Co., Ltd, Zhenjiang, China) were set as 400 rpm and 105.0 L/h, respectively. After a 24-h cultivation with a cell concentration of 8.05 g/L (approximate OD_{650nm} of 14.0), the culture was used as an inoculum for two-stage semi-continuous fermentation.

The two-stage semi-continuous process consisted of at least two 50-L mechanical stirred fermentors (Green Bio-engineering Co., Ltd, Zhenjiang, China). Temperature, DO concentration, pH, agitation speed and airflow rate were monitored on-line. The operational procedures were outlined in **Figure 1**. The first-stage fermentation started with the inoculation of the seeds into 35 L of media (V_1) and this was cultivated at 30°C with an aeration rate of 42.0 L/min and an agitation speed of 450 rpm under a pressure of 0.03 MPa. The first-stage cultivated broth

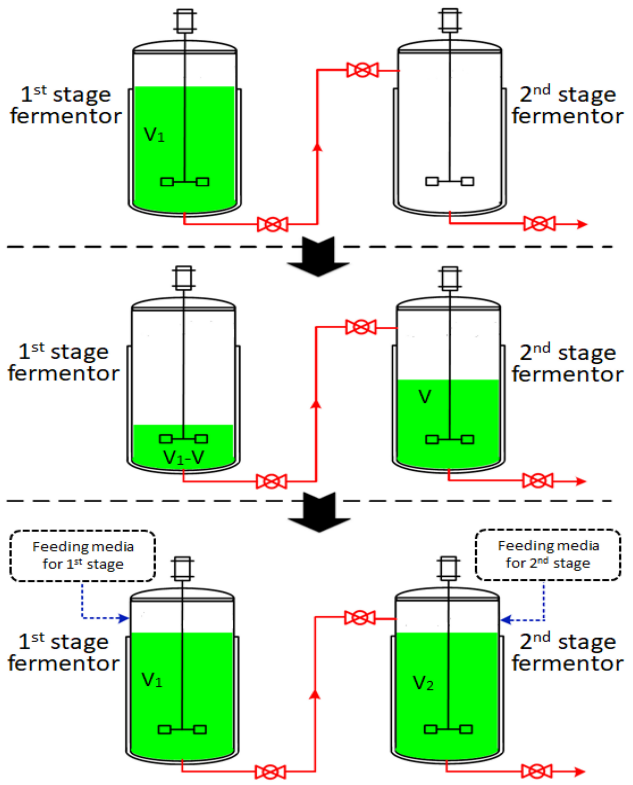

FIGURE 1 | A schematic diagram of a two-stage semi-continuous fermentation system for 2KGA production by *P. plecoglossicida* JUIM01 (V of first-stage cultivated broth in fermentor 1 was transferred to fermentor 2 as the inoculator. The feeding media (V and V_1-V) were fed into first- and second-stage fermentors, respectively. The second-stage cultivation proceeded until the glucose to be consumed was below 1.0 g/L).

was taken out to be used as the seed in the second-stage fermentor after a specific cultivation time (the time at which residual glucose concentration had decreased to specified levels). The feeding media of the first- and second-stages were fed into first- and second-stage fermentors with volumes of V and V_2-V (V_2 = 35.0 L), respectively. The first-stage fermentor maintained cultivation and was used as the seed for the next run. The second-stage fermentors were cultivated at 33°C, with an aeration rate of 42.0 L/min and an agitation speed of 450 rpm under a pressure of 0.03 MPa. Each second-stage fermentation ended when glucose concentration was below 1.0 g/L. Samples were withdrawn every four hours to determine the concentration of residual glucose, concentration of 2KGA, cell concentration and pH.

Analytical Methods

Cell growth was expressed as OD_{650nm} (optical density at 650 nm) or dry cell weight (DCW) (OD_{650nm} of 1.0 was equivalent to 0.575 g DCW/L). The culture supernatant was obtained by centrifuging broth at 3,500 × *g* for 20 min, diluted with H_2O and pH adjusted to 1.5 with 1 M HCl. The optical rotation degree and glucose concentration of the diluted supernatant were determined using a polarimeter (Precision Instrument Co., Ltd., Shanghai, China) and a biosensor analyzer (Shandong Academy of Sciences Institute of Biology, Jinan, China) at 25°C, respectively. 2KGA concentration was calculated with the following equation:

$$Y = -0.88\,X_1 + 0.5275\,X_2 \quad (1)$$

X_1 and X_2 represent 2KGA and glucose concentrations (g/L), respectively. Y represents the optical rotation degree (°). Coefficients −0.88 and 0.5275 represent the optical rotation degree of 10 g/L of 2KGA and 10 g/L of glucose, respectively.

2-Keto-Gluconic Acid productivity was defined as the amount of 2KGA produced per hour per liter. 2KGA yield was calculated as the amount of 2KGA produced divided by the amount of glucose consumed. The glucose consumption ratio was calculated as the amount of consumed glucose divided by the initial amount of glucose.

Statistical Analysis

All of the fermentations were performed in duplicate. One-way analysis of variance (ANOVA) and Duncan's test were used for statistical analysis.

RESULTS AND DISCUSSION

Effect of Glucose Concentration in First-Stage Fermentation on 2KGA Production Performance

Pure sugars and starch hydrolyzates have been widely used as the carbon sources for microbial organic acid production. Corn, wheat and rice starch are abundant inexpensive renewable resources which could reduce fermentation costs as substitutes for expensive pure sugars, however pure sugars give high final bioorganic acid concentrations and productivity. Our previous results have proven that RSHs showed similar 2KGA fermentation performances to those of pure glucose (Sun et al., 2012). Herein, on the basis of the previous study, a two-stage cultivation strategy was designed by cultivating a high density of *P. plecoglossicida* JUIM01 cells at a first-stage for 2KGA production during a second-stage. Glucose with concentrations of 80.0, 110.0, 140.0, 170.0, and 200.0 g/L was examined to determine its influence on the 2KGA production performance during the first-stage. As the summarized results in **Table 1** show, an increase in glucose concentration from 80.0 to 200.0 g/L led to prolonged cultivation periods from 12.5 h to 32.5 h. Our previous results also proved that a high glucose concentration of 200.0 g/L increased the fermentation time of *P. fluorescens* AR4 to 36 h (Sun et al., 2012). Accordingly, an initial glucose concentration of 200.0 g/L resulted in the highest 2KGA production of 175.28 g/L. 2KGA yields of 0.9549, 0.9746, and 0.9678 g/g were obtained from the fermentation using 110.0, 140.0, and 170.0 g/L of glucose, respectively. On the basis of the 2KGA yield, productivity and cell concentration, we chose 140.0 g/L as the initial glucose concentration for the second-stage fermentation due to it producing the highest total 2KGA, productivity

and cell concentration of 0.9746 g/g, 7.58 g/(L · h) and 3.91 g/L, respectively.

Fermentation Process at Glucose Concentration of 140 g/L in First-Stage Fermentation

Generally, the residual glucose concentration from the previous stage in semi-continuous or cell recycled cultures, depending on the cultivation time, provides the activated cells with high densities for next stage without a lag phase. **Figure 2** presented the time course of 2KGA batch fermentation by *P. plecoglossicida* JUIM01 at a glucose concentration of 140.0 g/L.

2-Keto-Gluconic Acid production and cell concentration increased rapidly to 26.76 g/L and 3.31 g/L, respectively, after the first 4-h fermentation. The exponential phase growth of *P. plecoglossicida* JUIM01 occurred from 4 h to 16 h with a rapid increase in 2KGA concentration to 135.29 g/L and cell concentration to 3.91 g/L. From 16 h to 24 h, fermentation entered a stationary phase with a maximum 2KGA concentration of 136.47 g/L and a gradual decrease of residual glucose to 0.10 g/L. Due to 2KGA accumulation, pH values decreased significantly from 6.75 to 4.61 and then remained at a relatively stable level of about 4.3. As for the two-stage cultivation, the optimal ending point for the first-stage was a cultivation time of 8∼10 h (residual glucose ranging from 20.00 to 55.00 g/L) with a high catalytic activity of *P. plecoglossicida* JUIM01 and 2KGA productivity of over 10.00 g/(L · h), which benefited the second-stage of fermentation.

Effect of Residual Glucose Concentration at First-Stage on 2KGA Production

The optimal residual glucose concentration of the first-stage of fermentation, depending on the fermentation time, provides the activated cells with high densities without a lag phase for the following stage experiments (Ji et al., 2014). On the basis of the time course of 2KGA batch fermentation by *P. plecoglossicida* JUIM01, 80% of the cultivated broth (28 L) from the first-stage was transferred to second fermentor for the second-stage of fermentation at the point when the residual glucose concentration of the first-stage reached between 13.27 and 55.02 g/L (corresponding fermentation

TABLE 1 | Summary of 2KGA production from different glucose concentrations at first-stage fermentation by *P. plecoglossicida* JUIM01.

Initial glucose concentration (g/L)	Residual glucose concentration (g/L)	Maximum cell concentration (g/L)	2KGA concentration (g/L)	2KGA yield (g/g)	Fermentation time (h)	2KGA productivity (g/L · h)
80.0	0.12 ± 0.04	3.70 ± 0.09	70.79 ± 2.28	0.8849 ± 0.0285	12.5 ± 0.6	5.67 ± 0.15
110.0	0.15 ± 0.08	3.83 ± 0.16	105.04 ± 1.68	0.9549 ± 0.0152	16.5 ± 0.6	6.37 ± 0.14
140.0	0.13 ± 0.06	3.91 ± 0.13	136.44 ± 2.74	0.9746 ± 0.0196	18.0 ± 0.7	7.58 ± 0.18
170.0	0.17 ± 0.07	3.32 ± 0.12	164.53 ± 1.62	0.9678 ± 0.0095	26.0 ± 0.7	6.33 ± 0.10
200.0	1.98 ± 0.63	3.18 ± 0.11	175.28 ± 6.14	0.8764 ± 0.0307	32.5 ± 1.9	5.40 ± 0.16

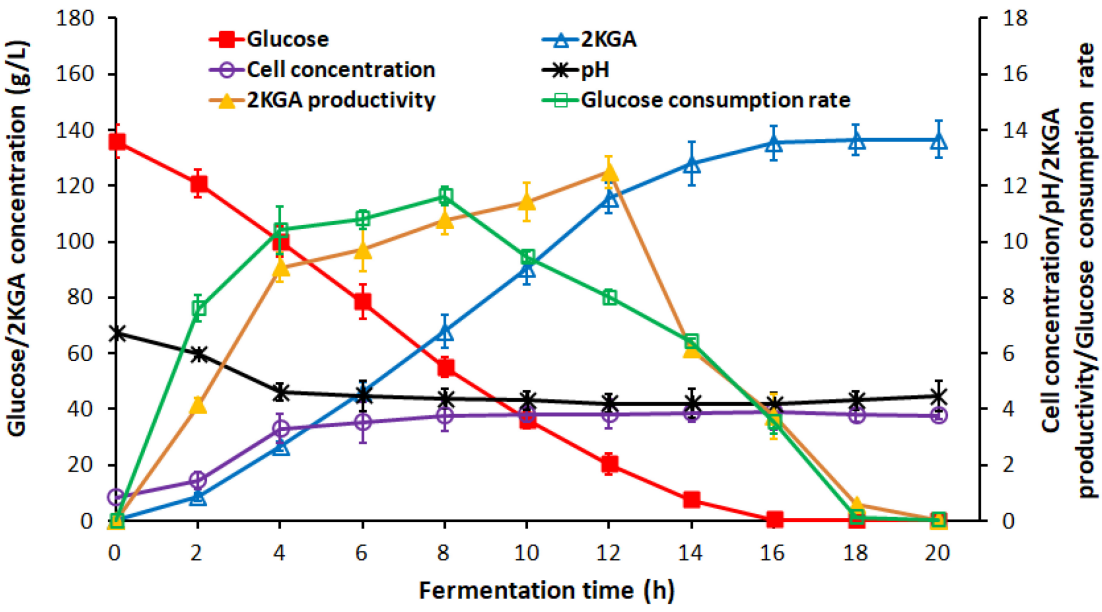

FIGURE 2 | Time course of 2KGA production, residual glucose concentration, cell concentration and pH during batch production at first-stage fermentation by *P. plecoglossicida* JUIM01 with an initial glucose concentration of 140.0 g/L.

occurred from 8.0 to 13.0 h). Seven liters of feeding media containing glucose at 300.0 g/L and $CaCO_3$ at 82.5 g/L were supplemented into the second-stage fermentor for the following fermentation.

The second-stage fermentation proceeded until the glucose was used up. The 2KGA fermentation performances were summarized in **Table 2**. 2KGA concentrations in the first-stage broth were 120.04, 109.70, 94.47, 83.51, and 74.94 g/L when the residual glucose had decreased to 13.27, 24.13, 36.38, 44.69, and 55.02 g/L (corresponding with fermentation times of 13.0, 11.5, 10.0, 9.0, and 8.0 h), respectively. Final cell concentrations in all of the experimental groups reached roughly 3.80 g/L in the broths. The 2KGA yield and productivity were at their highest levels of 0.9443 g/g and 9.51 g/(L · h), respectively, when the residual glucose concentration was 24.13 g/L (a fermentation time of 11.5 h).

After transferring 80% of the cultivated broth (28 L) from the first-stage to the second-stage fermentor and feeding 7 L of fresh feeding media, the glucose concentration in the second-stage fermentor increased to 70.60, 79.23, 89.10, 95.74, and 104.01 g/L as 2KGA concentrations decreased to 96.03, 87.76, 73.98, 66.81, and 58.75 g/L, respectively, and the cell densities also decreased correspondingly to about 3.0 g/L. At the end of the second-stage fermentation, the maximum productivity achieved was 8.56 g/(L · h) with 81.34 g/L of 2KGA and a 2KGA yield of 1.0266 g/g.

Considering the fermentation performance of both the first- and second-stages, the highest productivity of 8.05 g/(L · h) and yield of 0.9832 g/g were obtained when the residual glucose concentration was 24.13 g/L. Hence, it could be concluded that the broth in the first-stage could transfer to the second-stage fermentor for further fermentation when the residual glucose concentration was about 25.0 g/L (a fermentation time of 11.5 h) providing the live cells and glucose for the next stage.

Effect of Removing Broth Volumes of First-Stage on 2KGA Production

The cultivated broth in the first-stage contained live cells, residual glucose and produced 2KGA (Zhang et al., 2010). Removing volumes directly affected the remaining active cells, initial glucose level and 2KGA content for the next stage of fermentation. Accordingly, various broth volumes ranging from 50.0% to 80.0% (*v*/*v*) were taken after 11.5 h of first-stage fermentation, and transferred to second-stage fermentors to investigate the influence of removing volumes on 2KGA fermentation performance. As summarized in **Table 3**, after adding the

TABLE 2 | Effect of residual glucose concentration at first-stage on 2KGA production.

Parameters	Residual glucose concentration at first-stage (g/L)				
	13.27 ± 1.78	**24.13 ± 3.78**	**36.38 ± 3.90**	**44.69 ± 4.36**	**55.02 ± 2.80**
First stage					
Initial glucose (g/L)	140.0	140.0	140.0	140.0	140.0
Consumption of glucose (g/L)	126.73 ± 1.78	115.87 ± 3.78	103.62 ± 3.90	95.31 ± 4.36	84.98 ± 2.80
Initial cell concentration (g/L)	0.81 ± 0.08	0.79 ± 0.10	0.83 ± 0.08	0.81 ± 0.07	0.84 ± 0.04
Final cell concentration (g/L)	3.92 ± 0.04	3.83 ± 0.10	3.80 ± 0.04	3.78 ± 0.10	3.76 ± 0.08
Initial 2KGA (g/L)	0.30 ± 0.13	0.28 ± 0.03	0.27 ± 0.07	0.33 ± 0.06	0.31 ± 0.04
Final 2KGA (g/L)	120.04 ± 1.46	109.70 ± 3.48	94.97 ± 4.77	85.51 ± 3.62	74.94 ± 2.79
Produced 2KGA (g/L)	119.74 ± 1.58	109.42 ± 3.51	94.70 ± 4.84	85.18 ± 3.68	74.63 ± 2.83
2KGA yield (g/g)	0.9448 ± 0.0008	0.9443 ± 0.0005	0.9137 ± 0.0123	0.8938 ± 0.0023	0.8781 ± 0.0043
Fermentation time (h)	13.0	11.5	10.0	9.0	8.0
2KGA productivity (g/L · h)	9.21 ± 0.12	9.51 ± 0.31	9.47 ± 0.48	9.46 ± 0.41	9.33 ± 0.35
Second stage					
Glucose concentration after feeding media (g/L)	70.60 ± 1.40	79.23 ± 3.11	89.10 ± 3.13	95.74 ± 3.48	104.01 ± 2.26
2KGA after feeding media (g/L)	96.03 ± 1.16	87.76 ± 2.79	73.98 ± 3.81	66.81 ± 2.90	58.75 ± 2.22
Cell concentration after feeding media (g/L)	3.13 ± 0.03	3.06 ± 0.08	3.04 ± 0.04	3.02 ± 0.08	3.01 ± 0.07
Residual glucose concentration after fermentation (g/L)	0.14 ± 0.07	0.15 ± 0.07	0.21 ± 0.10	0.12 ± 0.06	0.17 ± 0.08
2KGA concentration after fermentation (g/L)	167.88 ± 1.00	169.10 ± 0.59	165.78 ± 0.13	165.02 ± 1.44	163.31 ± 0.87
Cell concentration after fermentation (g/L)	3.71 ± 0.08	3.90 ± 0.08	3.74 ± 0.06	3.81 ± 0.06	3.85 ± 0.07
Produced 2KGA at 2nd stage (g/L)	71.85 ± 2.16	81.34 ± 3.38	91.81 ± 3.94	98.21 ± 4.34	104.56 ± 3.09
2KGA yield at 2nd stage (g/g)	1.0176 ± 0.0104	1.0266 ± 0.0023	1.0303 ± 0.0080	1.0257 ± 0.0081	1.0052 ± 0.0079
Fermentation time at 2nd stage (h)	8.5	9.5	11.0	12.0	13.0
2KGA productivity at 2nd stage (g/L · h)	8.45 ± 0.25	8.56 ± 0.35	8.35 ± 0.36	8.18 ± 0.36	8.04 ± 0.24
In total*					
Total fermentation time (h)	21.5	21.0	21.0	21.0	21.0
Total 2KGA yield (g/g)	0.9760 ± 0.0058	0.9832 ± 0.0035	0.9638 ± 0.0007	0.9594 ± 0.0084	0.9494 ± 0.0051
Total 2KGA productivity (g/L · h)	7.81 ± 0.05	8.05 ± 0.03	7.89 ± 0.01	7.86 ± 0.07	7.78 ± 0.04

**, "In total" refers to the combination of first- and second- stage fermentation.*

TABLE 3 | Effect of removing broth volumes of first-stage on 2KGA production.

Parameters	V/V_1 (%)			
	50.0	**60.0**	**70.0**	**80.0**
First stage				
Initial glucose (g/L)	81.54 ± 1.91	92.04 ± 1.48	104.47 ± 0.91	115.26 ± 0.76
Residual glucose (g/L)	23.94 ± 2.74	24.01 ± 2.25	24.79 ± 2.89	23.49 ± 2.69
Consumption of glucose (g/L)	57.60 ± 1.95	68.03 ± 3.00	79.68 ± 3.61	91.77 ± 2.83
Initial cell concentration (g/L)	1.85 ± 0.06	1.54 ± 0.04	1.18 ± 0.02	0.82 ± 0.04
Final cell concentration (g/L)	3.62 ± 0.04	3.82 ± 0.09	3.90 ± 0.03	4.08 ± 0.16
Initial 2KGA (g/L)	55.72 ± 1.06	44.49 ± 0.72	33.10 ± 0.65	21.91 ± 0.16
Final 2KGA (g/L)	110.50 ± 2.59	109.03 ± 2.06	109.29 ± 3.75	109.16 ± 3.29
Increased 2KGA (g/L)	54.79 ± 3.22	64.54 ± 2.23	76.20 ± 3.17	87.25 ± 3.13
2KGA yield (g/g)	0.9508 ± 0.0337	0.9491 ± 0.0164	0.9564 ± 0.0129	0.9507 ± 0.0077
Fermentation time (h)	6.00 ± 0.50	7.00 ± 0.35	8.00 ± 0.35	10.00 ± 0.50
2KGA productivity (g/L · h)	9.15 ± 0.36	9.23 ± 0.26	9.53 ± 0.23	8.73 ± 0.18
Second stage				
Initial glucose (g/L)	160.47 ± 2.88	133.02 ± 1.40	106.44 ± 2.01	79.87 ± 3.37
Residual glucose (g/L)	0.10 ± 0.05	0.18 ± 0.06	0.15 ± 0.03	0.08 ± 0.01
Initial cell concentration (g/L)	1.81 ± 0.03	2.29 ± 0.04	2.73 ± 0.04	3.26 ± 0.08
Final cell concentration (g/L)	3.73 ± 0.07	3.82 ± 0.06	3.88 ± 0.07	3.89 ± 0.04
Initial 2KGA (g/L)	54.05 ± 2.67	65.39 ± 1.73	75.56 ± 1.95	87.02 ± 3.86
Final 2KGA (g/L)	214.34 ± 1.96	200.22 ± 1.71	184.68 ± 1.92	168.85 ± 2.49
Produced 2KGA (g/L)	160.29 ± 4.63	134.83 ± 3.44	109.12 ± 3.87	81.83 ± 6.35
2KGA yield (g/g)	0.9987 ± 0.0109	1.0135 ± 0.0152	1.0250 ± 0.0171	1.0238 ± 0.0364
Fermentation time (h)	19.5	16.0	13.0	9.5
2KGA productivity (g/L · h)	8.22 ± 0.24	8.43 ± 0.21	8.39 ± 0.30	8.61 ± 0.67
In total*				
Total 2KGA yield (g/g)	0.9743 ± 0.0089	0.9815 ± 0.0084	0.9823 ± 0.0102	0.9817 ± 0.0144
Total fermentation time (h)	25.5	23.0	21.0	19.5
Total 2KGA productivity (g/L · h)	8.41 ± 0.08	8.71 ± 0.07	8.79 ± 0.09	8.66 ± 0.13

**, "In total" refers to the combination of first- and second- stage fermentation.*

TABLE 4 | Effect of feeding glucose concentration on second-stage fermentation.

Parameters	Glucose concentration in feeding media (g/L)				
	250.0	**300.0**	**350.0**	**400.0**	**450.0**
Initial glucose (g/L)	90.35 ± 2.11	105.42 ± 1.24	120.62 ± 1.99	135.63 ± 1.68	150.24 ± 2.28
Residual glucose (g/L)	0.14 ± 0.06	0.15 ± 0.06	0.16 ± 0.07	0.19 ± 0.05	0.21 ± 0.03
Initial cell concentration (g/L)	2.74 ± 0.04	2.73 ± 0.04	2.74 ± 0.04	2.74 ± 0.03	2.73 ± 0.03
Final cell concentration (g/L)	3.99 ± 0.09	3.91 ± 0.03	3.84 ± 0.06	3.80 ± 0.06	3.73 ± 0.06
Initial 2KGA (g/L)	76.47 ± 1.43	76.52 ± 1.61	75.88 ± 1.07	75.38 ± 1.82	76.97 ± 0.57
Final 2KGA (g/L)	168.72 ± 2.07	184.26 ± 1.29	199.19 ± 1.12	215.21 ± 1.93	228.84 ± 2.48
Increased 2KGA (g/L)	92.25 ± 3.25	107.74 ± 1.89	123.31 ± 1.59	139.83 ± 2.06	151.87 ± 2.51
2KGA yield (g/g)	1.0209 ± 0.0210	1.0221 ± 0.0149	1.0224 ± 0.0107	1.0309 ± 0.0097	1.0108 ± 0.0042
Fermentation time (h)	11.5	13.0	14.5	16.0	19.0
2KGA productivity (g/L · h)	8.02 ± 0.28	8.29 ± 0.15	8.50 ± 0.11	8.74 ± 0.13	7.99 ± 0.13
Total 2KGA yield (g/g)*	0.9753 ± 0.0109	0.9801 ± 0.0062	0.9812 ± 0.0050	0.9872 ± 0.0081	0.9821 ± 0.0097
Total fermentation time (h)*	19.5	21.0	22.5	24.0	27.0
Total 2KGA productivity (g/L · h)*	8.65 ± 0.11	8.77 ± 0.06	8.85 ± 0.05	8.97 ± 0.08	8.48 ± 0.09

**, "total" refers to the combination of first- and second- stage fermentation.*

corresponding volumes (50.0%, 60.0%, 70.0%, and 80.0%, *v*/*v*) of fresh media into each first-stage fermentor to bring the final working volume to 35 L, the glucose concentrations changed to 81.54, 92.04, 104.47, and 115.26 g/L, cell densities decreased to 1.85, 1.54, 1.18, and 0.82 g/L, and 2KGA concentrations changed to 55.72, 44.49, 33.10, and 21.91 g/L, respectively. At

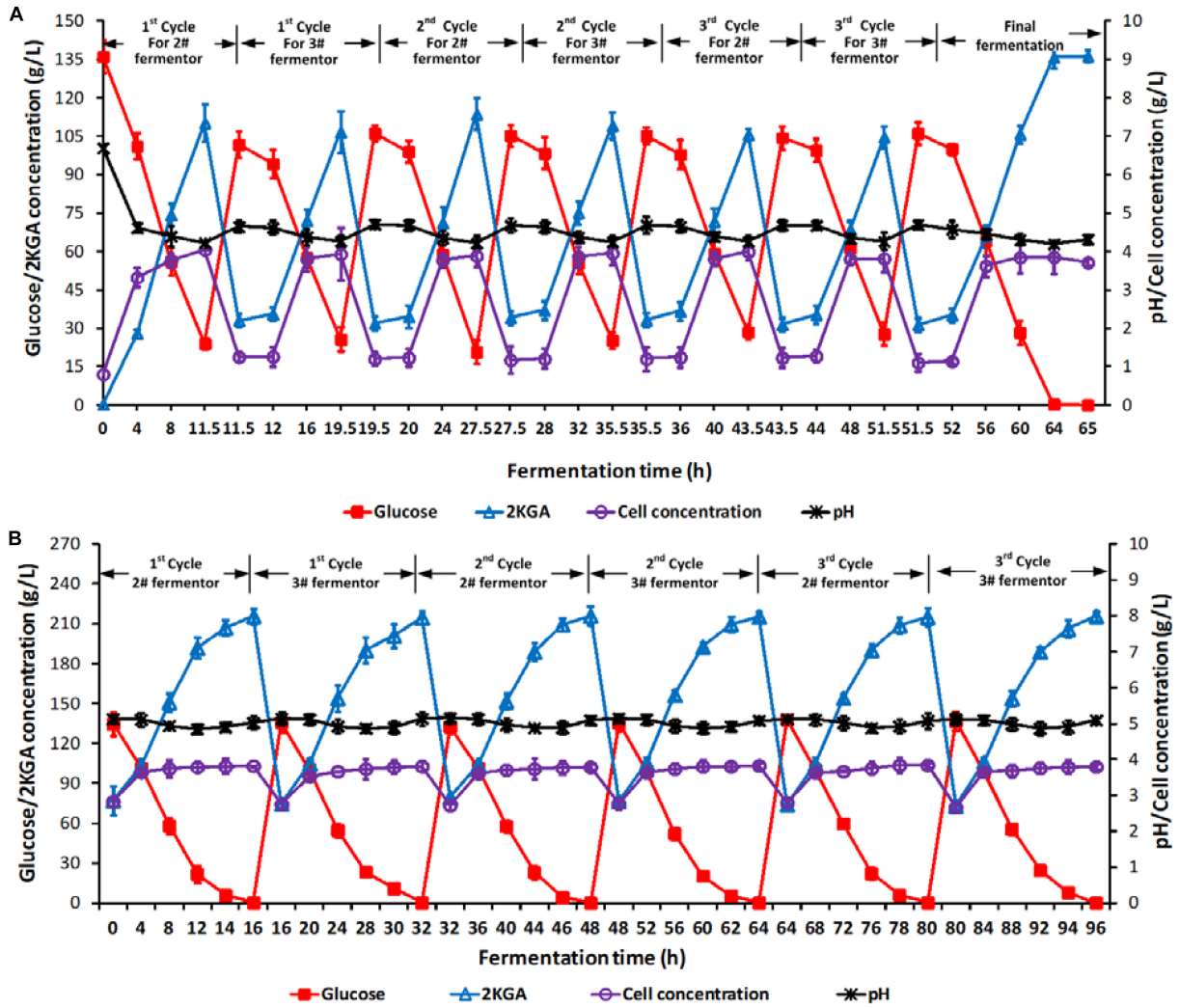

FIGURE 3 | Time courses of 2KGA production, residual glucose concentration, cell concentration and pH in a 3-cycle two-stage semi-continuous fermentation. Time courses of **(A)** 1# fermentor for the first-stage fermentation and **(B)** 2# and 3# fermentors for the second-stage fermentation. Each cycle lasted for 32 h. At the end of first-stage fermentation, 70% (*v*/*v*) of broth (24.5 L) in 1# fermentor was taken out as the inoculum for second-stage fermentation (2# or 3# fermentor), which was started by feeding 10.5 L of 400.0 g/L of glucose. Data are the means of three independent experiments ± standard deviations (n = 3) analyzed in duplicate.

the end, 2KGA concentrations in all experiments reached to about 110.0 g/L. The maximum cell concentration of 3.90 g/L, 2KGA yield of 0.9564 g/g and productivity of 9.53 g/(L · h) were obtained by removing 70.0% (v/v) of the broth (adding 70.0%, v/v, of fresh media). The glucose concentrations in the second-stage fermentation ranged from 79.87 g/L to 160.47 g/L after transferring 80.0%, 70.0%, 60.0% and 50.0% (*v*/*v*) of first-stage broth and feeding corresponding volumes (20%, 30%, 40%, and 50%, *v*/*v*) of media containing 300.0 g/L of glucose. As a consequence, resulting 2KGA concentrations were 160.29, 134.84, 109.12, and 81.83 g/L, respectively. A Maximum yield of 1.0250 g/g was observed with a productivity of 8.39 g/(L · h) when removing volume of first-stage broth was 70.0% (*v*/*v*).

Combining the first- and second-stage of fermentation, removing 70.0% (*v*/*v*) of the volume from the first-stage fermentor could be selected for following study with a total productivity of 8.79 g/(L · h) and yield of 0.9823 g/g, indicating that first-stage fermentation could produce 2KGA at 76.20 g/L and provide a high density of *P. plecoglossicida* JUIM01 cells for highly efficient 2KGA fermentation at the second-stage.

Effect of Feeding Glucose Concentration on Second- Stage Fermentation

A broth volume set at 70.0% (*v*/*v*) (24.5 L) was transferred into the second-stage fermentor, and 10.5 L of fresh media containing various glucose concentrations from 250.0 to 450.0 g/L were fed to investigate their effect on 2KGA fermentation performance. As presented in **Table 4**, after feeding various concentrations of glucose, the initial glucose concentrations in the second-stage fermentor changed with a range from 90.35 to 150.24 g/L with initial 2KGA concentrations of about 76.0 g/L. Increasing the

TABLE 5 | Comparison between the literature results cited and this work in 2KGA fermentation.

Organism	Raw material	Fermentation type	Total fermentation time (h)	2KGA production performance			Reference
				Concentration (g/L)	Productivity (g/L · h)	Yield (g/g)	
Serratia marcescens NRRL B-486	Glucose	Continuous	16∼40	/	/	0.92∼1.08	Minisenhermer et al., 1965
Pseudomonas fluorescens IFO 14808	Glucose	Batch	75	/	/	0.4	Tanimura et al., 2003
Pseudomonas aeruginosa IFO 3448	Cassava	Fed-batch	319	35	0.55	/	Chia et al., 2008
Pseudomonas fluorescens AR4	Rice starch	Semi-continuous	66	444.95	6.74	0.93	Sun et al., 2012
Pseudomonas fluorescens AR4	Corn starch hydrolyzate	Continuous	96	135.92	8.83 (steady state)	0.95	Sun et al., 2013
Arthrobacter globiformis C224	Rice starch hydrolyzate	Continuous	96∼120	124.74	11.23	0.97	Teng et al., 2013
Klebsiella pneumoniae ΔbudA	Glucose	Two-stage fed-batch	26	186	7.15	1.05	Sun et al., 2014
Pseudomonas fluorescens AR4	Glucose	Batch	64	195	3.05	1.07	Sun et al., 2015
Gluconobacter oxidans/pBBR-3510-ga2dh	Gluconic acid	Batch	45	486	10.08	1.01	Shi et al., 2015
Gluconobacter oxydans_tufB_ga2dh	Gluconic acid /glucose	Batch	45/18	453.3/321	10.07/17.83	0.94/1.19*	Li et al., 2016
Pseudomonas plecoglossicida JUIM01	Rice starch hydrolyzate/glucose	Two-stage semi-continuous	96	110.0 (first stage)/ 215.0 (second stage)	9.53 (first stage)/ 8.95 (second stage)	0.9867	In this work

**The yield of 1.19 g/g was calculated by 321 g/L 2KGA dividing 270 g/L of glucose, equivalent to a molar yield of 110.31%. However, the theoretical maximum yield from glucose to 2KGA should be no more than 1.08 g/g glucose. Although the yield reported by Li et al. (2016) is 99.1%, they didn't explain how this number was calculated in their manuscript.*

glucose concentration in the feeding media directly prolonged the fermentation time from 11.5 to 19.0 h, and led to final cell concentrations with a range from 3.99 to 3.73 g/L and 2KGA concentrations from 168.72 g/L to 228.83 g/L. A maximum 2KGA yield of 0.9872 g/g and a higher productivity of 8.97 g/(L · h) were observed by feeding 10.5 L of media containing 400.0 g/L of glucose, which was attributed to the increased produced 2KGA concentration of 139.83 g/L. Hence, feeding media containing 400 g/L of glucose is suitable for second-stage fermentation due to it producing the highest yield, highest produced 2KGA concentration and highest productivity.

2KGA Two-Stage Fermentation Under Optimal Conditions

Two stage semi-continuous fermentation of 2KGA under the optimal conditions by *P. plecoglossicida* JUIM01 was verified for 3 cycles. Briefly, the 11.5-h cultured broth of 70% (*v*/*v*) at the first-stage (1# fermentor) was taken out and transferred into 2# fermentor at the second-stage. 10.5 L of fresh media containing glucose at 400.0 g/L was added into 2# fermentor at the second-stage for another 16-h cultivation until the residual glucose was consumed completely. At the same time, 24.5 L of fresh media containing glucose at 140.0 g/L, corn syrup powder at 7.5 g/L, urea at 0.15 g/L, KH_2PO_4 at 0.1 g/L and $CaCO_3$ at 39.0 g/L was fed into the first-stage fermentor for a further 8-h cultivation with residual glucose of about 24.5 g/L, and 70.0% (*v*/*v*) of total broth volume was taken out and transferred to 3# fermentor at the second-stage. Similarly, 3# fermentor continued to ferment after feeding 10.5 L of fresh media containing glucose at 400.0 g/L until the residual glucose decreased to 0.1 g/L. Each of the two-stage semi-continuous cycles included one batch of first-stage fermentation (1# fermentor, cultivation time of 8.0 h) and one batch of second-stage fermentation (2# fermentor, fermentation time of 16.0 h), and one batch of first-stage fermentation (1# fermentor, cultivation time of 8.0 h) and one batch of second-stage fermentation (3# fermentor, fermentation time of 16.0 h). At the end of the 3rd cycle, all of the three fermentors would end with a residual glucose concentration of 0.1 g/L. **Figure 3** presented the total time courses of the first- (A, 1# fermentor) and second-stage (B, 2# and 3# fermentors) fermentation of *P. plecoglossicida* JUIM01.

As shown in **Figure 3A**, after every taking out 70% of the cultivated broth from 1# fermentor at the first-stage and feeding fresh media, the initial glucose, 2KGA, and cell concentrations in 1# fermentor showed stable levels of approximately 105.0, 33.0, and 1.20 g/L, respectively. At the end of each fermentation, the glucose concentration decreased to about 25.0 g/L, cell density increased to 3.90 g/L and 2KGA concentration increased to 110.0 g/L. The stable 2KGA yield of 0.98 g/g and productivity

of 9.5 g/(L · h) also indicated that the optimal removing volume of 70.0% (V/V_1) could provide a stable cell density and residual glucose for second-stage fermentation.

The initial glucose, 2KGA and cell concentrations in 2# and 3# fermentor (at the second-stage) had comparable levels of 135.0, 75.0, and 2.80 g/L, respectively (**Figure 3B**). After 16.0 h of fermentation, glucose was completely consumed with a final 2KGA concentration of 215.0 g/L and cell concentration of 3.80 g/L. Accordingly, the 2KGA produced from of each run in each fermentor was 139.0 g/L with a total 2KGA yield of 0.988 g/g and productivity of 8.95 g/(L · h), which indicated that the second-stage fermentation under the optimal conditions had a high 2KGA production performance.

During 3-cycle fermentation, 25480.0 g of glucose in total was added in 1# fermentor at the first-stage and 21749.0 g glucose was consumed, resulting in 20703.0 g 2KGA produced with a total yield of 0.9519 g/g. Similarly, 28930.0 g of glucose in total was consumed in 2# and 3# fermentors at the second-stage, and 29302.0 g 2KGA was produced with an average 2KGA production of 215.40 g/L and a total yield of 1.0129 g/g. Hence, combining the first- and second- stages, a total of 50680.0 g of glucose was consumed, and 50005.20 g of 2KGA was produced with an average produced 2KGA concentration of 204.10 g/L and a total yield of 0.9867 g/g.

Comparison of 2KGA Production by Different Culture Strategies

So far, four different fermentation processes including batch, fed-batch, semi-continuous and/or continuous fermentation have been used to produce 2KGA from glucose, cassava, RSH or corn starch hydrolyzate as substrates. 2KGA producing strains and their fermentation performance from this work and from literature reports were presented in **Table 5**. The 2KGA yields ranging from 0.92 g/g glucose to 1.08 g/g glucose were obtained using the continuous fermentation process by *S. marcescens* NRRL B-486 (Minisenhermer et al., 1965). Sun et al. (2014) developed a two-stage fermentation strategy using the first stage to maintain a neutral pH favoring cell growth and second stage which switched to acidic conditions favoring 2KGA accumulation, which produced a total of 186 g/L of 2KGA at 26 h with a conversion ratio of 0.98 mol/mol by *Klebsiella pneumoniae*. Our group had previously investigated 2KGA production strategies including batch, semi-continuous, continuous and even direct bioconversion of glucose using free resting cells of *P. fluorescens* AR4 (Sun et al., 2012, 2013, 2015). The strain *P. fluorescens* AR4 could convert 476.88 g/L of glucose into 444.96 g/L of 2KGA with a total productivity of 6.74 g/L and yield of 0.93 g/g during 4-run semi-continuous fermentation (Sun et al., 2012). At the steady state of continuous process, the amount of 2KGA was determined to be 135.92 g/L with 8.83 g/(L · h) average volumetric productivity and a 0.9510 g/g yield, and achieved a maximum 2KGA production of 195.0 g/L with 3.05 g/(L · h) total productivity and a 1.07 g/g yield during the 64-h direct bioconversion process. In this study, a two-stage semi-continuous fermentation of *P. plecoglossicida* JUIM01 consumed 50680.0 g of glucose and produced 50005.20 g of 2KGA with a total yield of 0.9867 g/g during a 3-cycle fermentation within 32 h. The average productivities of the first- and second- stages were calculated at 9.53 and 8.95 g/(L · h), respectively. Hence, two-stage semi-continuous fermentation inherited advantages such as high 2KGA production performance of semi-continuous process and avoided the lag time for cleaning, sterilization, and inoculation of each turnover. Additionally, the feeding media for the second-stage only consisted of glucose at a high concentration with no addition of either nitrogen or minerals, which would reduce the cost of industrial production.

CONCLUSION

A two-stage semi-continuous fermentation has been developed with the cooperation of 3 fermentors to enhance the 2KGA production performance by *P. plecoglossicida* JUIM01 using RSH as the substrate. A glucose concentration of 140.0 g/L was ideal for the first-stage fermentation due to its highest total 2KGA productivity of 7.58 g/(L · h) and cell concentration of 3.91 g/L. The optimal parameters for two-stage semi-continuous fermentation included 8.0-h fermentation time for the first-stage with a residual glucose concentration of about 25.0 g/L, 70.0% (*v*/*v*) of removing volume, and 400.0 g/L of feeding glucose for the second-stage fermentation. During 3-cycle fermentation, 50680.0 g of glucose was consumed, and 50005.20 g of 2KGA was obtained with a total yield of 0.9867 g/g by *P. plecoglossicida* JUIM01. In conclusion, the proposed two-stage semi-continuous fermentation showed a significant potential for industrial application based on its increased 2KGA production performance including concentration, yield and productivity from glucose in rice starch hydrolyzate, low input of feeding media, and decrease of processing period.

DATA AVAILABILITY STATEMENT

The raw data supporting the conclusions of this article will be made available by the authors, without undue reservation, to any qualified researcher.

AUTHOR CONTRIBUTIONS

W-JS and Z-HX conceived of the study and designed the experiments. LS and D-MW performed and analyzed results and drafted the manuscript. F-JC, J-SG, X-MZ, and J-SS performed partial experiments and analyzed results. All authors read and approved the manuscript.

FUNDING

This work was funded by the National Natural Science Foundation of China (31571885), Science and Technology Platform Construction Program of Jiangxi Province (2010DTZ01900), and the Priority Academic Program Development of Jiangsu Higher Education Institutions.

REFERENCES

Aguilar, F., Crebelli, R., Di Domenico, A., Dusemund, B., Frutos, M. J., Galtier, P., et al. (2016). Scientific opinion on the re-evaluation of erythorbic acid (E 315) and sodium erythorbate (E 316) as food additives. *EFSA J.* 14:4360. doi: 10.2903/j.efsa.2016.4360

Al Helal, A., Soames, A., Gubner, R., Iglauer, S., and Barifcani, A. (2018). Performance of erythorbic acid as an oxygen scavenger in thermally aged lean MEG. *J. Petrol. Sci. Eng.* 170, 911–921. doi: 10.1016/j.petrol.2018.06.073

Bauer, R., Katsikis, N., Varga, S., and Hekmat, D. (2005). Study of the inhibitory effect of the product dihydroxyacetone on *Gluconobacter oxydans* in a semi-continuous two-stage repeated-fed-batch process. *Bioproc. Biosyst. Eng.* 28, 37–43. doi: 10.1007/s00449-005-0009-0

Chia, M., Nguyen, T. B. V., and Choi, W. J. (2008). DO-stat fed-batch production of 2-keto-D-gluconic acid from cassava using immobilized *Pseudomonas aeruginosa*. *Appl. Microbiol. Biot.* 78, 759–765. doi: 10.1007/s00253-008-1374-9

Elseviers, M., Coomans, S. M. J., Lemmens, H. O. J., and Roper, H. W. W. (2000). Process for the production of 2-keto-D-glusonic acid. U.S. Patent No. 6,018,034.

Ji, X. J., Zhang, A. H., Nie, Z. K., Wu, W. J., Ren, L. J., and Huang, H. (2014). Efficient arachidonic acid-rich oil production by *Mortierella alpina* through a repeated fed-batch fermentation strategy. *Bioresource Technol.* 170, 356–360. doi: 10.1016/j.biortech.2014.07.098

Joven, R., Garcia, A., Arias, A., and Medina, J. (2015). Development of an active thermoplastic film with oxygen scavengers made of activated carbon and sodium erythorbate. *Packag. Technol. Sci.* 28, 113–121. doi: 10.1002/pts.2093

Li, K., Mao, X., Liu, L., Lin, J., Sun, M., Wei, D., et al. (2016). Overexpression of membrane-bound gluconate-2-dehydrogenase to enhance the production of 2-keto-D-gluconic acid by *Gluconobacter oxydans*. *Microb. Cell Fact.* 15:121. doi: 10.1186/s12934-016-0521-8

Liang, Y., Yu, K., Wang, J., Chen, J., Sun, B., and Shao, L. (2014). Erythorbic acid promoted synthesis of CdS quantum dots in aqueous solution and study on optical properties. *Colloids Surfaces A* 455, 129–135. doi: 10.1016/j.colsurfa.2014.04.049

Minisenhermer, T. J., Anderson, R. F., Lagoda, A. A., and Tyler, D. (1965). Production of 2-ketogluconic acid by *Serratia marcescens*. *Appl. Microbiol.* 13, 393–396. doi: 10.1128/aem.13.3.393-396.1965

Ping, L., Chen, F., Cui, F., Hu, W., Sun, W., Li, N., et al. (2018). Enhancement of quality retention of *Grifola frondosa* fruiting bodies by erythorbic acid treatment. *3 Biotech* 8:305. doi: 10.1007/s13205-018-1305-0

Shi, Y. Y., Li, K. F., Lin, J. P., Yang, S. L., and Wei, D. Z. (2015). Engineered expression vectors significantly enhanced the production of 2-keto-D-gluconic acid by *Gluconobacter oxidans*. *J. Agric. Food Chem.* 63, 5492–5498. doi: 10.1021/acs.jafc.5b01652

Sun, W. J., Chen, L., Ren, B. L., Zhang, J. G., and Liu, J. Z. (2006). Study on the application of phage-resistant strain *Pseudomonas fluorescens* AR4 in industrial production of 2-keto-D-gluconic acid. *J. Food Sci.* 11, 105–108.

Sun, W. J., Wang, Q. H., Luan, F., Man, Z. W., Cui, F. J., and Qi, X. H. (2019). The role of *kguT* gene in 2-ketogluconate-producing *Pseudomonas plecoglossicida* JUIM01. *Appl. Biochem. Biotechnol.* 187, 965–974. doi: 10.1007/s12010-018-2843-y

Sun, W. J., Xiao, F. F., Wei, Z., Cui, F. J., Yu, L., Yu, S. L., et al. (2015). Non-sterile and buffer-free bioconversion of glucose to 2-keto-gluconic acid by using *Pseudomonas fluorescens* AR4 free resting cells. *Process. Biochem.* 50, 493–499. doi: 10.1016/j.procbio.2015.01.011

Sun, W. J., Yun, Q. Q., Zhou, Y. Z., Cui, F. J., Yu, S. L., Zhou, Q., et al. (2013). Continuous 2-keto-gluconic acid (2KGA) production from corn starch hydrolysate by *Pseudomonas fluorescens* AR4. *Biochem. Eng. J.* 77, 97–102. doi: 10.1016/j.bej.2013.05.010

Sun, W. J., Zhou, Y. Z., Zhou, Q., Cui, F. J., Yu, S. L., and Sun, L. (2012). Semi-continuous production of 2-keto-gluconic acid by *Pseudomonas fluorescens* AR4 from rice starch hydrolysate. *Bioresour. Technol.* 110, 546–551. doi: 10.1016/j.biortech.2012.01.040

Sun, Y., Wei, D., Shi, J., Mojovi, L., Han, Z., and Hao, J. (2014). Two-stage fermentation for 2-ketogluconic acid production by *Klebsiella pneumoniae*. *J. Microbiol. Biotechn.* 24, 781–787. doi: 10.4014/jmb.1401.01038

Tanimura, R., Hamada, A., Ikehara, K., and Iwamoto, R. (2003). Enzymatic synthesis of 2-keto-D-gluconate and 2-keto-D-galactonate from D-glucose and D-galactose with cell culture of *Pseudomonas fluorescens* and 2-keto-galactonate from D-galactono 1,4-lactone with partially purified 2-ketogalactonate reductase. *J. Mol. Catal. B Enzym.* 23, 291–298. doi: 10.1016/s1381-1177(03)00092-4

Teng, W. H., Sun, W. J., Yu, B., Cui, F. J., Qian, J. Y., Liu, J. Z., et al. (2013). Continuous conversion of rice starch hydrolysate to 2-keto-D-gluconic acid by *Arthrobacter globiformis* C224. *Biotechnol. Bioproc. E* 18, 709–714. doi: 10.1007/s12257-012-0831-6

Walker, R. (1991). "Erythorbic acid and its sodium salt," in *Joint FAO/WHO Expert Committee on Food Additives (JEFCA)*, ed. Toxicological evaluation of certain food additives and contaminants (Geneva: World Health Organization), 27–60.

Wang, D. M., Sun, L., Sun, W. J., Cui, F. J., Gong, J. S., Zhang, X. M., et al. (2018). Purification, characterization and gene identification of a membrane-bound glucose dehydrogenase from 2-keto-D-gluconic acid industrial producing strain *Pseudomonas plecoglossicida* JUIM01. *Int. J. Biol. Macromol.* 118, 534–541. doi: 10.1016/j.ijbiomac.2018.06.097

Wei, Z., Yu, S. L., Sun, W. J., Zhou, Q., and Li, Z. B. (2008). Research progress on fermentation production of 2-keto-D-gluconic acid. *J. Food Sci.* 29, 636–639. (In Chinese)

Zhang, Y., Feng, X., Xu, H., Yao, Z., and Ouyang, P. (2010). ε-Poly-L-lysine production by immobilized cells of *Kitasatospora sp. MY* 5-36 in repeated fed-batch cultures. *Bioresour. Technol.* 101, 5523–5527. doi: 10.1016/j.biortech.2010.02.021

Conflict of Interest: W-JS and F-JC had coopereation with Parchn Sodium Isovitamin C Co. Ltd., by providing experimental materials including rice starch hydrolysate, and were/are not employed by company Parchn Sodium Isovitamin C Co. Ltd.

The remaining authors declare that the research was conducted in the absence of any commercial or financial relationships that could be construed as a potential conflict of interest.

frontiers in Bioengineering and Biotechnology

ORIGINAL RESEARCH
published: 17 March 2020
doi: 10.3389/fbioe.2020.00194

High Throughput Screening Platform for a FAD-Dependent L-Sorbose Dehydrogenase

Xiaoyu Shan[1,2,3], *Li Liu*[1,2,4], *Weizhu Zeng*[1], *Jian Chen*[1,2,4] *and Jingwen Zhou*[1,2,4]*

[1] School of Biotechnology and Key Laboratory of Industrial Biotechnology, Ministry of Education, Jiangnan University, Wuxi, China, [2] National Engineering Laboratory for Cereal Fermentation Technology, Jiangnan University, Wuxi, China, [3] The Key Laboratory of Carbohydrate Chemistry and Biotechnology, Ministry of Education, Jiangnan University, Wuxi, China, [4] Jiangsu Provisional Research Center for Bioactive Product Processing Technology, Jiangnan University, Wuxi, China

2-Keto-L-gulonic acid (2-KLG) is the direct precursor for the production of L-ascorbic acid (L-Asc) on industrial scale. Currently, the production of L-Asc in the industry is a two-step fermentation process. Owing to many unstable factors in the fermentation process, the conversion rate of L-sorbose to 2-KLG has remained at about 90% for many years. In order to further improve the production efficiency of 2-KLG, a FAD-dependent sorbose dehydrogenase (SDH) has been obtained in our previous research. The SDH can directly convert L-sorbose to 2-KLG at a very high efficiency. However, the enzyme activity of the SDH is relatively low. In order to further improve the enzyme activity of the SDH, a high throughput screening platform the dehydrogenase is essential. By optimizing the promoter, host and sorbosone dehydrogenase (SNDH), knockout of the aldosterone reductases and PTS related genes, a reliable platform for high-throughput screening of more efficient FAD-dependent SDH has been established. By using the high-throughput screening platform, the titer of the 2-KLG has been improved by 14.1%. The method established here could be useful for further enhancing the FAD-dependent SDH, which is important to achieve the efficient one-strain-single-step fermentation production of 2-KLG.

Keywords: 2-Keto-L-gulonic acid, promoter, sorbose dehydrogenase, sorbosone dehydrogenase, aldosterone reductase, L-sorbose-specific-PTS, error-prone PCR

OPEN ACCESS

Edited by:
Hui Wu,
East China University of Science and Technology, China

Reviewed by:
Zheng-Jun Li,
Beijing University of Chemical Technology, China
Liya Liang,
University of Colorado Boulder, United States

***Correspondence:**
Jingwen Zhou
zhoujw1982@jiangnan.edu.cn

Specialty section:
This article was submitted to Industrial Biotechnology, a section of the journal Frontiers in Bioengineering and Biotechnology

Received: *15 December 2019*
Accepted: *27 February 2020*
Published: *17 March 2020*

Citation:
Shan X, Liu L, Zeng W, Chen J and Zhou J (2020) High Throughput Screening Platform for a FAD-Dependent L-Sorbose Dehydrogenase. Front. Bioeng. Biotechnol. 8:194. doi: 10.3389/fbioe.2020.00194

INTRODUCTION

Vitamin C, also known as L-ascorbic acid (L-Asc), is an essential nutrient for human beings and occupies the largest global market among vitamins. It can affect cells by participating in the elimination of reactive oxygen species (Wenzel et al., 2004), promoting collagen production (May and Qu, 2005), and helping immune defense (Carr and Maggini, 2017). At present, the main L-Asc production method is the classical two-step fermentation process, which uses *Gluconobacter oxydans* to convert D-sorbitol to L-sorbose, and uses *Ketogulonigenium vulgare* and *Bacillus megaterium* to further convert L-sorbose to 2-keto-L-gulonic acid (2-KLG). The process has two fermentation steps and requires two times of sterilization, resulting in high energy consumption and long production period (Liu et al., 2011a,b). Besides, compared with commonly used single-fermentation fermentation, both regulation and breeding of mixed fermentation are more difficult (Kim et al., 2019). To achieve the one-step-single-strain production of 2-KLG is a long pursued goal for the vitamin C industry.

In order to achieve the one-step-single-strain production of 2-KLG, previous attempts could be divided into several groups: (1) Overexpression of sorbose dehydrogenase (SDH) and sorbosone dehydrogenase (SNDH) from *K. vulgare* in *G. oxydans* or other bacteria (Gao et al., 2014). Since the SDH from *K. vulgare* could also interact with D-sorbitol to form other byproducts, the yield of 2-KLG on D-sorbitol by this method remains to be lower than 65%. (2) Overexpression of 2,5-diketo-D-gluconate reductase from *Corynebacterium glutamicum* in *Erwinia sp*. that can product 2,5-diketo-D-gluconate from D-glucose (Anderson et al., 1985). For potential low enzyme activity or cofactor balance issues, 2-KLG titer could not be significantly improved by using the method. (3) Overexpression of SDH and SNDH from *G. oxydans* T100 in *G. oxydans* strains that can produce 2-KLG from D-sorbitol (Saito et al., 1997). When expressing the SDH gene from *G. oxydans* T100 in *E. coli*, the SDH cannot catalyze L- sorbose to 2-KLG, suggesting that it may be a major limiting step to increase the enzyme activity of this SDH. According to these previous reports, the main problems in achieving one-step-single-strain fermentation of 2-KLG include cofactor regeneration (Wang et al., 2016; Kim et al., 2019), identification of key enzymes, competition of intermediate metabolic byproducts (Richter et al., 2009).

In our recent report, we obtained a *G. oxydans* strain by high-throughput screening aided with 2-KLG dehydrogenase (Chen et al., 2019). A FAD-dependent SDH that can convert L-sorbose to 2-KLG with almost 100% conversion efficiency has been identified from the strain. However, the enzyme activity of the SDH is very low and can only produce several grams of 2-KLG by different optimization method. Based the previous reports about other SDHs that can convert L-sorbose to L-sorbosone or 2-KLG (Zhou et al., 2012; Gao et al., 2017), both substrate/product specificity and enzyme activity should be improved by high-throughput screening. Since the slow growth rate of *G. oxydans* and low transformation efficiency (Yao et al., 2017; Jin et al., 2019), *G. oxydans* itself is not suitable for high-throughput screening of efficient SDH. Therefore, it is essential to construct a high-throughput screening platform strain with fast growth and high transformation efficiency. Since the SDH could be functional expressed in *E. coli* to catalyze L-sorbose to 2-KLG, *E. coli* could be a good choice (Chen et al., 2019). Though D-sorbitol, L-sorbose, L-sorbosone and 2-KLG are not commonly acquired in *E. coli*, the aldosterone reductases and PTS-related proteins could affect the regular function of SDH and thus interrupt the high-throughput screening process.

This study was focused on establishment of a high-throughput screening platform of a FAD-dependent SDH from *G. oxydans* WSH-003 based on *E. coli*, and then improve the enzyme activity of the SDH. By optimizing the promoter of the SDH, it was found that introduction of SDH in *E. coli* not only produce 2-KLG, there are also some byproducts could be found. In order to achieve more reliable screening process, the aldosterone reductases and PTS related genes are knockout consequently, combined with the co-expression of a SNDH. By using the high-throughput screening system, the titer of the 2-KLG has been improved by 14.1%. The method established here could be useful for further enhancing the FAD-dependent SDH, which is important to achieve the efficient one-strain-single-step fermentation production of 2-KLG.

TABLE 1 | Primers used for promoter optimization.

Primer	Sequence 5′-3′
infC-rplT-F	gcgcggatcttccagagattctgaatacgttaacgaattgacgc
infC-rplT-R	agttcttctcccttacccatacctttattcctccaattgtttaagac
lpp-F	gcgcggatcttccagagatttgaatccgatggaagcatcctg
lpp-R	agttcttctcccttacccattattaataccctctagattgagttaatctc
cspA-F	cgcggatcttccagagattattgctgtttacggtcctgatg
cspA-R	agttcttctcccttacccatagtgtattacctttaataattaagtgtgcc
dnaKJ-F	gcggatcttccagagatttcttgtcctgccatatcgcg
dnaKJ-R	agttcttctcccttacccatctaaacgtctccactatatattcgg
csrA-F	gcgcggatcttccagagatttacctgcagcgttagccagtg
csrA-R	agttcttctcccttacccatagtgtattacctttaataattaagtgtgcc
SDH-R	gttcttctcccttacccattcaggcgttcccctgaatgaaatc
infC-rplT-*SDH*-F	aacaattggaggaataaggtatgacgagcggttttgattacatcg
lpp-*SDH*-F	caatctagagggtattaataatgacgagcggttttgattacatcg
cspA-*SDH*-F	attattaaaggtaatacactatgacgagcggttttgattacatcg
dnaKJ-*SDH*-F	tatatagtggagacgtttagatgacgagcggttttgattacatcg
csrA-*SDH*-F	aatctttcaaggagcaaagaatgacgagcggttttgattacatcg

MATERIALS AND METHODS

Genes, Plasmids, and Strains

E. coli JM109 was used for plasmid construction and preservation. *E. coli* BL21 (DE3) was used for gene expression research. The plasmids pCas and pTarget required for gene knockout were provided by Shanghai Institute of Plant Physiology and Ecology (Jiang et al., 2015). *G. oxydans* WSH-004 was screened in our previous research (Chen et al., 2019).

Plasmid Construction and Gene Expression

Five constitutive promoters with different strength ($P_{infC-rplT}$, P_{lpp}, P_{dnaKJ}, P_{cspA}, P_{csrA}) have been selected to express SDH (Zhou et al., 2017). These promoters were obtained by PCR amplification using the *E. coli* K12 genome as the template. SDH gene was PCR-amplified from the genomic DNA of *G. oxydans* WSH-004. The target gene SDH and these promoters were ligated into the vector pMD19-T-Simple by a one-step cloning kit (Takara, Dalian, China). All the primers used for expression of SDH are listed **Table 1**. These plasmids have also been transformed into *E. coli* K12substr. W3110, *E. coli* K12substr. MG1655, *E. coli* JM109 for selecting optimum *E. coli* host.

Culture Conditions

E. coli strains with plasmids are plated on LB plates with 100 mg/L of ampicillin and cultured overnight. A single colony is picked into a 14 mL shaker tube containing 4 ml LB medium and then cultured for 9–10 h as seed culture. The seed culture was then inoculated with an inoculation ratio of 2% into a 250 mL shake flask containing 25 mL of LB medium with 1% L-sorbose,

firstly incubated at 37°C for 3 h, and then transferred to 25, 30, 37, and 40°C, respectively, for optimizing the temperature for enzyme expression.

Simultaneous Overexpression of SDH and SNDH

For simultaneous overexpression of SDH and SNDH, the highest yielding constitutive promoter P_{cspA} was selected as pMD19-cspA-SDH. *E. coli* BL21(DE3) competent cell was simultaneously transfected into pMD19-cspA-SDH and pET28a-SNDH. Both SDH and SNDH were from *G. oxydans* WSH-004. Single colonies were picked into seed culture medium for 9 h, then transferred to a 250 mL shake flask containing 25 mL of LB medium with 1% L-sorbose by 2% inoculum, then incubated at 37°C for 2–3 h until about OD_{600} = 0.6–1, adding IPTG with a final concentration of 0.3 mM, transferring to a 30°C shaker for subsequent fermentation, taking samples at different times and used HPLC to detect for 2-KLG yield.

For optimizing sorbosone dehydrogenase (SNDH) from different sources, five SNDH from other sources were synthesize the five SNDH genes. To construct plasmids for overexpression of SNDH in *E. coli* BL21 (DE3), SNDH genes were inserted into the *Hin*dIII/*Eco*RI site of pET28(a)+. These plasmids containing SNDH werer transformed into *E. coli* BL21 (DE3) strain containing SDH plasmid to achieve the co-expression of SDH and SNDH in *E. coli*.

Knockout of Aldosterone Reductase Genes

The aldosterone reductase genes, *yiaK, ahr, dkgA, dkgB, yahK, yajO, ydjG, yeaE*, have been amplified from genomic DNA of *E. coli* BL21 (DE3) by using *yiaK*-UP-F/R, *yiaK*-Down-F/R, *ahr*-UP-F/R, *ahr*-Down-F/R, *dkgA*-UP-F/R, *dkgA*-Down-F/R, *dkgB*-UP-F/R, *dkgB*-Down-F/R, *yahK*-UP-F/R, *yahK*-Down-F/R, *yajO*-UP-F/R, *yajO*-Down-F/R, *ydjG*-UP-F/R, *ydjG*-Down-F/R, *yeaE*-UP-F/R, *yeaE*-Down-F/R, respectively, to obtain upstream and downstream homology arm fragments. These genes of homologous arm were obtained by overlapping PCR using PrimerSTAR DNA polymerase. All the primers are listed in **Table 2**. The pCas plasmid can generate sgRNA located on the pTarget plasmid under IPTG induction, and the pCas plasmid itself will be incubated at 42°C. A series of pTarget plasmids were constructed containing the target gene N20-sgRNA of aldosterone reductase genes by primer sequences listed in **Table 2**. Knockout of these genes by CRISPR/Cas9 are performed according to the previous report (Jiang et al., 2015).

Knockout of Related Genes About L-Sorbose-Specific-PTS

By using the CRISPR/Cas9 technology, continued to knock out six related genes (*ptsG, fruA, pfkA*, *ptsH*, *ptsI*, *glcA*) in L-sorbose-specific PTS was based on the original strain *E. coli* BL21 (DE3) and *E. coli* BL21 (DE3)-8. A series of pTarget plasmids were constructed containing the target gene N20-sgRNA of aldosterone reductase genes by primer sequences listed in **Table 3**. Knockout of these genes by CRISPR/Cas9 are performed according to the previous report (Jiang et al., 2015). Using the *E. coli* BL21 (DE3) genome as a template, respectively, amplify using PrimerSTAR DNA polymerase, using *ptsG*-UP-F/R, *ptsG*-Down-F/R, *fruA*-UP-F/R, *fruA*-Down-F/R, *glcA*-UP-F/R,

TABLE 2 | Primers used for knockout aldosterone reductases.

Primer	Sequence 5′-3′
yahK-UP-F	ccagggagtggggcaatctgaatatg
yahK-UP-R	attatgtggcgcagctactgtattccgccccacaatttcatgacccggca
yahK-Down-F	tgccgggtcatgaaattgtggggcggaatacagtagctgcgccacataat
yahK-Down-R	ccaggcactatcagaaatcgctcat
yahK-sgRNA-F	gtggctcctttgttgtgtgcgttttagagctagaaatagcaagtt
yahK-sgRNA-R	gcacacaacaaaggagccacactagtattatacctaggactgagc
dkgA-UP-F	aggaggaacgtatggctaatccaac
dkgA-UP-R	cttccggctctgcatgatgatgtccggtgatggatctggaagttgcacac
dkgA-Down-F	gtgtgcaacttccagatccatcaccggacatcatcatgcagagccggaag
dkgA-Down-R	gctgccatgattgctgacaatatc
dkgA-sgRNA-F	ccattagcgcaaggagggaagttttagagctagaaatagcaagtt
dkgA-sgRNA-R	ttccctccttgcgctaatggactagtattatacctaggactgagc
dkgB-UP-F	gccagaatcgcaaaaatcctctgca
dkgB-UP-R	agaggcttaatcccattcaggagcccggccagtggattagagtcagatca
dkgB-Down-F	tgatctgactctaatccactggccgggctcctgaatgggattaagcctct
dkgB-Down-R	gcgctggtacgttaacggattcca
dkgB-sgRNA-F	gaagggttgacgcgtgagatgttttagagctagaaatagcaagtt
dkgB-sgRNA-R	atctcacgcgtcaacccttcactagtattatacctaggactgagc
ahr-UP-F	ggctggaacgcttaaatgatgcttc
ahr-UP-R	gcggtaatcagatcaactgcgagcacttatgagctgcgtaagctgatgcg
ahr-Down-F	cgcatcagcttacgcagctcataagtgctcgcagttgatctgattaccgc
ahr-Down-R	cgttgtggattatacctgtcgcacg
ahr-sgRNA-F	caaaatagggctgccagtcggttttagagctagaaatagcaagtt
ahr-sgRNA-R	cgactggcagccctattttgactagtattatacctaggactgagc
yeaE-UP-F	cgcgtgtatctgaatccacaaga
yeaE-UP-R	ggcattgaactcggtttaaccctcacaatatcagcgcggcacaagtattg
yeaE-Down-F	caatacttgtgccgcgctgatattgtgagggttaaaccgagttcaatgcc
yeaE-Down-R	cgggtattggtgtgcagtggaac
yeaE-sgRNA-F	atctgctgttgctggcaccagttttagagctagaaatagcaagtt
yeaE-sgRNA-R	tggtgccagcaacagcagatactagtattatacctaggactgagc
yajO-UP-F	tcggcgtctatctttgtcatcagac
yajO-UP-R	gtaatcacgcatggacactgccggaattatcggtacatcgcgggaagaac
yajO-Down-F	gttcttcccgcgatgtaccgataattccggcagtgtccatgcgtgattac
yajO-Down-R	tctggaaatggccaccagccatg
yajO-sgRNA-F	gcccggtttactcaacaaccgttttagagctagaaatagcaagtt
yajO-sgRNA-R	ggttgttgagtaaaccgggcactagtattatacctaggactgagc
ydjG-UP-F	tcatcttccagcttctcaagatcgc
ydjG-UP-R	cctttaggcacaacggatattacgc ccgctatgtcgtgataatggcattg
ydjG-Down-F	caatgccattatcacgacatagcgg gcgtaatatccgttgtgcctaaagg
ydjG-Down-R	acaaaccgtaacggcagtctgtggg
ydjG-sgRNA-F	agctggcttctacctcttcggttttagagctagaaatagcaagtt
ydjG-sgRNA-R	cgaagaggtagaagccagctactagtattatacctaggactgagc
yiaK-UP-F	ccatgtagatcttgcccattgcg
yiaK-UP-R	gcgcgatatgtccaaaaatcatgacctcaaatgtcactttcatcccaggc
yiaK-Down-F	gcctgggatgaaagtgacatttgaggtcatgatttttggacatatcgcgc
yiaK-Down-R	ttcaagtcgcatgtgcagcaacct
yiaK-sgRNA-F	ggcgcaaaagagtgtcgcatgttttagagctagaaatagcaagtt
yiaK-sgRNA-R	atgcgacactcttttgcgccactagtattatacctaggactgagc

glcA-Down-F/R, *ptsI-ptsH*-UP-F/R, *ptsI-ptsH*-Down-F/R, as a pair primer to obtain upstream and downstream homology arm fragments. These genes of homologous arm were obtained by overlapping PCR using PrimerSTAR DNA polymerase. All the primers are listed in **Table 3**.

Error-Prone PCR

Error-prone PCR of SDH was performed by the GeneMorph II Random Mutagenesis Kit (Agilent, Santa Clara, CA) with pMD19-cspA-SDH as a template by using primer pair 5′-TTC CAGAGATTATTGCTGTTTACGG-3′/5′-GTGAAAAGTTCT TCTCCCTTACCCA-3′. The amplified fragment carrying A tail was directly cloned with the vector pMD19-Simple transformed into *E. coli* BL21 (DE3) derivative strains mentioned above. For primary screening, the colonies appeared on the LB plates with ampicillin were picked up into 96-deep well plates by QPix420 (MD, Genetix, UK). These cultured cells in the deep-well plate were cultured at 37°C for 2–3 h, then moved to culture at 30°C for 20–24 h. For high-throughput screening, 40 uL of supernatant was transferred into another 96-well plate, then mixed with buffer containing 2-KLG reductase and NADH to a total volume 200 uL. The last one of each 96-well plate was set as a control. The absorbance at 340 nm, which is the optimum absorbance for NADH, was detected by a microplate reader (BioTek, Winooski, VT).

TABLE 3 | Primers used for knockout of PTS related genes.

Primer	Sequence 5′-3′
ptsG-UP-F	actcaccttaccttgcgccggtacc
ptsG-UP-R	gtaccgaaaatcgcctgaacaccagaaccgcctgcttctgccataacatg
ptsG-Down-F	catgttatggcagaagcaggcggttctggtgttcaggcgattttcggtac
ptsG-Down-R	ggcgcaattaccgacaactggcagc
ptsG-sgRNA-F	tccttcatttggccgccgatgttttagagctagaaatagcaagtt
ptsG-sgRNA-R	atcggcggccaaatgaaggaactagtattatacctaggactgagc
fruA-UP-F	caacgccaggttttgtgcaatatt
fruA-UP-R	cggtaaaaatgtctggctgggtgatagcgaaagcagcgtaataaaaggtg
fruA-Down-F	cacctttattacgctgctttcgctatcacccagccagacatttttaccg
fruA-Down-R	tgaaacctaaccgccgcgagctgga
fruA-sgRNA-F	aaactgatggcaccacacgggttttagagctagaaatagcaagtt
fruA-sgRNA-R	ccgtgtggtgccatcagtttactagtattatacctaggactgagc
glcA-UP-F	cggcatcactgatagaaaaacaggtg
glcA-UP-R	gacatgtcgctggagcaataaccctatcgaccacggcgcagcaaatcaac
glcA-Down-F	gttgatttgctgcgccgtggtcgatagggttattgctccagcgacatgtc
glcA-Down-R	gcgaaagtggttgatcagcaaaacg
glcA-sgRNA-F	agaacggcacaagaaccgacgttttagagctagaaatagcaagtt
glcA-sgRNA-R	gtcggttcttgtgccgttctactagtattatacctaggactgagc
pfkA-UP-F	ttgatatcgtgacttcctggccggg
pfkA-UP-R	gctgttcgttctggatacctacgcacgctgtaacggtctagctgtaccat
pfkA-Down-F	atggtacagctagaccgttacagcgtgcgtaggtatccagaacgaacagc
pfkA-Down-R	actgttcgtacaattcgcgcgttgg
pfkA-sgRNA-F	gaagtgatgggccgttattggttttagagctagaaatagcaagtt
pfkA-sgRNA-R	caataacggcccatcacttcactagtattatacctaggactgagc
ptsI-ptsH-UP-F	gcaggtatctcttctggagcagctg
ptsI-ptsH-UP-R	ccagcgtcattaactcgtccgttgtagcggtaatggtaacttcttgctgg
ptsI-ptsH-Down-F	ccagcaagaagttaccattaccgctacaacggacgagttaatgacgctgg
ptsI-ptsH-Down-R	gcgaaagtggttgatcagcaaaacg
ptsI-ptsH-sgRNA-F	gttgtgactatctccgcagagttttagagctagaaatagcaagtt
ptsI-ptsH-sgRNA-R	tctgcggagatagtcacaacactagtattatacctaggactgagc

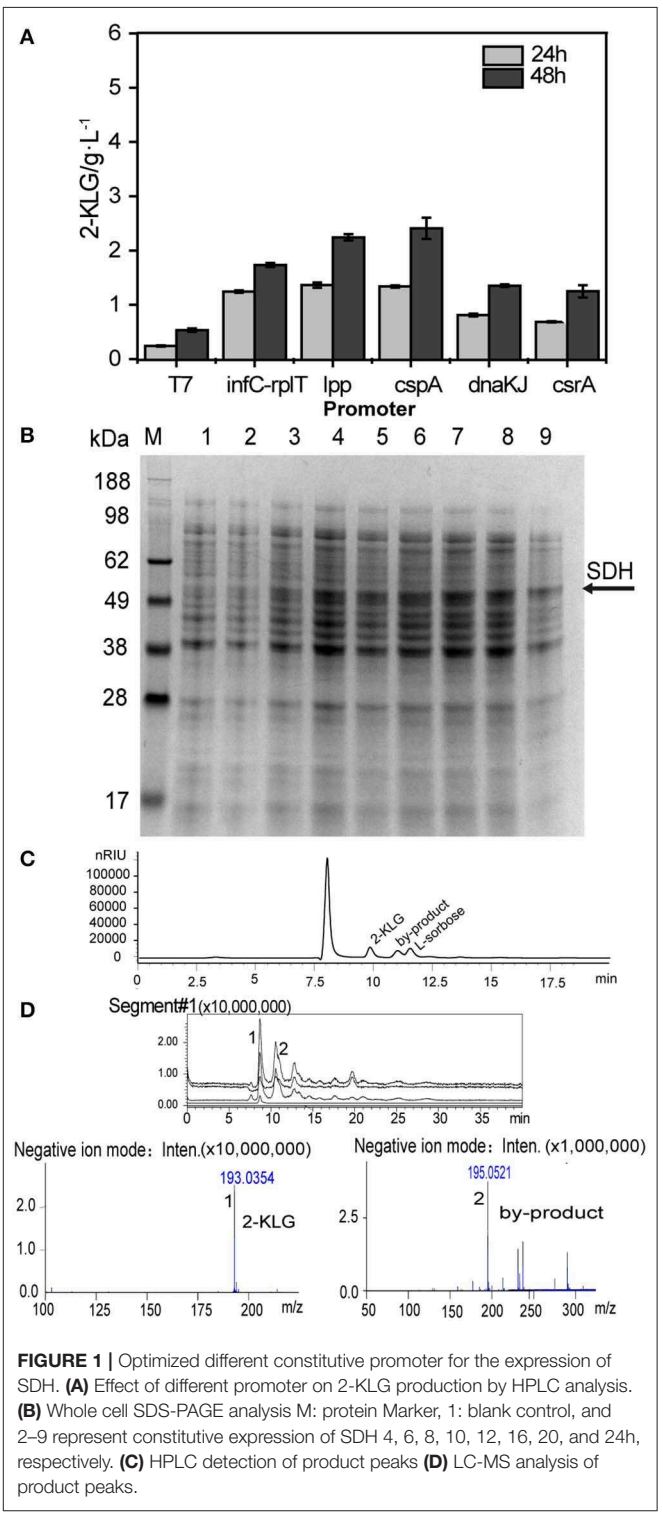

FIGURE 1 | Optimized different constitutive promoter for the expression of SDH. **(A)** Effect of different promoter on 2-KLG production by HPLC analysis. **(B)** Whole cell SDS-PAGE analysis M: protein Marker, 1: blank control, and 2–9 represent constitutive expression of SDH 4, 6, 8, 10, 12, 16, 20, and 24h, respectively. **(C)** HPLC detection of product peaks **(D)** LC-MS analysis of product peaks.

HPLC and Liquid Chromatography Ion Trap Time-Of-Flight Mass Spectrometry (LCMS-IT-TOF) Assays

L-sorbose and 2-KLG were determined by a HPLC equipped with an Aminex HPX-87H column (Bio-Rad, Hercules, CA) at 35°C with a flow rate of 0.5 mL/min and 5 mmol/L H_2SO_4 as the eluent (Gao et al., 2014). For LC-MS analysis, a Shimadzu LCMS-IT-TOF (Shimadzu, Kyoto, Japan) equipped with an Aminex HPX-87H column was used. The HPLC conditions for LCMS-IT-TOF analysis is: 35°C with a flow rate of 0.5 mL/min and 5 mmol/L formic acid as the eluent. IT-TOF detection was performed with an ESI source in negative ion mode at the followed conditions: detector voltage, 1.60 kV; nebulizing gas (N2) flow, 1.5 L/min; drying gas (N2) flow, 200 kPa; ion accumulation time, 30 ms; and scan range (*m/z*), 100–300 for MS1(Chen et al., 2019).

RESULTS

Overexpression of the FAD-Dependent L-Sorbose Dehydrogenase in *E. coli*

Five *E. coli* BL21 (DE3) strains that express the FAD-dependent SDH with different promoters were constructed and applied for the shake flask culture to produce 2-KLG with 10 g/L of L-sorbose as a substrate. The sampled culture broth was then detected by HPLC (**Figure 1A**). T7 and five constitutive promoters were applied to optimize the expression of SDH in *E. coli*. The results showed that the promoter P_{cspA} could achieve to 2.42 g/L, which is the highest 2-KLG titer among the strains. SDS-PAGE results showed that the promoter P_{cspA} could significantly express SDH, which has a molecular weight of SDH was 57.6 kDa (**Figure 1B**). Since both the titer and the conversion ratio is relatively low, it cannot be directly applied for the high-throughput screening of the SDH. The HPLC and LC-MS results showed that besides the L-sorbose and 2-KLG, there is also an unknown byproduct (**Figures 1C,D**). This by-product was produced in the middle of the fermentation stage. As the fermentation progresses, the by-product gradually decreased. At the end of the fermentation, the by-product peak was almost disappeared.

Optimized Production of 2-KLG From L-Sorbose

By expressing the SDH with the optimum promoter P_{cspA} in different *E. coli* strains, it was found that SDH could convert L-sorbose to 2-KLG in *E. coli* K-12 substr. W3110, *E. coli*

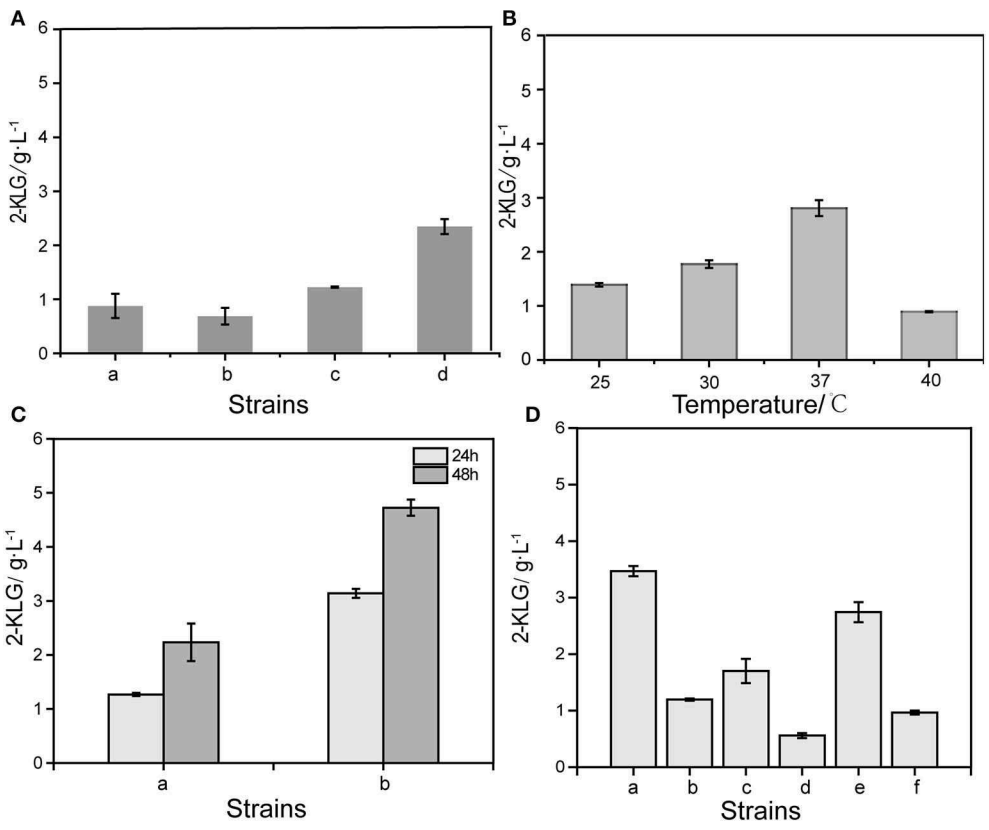

FIGURE 2 | Optimized different conditions of 2-KLG yield from L-sorbose. **(A)** Optimized host cells for expression of sorbose dehydrogenase. a: *E.coli* JM109, b: *E.coli* K-12substr.W3110, c: *E.coli* K-12substr.MG1655, d: *E.coli* BL21(DE3). **(B)** Optimized the effect of culture temperature on the yield of 2-KLG. **(C)** Effect of co-expression of SDH/SNDH on 2-KLG production. a: Control, b: T-cspA-SDH/pET28a-SNDH. **(D)** Optimized the effects of different sources of sorbosone dehydrogenase (SNDH) on the yield of 2-KLG. a: sndh-WSH-004, b: sndh-02655, c: sndh-02935, d: sndh-03750, e: sndh-04500, f: sndh-19405.

TABLE 4 | Strains deficient in aldosterone reductases and PTS system.

Strains	Genotypes
E. coli BL21 (DE3)-3	Δ *ptsG:* Δ *fruA:* Δ *glcA*
E. coli BL21 (DE3)-4	Δ *ptsG:* Δ*fruA:* Δ *glcA:* Δ *pfkA*
E. coli BL21 (DE3)-6	Δ *ptsG:* Δ*fruA:* Δ *glcA:* Δ *pfkA* Δ*ptsH:* Δ*ptsI*
E. coli BL21 (DE3)-8	Δ*dkgB:* Δ *ahr:* Δ *yajO:* Δ *yiaK:* Δ *yahK:* Δ *ydjG:* Δ *yeaE:* Δ*dkgA*
E. coli BL21(DE3)-8-SDH	Δ*dkgB:* Δ *ahr:* Δ *yajO:* Δ *yiaK:* Δ *yahK:* Δ *ydjG:* Δ *yeaE:* Δ*dkgA*, SDH
E. coli BL21(DE3)-8-SDH-SNDH	Δ*dkgB:* Δ *ahr:* Δ *yajO:* Δ *yiaK:* Δ *yahK:* Δ *ydjG:* Δ *yeaE:* Δ*dkgA*, SDH, SNDH
E. coli BL21 (DE3)-11	Δ*dkgB:* Δ*ahr*: Δ*yajO*: Δ*yiaK*: Δ*yahK*: Δ*ydjG*: Δ*yeaE*: Δ*dkgA*: Δ*ptsG*: Δ*fruA*: Δ*glcA*
E. coli BL21 (DE3)-12	Δ*dkgB:* Δ*ahr*: Δ*yajO*: Δ*yiaK*: Δ*yahK*: Δ*ydjG*: Δ*yeaE*: Δ*dkgA*: Δ*ptsG*: Δ*fruA*: Δ*glcA*: Δ *pfkA*
E. coli BL21 (DE3)-13	Δ*dkgB:* Δ*ahr*: Δ*yajO*: Δ*yiaK*: Δ*yahK*: Δ*ydjG*: Δ*yeaE*: Δ*dkgA*: Δ*ptsG*: Δ*fruA*: Δ*glcA*: Δ *ptsH*: Δ *ptsI*
E. coli BL21 (DE3)-14	Δ*dkgB:* Δ*ahr*: Δ*yajO*: Δ*yiaK*: Δ*yahK*: Δ*ydjG*: Δ*yeaE*: Δ*dkgA*: Δ*ptsG*: Δ*fruA*: Δ*glcA*: Δ *pfkA*: Δ *ptsH*: Δ *ptsI*

K-12 substr. MG1655, *E. coli* JM109 and *E. coli* BL21 (DE3) (**Figure 2A**). The result showed that the SDH could yield highest 2-KLG titer in *E. coli* BL21 (DE3), while the 2-KLG titers in the other three strains are low. Then the *E. coli* BL21 (DE3) was selected as the host for the downstream experiments. The *E. coli* BL21 (DE3) strain with the plasmid pMD19-cspA-SDH was subjected to shake flask fermentation at 4 different temperatures to obtain the optimum temperature for enzyme expression (**Figure 2B**). The results showed that the optimum temperature for 2-KLG production was 37°C, under which the 2-KLG titer could reached to 2.83 g/L. Furthermore, when simultaneous expression of pMD19-cspA-SDH and pET28a-SNDH in *E. coli* BL21 (DE3), the 2-KLG titer could be further improved to 2.54 g/L at 48 h (**Figure 2C**). Base on the results, different SNDH have been co-expressed. The results showed that co-expression of SNDH from WSH-004 could achieve the highest 2-KLG titer (**Figure 2D**).

Effects of Aldosterone Reductases Knockout on 2-KLG Production in *E. coli*

By knocking out the 8 aldosterone reductase gene using the CRISPR/Cas9 technology, an *E. coli* strain without aldosterone reductases, *E. coli* BL21(DE3)-8 (**Table 4**) has been obtained. Then the SDH or SDH/SNDH was transferred into the aldosterone reductases defective strain to form *E. coli* BL21(DE3)-8-SDH and *E. coli* BL21(DE3)-8-SDH-SNDH. By culture of *E. coli* BL21(DE3)-8-SDH in shake flasks using 10 g/L of L-sorbose as the substrate, the 2-KLG titer was slightly decreased from 2.58 to 2.32 g/L, while the 2-KLG titer of *E. coli* BL21(DE3)-8-SDH-SNDH was increased from 4.43 to 5.85 g/L. The results suggested that the aldosterone reductases could play important roles in the function of SDH and SNDH.

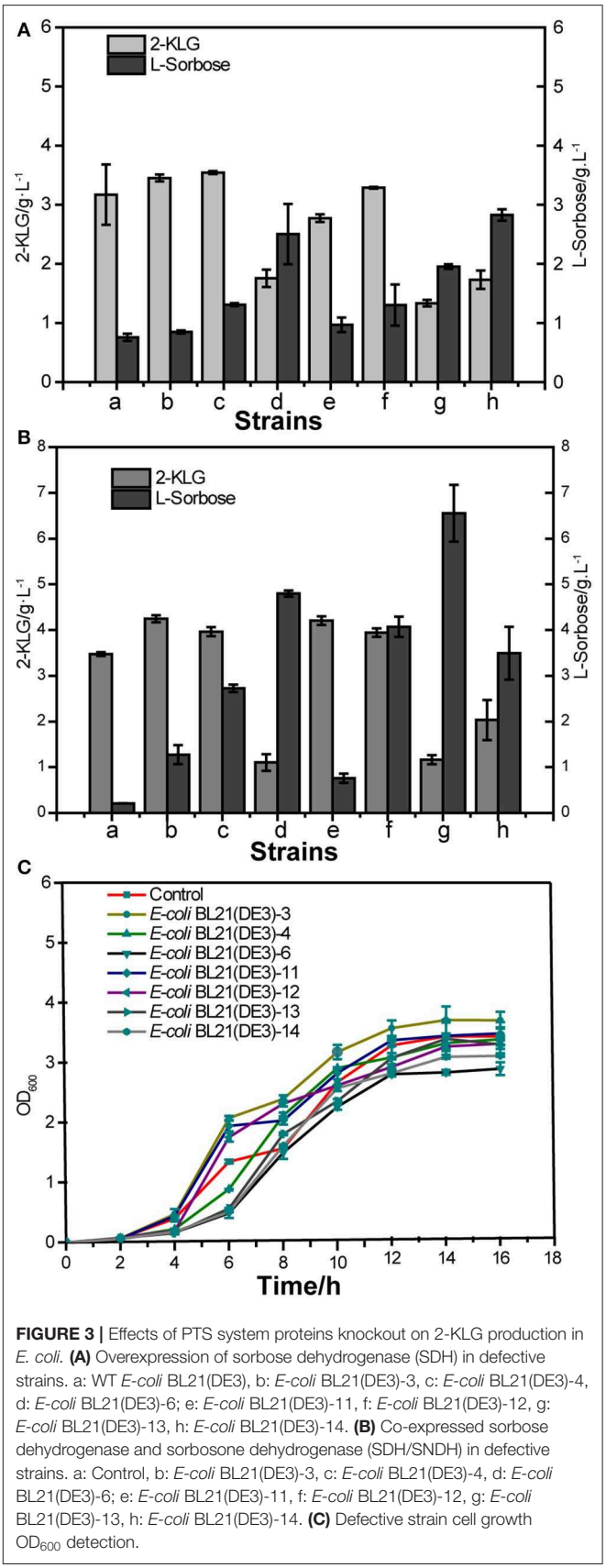

FIGURE 3 | Effects of PTS system proteins knockout on 2-KLG production in *E. coli*. **(A)** Overexpression of sorbose dehydrogenase (SDH) in defective strains. a: WT *E-coli* BL21(DE3), b: *E-coli* BL21(DE3)-3, c: *E-coli* BL21(DE3)-4, d: *E-coli* BL21(DE3)-6; e: *E-coli* BL21(DE3)-11, f: *E-coli* BL21(DE3)-12, g: *E-coli* BL21(DE3)-13, h: *E-coli* BL21(DE3)-14. **(B)** Co-expressed sorbose dehydrogenase and sorbosone dehydrogenase (SDH/SNDH) in defective strains. a: Control, b: *E-coli* BL21(DE3)-3, c: *E-coli* BL21(DE3)-4, d: *E-coli* BL21(DE3)-6; e: *E-coli* BL21(DE3)-11, f: *E-coli* BL21(DE3)-12, g: *E-coli* BL21(DE3)-13, h: *E-coli* BL21(DE3)-14. **(C)** Defective strain cell growth OD_{600} detection.

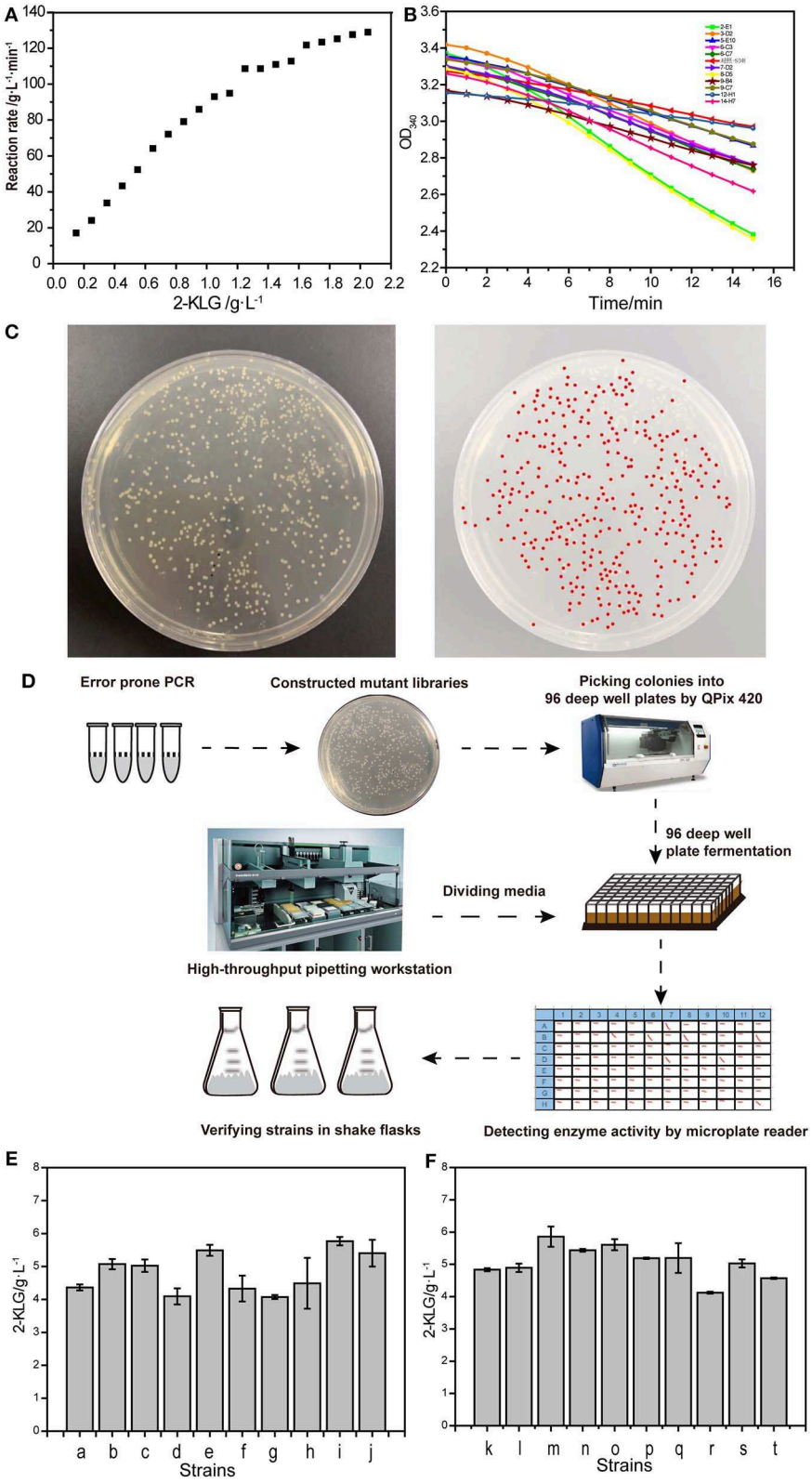

FIGURE 4 | High-throughput screening system. **(A)** Reaction rate of 2-KLG reductase with different concentrations of 2-KLG. **(B)** High-throughput preliminary screening visual map based on microplate reader. **(C)** A typical colony EP-PCR result. **(D)** The workflow of high-throughput screening method. **(E)** Verify of the strains in shake flasks (batch 1). a: Control, b: co-2-E1, c: co-8-D5, d: co-9-B4, e: co-6-F7, f: co-6-C3, g: co-5-E10, h: co-3-D2, i: co-15-A7, j: co-16-B6. **(F)** Verify of the strains in shake flasks (batch 2). k: Control, l: co-20-A1, m: co-28-B1, n: co-19-C1, o: co-15-D1, p: co-33-E1, q: co-6-F1, r: co-8-G1, s: co-25-H1, t: co-5-H5.

Effects of PTS System Proteins Knockout on 2-KLG Production in *E. coli*

Seven PTS system proteins knockout strains were constructed to evaluate the effect of these proteins on the 2-KLG production, i. e., *E. coli* BL21 (DE3)-3, *E. coli* BL21 (DE3)-4, *E. coli* BL21 (DE3)-6, *E. coli* BL21 (DE3)-11, *E. coli* BL21 (DE3)-12, *E. coli* BL21 (DE3)-13, *E. coli* BL21 (DE3)-14 (**Table 4**). Then SDH or SDH/SNDH were overexpressed in these strains, respectively. The results of shake flask fermentation showed that knockout of *ptsH* and *ptsI* could significantly improve the 2-KLG titer in strains either overexpression of SDH or SDH/SNDH (**Figures 3A,B**). The results also showed that knocking out *ptsH* and *ptsI* had a great effect on the growth of the cells in the early stage, while the cell growth could achieve the similar level to that of the control strain (**Figure 3C**).

High Throughput Screening of Sorbose Dehydrogenase in *E. coli*

It was determined that the optimal limited range for detection of 2-KLG with 2-KLG reductase was 0–0.23 (g/L) (**Figure 4A**). A series of mutants was obtained by using the mutation kit. The initial screening was performed by using microplate reader (**Figure 4B**). Around 1.3×10^4 mutants were screened for each round. **Figure 4C** showed one typical colony EP-PCR result by using the workflow shown in **Figure 4D**. The optimum mutants obtained by preliminary screening were subjected for rescreening with shake flasks. Six strains with higher 2-KLG titer was obtained by rescreening (**Figures 4E,F**), namely co-2-E1, co-16-B6, co-8-D5, co-6-F7, co-15-A7, co-28-B1, increased by 7.1, 10.4, 6.6, 11.3, 14.1, and 10.2%, respectively. The specific amino acid mutations of these beneficial mutants were shown in **Table 5**. The results showed that the method established here can be used for high-throughput screening of enhanced SDH. In theory, when the GeneMorph II Random Mutagenesis Kit could yield the similar the probability of mutation of the target gene to A, T, G, and C base. However, 80% of the target gene was mutated to A or T base in the screened SDH, indicating that the gene may have a preference for A or T bases.

TABLE 5 | Mutation sites in SDHs.

Mutants	Mutation sites
co-2-E1	Cys17Arg, Gly134Asp, Ile234Val, Val280Met, Trp316Arg, Thr325Asn
co-16-B6	Lys313Glu, Glu274Ile
co-8-D5	Leu44Gln, Glu66Gly, Tyr78Phe, Gly141Val, Asn147Ile, Val159Ala, Ile221Phe, Arg273His, Thr304Ala, Asp407Val, Val490Asp
co-6-F7	Thr443Ile, Gly276Asp
co-15-A7	His59Gln, Glu243Gly, Met326Leu, Ser349Pro
co-28-B1	Lys53Arg, Thr65Ala, Thr96Ala, Asp118His, Val119Asp, Ser146Thr, Asn152Thr, Ile234Asn, Asn236Asp, Ser348Thr, Gly377Trp, Ser510Thr

DISCUSSION

SDH with high substrate/product specificity and high enzyme activity is vital for achieving one-step-single-strain production of 2-KLG from D-sorbitol. A FAD-dependent SDH obtained by our previous work has high substrate/product specificity while low enzyme activity was used to improve the enzyme activity by high-throughput screening. By optimizing the promoter, hosts and SNDHs, knockout of the aldosterone reductases and PTS related genes, a reliable platform for high-throughput screening of more efficient FAD-dependent SDH has been established. By using the high-throughput screening system, the titer of the 2-KLG has been improved by 14.1%.

At present, most of the recent researches on the one-step-single-strain production of L-Asc were carried out in the *G. oxydans* (**Table 6**) (Wang et al., 2018). The SDH has a similar sequence to that of the *G. oxydans* T100, which could directly convert D-sorbitol to 2-KLG (Saito et al., 1997). When overexpression of the SDH from *G. oxydans* T100 in another *G. oxydans* G624, the titer of 2-KLG could achieve to 130 g/L (Saito et al., 1997). However, when synthesize the SDH and SNDH from *G. oxydans* T100 in *G. oxydans* strains available in our lab, no more than 10 g/L of 2-KLG could be obtained. Unlike a majority of the common enzymes, these SDHs from *G. oxydans* are highly hypercritical to strains without any known disciplines according to our experiments, such as: (1) The SDHs from one *G. oxydans* strain cannot be functional in other *G. oxydans* strains and other common bacteria; (2) *E. coli* strains express the SDHs could have the ability to convert L-sorbose to 2-KLG, while the broken cells cannot, even with common exogenous electron acceptors for dehydrogenases (DCIP, PMS). These strange phenomena significantly affect the further rational engineering of the SDHs from *G. oxydans*. Since the slow growth rate of *G. oxydans* and low transformation efficiency (Yao et al.,

TABLE 6 | Production of -KLG by different microorganisms.

Microorganisms (year)	Substrate	Concentration (g/L)	Titer (g/ L)	Yield (mol/ mol)
G. oxydans T-100 (1997)	D-Sorbitol	50	7.0	13.1%
P.putida IFO3738 (2001)	D-Sorbitol	50	11.6	21.8%
G.oxydans (pGUC-k0203-GS-k0095-pqqABCDE) (2014)	D-Sorbitol	150	39.2	24.5%
G. oxydans-ss-pqqABCDE (2016)	D-Sorbitol	150	44.5	27.8%
G. melanogenus Z84 (1990)	D-Sorbitol	100	60.0	55.7%
G. oxydans NB6939 (pSDH-tufB1) (1997)	D-Sorbitol	150	130.0	81.3%

2017; Jin et al., 2019), *G. oxydans* itself is not suitable for high-throughput screening of efficient SDH. *E. coli* could be a common host for the high-throughput screening of enzymes by using error-prone PCR.

By optimizing the promoters and the host of *E. coli*, it was found that not only the conversion ratio of L-sorbose to 2-KLG was low, there was also some byproducts that may be associated with the SDH. In order to decrease the accumulation of by-product, several means have been attempted, such as coexpression of SNDH (Fu et al., 2007; Du et al., 2013), blocked the potential competition pathway of L-sorbose to 2-KLG by knocking out the aldosterone reductase genes (Yum et al., 1998; Penning, 2015). According to reports in the gene of *Klebsiella*, the transport of L-sorbose into bacteria requires the L-sorbose-specific phosphotransferase system (PTS) (Slater et al., 1981; Wehmeier et al., 1995; Yebra et al., 2000). Therefore, knockout of PTS related genes in *E. coli* has also been attempted, including PtsG (glucose phosphoryl transferase) (Han et al., 2004), FruA (fructose phosphoryl transferase), PfkA (phosphofructokinase) (Vinopal et al., 1975), PtsH (phosphorylated carrier protein), PtsI (phosphotransferase I) (Woodward and Charles, 1982), and GlcA (glycolate transporter) (Sprenger and Lengeler, 1984). Though the interactions of SDH with these genes remains unclear, our results demonstrated that knockout of some of the genes could significantly enhance the function of SDH in *E. coli*, which could benefit the high-throughput screening of enhanced SDH in *E. coli*.

After investigated a majority of the SDHs reported in *G. oxydans* in our lab, the enzyme activity in either *G. oxydans* or *E. coli* is far away from the requirement for competition with the current industrial scale vitamin C process. Though it has been reported that the *G. oxydans* strain can be directly mutagenized to enhance its performance in 2-KLG production (Park et al., 2012; Zhu et al., 2012; Yang et al., 2017), there was no reports on the directed evolution of SDH from *G. oxydans*. In this study, it was found that only overexpression of SDH in *E. coli* BL21 (DE3) could produce 2-KLG. Though the current mixed fermentation system for the production of 2-KLG has been extensively studied (Takagi et al., 2010; Yang et al., 2015), production of 2-KLG in *E. coli* are rarely investigated. The results presented here could provide a useful reference for the metabolic engineering of L-sorbose to 2-KLG in *E. coli*. In this work, overexpression of a FAD-dependent SDH from *G. oxydans* WSH-004 in *E. coli* was studied. Owing to its unique characteristics, this SDH could be used to directly produce 2-KLG from L-sorbose with high substrate/product specificity. A platform strain suitable for high-throughput screening of SDH was constructed. The screening platform strain constructed here should be a model strain suitable for further enhancing the production of 2-KLG by either *G. oxydans* or other bacteria.

DATA AVAILABILITY STATEMENT

The raw data supporting the conclusions of this article will be made available by the authors, without undue reservation, to any qualified researcher.

AUTHOR CONTRIBUTIONS

JZ and JC provided the main core ideas of the experimental design. WZ, LL, and XS mainly searched for references, designed of experimental methods, purchase of consumables and reagents used in the experimental process, operated experiment and analysis of data, drawing of charts, and writing of articles.

FUNDING

This work was supported by grants from the National Natural Science Foundation of China (Key Program, 31830068), the National Science Fund for Excellent Young Scholars (21822806), the Fundamental Research Funds for the Central Universities (JUSRP51701A), the National First-class Discipline Program of Light Industry Technology and Engineering (LITE2018-08), the Distinguished Professor Project of Jiangsu Province, and the 111 Project (111-2-06).

REFERENCES

Anderson, S., Marks, C. B., Lazarus, R., Miller, J., Stafford, K., Seymour, J., et al. (1985). Production of 2-Keto-L-Gulonate, an intermediate in L-Ascorbate synthesis, by a genetically modified *Erwinia herbicola*. *Science* 230, 144–149. doi: 10.1126/science.230.4722.144

Carr, A. C., and Maggini, S. (2017). Vitamin C and immune function. *Nutrients* 9:25. doi: 10.3390/nu9111211

Chen, Y., Liu, L., Shan, X., Du, G., Zhou, J., and Chen, J. (2019). High-throughput screening of a 2-Keto-L-Gulonic acid-producing *Gluconobacter oxydans* strain based on related dehydrogenases. *Front. Bioeng. Biotechnol.* 7:385. doi: 10.3389/fbioe.2019.00385

Du, J., Bai, W., Song, H., and Yuan, Y. J. (2013). Combinational expression of sorbose/sorbosone dehydrogenases and cofactor pyrroloquinoline quinone increases 2-keto-L-gulonic acid production in *Ketogulonigenium vulgare-Bacillus* cereus consortium. *Metab. Eng.* 19, 50–56. doi: 10.1016/j.ymben.2013.05.006

Fu, S., Zhang, W., Guo, A., and Wang, J. (2007). Identification of promoters of two dehydrogenase genes in *Ketogulonicigenium vulgare* DSM 4025 and their strength comparison in *K-vulgare* and *Escherichia coli*. *Appl. Microbiol. Biotechnol.* 75, 1127–1132. doi: 10.1007/s00253-007-0930-z

Gao, L., Hu, Y., Liu, J., Du, G., Zhou, J., and Chen, J. (2014). Stepwise metabolic engineering of *Gluconobacter oxydans* WSH-003 for the direct production of 2-keto-L-gulonic acid from D-sorbitol. *Metab. Eng.* 24, 30–37. doi: 10.1016/j.ymben.2014.04.003

Gao, Y., Zeng, W., Zhou, J., and Chen, J. (2017). Purification and characterization of L-sorbose dehydrogenase and L-sorbosone dehydrogenase from *Ketogulonicigenium vulgare* WSH-001. *Wei Sheng Wu Hsueh Pao Acta Microbiol. Sin.* 57, 1546–1554. doi: 10.13343/j.cnki.wsxb.20160499

Han, C., Zhang, W. C., You, S., and Huang, L. Y. (2004). Knockout of the ptsG Gene in *Escherichia coli* and cultural characterization of the mutants. *Chin. J. Biotechnol.* 20, 16–20. doi: 10.13345/j.cjb.2004.01.004

Jiang, Y., Chen, B., Duan, C., Sun, B., Yang, J., and Yang, S. (2015). Multigene editing in the *Escherichia coli* genome via the CRISPR-Cas9 system. *Appl. Environ. Microbiol.* 81, 2506–2514. doi: 10.1128/AEM.04023-14

Jin, C., Hou, W., Yao, R., Zhou, P., Zhang, H., and Bao, J. (2019). Adaptive evolution of *Gluconobacter oxydans* accelerates the conversion rate of

non-glucose sugars derived from lignocellulose biomass. *Bioresour. Techn.* 289:121623. doi: 10.1016/j.biortech.2019.121623

Kim, T. S., Hui, G., Li, J., Kalia, V. C., Muthusamy, K., Sohng, J. K., et al. (2019). Overcoming NADPH product inhibition improves D-sorbitol conversion to L-sorbose. *Sci. Rep.* 9:815. doi: 10.1038/s41598-019-48082-8

Liu, L., Li, Y., Zhang, J., Zhou, Z., Liu, J., Li, X., et al. (2011a). Complete genome sequence of the industrial strain *Ketogulonicigenium vulgare* WSH-001. *J. Bacteriol.* 193, 6108–6109. doi: 10.1128/JB.06007-11

Liu, L., Li, Y., Zhang, J., Zou, W., Zhou, Z., Liu, J., et al. (2011b). Complete genome sequence of the industrial strain *Bacillus megaterium* WSH-002. *J. Bacteriol.* 193, 6389–6390. doi: 10.1128/JB.06066-11

May, J. M., and Qu, Z. C. (2005). Transport and intracellular accumulation of vitamin C in endothelial cells: relevance to collagen synthesis. *Arch. Biochem. Biophys.* 434, 178–186. doi: 10.1016/j.abb.2004.10.023

Park, C. S., Yang, H. J., Kim, D. H., Kang, D. O., Kim, M. S., and Choi, N. S. (2012). A screening method for beta-glucan hydrolase employing Trypan Blue-coupled beta-glucan agar plate and beta-glucan zymography. *Biotechnol. Lett.* 34, 1073–1077. doi: 10.1007/s10529-012-0873-z

Penning, T. M. (2015). The aldo-keto reductases (AKRs): overview. *Chem. Biol. Interact.* 234, 236–246. doi: 10.1016/j.cbi.2014.09.024

Richter, N., Neumann, M., Liese, A., Wohlgemuth, R., Eggert, T., and Hummel, W. (2009). Characterisation of a recombinant NADP-dependent glycerol dehydrogenase from *Gluconobacter oxydans* and its application in the production of L-Glyceraldehyde. *Chembiochem* 10, 1888–1896. doi: 10.1002/cbic.200900193

Saito, Y., Ishii, Y., Hayashi, H., Imao, Y., Akashi, T., Yoshikawa, K., et al. (1997). Cloning of genes coding for L-sorbose and L-sorbosone dehydrogenases from *Gluconobacter oxydans* and microbial production of 2-Keto-L-Gulonate, a precursor of L-ascorbic acid, in a recombinant *G-oxydans* strain. *Appl. Environ. Microbiol.* 63, 454–460. doi: 10.1128/AEM.63.2.454-460.1997

Slater, A. C., Jones-Mortimer, M. C., and Kornberg, H. L. (1981). L-Sorbose phosphorylation in *Escherichia coli* K-12. *Biochim. Biophys. Acta.* 646, 365–367. doi: 10.1016/0005-2736(81)90346-1

Sprenger, G. A., and Lengeler, J. W. (1984). L-Sorbose metabolism in *Klebsiella pneumoniae* and Sor+ derivatives of *Escherichia coli* K-12 and chemotaxis toward sorbose. *J. Bacteriol.* 157, 39–45. doi: 10.1128/JB.157.1.39-45.1984

Takagi, Y., Sugisawa, T., and Hoshino, T. (2010). Continuous 2-Keto-l-gulonic acid fermentation by mixed culture of *Ketogulonicigenium vulgare* DSM 4025 and *Bacillus megaterium* or *Xanthomonas maltophilia*. *Appl. Microbiol. Biotechnol.* 86, 469–480. doi: 10.1007/s00253-009-2312-1

Vinopal, R. T., Clifton, D., and Fraenkel, D. G. (1975). PfkA locus of *Escherichia coli*. *J. Bacteriol.* 122, 1162–1171. doi: 10.1128/JB.122.3.1162-1171.1975

Wang, P., Zeng, W., Xu, S., Du, G., Zhou, J., and Chen, J. (2018). Current challenges facing one-step production of l-ascorbic acid. *Biotechnol. Adv.* 36, 1882–1899. doi: 10.1016/j.biotechadv.2018.07.006

Wang, P. P., Xia, Y., Li, J. H., Kang, Z., Zhou, J. W., and Chen, J. (2016). Overexpression of pyrroloquinoline quinone biosynthetic genes affects L-sorbose production in *Gluconobacter oxydans* WSH-003. *Biochem. Eng. J.* 112, 70–77. doi: 10.1016/j.bej.2016.04.011

Wehmeier, U. F., Wöhrl, B. M., and Lengeler, J. W. (1995). Molecular analysis of the phosphoenolpyruvate-dependent L-sorbose: phosphotransferase system from *Klebsiella pneumoniae* and of its multidomain structure. *Mol. Gen. Genet.* 246, 610–618. doi: 10.1007/bf00298968

Wenzel, U., Nickel, A., Kuntz, S., and Daniel, H. (2004). Ascorbic acid suppresses drug-induced apoptosis in human colon cancer cells by scavenging mitochondrial superoxide anions. *Carcinogenesis* 25, 703–712. doi: 10.1093/carcin/bgh079

Woodward, M. J., and Charles, H. P. (1982). Genes for l-sorbose utilization in *Escherichia coli*. *J. Gen. Microbiol.* 128, 1969–1980. doi: 10.1099/00221287-128-9-1969

Yang, W., Han, L., Mandlaa, M., Zhang, H., Zhang, Z., and Xu, H. (2017). A plate method for rapid screening of *Ketogulonicigenium vulgare* mutants for enhanced 2-keto-L-gulonic acid production. *Braz. J. Microbiol.* 48, 397–402. doi: 10.1016/j.bjm.2017.02.002

Yang, Y., Gao, M., Yu, X. D., Zhang, Y. H., and Lyu, S. X. (2015). Optimization of medium composition for two-step fermentation of vitamin C based on artificial neural network-genetic algorithm techniques. *Biotechnol. Biotechnol. Equip.* 29, 1128–1134. doi: 10.1080/13102818.2015.1063970

Yao, R., Hou, W., and Bao, J. (2017). Complete oxidative conversion of lignocellulose derived non-glucose sugars to sugar acids by *Gluconobacter oxydans*. *Bioresour. Technol.* 244, 1188–1192. doi: 10.1016/j.biortech.2017.08.078

Yebra, M. J., Veyrat, A., Santos, M. A., and Pérez-Martínez, G. (2000). Genetics of L-sorbose transport and metabolism in *Lactobacillus casei*. *J. Bacteriol.* 182, 155–163. doi: 10.1128/jb.182.1.155-163.2000

Yum, D. Y., Lee, B. Y., Hahm, D. H., and Pan, J. G. (1998). The yiaE gene, located at 80.1 minutes on the *Escherichia coli* chromosome, encodes a 2-ketoaldonate reductase. *J. Bacteriol.* 180, 5984–5988. doi: 10.1128/JB.180.22.5984-5988.1998

Zhou, J., Du, G., and Chen, J. (2012). Metabolic engineering of microorganisms for vitamin C production. *Subcell. Biochem.* 64, 241–259. doi: 10.1007/978-94-007-5055-5_12

Zhou, S., Ding, R., Chen, J., Du, G., Li, H., and Zhou, J. (2017). Obtaining a panel of cascade promoter-5′-UTR complexes in *Escherichia coli*. *ACS Synth. Biol.* 6, 1065–1075. doi: 10.1021/acssynbio.7b00006

Zhu, Y. B., Liu, J. D., Liu, J., Du, G. C., Zhou, J. W., and Chen, J. (2012). A high throughput method to screen companion bacterium for 2-keto-L-gulonic acid biosynthesis by co-culturing *Ketogulonicigenium vulgare*. *Process Biochem.* 47, 1428–1432. doi: 10.1016/j.procbio.2012.05.010

Conflict of Interest: The authors declare that the research was conducted in the absence of any commercial or financial relationships that could be construed as a potential conflict of interest.

frontiers in Bioengineering and Biotechnology

MINI REVIEW
published: 20 March 2020
doi: 10.3389/fbioe.2020.00207

A Review of the Biotechnological Production of Methacrylic Acid

*Juliana Lebeau, John P. Efromson and Michael D. Lynch**

Department of Biomedical Engineering, Duke University, Durham, NC, United States

Industrial biotechnology can lead to new routes and potentially to more sustainable production of numerous chemicals. We review the potential of biobased routes from sugars to the large volume commodity, methacrylic acid, involving fermentation based bioprocesses. We cover the key progress over the past decade on direct and indirect fermentation based routes to methacrylic acid including both academic as well as patent literature. Finally, we take a critical look at the potential of biobased routes to methacrylic acid in comparison with both incumbent as well as newer greener petrochemical based processes.

Keywords: methacrylic acid, methyl-methacrylate, fermentation, sustainability, bioprocessing

OPEN ACCESS

Edited by:
Lucia Gardossi,
University of Trieste, Italy

Reviewed by:
Sujit Jagtap,
University of Illinois at Urbana-Champaign, United States
Farshad Darvishi,
University of Maragheh, Iran

****Correspondence:***
Michael D. Lynch
michael.lynch@duke.edu

Specialty section:
This article was submitted to Industrial Biotechnology, a section of the journal Frontiers in Bioengineering and Biotechnology

Received: *22 January 2020*
Accepted: *02 March 2020*
Published: *20 March 2020*

Citation:
Lebeau J, Efromson JP and Lynch MD (2020) A Review of the Biotechnological Production of Methacrylic Acid. Front. Bioeng. Biotechnol. 8:207. doi: 10.3389/fbioe.2020.00207

INTRODUCTION

Methacrylic acid (MA) and its ester (methyl methacrylate, MMA) are primarily polymerized into polymethylmethacrylate (PMMA) which is used in the production of acrylic glass (Dormer et al., 1998). Acrylic glass is used in components of electronics, automobile parts, lights (LEDs), signs, and displays (Brydson, 1999; Nagai and Ui, 2004; Ali et al., 2015)[1]. Notably, PMMA has a high biocompatibility and low acute toxicity enabling use in medical applications (Frazer et al., 2005). MMA pricing ranges from \$1.75 to \$2.25 /kg[2,3,4] with an annual market that will exceed \$8 billion USD by 2025, growing at a rate of 8–9% per year.

This increasing demand for MA is not only due to increased demand for acrylic glass, but also the increasing number of new applications for MMA (Brydson, 1999). MMA will continue to be a critical monomer in the future with currently no equivalent replacement (Ali et al., 2015). As demand will continue to grow, more sustainable methods of production need to be considered. Numerous efforts have been made to increase sustainability and reduce waste in petrochemical processes. Recent advances in chemical processes have enabled alternative petrochemical feedstocks and reduced waste (Johnson et al., 2009; Witczak et al., 2010). Additionally, the International Energy Agency in 2012 designated MA as a suitable target for the design of a bio-based process (Burk and Van Dien, 2016)[1].

Both petrochemical processes and biobased routes have their own strengths and weaknesses. In this review, we discuss the current states of and recent advances in both petrochemical and biobased routes to MMA. We review different bio-based routes as well as the performance requirements of

[1]PMMA Market Size Worth \$8.16 Billion By 2025|CAGR: 8.4%. https://www.grandviewresearch.com/press-release/global-polymethyl-methacrylate-pmma-industry.
[2]PMMA Production, Price and Market Demand. Plastics Insight https://www.plasticsinsight.com/resin-intelligence/resin-prices/pmma/.
[3]https://dataweb.usitc.gov/
[4]https://www.plasticsinsight.com/resin-intelligence/resin-prices/pmma/ and https://www.grandviewresearch.com/press-release/global-polymethyl-methacrylate-pmma-industry

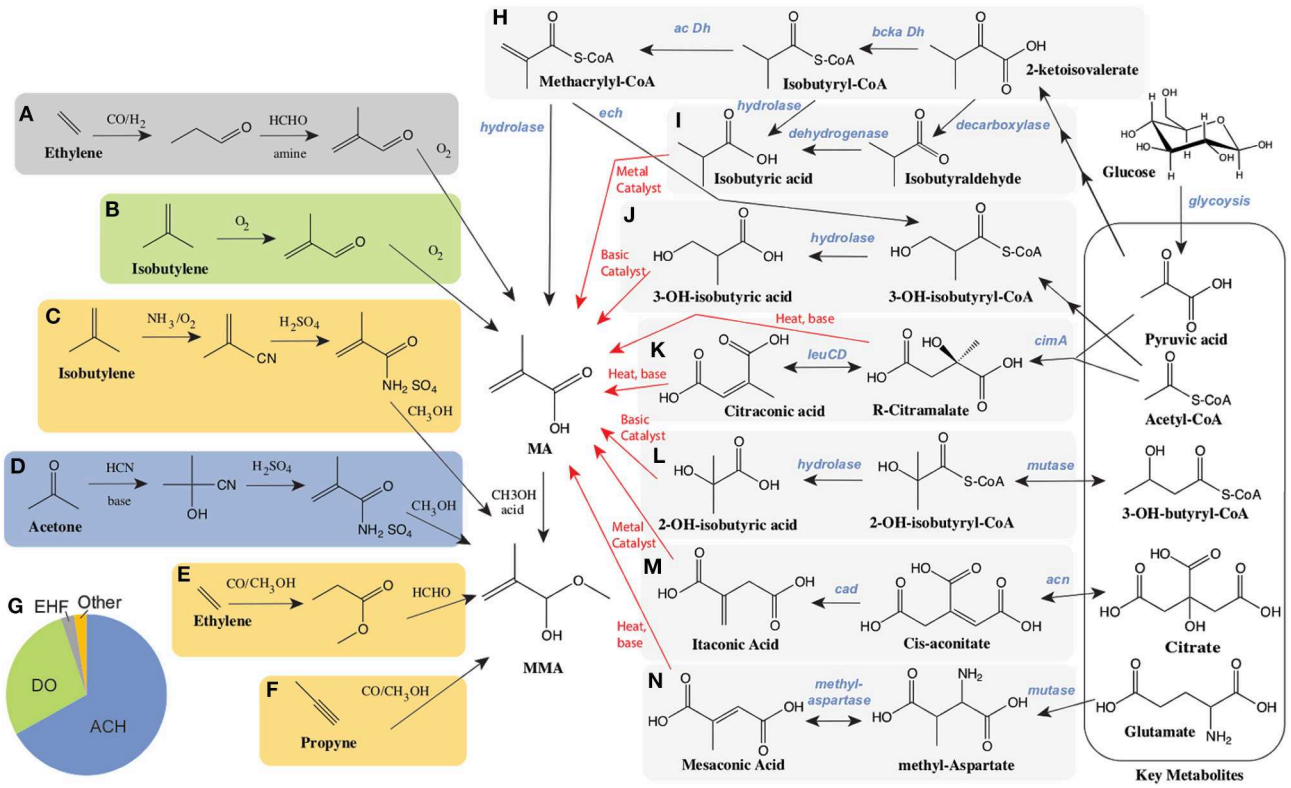

FIGURE 1 | Current petrochemical routes and proposed bioprocessing alternatives for the manufacture of MA/MMA. Petrochemical routes **(A–G)**. The C2 manufacturing routes of MA using ethylene as starting material include **(A)** BASF's ethylene hydroformylation (EHF) to propionaldehyde followed by condensation to methacrolein before oxidation and esterification to MMA and **(E)** the Alpha process where ethylene is converted to MMA *via* methyl propionate. The C3 routes include: **(D)** the Acetone Cyanohydrin (ACH) process starting from acetone and hydrogen cyanohydrin, and **(F)** the propyne route with the carbonylation and esterification of methyl acetylene. The C4 routes, starting from isobutylene include **(B)**, Direct Oxidation (DO) process and **(C)** Asahi's process reliant on ammonia. **(G)** The global breakdown of MMA supply by process technology. Alternative biological routes to produce MA from sugars such as glucose **(H–N)**. Bioconversion steps and chemical conversions are shown as black and red arrows respectively. **(H)** Direct biosynthesis of MA through the intermediates keto-isovalerate, isobutyryl-CoA and methacrylyl-CoA reliant on a branched chain keto-acid dehydrogenase (bcka Dh) and an acyl-CoA dehydrogenase (ac Dh). **(I)** Production of isobutyrate either from keto-isovalerate through isobutyraldehyde, or alternatively through isobutyryl-CoA. **(J)** The conversion of methacrylyl-CoA to 3-hydroxy-isobutyrate (3HIBA) is reliant on an enoyl-CoA hydratase (ech). Citramalate is produced from acetyl-CoA and pyruvate *via* a citramalate synthase (*cimA*) and can then be converted to citraconate *via* isopropylmalate isomerase such as encoded by the *leuCD* genes. Both citramalate and citraconate can be converted chemically to MA. **(L)** 2-hydroxy-isobutyrate (2HIBA) can be produced from 3-hydroxybutyryl-CoA through a mutase and hydrolase. **(M)** Itaconic acid is derived from citric acid through the intermediate cis-aconitate *via* two enzymes: aconitase (acn) and cis-aconitate decarboxylase (cad). **(N)** Mesaconic acid is synthesized from glutamate through methyl-aspartate using a mutase and methylaspartase.

any biobased process to compete with advanced petrochemical technologies. Lastly, we discuss the potential of future bio-based routes to MMA as well as the key barriers for a bioprocess to compete with petrochemistry including conversion yields and feedstock costs.

PETROCHEMICAL ROUTES

Currently, MMA is produced *via* one of several processes from a few key petrochemical feedstocks as illustrated in **Figures 1A–G**. Over 65% of MMA is produced *via* the Acetone CyanoHydrin (ACH) route, developed in the 1930's (**Figure 1D**) (Nagai and Ui, 2004). The use of toxic hydrogen cyanide, as well as concentrated acids are a primary concern with the ACH route, as is the negative impact of significant waste (ammonium bisulfate) generation and treatment (Nagai and Ui, 2004; Mahboub et al., 2018). A competitive route, Direct Oxidation (and similar processes), relies on isobutylene as a feedstock (**Figure 1B**) and is primarily commercial in Asia (Nagai and Ui, 2004; The Chemical Engineer, 2008; Mahboub et al., 2018). Concerns over safety, costs, and the environmental impact of the ACH route have driven efforts to find alternative routes to produce MMA (Adom et al., 2014). Important among these is the hydroformylation of ethylene and related chemistry (**Figures 1A,E**). The low costs of ethylene compared to acetone and isobutylene, as well as decreased waste and lower investment costs have made these processes attractive. In 2019, there were announcements related to the potential construction of new MMA plants using ethylene as a feedstock. If constructed these plants would be operational between 2024 and 2026 (Sale, 2019).

BIOPROCESSING ALTERNATIVES

The use of biotechnology to provide alternative routes for the production of chemicals has had several successful outcomes (Chen et al., 2013; Valdehuesa et al., 2013; Van Dien, 2013; Barton et al., 2015; De Carvalho et al., 2018). Fermentation based routes to MMA utilizing more sustainable feedstocks represent one potential alternative to petrochemistry. Biobased routes may provide both long term environmental and economic sustainability. Given the competitiveness of the market, the development of biobased PMMA has become a priority of many of the current producers (ChiMei Corp., Mitsubishi Corp., Evonik Ind., Sumitomo Chemicals and Arkema) (Bio PMMA Market Trends, 2017)[1,5]. Previous work on the conversion of sugar to MA or MMA using engineered biocatalysts has focused on the evaluation or development of one of several pathways, as illustrated in **Figures 1H–N**, ranging from the direct production of MA to the combined use of biochemical and traditional chemistry to produce MA from glucose. In these bio-chemocatalytic routes, key intermediates are produced biologically and subsequently converted to MA. Intermediates evaluated to date include both 2- and 3- hydroxyisobutyric acids, which are converted to MA *via* dehydration, as well as several 5 carbon organic acids (citraconic, citramalic, itaconic, and mesaconic acids), which have the potential to be converted to MA either by decarboxylation or decarboxylation along with dehydration using an inexpensive hot pressurized water process. (**Figures 1K,M,N**) Significant work over the past decade on these routes has been made in the development of a variety of microorganisms for the biological production of target intermediates, as well as in their subsequent chemical conversions to MA. We will discuss each route in turn.

Direct Production of Methacrylic Acid

As illustrated in **Figure 1H**, there is a direct route from glucose to MA. The biochemical steps involved are primarily derived from valine catabolism, *via* the natural intermediate methacrylyl-CoA (Bachhawat et al., 1957; Rendina and Coon, 1957; Massey et al., 1976). In valine catabolism, methacrylyl-CoA is hydrated to 3-hydroxyisobutyryl-CoA, hydrolysed to 3-hydroxyisobutyrate (**Figure 1J**) and subsequently oxidized to methylmalonate semialdehyde, which enters central metabolism through another oxidation to propionyl-CoA (Bachhawat et al., 1957). Bypassing the later steps of valine degradation by expression of a CoA hydrolase/thioesterase with engineered activity on methacrylyl-CoA, can lead to the direct production of MA. Numerous enzymes have been proposed to perform the conversion of methacrylyl-CoA to MA, which may all need to be engineered for this activity (Burgard et al., 2009). Despite these theoretical descriptions no production has been demonstrated (Burgard et al., 2009). To our knowledge, only one study of microbial bioproduction of MA from glucose was reported reaching a titer of 170uM (14.6mg/L) in shake flasks (Eastham et al., 2018). In this work expression of an acyl-CoA oxidase (ACX4) converts isobutyryl-CoA to methacrylyl-CoA, which is transformed to MA *via* a promiscuous thioesterase (Hayashi et al., 1999; Eastham et al., 2018).

One potential reason for so little success in the biosynthesis of MA is likely due to its acute toxicity. In *E. coli* the concentration of MA reducing growth rate by 50% is only 13.2mM (1.1g/L) (Webb et al., 2018). The toxicity of MA, its esters, and methacryly-CoA has been investigated in numerous *in vivo* studies in both eukaryotes and prokaryotes. The main mechanisms identified were the radical reactivity of MA and derivatives with cellular nucleophiles such as glutathione. MA has also been shown to directly induce DNA damage and inhibit key metabolic enzymes (Plaga et al., 2000; Ansteinsson et al., 2013; Arya et al., 2013; Curson et al., 2014; Murakami et al., 2019). This toxicity makes its direct biological production highly limited in any of the potential microbial hosts considered. (Lipscomb et al., 2011, 2012; Jarboe et al., 2013; Lam et al., 2014; Mukhopadhyay, 2015).

Isobutyric Acid

As depicted in **Figures 1H,I**, another route to MA leveraging valine catabolism relies on the biological production of isobutyric acid (IBA), with subsequent oxidation to MA. This route is attractive as significant progress has been made to date on IBA production in engineered hosts. A recent study highlights that *S. cerevisiae* naturally possesses an Ehrlich pathway (Yu et al., 2016), which enables it to produce isobutyrate. However, reported titers of IBA (387.4 mg/L) (Yu et al., 2016) remain relatively low. In contrast, IBA synthesis from glucose in engineered *E. coli* has been reported at titers of 90 g/L, volumetric productivities of 1g/L-h, and yields of 0.39g IBA/g glucose (80% of the theoretical maximum) (Zhang et al., 2011; Xiong et al., 2015). In this work, isobutyraldehyde was first produced from 2-keto-isovalerate using an α-ketoisovalerate decarboxylase (*kivd*) from *Lactococcus lacti*, followed by oxidation to IBA utilizing a phenylacetaldehyde dehydrogenase (*padA*) from *E. coli* (Zhang et al., 2011; Xiong et al., 2015). While these bioprocesses are promising, achieving high chemical conversion yields have proven more challenging. Dehydrogenation has been performed on both IBA to produce MA as well as on methyl-IBA to produce MMA. To date yields of only 40 and 60%, respectively, have been demonstrated. Yields are limited by significant byproduct (carbon dioxide and diisopropyl ketone) formation (McDaniel and Young, 1963; Wilhelm Gruber and Ginter Schröder, 1983; Macho et al., 2004).

Hydroxy Isobutyric Acids

Routes through biosynthesized hydroxy-isobutyrates (HIBAs) can be coupled with dehydration reactions to produce MA and are considered as alternative chemical conversions to the dehydrogenation of IBA (**Figures 1J,L**). Both 3-hydroxy-isobutyrate (3-HIBA), derived from valine catabolism as discussed above, as well as its isomer 2-hydroxy-isobutyrate (2-HIBA), have been considered as biological end products (Volker and Schindelmann, 1969; Burgard et al., 2009; Rohwerder and Müller, 2010; Dubois et al., 2011; Burk et al., 2012; Marx et al., 2016). The conversion of 3-HIBA to MA has been reported

[5] *Synthetic and Bio PMMA Market Size - Industry Share Report 2022*. Global Market Insights, Inc. https://www.gminsights.com/industry-analysis/synthetic-and-bio-based-pmma-polymethyl-methacrylate-market-size.

with conversions from 20 to > 90% (Volker and Schindelmann, 1969; Marx et al., 2016) while the dehydration of 2-HIBA has been accomplished at conversion yields of 71.5% (Pirmoradi and Kastner, 2017). As mentioned above, 3-HIBA is a natural intermediate in valine catabolism. Engineering efforts have resulted in 3-HIBA titers ranging from 150 mg/L (Dellomonaco et al., 2011) to 2.3 g/L (Lang et al., 2015), often produced along with significant amounts of IBA (Lang et al., 2014; Xiong et al., 2015; Jawed et al., 2016; Marx et al., 2016).

2-HIBA-CoA (**Figure 1l**) was originally found to be a natural metabolite in a pathway that has evolved in the biodegradation of *tert* -butyl ether (Rohwerder et al., 2006). The production of 2-HIBA-CoA *via* a mutase from *A. tertiaricarbonis* is dependent on a B12-dependent mutase involving free radical isomerization (Yaneva et al., 2012; Kurteva-Yaneva et al., 2015). In addition, this enzyme has stereospecificity for (S)-3-hydroxybutyryl-CoA as a substrate (Kurteva-Yaneva et al., 2015). While (R)-3-hydroxybutyryl-CoA, a precursor to polyhydroxyalkanoates, is readily produced from acetoacetyl-CoA in numerous organisms (Madison and Huisman, 1999; Chen and Jiang, 2017), (S)-3-hydroxybutyryl-CoA and (S)-3-hydroxyacyl-CoAs more generally are intermediates in fatty acid biosynthesis. Engineering of pathways with (S)-3-hydroxyacyl-CoA intermediates have been a focus in the production of alcohols as well as fatty acids (Dellomonaco et al., 2011; Lynch et al., 2014; Kim et al., 2015; Wang et al., 2019). 2-HIBA has been produced from both (S)-3-hydroxybutyryl-CoA, *via* mutases similar to that originally characterized, as well as (R)-3-hydroxybutyryl-CoA through the discovery of (R) specific mutases. (R) specific mutases are also vitamin B12 dependent. Biocatalysis reliant on B12 dependent enzymes often require vitamin supplementation, and can suffer from enzyme inactivation, requiring reactivation (Daniel et al., 1998; Mori and Toraya, 1999). To date 2-HIBA biosynthesis has been reported in engineered microbes at titers as high as 6.4g/L (Burgard et al., 2009; Hoefel et al., 2010; Reinecke et al., 2011; Soucaille and Boisart, 2011; Rohde et al., 2017).

Citramalic/Citraconic Acids

Citramalate is a naturally occurring diacid and an intermediate in the isoleucine biosynthesis pathway of some anaerobic bacteria (Buckel and Barker, 1974; Howell et al., 1999; Risso et al., 2008). Citramalate is synthesized from the central metabolites pyruvic acid and acetyl-CoA using a single enzyme, citramalate synthase (*cimA*), as depicted in **Figure 1K**. This enzyme has been successfully utilized in pathways enabling the biosynthesis of 1-propanol and 1-butanol through the intermediate citramalate. In these studies directed evolution of citramalate synthase resulted in feedback resistant mutants with improved activity (Atsumi and Liao, 2008). Citramalate has limited toxicity to microbes when compared to MA where concentrations of ∼25g/L are required to inhibit growth by 50% (Webb et al., 2018). Citramalate can be converted to MA *via* a relatively simple process involving simultaneous decarboxylation and dehydration with citraconate as an intermediate. The simplest conversion uses only hot pressurized water and has achieved conversion yields as high as 81% (de Jong et al., 2012). Although this chemistry is inexpensive, catalyst development may be needed to improve yields and selectivity. Recent successes in bioengineering highlight the potential of citramalate as an intermediate to MA. Using engineered *E. coli* expressing a mutant citramalate synthase, titers ranging from 46.5 g/L to as high as 80 g/L have been reported with yields of 58% of theoretical (Johnson et al., 2009; Wu and Eiteman, 2016; Parimi et al., 2017; Webb et al., 2018). Additionally, significant systems characterization of these engineered strains has been reported (Webb et al., 2019).

Itaconic Acid

Itaconic acid has long been produced *via* biotechnology primarily utilizing wild type or engineered *Aspergillus terreus* strains (Steiger et al., 2013; Hevekerl et al., 2014; Bafana and Pandey, 2018; Kuenz and Krull, 2018). Itaconic acid is also produced from citrate through the intermediate cis-aconitate which is decarboxylated to itaconate as illustrated in **Figure 1M**. Titers in the range of 120–220 g/L have been reported with itaconate yields ranging from 0.45 to as high as 0.58 g itaconic acid/ g glucose and maximal production rates from 0.45 to 1g/L-h (Hevekerl et al., 2014; Huang et al., 2014; Krull et al., 2017a; Tehrani et al., 2019). In addition, the chemical decarboxylation of itaconic acid to MA has been demonstrated *via* several different catalytic routes, mostly reliant on metal catalysts. Some of these processes have demonstrated conversion yields as high as 40% at over 90% selectivity (Le Nôtre et al., 2014; Lansing et al., 2017; Bohre et al., 2019). However, the current cost of itaconic acid ranges from $1.80 to $2.00/kg (Kuenz and Krull, 2018), which is similar to the price of MMA. At this pricing and 100% conversion of itaconic acid to MA (with loss of carbon dioxide), a price of $2.70–$3.00/kg could be expected for MA alone (not including the cost of esterification). This is 20–70% higher than estimated petrochemical based pricing for MA. The route to MA through itaconic acid may well be the most mature, with previous scale up and commercial production but key improvements to reduce costs would include improving the yield of fermentation, as well as increasing the volumetric rate of production by at least 2 fold (Bafana and Pandey, 2018). Recent efforts have been aimed at engineering organisms beyond *A. terreus* including *U. maydis*, *Y. lipolytica*, and *E. coli* (Krull et al., 2017b; Tehrani et al., 2019; Zhao et al., 2019).

Mesaconic Acid

Lastly, another attractive potential route to MA is through mesaconic acid. Mescaconic acid is produced from the amino acid glutamate. Glutamic acid production *via* fermentation is a mature technology, primarily reliant on engineered *Corynebacterium glutamicum* (Kimura, 2003; Wendisch et al., 2016). Mesaconate production relies on several natural pathways for glutamate catabolism and/or carbon fixation (**Figure 1N**), wherein a mutase converts glutamate to methyl aspartate, which through the action of a methyl aspartase is converted to mesaconate (Wang and Zhang, 2015). Similarly to the HIBA-CoA mutase described above, the glutamate mutase is also a B12 dependent enzyme reliant on free radical chemistry and requires vitamin supplementation and continuous enzyme reactivation (Chih and Marsh, 2000; Wang and Zhang, 2015). Methyl

TABLE 1 | Comparison of maturity and challenges for biobased routes to MA.

Maturity	Route	Best demonstrated performance	Bioprocess challenges	Chemistry challenges
1	Itaconic acid/decarboxylation	220g/L (*U. maydis*) (Tehrani et al., 2019) 0.45 g/L-h 51% bioprocess yield 48% conversion to MA (Johnson et al., 2009, 2012; Pirmoradi and Kastner, 2017)	Fermentation rates & yields	Yield, catalyst costs
2	Citramalic acid/decarboxylation & dehydration	80g/L (*E. coli*) (Webb et al., 2018) 1.85 g/L-h 58% bioprocess yield 81% conversion to MA (Johnson et al., 2009, 2012; Pirmoradi and Kastner, 2017)	Fermentation rates & yields	Yield, catalyst development
3	Isobutyric acid/dehydrogenation	90g/L (*E. coli*) (Xiong et al., 2015) 0.625 g/L-h 80% bioprocess yield 40–60% conversion to MA (Pirmoradi and Kastner, 2017)	Fermentation rates & yields	Catalyst development
4	2-HIBA/dehydration	6.4g/L (*C. necator H16)* (Hoefel et al., 2010) 0.09 g/L-h 6.3% bioprocess yield 71.5% conversion to MA (Pirmoradi and Kastner, 2017)	Enzymology	Yield, catalyst development
5	Mesaconic acid/decarboxylation	23g/L (*E. coli*) (Wang et al., 2018) 0.36 g/L-h 64% bioprocess yield 52% conversion to MA (Pirmoradi and Kastner, 2017)	Enzymology	Yield, catalyst development
6	Methacrylic acid production	0.0146g/L (*E. coli*) (Eastham et al., 2018) 0.0007 g/L-h 0.62% bioprocess yield	Rates, yields, engineering resistance	NA

aspartase shares a reaction mechanism with aspartases converting aspartate to fumarate (de Villiers et al., 2012). Heterologous expression of these enzymes from *C. tetanomorphum* in *E. coli* enabled mesaconic acid titers approaching 23 g/L (Wang and Zhang, 2015; Wang et al., 2018). The same basic chemical conversions producing MA from citramalate can convert mesaconic acid to MA although yields still require optimization and possible catalyst/process development (Johnson et al., 2012). While glutamate is basically a commodity chemical in its own right with prices estimated from \$1.70–\$1.95/kg (\$2.00–2.25/kg of monosodium glutamate)[3], assuming a yield of MA from glutamate of 0.58g/g, one could predict a potential MA cost of ∼\$2.90/kg which is not competitive with current pricing for MA. Cost reductions in glutamate production will be needed for this route to be competitive.

FUTURE OUTLOOK

We can, admittedly subjectively, assess the relative maturity and remaining technical challenges for each of the proposed fermentation based routes to MA, as given in **Table 1**. In our opinion, the three most promising routes, when considering both the strain and bioprocess development, as well as final chemical conversions, are the routes through itaconic, citramalic, and isobutyric acids. All of these routes are well past proof of concept stages, but still will require optimization.

While **Table 1** has attempted to rank order the maturity of possible biobased routes to MA, all of the potential biological routes for MA from sugar, as described above, have a similar yield, 1 mole of MA from 1 mole of hexose, which translates in the case of glucose to a maximal theoretical yield of 0.477 gram of MA per gram of glucose. This yield is a common challenge to all of these routes. At theoretical yield, and glucose costs of \$0.20/lb (\$0.44/kg)[6,7] this translates to a cost of \$0.92/kg of MA for feedstock alone. This represents a major challenge to these biological routes, wherein they not only need to compete with the ACH manufacturing technology, but also newer ethylene based processes. In the case of the ACH process, converting acetone (\$0.94/kg), HCN (\$0.66/kg) and sulfuric acid (\$0.13/kg) to MMA, we can estimate the cost of feedstocks for MA (which is not isolated as an intermediate in this process) at roughly \$1/kg[3]. In this case, on a feedstock cost basis, glucose based routes have the potential to compete. However, the *greener* petroleum based routes converting ethylene (\$0.76/kg), syngas (CO/H_2, \$0.07/kg), and methanol (\$0.37/kg) or formaldehyde (\$0.63/kg) to MA (**Figures 1A,E**), would have estimated costs for feedstocks of only \$0.50/kg of MA[3]. This is half that of biobased routes, discussed in **Figure 1**.

While the proposed routes to MA have a maximal yield of 0.477 gram of MA per gram of glucose, there is room for improvement. The theoretical yield for MA from glucose is ∼0.63g/g. A key limitation of these pathways is the wasting of electrons, as illustrated in **Figure 2**. While we often use the term "renewable carbon," it is in actuality usually renewable reducing

[6] *The Sweet and Sour History of Sugar Prices*|*Winton*. Winton https://www.winton.com/longer-view/the-sweet-and-sour-history-of-sugar-prices.

[7] Sugar Prices - 37 Year Historical Chart. https://www.macrotrends.net/2537/sugar-prices-historical-chart-data.

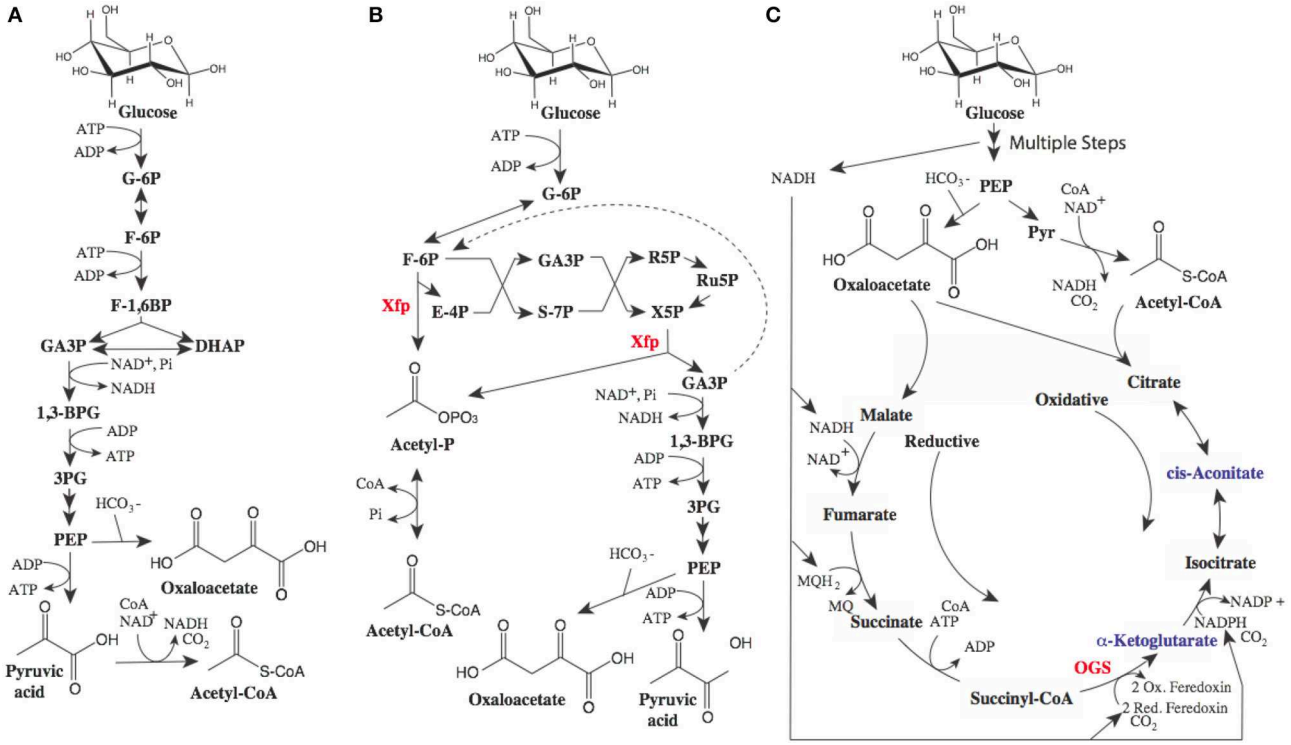

FIGURE 2 | Potential metabolic pathways to optimize MA yields. **(A)** glycolytic metabolism, **(B)** Bifidobacterium shunt, and **(C)** reductive TCA cycle. In glycolysis **(A)** 0.5 moles of glucose are converted to 1 mole of pyruvate (or alternatively 1 mole of oxaloacetate) and one mole of NADH (1 pair or electrons). Pyruvate can be oxidized to acetyl-CoA generating another mole of NADH. **(B)** The Bifidobacterium shunt phosphoketolase enzyme (xfp) (Fandi et al., 2001) has activity as both an erythrose-4-phosphate (E4P) and xylulose-5-phosphate (X5P) phosphoketolase producing acetyl-phosphate (acetyl-P). Recycling 2 moles of glyceraldehyde-3-phosphate (GA3P) through triosephosphate isomerase and the reversible fructose bisphosphate aldolase can lead to improved yield (dashed line) **(C)**. Inclusion of 2-oxoglutarate synthase (OGS) in anaerobic production could lead metabolism where oxidative flux through the TCA cycle is balanced by reductive flux wherein electrons from glycolysis are consumed. Balanced TCA flux can lead to higher yields of alpha-ketoglutarate derived products such as mesaconic acid as well as cis-aconitate derived products such as itaconic acid. Additional abbreviations: glucose-6-phosphate (G-6P), fructose-6-phosphate (F-6P), fructose-1,6-bisphosphate (F-1,6BP), dihydroxyacetone phosphate (DHAP), 1,3 bisphosphoglycerate (1,3BPG), 3 phosphoglycerate (3PG), phosphoenolpyruvate (PEP).

equivalents or electrons which are of the most value. The current biobased routes to MA described above all produce excess electrons. These electrons need to be oxidized for metabolism and production to proceed, either aerobically using oxygen, or anaerobically with another electron acceptor requiring the committed formation of unwanted fermentation byproducts. In addition, wasted pairs of electrons are accompanied by wasted carbon.

Fortunately, potential metabolic solutions to improve yields have been described, generally relying on the use of multiple metabolic routes in combination. For example, the combination of oxidative routes (described above) where excess electrons are generated and reductive routes where excess electrons can be utilized, can lead to improved yields. A good example of an oxidative route to the intermediate acetyl-CoA would be the bifidobacterium shunt, or non-oxidative glycolysis, as depicted in **Figure 2B** (Bogorad et al., 2013; Lin et al., 2018). This metabolic shunt has the potential to produce acetyl-CoA while conserving electrons and carbon, increasing maximal yields. In the best case (where some of the three carbon intermediates can be recaptured in the oxidative pathway, dashed line **Figure 2B**), maximal yields of MA reach theoretical yields of 0.63g/g. Non-oxidative glycolysis is useful for the routes to MA utilizing acetyl-CoA or pyruvate and acetyl-CoA (**Figure 1**). When evaluating the routes reliant on tricarboxylic acid (TCA) cycle intermediates or derivatives, consuming excess electrons produced *via* glycolysis in a reductive route can increase yields as demonstrated in **Figure 2C**. This would require expression of key enzymes from a natural reductive TCA cycle including 2-oxoglutarate synthase [OGS, which it should be noted is an oxygen sensitive enzyme (Hughes et al., 1998)]. A similar approach was used to increase 1,4-butanediol yield from TCA intermediates, albeit not requiring OGS (Yim et al., 2011). Again, this metabolism has the potential to increase theoretical yields of MA (from the mesaconic or itaconic acid intermediates) to the theoretical maximum of 0.63g/g.

With maximal yields of 0.63g/g, sugar costs of less than $0.32/kg ($0.145/lb) would still be needed for biobased routes to have feedstock costs comparable to newer ethylene based petrochemical processes. Sugar costs are a challenge in the bioeconomy in general, particularly for biobased commodities and especially for biofuels (Chen et al., 2013;

NREL, 2013; Taylor et al., 2015; Rosales-Calderon and Arantes, 2019). These costs may well be achievable with second generation cellulosic based sugars as technologies for their production mature (Youngs and Somerville, 2012; Kühner, 2013; Liu et al., 2019). Previous estimates suggest cellulosic sugars can reach costs as low as $0.26/kg (Soare, 2013). Future changes in the legislative landscape, including potential carbon taxes or fines, may also help biobased routes compete (Rajni et al., 2006; Mustafa and Balat, 2009; Information Technology and Innovation Foundation, 2018; EPA, 2019). However, it is likely that technical developments to increase yields (as well as rates and titers), lower sugar costs, and legislative changes will be required for any potential biobased process to MA or MMA to take hold in the market.

AUTHOR CONTRIBUTIONS

JE extracted 10 year average chemical prices from the United States International Trade Commission (https://dataweb.usitc.gov/). JL, JE, and ML wrote, revised, and edited the manuscript.

FUNDING

The authors declare that this study received funding from DMC Biotechnologies, Inc. The funder was not involved in the study design, collection, analysis, interpretation of data, the writing of this article or the decision to submit it for publication. We would also like to acknowledge the following support: ONR YIP #12043956, and DOE EERE grant #EE0007563.

REFERENCES

Adom, F., Dunn, J. B., Han, J., and Sather, N. (2014). Life-cycle fossil energy consumption and greenhouse gas emissions of bioderived chemicals and their conventional counterparts. *Environ. Sci. Technol.* 48, 14624–14631. doi: 10.1021/es503766e

Ali, U., Khairil, J., and Buang, N. A. (2015). A review of the properties and applications of Poly (Methyl Methacrylate) (PMMA). *Polymer Rev.* 55, 678–705. doi: 10.1080/15583724.2015.1031377

Ansteinsson, V., Kopperud, H. B., Morisbak, E., and Samuelsen, J. T. (2013). Cell toxicity of methacrylate monomers-the role of glutathione adduct formation. *J. Biomed. Mater. Res.* 101, 3504–3510. doi: 10.1002/jbm.a.34652

Arya, A. S., Lee, S. A., and Eiteman, M. A. (2013). Differential sensitivities of the growth of Escherichia coli to acrylate under aerobic and anaerobic conditions and its effect on product formation. *Biotechnol. Lett.* 35, 1839–1843. doi: 10.1007/s10529-013-1282-7

Atsumi, S., and Liao, J. C. (2008). Directed evolution of *Methanococcus jannaschii* citramalate synthase for biosynthesis of 1-propanol and 1-butanol by *Escherichia coli*. *Appl. Environ. Microbiol.* 74, 7802–7808. doi: 10.1128/AEM.02046-08

Bachhawat, B. K., Coon, M. J., Kupiecki, F. P., Nagle, R., and Robinson, W. G. (1957). Coenzyme A thiol esters of isobutyric, methacrylic, and beta-hydroxyisobutyric acids as intermediates in the enzymatic degradation of valine. *J. Biol. Chem.* 224, 1–11.

Bafana, R., and Pandey, R. A. (2018). New approaches for itaconic acid production: bottlenecks and possible remedies. *Crit. Rev. Biotechnol.* 38, 68–82. doi: 10.1080/07388551.2017.1312268

Barton, N. R., Burgard, A. P., Burk, M. J., Crater, J. S., Osterhout, R. E., Pharkya, P., et al. (2015). An integrated biotechnology platform for developing sustainable chemical processes. *J. Ind. Microbiol. Biotechnol.* 42, 349–360. doi: 10.1007/s10295-014-1541-1

Bio PMMA Market Trends (2017). *Statistics, Research Report 2022* - Fractovia.org. Available online at: https://www.fractovia.org/news/industry-research-report/synthetic-and-bio-based-pmma-polymethyl-methacrylate-market (accessed Febraury 21, 2020).

Bogorad, I. W., Lin, T.-S., and Liao, J. C. (2013). Synthetic non-oxidative glycolysis enables complete carbon conservation. *Nature* 502, 693–697. doi: 10.1038/nature12575

Bohre, A., Novak, U., Grilc, M., and Likozar, B. (2019). Synthesis of bio-based methacrylic acid from biomass-derived itaconic acid over barium hexa-aluminate catalyst by selective decarboxylation reaction. *Mol Catalysis* 476:110520. doi: 10.1016/j.mcat.2019.110520

Brydson, J. A. (ed.). (1999). "Acrylic plastics". In: *Plastics Materials, 7th Edn.* (Elsevier), 398–424. doi: 10.1016/B978-075064132-6/50056-5

Buckel, W., and Barker, H. A. (1974). Two pathways of glutamate fermentation by anaerobic bacteria. *J. Bacteriol.* 117, 1248–1260. doi: 10.1128/JB.117.3.1248-1260.1974

Burgard, A. P., Burk, M. J., Osterhout, R. E., and Pharkya, P. (2009). *Microorganisms for the Production of Methacrylic Acid*. Patent No US8241877B2. Genomatica, Inc.

Burk, M. J., Burgard, A. P., Osterhout, R. E., Sun, J., and Pharkya, P. (2012). *Microorganisms for Producing Methacrylic Acid and Methacrylate Esters and Methods Related Thereto*. Patent No US9133487B2. Genomatica, Inc.

Burk, M. J., and Van Dien, S. (2016). Biotechnology for chemical production: challenges and opportunities. *Trends Biotechnol.* 34, 187–190. doi: 10.1016/j.tibtech.2015.10.007

Chen, G.-Q., and Jiang, X.-R. (2017). Engineering bacteria for enhanced polyhydroxyalkanoates (PHA) biosynthesis. *Synth. Syst. Biotechnol.* 2, 192–197. doi: 10.1016/j.synbio.2017.09.001

Chen, X., Zhou, L., Tian, K., Kumar, A., Singh, S., Prior, B. A., et al. (2013). Metabolic engineering of *Escherichia coli*: a sustainable industrial platform for bio-based chemical production. *Biotechnol. Adv.* 31, 1200–1223. doi: 10.1016/j.biotechadv.2013.02.009

Chih, H.-W., and Marsh, E. N. G. (2000). Mechanism of glutamate mutase: identification and kinetic competence of acrylate and glycyl radical as intermediates in the rearrangement of glutamate to methylaspartate. *J. Am. Chem. Soc.* 122, 10732–10733. doi: 10.1021/ja002488+

Curson, A. R. J., Burns, O. J., Voget, S., Daniel, R., Todd, J. D., McInnis, K., et al. (2014). Screening of metagenomic and genomic libraries reveals three classes of bacterial enzymes that overcome the toxicity of acrylate. *PLoS ONE* 9:e97660. doi: 10.1371/journal.pone.0097660

Daniel, R., Bobik, T. A., and Gottschalk, G. (1998). Biochemistry of coenzyme B12-dependent glycerol and diol dehydratases and organization of the encoding genes. *FEMS Microbiol. Rev.* 22, 553–566. doi: 10.1111/j.1574-6976.1998.tb00387.x

De Carvalho, J. C., Magalhaes, A. I., and Soccol, C. R. (2018). Biobased itaconic acid market and research trends—Is it really a promising chemical. *Chim. Oggi-Chem. Today* 36, 56–58.

de Jong, E., Higson, A., Walsh, P., and Wellisch, M. (2012). *Bio-based chemicals value added products from biorefineries.* IEA Bioenergy, Report. Available online at: https://www.ieabioenergy.com/wp-content/uploads/2013/10/Task-42-Biobased-Chemicals-value-added-products-from-biorefineries.pdf

de Villiers, M., Puthan Veetil, V., Raj, H., de Villiers, J., and Poelarends, G. J. (2012). Catalytic mechanisms and biocatalytic applications of aspartate and methylaspartate ammonia lyases. *ACS Chem. Biol.* 7, 1618–1628. doi: 10.1021/cb3002792

Dellomonaco, C., Clomburg, J. M., Miller, E. N., and Gonzalez, R. (2011). Engineered reversal of the β-oxidation cycle for the synthesis of fuels and chemicals. *Nature* 476, 355–359. doi: 10.1038/nature10333

Dormer, W, Gomes, R, Meek, M. E, World Health Organization and International Programme on Chemical Safety (1998). *Methyl Methacrylate.* World Health Organization. Available online at: https://apps.who.int/iris/handle/10665/42030

Dubois, J.-L., Okumura, K., Kobayashi, Y., and Hiraoka, R. (2011). *Improved Process of Dehydration Reactions*. Patent No US9914699B2. Arkema.

Eastham, G. R., Stephens, G., and Yiakoumetti, A. (2018). *Process for the Biological Production of Methacrylic Acid and Derivatives Thereof*. Patent No US20180171368A1. Lucite International UK Ltd.

EPA (2019). The economics of climate change. *Finance Dev.* 56. Available online at: https://www.imf.org/external/pubs/ft/fandd/2019/12/pdf/fd1219.pdf

Fandi, K. G., Ghazali, H. M., Yazid, A. M., and Raha, A. R. (2001). Purification and N-terminal amino acid sequence of fructose-6-phosphate phosphoketolase from Bifidobacterium longum BB536. *Lett. Appl. Microbiol.* 32, 235–239. doi: 10.1046/j.1472-765X.2001.00895.x

Frazer, R. Q., Byron, R. T., Osborne, P. B., and West, K. P. (2005). PMMA: an essential material in medicine and dentistry. *J. Long Term Eff. Med. Implants* 15, 629–639. doi: 10.1615/JLongTermEffMedImplants.v15.i6.60

Hayashi, H., Iwata, K., Matsuoka, M., Hayashi, H., Takemiya, T., Yasuda S., et al. (1999). A novel acyl-CoA oxidase that can oxidize short-chain acyl-CoA in plant peroxisomes. *J. Biol. Chem.* 274, 12715–12721. doi: 10.1074/jbc.274.18.12715

Hevekerl, A., Kuenz, A., and Vorlop, K.-D. (2014). Influence of the pH on the itaconic acid production with *Aspergillus terreus*. *Appl. Microbiol. Biotechnol.* 98, 10005–10012. doi: 10.1007/s00253-014-6047-2

Hoefel, T., Wittmann, E., Reinecke, L., and Weuster-Botz, D. (2010). Reaction engineering studies for the production of 2-hydroxyisobutyric acid with recombinant *Cupriavidus necator* H 16. *Appl. Microbiol. Biotechnol.* 88, 477–484. doi: 10.1007/s00253-010-2739-4

Howell, D. M., Xu, H., and White, R. H. (1999). (R)-citramalate synthase in methanogenic archaea. *J. Bacteriol.* 181, 331–333. doi: 10.1128/JB.181.1.331-333.1999

Huang, X., Lu, X., Li, Y., Li, X., and Li, J.-J. (2014). Improving itaconic acid production through genetic engineering of an industrial *Aspergillus terreus* strain. *Microb. Cell Fact.* 13:119. doi: 10.1186/s12934-014-0119-y

Hughes, N. J., Clayton, C. L., Chalk, P. A., and Kelly, D. J. (1998). Helicobacter pylori porCDAB and oorDABCGenes encode distinct pyruvate: flavodoxin and 2-Oxoglutarate: acceptor oxidoreductases which mediate electron transport to NADP. *J. Bacteriol.* 180, 1119–1128. doi: 10.1128/JB.180.5.1119-1128.1998

Information Technology and Innovation Foundation (2018). *Carbon Tax Could Support Innovation and Economic Growth While Lowering Cost to Reduce Carbon.* Emissions: New ITIF Report Finds.

Jarboe, L. R., Royce, L. A., and Liu, P. (2013). Understanding biocatalyst inhibition by carboxylic acids. *Front. Microbiol.* 4:272. doi: 10.3389/fmicb.2013.00272

Jawed, K., Mattam, A. J., Fatma, Z., Wajid, S., Abdin, M. Z., Yazdani, S. S., et al. (2016). Engineered production of short chain fatty acid in *Escherichia coli* using fatty acid synthesis pathway. *PLoS ONE* 11:e0160035. doi: 10.1371/journal.pone.0160035

Johnson, D. W., Eastham, G. R., Poliakoff, M., and Huddle, T. A. (2009). *Method of Producing Arcylic and Methacrylic Acid*. Patent No US8933179B2. Lucite International UK Ltd.

Johnson, D. W., Eastham, G. R., Poliakoff, M., and Huddle, T. A. (2012). *Process for the Production of Methacrylic Acid and Its Derivatives and Polymers Produced Therefrom*. Patent No US20150094438A1. Lucite International UK Ltd.

Kim, S., Clomburg, J. M., and Gonzalez, R. (2015). Synthesis of medium-chain length (C6-C10) fuels and chemicals via β-oxidation reversal in Escherichia coli. *J. Ind. Microbiol. Biotechnol.* 42, 465–475. doi: 10.1007/s10295-015-1589-6

Kimura, E. (2003). Metabolic engineering of glutamate production. *Adv. Biochem. Eng. Biotechnol.* 79, 37–57. doi: 10.1007/3-540-45989-8_2

Krull, S., Eidt, L., Hevekerl, A., Kuenz, A., and Prüße, U. (2017b). Itaconic acid production from wheat chaff by *Aspergillus terreus*. *Process Biochem.* 63, 169–176. doi: 10.1016/j.procbio.2017.08.010

Krull, S., Hevekerl, A., Kuenz, A., and Prüße, U. (2017a). Process development of itaconic acid production by a natural wild type strain of Aspergillus terreus to reach industrially relevant final titers. *Appl. Microbiol. Biotechnol.* 101, 4063–4072. doi: 10.1007/s00253-017-8192-x

Kuenz, A., and Krull, S. (2018). Biotechnological production of itaconic acid—things you have to know. *Appl. Microbiol. Biotechnol.* 102, 3901–3914. doi: 10.1007/s00253-018-8895-7

Kühner, S. (2013). *Feedstock Costs. Deliverable D*1 1. Available online at: http://www.bioboost.eu/uploads/files/bioboost_d1.1-syncom_feedstock_cost-vers_1.0-final.pdf

Kurteva-Yaneva, N., Zahn, M., Weichler, M. T., Starke, R., Harms, H., Müller, R. H., et al. (2015). Structural basis of the stereospecificity of bacterial B12-dependent 2-hydroxyisobutyryl-CoA mutase. *J. Biol. Chem.* 290, 9727–9737. doi: 10.1074/jbc.M115.645689

Lam, F. H., Ghaderi, A., Fink, G. R., and Stephanopoulos, G. (2014). Biofuels. *Engineering alcohol tolerance in yeast. Science* 346, 71–75. doi: 10.1126/science.1257859

Lang, K., Buehler, K., and Schmid, A. (2015). Multistep synthesis of (S)-3-hydroxyisobutyric acid from glucose using *Pseudomonas taiwanensis* VLB120 B83 T7 catalytic biofilms. *Adv. Synth. Catal.* 357, 1919–1927. doi: 10.1002/adsc.201500205

Lang, K., Zierow, J., Buehler, K., and Schmid, A. (2014). Metabolic engineering of Pseudomonas sp. strain VLB120 as platform biocatalyst for the production of isobutyric acid and other secondary metabolites. *Microb. Cell Fact.* 13:2. doi: 10.1186/1475-2859-13-2

Lansing, J. C., Murray, R. E., and Moser, B. R. (2017). Biobased methacrylic acid via selective catalytic decarboxylation of itaconic acid. *ACS Sustain. Chem. Eng.* 5, 3132–3140. doi: 10.1021/acssuschemeng.6b02926

Le Nôtre, J., Witte-van Dijk, S. C. M., van Haveren, J., Scott, E. L., and Sanders, J. P. M. (2014). Synthesis of bio-based methacrylic acid by decarboxylation of itaconic acid and citric acid catalyzed by solid transition-metal catalysts. *ChemSusChem* 7, 2712–2720. doi: 10.1002/cssc.201402117

Lin, P. P., Jaeger, A. J., Wu, T. Y., Xu, S. C., Lee, A. S., Gao, F., et al. (2018). Construction and evolution of an *Escherichia coli* strain relying on nonoxidative glycolysis for sugar catabolism. *Proc. Natl. Acad. Sci. U.S.A.* 115, 3538–3546. doi: 10.1073/pnas.1802191115

Lipscomb, T. E. W., Lynch, M. D., and Gill, R. T. (2011). *Methods, Systems and Compositions for Increased microorganism Tolerance to and Production of 3-Hydroxypropionic Acid (3-hp).* Patent No US8883464B2. Cargill, Inc., University of Colorado at Boulder.

Lipscomb, T. W., Lipscomb, M. L., and Gill, R. T. (2012). "Metabolic engineering of recombinant *E. coli* for the production of 3-hydroxypropionate," in *Engineering Complex Phenotypes in Industrial Strains,* ed R. Patnaik (John Wiley & Sons, Inc). doi: 10.1002/9781118433034

Liu, C.-G., Xiao, Y., Xia, X. X., Zhao, X. Q., Peng, L., Srinophakun, P., et al. (2019). Cellulosic ethanol production: progress, challenges and strategies for solutions. *Biotechnol. Adv.* 37, 491–504. doi: 10.1016/j.biotechadv.2019.03.002

Lynch, M., Louie, M., Copley, S., and Spindler, E. (2014). *Microorganisms and Methods for the Production of Fatty Acids and Fatty Acid Derived Products*. Patent No US10337038B2. Cargill, Inc.

Macho, V., Králik, M., Chromá, V., Cingelová, J., and Mikulec, J. (2004). The oxidative dehydrogenation of methyl isobutyrate to methyl methacrylate. *Petroleum and Coal.* 46, 69–80.

Madison, L. L., and Huisman, G. W. (1999). Metabolic engineering of Poly(3-Hydroxyalkanoates): from DNA to plastic. *Microbiol. Mol. Biol. Rev.* 63, 21–53. doi: 10.1128/MMBR.63.1.21-53.1999

Mahboub, M. J. D., Dubois, J.-L., Cavani, F., Rostamizadeh, M., and Patience, G. S. (2018). Catalysis for the synthesis of methacrylic acid and methyl methacrylate. *Chem. Soc. Rev.* 47, 7703–7738. doi: 10.1039/C8CS00117K

Marx, A., Poetter, M., Buchholz, S., May, A., Siegert, H., Alber, B., et al. (2016). *Process for Preparing Methacrylic Acid or Methacrylic Esters*. Patent No US20100291644A1. Evonik Roehm GmbH

Massey, L. K., Sokatch, J. R., and Conrad, R. S. (1976). Branched-chain amino acid catabolism in bacteria. *Bacteriol. Rev.* 40, 42–54. doi: 10.1128/MMBR.40.1.42-54.1976

McDaniel, E. L., and Young, H. S. (1963). Catalytic dehydrogenation of methyl isobutyrate to methyl methacrylate over alumina catalysts. *Industr. Eng. Chem. Product Res. Dev.* 2, 287–292. doi: 10.1021/i360008a009

Mori, K., and Toraya, T. (1999). Mechanism of reactivation of coenzyme B12-dependent diol dehydratase by a molecular chaperone-like reactivating factor. *Biochemistry* 38, 13170–13178. doi: 10.1021/bi9911738

Mukhopadhyay, A. (2015). Tolerance engineering in bacteria for the production of advanced biofuels and chemicals. *Trends Microbiol.* 23, 498–508. doi: 10.1016/j.tim.2015.04.008

Murakami, Y., Kawata, A., Suzuki, S., and Fujisawa, S. (2019). Cytotoxicity and pro-inflammatory properties of aliphatic Alpha, Beta-unsaturated acid and ester monomers in RAW264.7 cells and their chemical reactivity. *In vivo* 33, 313–323. doi: 10.21873/invivo.11477

Mustafa, B., and Balat, H. (2009). Recent trends in global production and utilization of bio-ethanol fuel. *Appl. Energy* 86, 2273–2282. doi: 10.1016/j.apenergy.2009.03.015

Nagai, K., and Ui, T. (2004). Trends and future of monomer-MMA technologies. *Sumitomo Chem.* 2, 4–13.

NREL (2013). *NREL Proves Cellulosic Ethanol Can Be Cost Competitive (Fact Sheet)*.

Parimi, N. S., Durie, I. A., Wu, X., Niyas, A. M. M., and Eiteman, M. A. (2017). Eliminating acetate formation improves citramalate production by metabolically engineered *Escherichia coli*. *Microb. Cell Fact.* 16:114. doi: 10.1186/s12934-017-0729-2

Pirmoradi, M., and Kastner, J. R. (2017). Synthesis of methacrylic acid by catalytic decarboxylation and dehydration of carboxylic acids using a solid base and subcritical water. *ACS Sustain. Chem. Eng.* 5, 1517–1527. doi: 10.1021/acssuschemeng.6b02201

Plaga, W., Vielhaber, G., Wallach, J., and Knappe, J. (2000). Modification of Cys-418 of pyruvate formate-lyase by methacrylic acid, based on its radical mechanism. *FEBS Lett.* 466, 45–48. doi: 10.1016/S0014-5793(99)01752-4

Rajni, H. K., Tornvall, U., Gustafsson, L., and Boerjesson, P. (2006). Industrial biotechnology for the production of bio-based chemicals – a cradle-to-grave perspective. *TRENDS Biotechnol.* 25, 119–124. doi: 10.1016/j.tibtech.2007.01.001

Reinecke, L., Schaffer, S., Marx, A., Poetter, M., and Haas, T. (2011). *Recombinant Cell Producing 2-Hydroxyisobutyric Acid*. Patent No US20110171702A1. Evonik Roehm GmbH.

Rendina, G., and Coon, M. J. (1957). Enzymatic hydrolysis of the coenzyme a thiol esters of β-hydroxypropionic and β-hydroxyisobutyric acids. *J. Biol. Chem.* 225, 523–534.

Risso, C., Van Dien, S. J., Orloff, A., Lovley, D. R., and Coppi, M. V. (2008). Elucidation of an alternate isoleucine biosynthesis pathway in Geobacter sulfurreducens. *J. Bacteriol.* 190, 2266–2274. doi: 10.1128/JB.01841-07

Rohde, M.-T., Tischer, S., Harms, H., and Rohwerder, T. (2017). Production of 2-Hydroxyisobutyric Acid from Methanol by Methylobacterium extorquens AM1 Expressing (R)-3-Hydroxybutyryl Coenzyme A-Isomerizing Enzymes. *Appl. Environ. Microbiol.* 83:e02622–16. doi: 10.1128/AEM.02622-16

Rohwerder, T., Breuer, U., Benndorf, D., Lechner, U., and Müller, R. H. (2006). The alkyl tert-butyl ether intermediate 2-hydroxyisobutyrate is degraded via a novel cobalamin-dependent mutase pathway. *Appl. Environ. Microbiol.* 72, 4128–4135. doi: 10.1128/AEM.00080-06

Rohwerder, T., and Müller, R. H. (2010). Biosynthesis of 2-hydroxyisobutyric acid (2-HIBA) from renewable carbon. *Microb. Cell Fact.* 9:13. doi: 10.1186/1475-2859-9-13

Rosales-Calderon, O., and Arantes, V. (2019). A review on commercial-scale high-value products that can be produced alongside cellulosic ethanol. *Biotechnol. Biofuels* 12:240. doi: 10.1186/s13068-019-1529-1

Sale, K. (2019). *EPCA'19: Roehm to build 250,000 tonne/year MMA plant in US Gulf Coast, start-up by 2024*. Icis. Available online at: https://www.icis.com/explore/resources/news/2019/10/08/10426307/epca-19-roehm-to-build-250-000-tonne-year-mma-plant-in-us-gulf-coast-start-up-by-2024 (accessed Febraury 17, 2020).

Soare, A. (2013). *Cellulosic Chemicals and Fuels Race to Compete with First-Gen Sugar Economics*. https://members.luxresearchinc.com/research/report/12706 (accessed Febraury 17, 2020).

Soucaille, P., and Boisart, C. (2011). *Enzymatic Production of 2-HydroxyIsobutyrate (2-hiba)*. Patent No US20110151530A1. Metabolic Explorer SA.

Steiger, M. G., Blumhoff, M. L., Mattanovich, D., and Sauer, M. (2013). Biochemistry of microbial itaconic acid production. *Front. Microbiol.* 4:23. doi: 10.3389/fmicb.2013.00023

Taylor, R., Nattrass, L., Alberts, G., Robson, P., Chudziak, C., Bauen, A., et al. (2015). *From the Sugar Platform to Biofuels and Biochemicals*. Final report for the European Commission Directorate-General Energy.

Tehrani, H. H., Becker, J., Bator, I., Saur, K., Meyer, S., Lóia, A. C. R., et al. (2019). Integrated strain-and process design enable production of 220 g L- 1 itaconic acid with Ustilago maydis. *Biotechnol. Biofuels* 12, 1–11. doi: 10.1186/s13068-019-1605-6

The Chemical Engineer (2008). Evonik develops new process for methyl methacrylate. *Focus Catal.* 2008, 6–7. doi: 10.1016/S1351-4180(08)70573-7

Valdehuesa, K. N. G., Liu, H., Nisola, G. M., Chung, W. J., Lee, S. H., et al. (2013). Recent advances in the metabolic engineering of microorganisms for the production of 3-hydroxypropionic acid as C3 platform chemical. *Appl. Microbiol. Biotechnol.* 97, 3309–3321. doi: 10.1007/s00253-013-4802-4

Van Dien, S. (2013). From the first drop to the first truckload: commercialization of microbial processes for renewable chemicals. *Curr. Opin. Biotechnol.* 24, 1061–1068. doi: 10.1016/j.copbio.2013.03.002

Volker, T., and Schindelmann, E. (1969). *Preparation of Methacrylic Compounds by Dehydration of Alpha - Hydroxybutyric Acid Compounds*. Patent No US3487101A. Lonza Ltd.

Wang, J., Wang, J., Tai, Y. S., Zhang, Q., Bai, W., Zhang, K., et al. (2018). Rerouting carbon flux for optimized biosynthesis of mesaconate in *Escherichia coli*. *Appl. Microbiol. Biotechnol.* 102, 7377–7388. doi: 10.1007/s00253-018-9135-x

Wang, J., and Zhang, K. (2015). Production of mesaconate in *Escherichia coli* by engineered glutamate mutase pathway. *Metab. Eng.* 30, 190–196. doi: 10.1016/j.ymben.2015.06.001

Wang, L., Chauliac, D., Moritz, B. E., Zhang, G., Ingram, L. O., Shanmugam, K. T., et al. (2019). Metabolic engineering of *Escherichia coli* for the production of butyric acid at high titer and productivity. *Biotechnol. Biofuels* 12:62. doi: 10.1186/s13068-019-1408-9

Webb, J., Springthorpe, V., Rossoni, L., Minde, D. P., Langer, S., Walker, H., et al. (2019). Systems analyses reveal the resilience of *Escherichia coli* physiology during accumulation and export of the nonnative organic acid citramalate. *mSystems* 4:e00187–19. doi: 10.1128/mSystems.00187-19

Webb, J. P., Arnold, S. A., Baxter, S., Hall, S. J., Eastham, G., Stephens, G., et al. (2018). Efficient bio-production of citramalate using an engineered *Escherichia coli* strain. *Microbiology* 164, 133–141. doi: 10.1099/mic.0.000581

Wendisch, V. F., Jorge, J. M. P., Pérez-García, F., and Sgobba, E. (2016). Updates on industrial production of amino acids using Corynebacterium glutamicum. *World J. Microbiol. Biotechnol.* 32:105. doi: 10.1007/s11274-016-2060-1

Wilhelm Gruber, D., and Ginter Schröder, O.-R. (1983). *Process for Producing Methacrylic Acid by Oxidative Dehydration of Isobutyric Acid and Catalyst Therefor*. Patent No US4370490A. Evonik Roehm GmbH. Available online at: https://patents.google.com/patent/US4370490A/en.

Witczak, T., Grzesik, M., Skrzypek, J., and Witczak, M. (2010). Liquid-phase esterification of methacrylic acid with methanol catalyzed by heteropolyacid. *Int. J. Chem. Reactor Eng.* 8, 1–6. doi: 10.2202/1542-6580.2128

Wu, X., and Eiteman, M. A. (2016). Production of citramalate by metabolically engineered *Escherichia coli*. *Biotechnol. Bioeng.* 113, 2670–2675. doi: 10.1002/bit.26035

Xiong, M., Yu, P., Wang, J., and Zhang, K. (2015). Improving engineered *Escherichia coli* strains for high-level biosynthesis of isobutyrate. *Aims Energy* 2, 60–74. doi: 10.3934/bioeng.2015.2.60

Yaneva, N., Schuster, J., Schäfer, F., Lede, V., Przybylski, D., Paproth, T., et al. (2012). Bacterial Acyl-CoA mutase specifically catalyzes coenzyme B12-dependent isomerization of 2-hydroxyisobutyryl-CoA and (S)-3-hydroxybutyryl-CoA. *J. Biol. Chem.* 287, 15502–15511. doi: 10.1074/jbc.M111.314690

Yim, H., Haselbeck, R., Niu, W., Pujol-Baxley, C., Burgard, A., Boldt, J., et al. (2011). Metabolic engineering of *Escherichia coli* for direct production of 1,4-butanediol. *Nat. Chem. Biol.* 7, 445–452. doi: 10.1038/nchembio.580

Youngs, H., and Somerville, C. (2012). Development of feedstocks for cellulosic biofuels. *F1000 Biology Reports* 4:10. doi: 10.3410/B4-10

Yu, A.-Q., Juwono, N. K. P., Foo, J. L., Leong, S. S. J., and Chang, M. W. (2016). Metabolic engineering of *Saccharomyces cerevisiae* for the overproduction of short branched-chain fatty acids. *Metabolic Eng.* 34, 36–43. doi: 10.1016/j.ymben.2015.12.005

Zhang, K., Woodruff, A. P., Xiong, M., Zhou, J., and Dhande, Y. K. (2011). A synthetic metabolic pathway for production of the platform chemical isobutyric acid. *ChemSusChem* 4, 1068–1070. doi: 10.1002/cssc.201100045

Zhao, C., Cui, Z., Zhao, X., Zhang, J., Zhang, L., Tian, Y., et al. (2019). Enhanced itaconic acid production in *Yarrowia lipolytica* via heterologous expression of a mitochondrial transporter MTT. *Appl. Microbiol. Biotechnol.* 103, 2181–2192. doi: 10.1007/s00253-019-09627-z

Conflict of Interest: ML has a financial interest in DMC Biotechnologies, Inc.

The remaining authors declare that the research was conducted in the absence of any commercial or financial relationships that could be construed as a potential conflict of interest.

Advantages of publishing in Frontiers

OPEN ACCESS
Articles are free to read for greatest visibility and readership

FAST PUBLICATION
Around 90 days from submission to decision

HIGH QUALITY PEER-REVIEW
Rigorous, collaborative, and constructive peer-review

TRANSPARENT PEER-REVIEW
Editors and reviewers acknowledged by name on published articles

Frontiers
Avenue du Tribunal-Fédéral 34
1005 Lausanne | Switzerland

Visit us: www.frontiersin.org
Contact us: frontiersin.org/about/contact

REPRODUCIBILITY OF RESEARCH
Support open data and methods to enhance research reproducibility

DIGITAL PUBLISHING
Articles designed for optimal readership across devices

FOLLOW US
@frontiersin

IMPACT METRICS
Advanced article metrics track visibility across digital media

EXTENSIVE PROMOTION
Marketing and promotion of impactful research

LOOP RESEARCH NETWORK
Our network increases your article's readership